



The chemical weathering of rocks and migration of elements in the boreal zone (North-West Russia)

Ekaterina Vasyukova

► To cite this version:

Ekaterina Vasyukova. The chemical weathering of rocks and migration of elements in the boreal zone (North-West Russia). Earth Sciences. Université Paul Sabatier - Toulouse III, 2009. English. NNT : . tel-00410508

HAL Id: tel-00410508

<https://theses.hal.science/tel-00410508>

Submitted on 21 Aug 2009

HAL is a multi-disciplinary open access archive for the deposit and dissemination of scientific research documents, whether they are published or not. The documents may come from teaching and research institutions in France or abroad, or from public or private research centers.

L'archive ouverte pluridisciplinaire **HAL**, est destinée au dépôt et à la diffusion de documents scientifiques de niveau recherche, publiés ou non, émanant des établissements d'enseignement et de recherche français ou étrangers, des laboratoires publics ou privés.



Université
de Toulouse



THÈSE

En vue de l'obtention du

DOCTORAT DE L'UNIVERSITÉ DE TOULOUSE

Délivré par *l'Université Toulouse III - Paul Sabatier*
Discipline ou spécialité : *Géochimie de surface*

Présentée et soutenue par

Ekaterina VASYUKOVA

Le 27 janvier 2009

Altération chimique des roches et migration des éléments dans la zone boréale (Nord-Ouest de la Russie)

**The chemical weathering of rocks and migration of elements in
the boreal zone (North-West Russia)**

JURY

A. Dia	DR CNRS, Géosciences Rennes	Rapporteur
J. Ingri	Professeur Luleå University of Technology	Rapporteur
S. Lapitsky	DR Université d'Etat de Moscou	Rapporteur
F. Martin	Professeur UPS, LMTG Toulouse	Examinateur
V. Shevchenko	CR Académie des Sciences, Moscou	Examinateur
B. Dupré	DR CNRS, OMP Toulouse	Directeur de thèse
O. Pokrovsky	CR1 CNRS, LMTG Toulouse	Directeur de thèse
A. Shishkin	Professeur SPbSTU, St.Pétersbourg	Co-directeur de thèse

Ecole doctorale : *Sciences de l'Univers, de l'Environnement et de l'Espace*

Unité de recherche : *Laboratoire des Mécanismes et Transferts en Géologie*

Directeur(s) de Thèse : *Bernard Dupré, DR CNRS, Toulouse*

Oleg Pokrovsky, CR1 CNRS, LMTG Toulouse

Alexander Shishkin, Professeur SPbSTU, St.Pétersbourg



Université
de Toulouse



THÈSE

En vue de l'obtention du

DOCTORAT DE L'UNIVERSITÉ DE TOULOUSE

Délivré par *l'Université Toulouse III - Paul Sabatier*
Discipline ou spécialité : *Géochimie de surface*

Présentée et soutenue par

Ekaterina VASYUKOVA

Le 27 janvier 2009

Altération chimique des roches et migration des éléments dans la zone boréale (Nord-Ouest de la Russie)

**The chemical weathering of rocks and migration of elements in
the boreal zone (North-West Russia)**

JURY

A. Dia	DR CNRS, Géosciences Rennes	Rapporteur
J. Ingri	Professeur Luleå University of Technology	Rapporteur
S. Lapitsky	DR Université d'Etat de Moscou	Rapporteur
F. Martin	Professeur UPS, LMTG Toulouse	Examinateur
V. Shevchenko	CR Académie des Sciences, Moscou	Examinateur
B. Dupré	DR CNRS, OMP Toulouse	Directeur de thèse
O. Pokrovsky	CR1 CNRS, LMTG Toulouse	Directeur de thèse
A. Shishkin	Professeur SPbSTU, St.Pétersbourg	Co-directeur de thèse

Ecole doctorale : *Sciences de l'Univers, de l'Environnement et de l'Espace*

Unité de recherche : *Laboratoire des Mécanismes et Transferts en Géologie*

Directeur(s) de Thèse : *Bernard Dupré, DR CNRS, Toulouse*

Oleg Pokrovsky, CR1 CNRS, LMTG Toulouse

Alexander Shishkin, Professeur SPbSTU, St.Pétersbourg

Acknowledgements

This PhD thesis has been elaborated from October 2005 till November 2008 between the University Paul Sabatier of Toulouse, France, and Saint-Petersburg State Polytechnic University, Russia, within the French government scholarship programme for a double-supervised dissertation.

In the first place, I would like to address my acknowledgements to my scientific directors – Bernard Dupré and Alexander Shishkin – for the offered topic for this thesis, for their professional supervision each in his own manner, and for giving me their constant support and criticism throughout all stages of the research program which contributed to the success of this work.

I am deeply thankful to my co-supervisor Oleg Pokrovsky for guiding me throughout the dissertation and discovering for me the world of geochemistry. I thank him for the invaluable help from the field work and laboratory experiments till the manuscript preparation, permanent availability, talent and endless understanding in the moments of disappointment.

I would like to thank kindly Jérôme Viers who helped me a lot during this time, especially on isotope geochemistry, inveigled me into the cuisine of “salle blanche”, and with gentleness and patience invested time (and maybe nerves) throughout my French language mastering.

I am also very grateful to Priscia Oliva for very agreeable moments of working together, for transmitting her knowledge, helpful discussions and her sympathy towards me.

Finally, I would like to express my sincere gratitude to François Martin, who took me under his wing, and not only brought me into mineralogy, but also encouraged and supported with all his kindness especially during the last most important and difficult stage of the PhD. I had a great pleasure to work with him and to derive my strength and inspiration from his optimism and sense of humour.

I am thankful to all these people for the freedom I enjoyed during our work together and for the knowledge and confidence they brought towards me.

I would also like to thank the opponents Aline Dia, Johan Ingri and Sergey A. Lapitsky of this thesis for having accepted to judge my work and for the interest they showed in it.

Without the support of technical and engineering staff at LMTG, I would have been lost sometimes with my experiments and analysis, so big thanks go to Carole Boucayrand, Carole Causserand, Maïté Carayon, Fabienne de Parceval, Frédéric Candaudap, Sébastien Gardoll, Cyril Zouiten, Thierry Aigouy, Philippe de Parceval, and Pierre Brunet.

I am also very grateful to geologists from the Moscow State University – Yana, Andrey and Dmitriy Bychkovy – for their professional help with data, maps and team work in the field trip where I was initiated into geologists, but also for wonderful ambience during the summer expedition 2007 in Karelia.

Certainly, I would like to mention, without paying special attention to the order, my friends from Toulouse but at the same time from all over the world who shared nice moments with me during this fascinating journey: Elena, Ludmila, Nastya, Teresa, Camille, Ana, Riccardo, Sergey, Pierre, Chris, Guilhem, Guiseppe, Quintin, Gwénaël, Yann, Fabrice and many others from LMTG. Special thanks go to Laurent – the best office-mate – for his patience, readiness to help whatever was the need, time spent together, and chronically good mood.

I would like to finish with the people who are precious to me:

My parents, Irina and Vladimir, who brought me to this level of education, always leaving me a choice in my professional orientation. They are my invaluable encouragement since I was born and especially over these years far away from home. I thank all my family for their support, patience and faith in me.

And finally, I reserve a particular mention to Ilya, who always knew how to inspire me even in the most difficult moments. I am deeply indebted to you for everything that you had to put away throughout this time and that you did sincerely to make these years the most precious time of my life. A part of this work belongs to you.

To Ilya and my family

Abstract

The objective of this thesis is to improve our understanding of the weathering processes of mafic silicate rocks and element speciation and migration in the boreal environments (White Sea basin, North-Western Russia). Specific goals are to *i*) characterize and describe the mechanisms governing the chemical weathering and mineral formation in subarctic zone, *ii*) assess the role of the rock lithology (granitic environment vs. basaltic) in trace elements (TE) speciation and organo-mineral colloids formation in surface waters of boreal high latitude river basins, and *iii*) reveal the pH-dependence of TE speciation in order to predict possible changes in elements bioavailability in natural water due to their acidification caused by environmental changes. The main originality of the work is to combine, for the first time on the same natural objects, the geochemical, isotope, physico-chemical and mineralogical techniques to better understand the factors that control biogeochemical cycling of elements in the subarctic region.

The first part is devoted to general introduction and the insight into the problems. The second chapter is aimed at studying the geochemical migration and partition of major and trace elements between rock and soil reservoirs during chemical weathering process. In particular, we investigate soil forming processes on mafic rocks under strong influence of glacier moraine in North-Western Russia, and related surface water hydrochemistry, and provide the estimation of mafic rocks weathering intensity in view the importance of weathering of these rocks in atmospheric CO₂ consumption. The third chapter gives a quantitative characterization of TE colloidal speciation in pristine, organic-rich rivers and surface waters where the role of colloidal status of elements and their transport in surface waters is addressed. In this part we compare two contrasting techniques, dialysis and ultrafiltration, both used for the assessment of the elements speciation in water, and we test the role of the rock lithology (granitic vs. basaltic catchments) in colloids formation and their chemical nature. The fourth chapter describes the results of experimental modeling conducted with natural surface waters at different pH using the equilibrium dialysis technique. We evaluate the complexation of TE with natural organo-mineral colloids present in boreal surface waters and quantify empirical distribution coefficients of TE between dissolved and colloidal pools as a function of pH. Investigations carried out in this part of the study should contribute to the prediction of water acidification phenomena expected to be mostly pronounced in the Arctic due to global climate warming.

Keywords: geochemistry, boreal zone, subarctic, trace element, colloid, speciation, natural waters, ultrafiltration, dialysis, podzol, mafic rock, chemical weathering.

Résumé

Cette thèse a pour but d'améliorer notre compréhension des processus d'altération des roches mafiques silicatées, de la spéciation des éléments et de leur migration dans le milieu boréal (bassin versant de la mer Blanche, Nord-Ouest de la Russie). Les objectifs principales du travail sont *i*) de caractériser et décrire les mécanismes responsables de l'altération chimique et de la formation des minéraux dans la zone subarctique, *ii*) évaluer le rôle de la lithologie (environnement granitique versus basaltique) dans la spéciation des éléments traces (ET) et la formation des colloïdes organo-minéraux dans les eaux de surface des bassins versants boréaux des hautes latitudes, et *iii*) révéler la dépendance de la spéciation des ET en fonction du pH de la solution pour prédire des changements éventuels dans la bioaccumulation des éléments dans les eaux naturelles à cause de leur acidification. L'originalité de cette thèse est de combiner, pour la première fois sur les mêmes objets naturels, les techniques physico-chimique, minéralogique et isotopique afin de mieux comprendre les facteurs qui contrôlent les cycles biogéochimiques des éléments dans les régions subarctiques.

La première partie de la thèse consiste en une introduction générale de la problématique. Le deuxième chapitre est consacré à l'étude de la migration géochimique et de la partition des éléments majeurs et traces entre la roche et le sol au cours du processus d'altération chimique. Notamment, nous étudions le processus de la formation des sols sur les roches mafiques soumis à une forte influence de la moraine glaciaire (dans la zone Nord-Ouest de la Russie), ainsi que la chimie des eaux associées. Nous présentons l'estimation de l'intensité d'altération des roches mafiques en lien avec la consommation du CO₂ atmosphérique. La troisième partie de la thèse est consacrée à la caractérisation quantitative de la spéciation colloïdale des ET dans les rivières et les eaux de surface naturelles. Le rôle du statut colloïdal des éléments, ainsi que de leur transport dans les eaux de surface est considéré. Dans cette partie, nous réalisons une comparaison de deux techniques contrastantes, dialyse et ultrafiltration, utilisées pour l'estimation de la spéciation des éléments dans l'eau. Nous contrôlons le rôle de la lithologie des roches (bassins versants granitiques vs. basaltiques) dans la formation des colloïdes et leur nature chimique. Le quatrième chapitre comprend les résultats d'une modélisation expérimentale conduite sur les eaux naturelles de surface à différents pH en utilisant la technique de dialyse en équilibre. Nous évaluons la complexation des ET avec les colloïdes organo-minéraux naturels présents dans les eaux de surface boréales, et estimons les coefficients de distribution empiriques des ET entre les fractions colloïdale et dissoute en fonction du pH. L'étude menée dans cette partie vise à contribuer à la prévision du phénomène d'acidification supposé être prononcé dans les régions Arctiques suite au réchauffement climatique global.

Mots clés: géochimie, zone boréale, subarctic, élément trace, colloïde, spéciation, eaux naturelles, ultrafiltration, dialyse, podzol, roche mafic, altération chimique.

Резюме

Данная диссертация направлена на изучение процессов химического выветривания магматических силикатных горных пород, форм нахождения и миграции элементов в бореальных ландшафтах (бассейн Белого моря, Северо-Запад России). В рамках работы были поставлены следующие задачи: i) охарактеризовать и описать механизмы, ответственные за химическое выветривание и образование минералов в субарктической зоне, ii) оценить роль литологии (гранитные водосборные бассейны против базальтовых) в распределении форм нахождения микроэлементов и формировании органо-минеральных коллоидов в поверхностных водах бассейнов бореальных рек, и iii) выявить зависимость форм нахождения элементов от pH раствора с целью предсказать возможные изменения в биоаккумуляции элементов в природных водах вследствие их асидификации, вызванной влиянием на окружающую среду. Научная новизна диссертации заключается в объединении геохимического, изотопного, физико-химического и минералогического методов исследований, примененных впервые на одних и тех же природных объектах, с целью выявления факторов, контролирующих биогеохимические циклы элементов в субарктической зоне.

В первой главе работыдается общее введение в проблематику. Вторая глава посвящена изучению геохимической миграции и распределения макро- и микроэлементов между горными породами и почвами в процессе химического выветривания. В частности, мы исследовали процесс формирования почв на основных породах, подверженных сильному влиянию ледниковых моренных отложений в северо-западной части России, а также химический состав соответствующих поверхностных вод. Была дана оценка интенсивности выветривания основных горных пород в виду его важности в процессе потребления атмосферного углекислого газа. Третья глава посвящена количественной оценке коллоидных форм микроэлементов в реках и поверхностных водах, богатых органическим веществом и неподверженных антропогенному воздействию. В этой части проводится сравнение двух контрастных методов, диализа и ультрафильтрации, используемых для оценки форм нахождения элементов в воде, а также оценивается роль литологии подстилающих горных пород (кислых и основных) в формировании коллоидных веществ и их химическом составе. В четвертой главе дается описание результатов экспериментального моделирования

проведенного с природными поверхностными водами при различных рН с помощью метода равновесного диализа. Проведена оценка комплексации микроэлементов с природными органо-минеральными коллоидами, присутствующими в бореальных поверхностных водах, а также расчет эмпирических коэффициентов распределения микроэлементов между растворенной и коллоидной фазой как функция рН. Исследования, проведенные в этой части работы, призваны внести вклад в прогнозирование феномена асидификации природных вод, который может быть более выраженным в арктических регионах вследствие глобального потепления климата.

Ключевые слова: геохимия, бореальная зона, субарктический, микроэлементы, коллоиды, формы нахождения, природные воды, ультрафильтрация, диализ, подзол, основные породы, химическое выветривание.

CONTENTS

Acknowledgements	5
Abstract	7
Key words	7
Résumé	8
Mots clés	9
Резюме	9
Ключевые слова	10
Letter combinations	15
Chapter 1. General introduction	17
1.1. Background of the study.....	19
1.1.1. Speciation of elements in boreal zone.....	19
1.1.2. Nature of colloids and their role in mobilisation of trace elements.....	22
1.1.3. Methods of colloids' separation.....	25
1.1.4. Change of trace element speciation in the light of the global climate warming.....	26
1.1.5. Podzols in boreal zone.....	27
1.1.6. Role of chemical weathering in elements transport to the oceans and associated CO ₂ consumption.....	30
1.2. Description of the region.....	32
1.2.1. Characteristics of the boreal zone.....	32
1.2.2. Study site.....	33
1.3. Objectives and scope of the study.....	35
1.4. Thesis organisation.....	36
Chapter 2. Chemical weathering of mafic rocks in boreal subarctic environment (North-West Russia) under glacial moraine deposits	39
Abstract.....	41
2.1. Introduction.....	42
2.2. Geological and geographical setting.....	46
2.2.1. Lithology, soils, and vegetation.....	46

2.2.1.1. Vetryny Belt paleorift.....	49
2.2.1.2. Kivakka layered intrusion.....	49
2.2.2. Climate and hydrology.....	50
2.3. Materials and methods.....	50
2.3.1. Sampling of rocks, soils, surface waters and soil pore waters.....	50
2.3.2. Analytical techniques.....	51
2.3.2.1. Mineralogical and chemical analysis of rocks and soils.....	51
2.3.2.2. Chemical analysis of river, surface swamp and soil pore waters.....	60
2.3.2.3. Isotope analysis of river waters and soils.....	61
2.4. Results.....	62
2.4.1. Bedrock mineralogy and chemistry.....	62
2.4.2. Soil mineralogy.....	63
2.4.2.1. Evolution of the soil chemical composition as a function of depth.....	67
2.4.3. Hydrochemistry.....	68
2.5. Discussion.....	69
2.5.1. Moraine influence over the full depth of soil profile.....	69
2.5.1.1. Major elements.....	69
2.5.1.2. REE upper crust normalized diagrams.....	72
2.5.1.3. Extended upper crust normalized diagrams.....	74
2.5.2. Actual weathering processes: waters versus soils and rocks.....	75
2.5.6. Isotope study.....	80
2.5.7. Chemical weathering rates.....	83
2.6. Conclusions.....	84
References.....	86

Chapter 3. Trace elements in organic- and iron-rich surficial fluids of boreal zone: Assessing colloidal forms via dialysis and ultrafiltration.....	97
Preface.....	99
Abstract.....	101
3.1. Introduction.....	102
3.2. Sample area.....	104
3.3. Materials and methods.....	106
3.3.1. Sampling, filtration and dialysis.....	106

3.3.2. Analysis.....	109
3.4. Results and discussion.....	110
3.4.1. Comparison between dialysis and ultrafiltration.....	110
3.4.2. Major and trace element speciation.....	113
3.4.2.1. Organic carbon and iron.....	113
3.4.2.2. Alkali metals, alkaline earths, divalent transition and heavy metals.....	115
3.4.2.3. Trivalent metals: Al, Ga, Y and REE.....	117
3.4.2.4. Tetravalent metals: Ti, Zr, Hf and Th.....	121
3.4.2.5. Other trace elements: V, Cr, Mo, W, As, Sb, Sn, Nb and U.....	122
3.4.3. Effect of lithology on element distribution among various types of colloid.....	125
3.4.4. Thermodynamic analysis.....	128
3.5. Conclusions.....	130
References.....	132

Chapter 4. Experimental measurement of trace elements association with natural organo-mineral colloids using dialysis.....	139
Abstract.....	141
4.1. Introduction.....	142
4.2. Materials and methods.....	144
4.2.1. Sampling.....	144
4.2.2. Dialysis procedure and analyses.....	147
4.3. Results.....	148
4.3.1. Methodology of dialysis at different pH.....	149
4.3.2. The pH-dependence of the percentage of dissolved form and the distribution coefficient K_d of the trace elements.....	149
4.3.3. Thermodynamic modeling of metal complexation with dissolved organic matter.....	152
4.4. Discussion.....	164
4.4.1. Possible artifacts of dialysis procedure and colloids aggregation.....	164
4.4.2. Relative role of organic matter vs. adsorption or coprecipitation of trace elements with Fe-rich colloids.....	165

4.5. Conclusions and implications: change of trace elements speciation and bioavailability during acidification of surface waters.....	168
References.....	170
Chapter 5. Conclusions and perspectives.....	177
5.1. Conclusions.....	179
5.2. Perspectives.....	182
Bibliography.....	185
List of figures.....	206
List of tables.....	209
ANNEXES.....	211

Letter combinations and abbreviations

AAS	Atomic Absorption Spectrometry
Alk	Alkalinity (concentration)
DOC	Dissolved Organic Carbon (concentration)
FA	Fulvic Acid
HA	Humic Acid
HPLC	High Performance Liquid Chromatography
ICP-AES	Inductively-Coupled Plasma Atomic Emission Spectrometry
ICP-MS	Inductively-Coupled Plasma Mass Spectrometer
K _d	Iron-normalized trace element partition coefficient between dissolved and colloidal fraction
LOI	Loss On Ignition
OC	Organic Carbon
OM	Organic Matter
TE	Trace Elements
STEM	Scanning Transmission Electronic Microscopy
SEM	Scanning Electron Microscopy
UF	Ultrafiltration
WHAM	Windermere Humic Aqueous Model
XRD	X-Ray Diffractometry

Chapter 1

General introduction



1.1. Background of the study

1.1.1. Speciation of elements in boreal zone

One of the major goals of the geochemistry is to quantify the element fluxes occurring between different reservoirs represented by continents, oceans and atmosphere, and to identify the mechanisms which control these fluxes. This exchange takes place at all scales, from the globe surface to a smaller scale of a soil or soil horizon. Figure 1.1 (after Viers et al., 2007) illustrates these matter transfer processes at a river basin scale, and defines the main processes which control these exchanges.

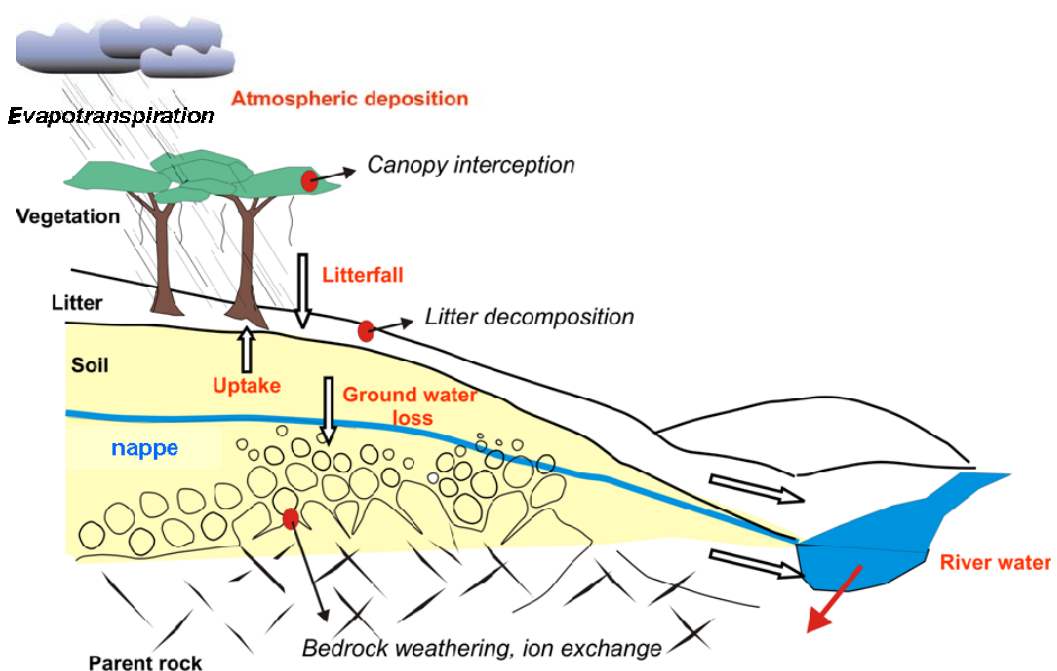


Fig. 1.1. Scheme describing the main matter exchange between different reservoirs (soil-rock system, vegetation, and atmosphere) of a watershed (after Viers et al., 2007).

The understanding of the role of continental erosion on the biogeochemical cycles of elements requires thorough studies on the interactions between different biogeochemical reservoirs (oceans, atmosphere, biosphere, and hydrosphere). Chemical and physical erosion of continental rocks plays a fundamental role in these processes. It can be mechanical, initiated by physical processes, gravity, temperature contrasts, frosting and defrosting, or chemical, initiated by dissolution of minerals under the influence of water and dissolved substances which it contains. During these processes,

some chemical elements remain *in situ* in the form of newly-formed minerals, and constitute a soil together with primary minerals. Other elements are exported with water flows in dissolved (< 0.22 or 0.45 µm) or particulate (> 0.22 or 0.45 µm) form. Water flows are responsible of 90% of the substances transfer from continent to the ocean, and for many elements this transport mostly occurs in particulate form (Gaillardet et al., 2003; Viers et al., 2007, 2008). At the same time, there is a growing understanding of the importance of colloidal¹ fluxes, which can represent an essential part of flux for many usually insoluble elements (Viers et al., 2007). This colloidal transport is especially important for the boreal regions of the world, where river contain high concentration of dissolved organic matter and iron. Thus, quantitative and qualitative estimation of fluxes of dissolved and particulate matter exported with water flows is essential to acquire better understanding of the process of continental weathering.

Boreal² regions of the Russian Arctic play a crucial role in the transport of elements from continents to the ocean at high latitudes. In view of the importance of these circumpolar zones for our understanding of ecosystem response to global warming, it is very timely to carry out detailed regional studies of trace elements³ (TE) geochemistry in boreal landscapes. These zones represent one of the most important organic carbon reservoirs in the form of peat bogs, wetlands and soils very rich in organic matter. As a consequence, trace elements in water are likely to be transferred in

¹ **Colloids** are defined as small particles, organic or inorganic, having the size between 1 µm and 1 nm (Stumm and Morgan, 1996).

² **Boreal** is defined by W. Köppen (1931) as the zone having a definite winter with snow, and a short summer, generally hot. It includes a large part of North America between the Arctic Zone and about 40°N, extending to 35°N in the interior. In Central Europe and in Asia the boreal zone extends southward from the tundra to 40°–50°N. 2. A biogeographical zone or region characterized by a northern type of fauna or flora. The term boreal region is used mainly by American biologists, and includes the area between the mean summer isotherm of 18°C or 64.4°F (roughly 45°N latitude) and the Arctic Zone.

³ **Trace elements** (TE) are defined as elements that are present at low concentrations (1 mg/l or less) in natural waters. This means that trace elements are not considered when “total dissolved solids” are calculated in rivers, lakes, or groundwaters, because their combined mass is not significant compared to the sum Na^+ , K^+ , Ca^{2+} , Mg^{2+} , H_4SiO_4 , HCO_3^- , CO_3^{2-} , SO_4^{2-} , Cl^- , and NO_3^- . Being TEs in natural waters does not necessarily qualify them as TEs in rocks (Gaillardet et al., 2003). In general, this definition covers almost all elements of the periodical table but this thesis is focused on the most commonly used elements such as trace metals and metalloids of a considerable geochemical importance.

the form of organic and organo-mineral colloids as it was shown in several recent studies on the estuaries of major Siberian rivers (e.g., Martin et al., 1993; Dai and Martin, 1995). There is a large amount of previous studies which addressed the speciation⁴ and transport of trace elements in water in tropical (Viers et al., 1997; Braun et al., 1998; Dupré et al., 1999) and temperate (Pokrovsky et al., 2005a,) zones. Despite the increasing interest to boreal permafrost⁵-dominated areas among aquatic geochemists, these particular zones remain much less investigated. In contrast with the west European environments lying at the Baltic Sea and North Sea coast in a relatively mild climate, the understanding of the geochemistry of ecosystems situated at the Arctic sea coast, including White Sea, is still largely insufficient. Indeed, geochemical processes in the “eastern” boreal zone undergo in different climatic conditions, with higher temperature variations in winter and summer. In comparison to the western boreal zone, in the eastern part the precipitation is much less influenced by marine aerosols. The influence of atmospheric pollution, local anthropogenic pressure and anthropogenically induced concentrations in precipitates, as well as the effect of acidic rains, are more pronounced in the Western Europe compared to pristine zone of the Russian Arctic. Landscape properties in these two parts also differ, in particular, more important proportion of wetland areas in eastern boreal zone provides higher concentrations of dissolved (< 0.22 µm) organic matter (from 10 to 150 mg/l) and Fe (up to 10 mg/l) in surface waters. As a consequence, in eastern boreal regions, the nature of dissolved organic matter, iron and aluminium colloids, as well as the estuarine behaviour of TE, may be different from that observed in the “model” Kalix river, draining the western boreal zone in northern Sweden, which has been very thoroughly studied over the past decades (Pontér et al., 1990, 1992; Ingri and Widerlund, 1994; Ingri et al., 1997, 2000, 2005, 2006; Land and Öhlander, 1997, 2000; Porcelli et al., 1997; Andersson et al., 1998, 2001; Land et al., 2000; Dahlqvist et al., 2004, 2005, 2007; van Dongen et al., 2008). Except for a few works on trace elements measurements in the Russian Arctic (Dai and Martin, 1995; Guieu et al., 1996; Moran and Woods, 1997; Zhulidov et al., 1997), studies addressing colloidal vs. dissolved

⁴ **Speciation** is defined as chemical form in which the metals occur in the solid and solution phase.

⁵ **Permafrost** describes a thermal condition in soil or rock when the temperature of the ground remains below 0°C for two or more years.

forms and transport of TE in organic-rich waters from pristine permafrost landscapes are scarce (Ingri et al., 2000; Pokrovsky and Schott, 2002; Dahlqvist et al., 2004; Pokrovsky et al., 2006a).

Over the last several decades, a revolutionary change of attitude towards the importance of metal speciation has occurred and considerable research effort has been devoted to measuring the concentrations of biologically important trace elements in soil and surface water. At the present time, it is generally recognized by environmental scientists that the particular behaviour of trace metals in the environment is determined by their specific physico-chemical forms rather than by their total concentration. The speciation affects the extent to which the chemical element participates in various transport and transformation processes (Gustafsson and Gschwend, 1997). The research in this field requires a multidisciplinary approach, i.e., combination of chemical, geological, hydrological, (micro)biological studies.

1.1.2. Nature of colloids and their role in mobilisation of trace elements

In order to understand the role of colloids in aquifer systems, it is important to determine their occurrence and origin.

Natural colloids can be found in different milieus: natural surface and groundwater, sea and ocean, as well as soil pore water. Fig. 1.2 (after Gaillardet et al., 2003) shows an example of the distribution of a number of mineral and organic species which are present in natural environment as a function of their size.

Colloids in surface water (Gustafsson and Gschwend, 1997; in this study we define colloids as entities between 1 nm and 0.22 µm size) originate, in general, from the soil horizons, and can be organic, inorganic and organo-mineral (Ingri and Widerlund, 1994; Gustafsson and Gschwend, 1997; Viers et al., 1997; Gustafsson et al., 2000; Dahlqvist et al., 2004, 2007; Pokrovsky et al., 2005a, 2006a; Allard, 2006; Andersson et al., 2006; Allard and Derenne, 2007). Degradation of plant litter on the soil's surface yields a family of organic colloids (soluble humic substances, i.e., humic and fulvic acids) which constitute, in an insoluble form, the upper mineral soil horizon. They are usually combined with mineral soils particles creating either organo-mineral clay-humic complexes (i.e., Fe and Al hydroxides stabilized by organic matter) in well-drained environments, or dispersed complexes if the soil is not drained enough. In this

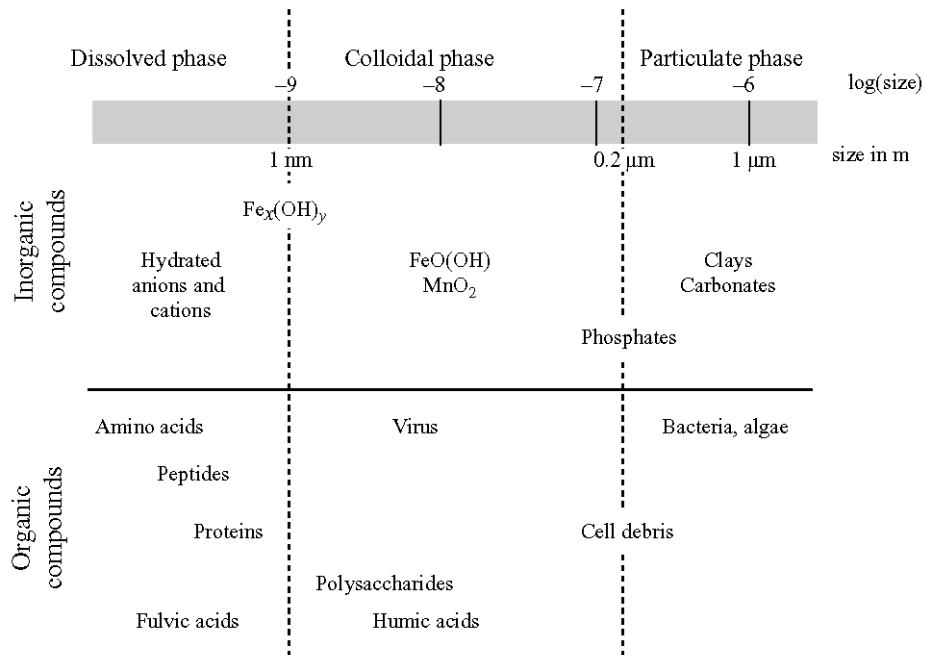


Fig. 1.2. Distribution of mineral and organic colloids as a function of size in aquatic systems (after Gaillardet et al., 2003).

upper horizon, trace elements are also present in colloidal form, being released from the decomposition of the plant litter. In boreal regions, the presence of wetlands, abundant precipitation and sufficient plant production creates favourable conditions for formation of organic rich soils, providing high concentrations of organic matter in surficial waters and thus, colloidal status of many elements in waters.

Mineral inorganic colloids are most commonly represented by metal oxyhydroxides (e.g., iron-, aluminium- and manganese-oxyhydroxides), siliceous phases and clays. They are formed during intensive chemical weathering⁶ of primary soil minerals (silicates and multiple oxides) in the upper soil horizon. This process is usually called a podzolisation process (e.g., Duchaufour, 1951, 1997; Buurman and Jongmans, 2005). It takes place in an aggressive acid medium created by plant litter decomposition products, and is controlled by the influence of a mixture of organic acids and complexing agents. Cations Ca^{2+} , Mg^{2+} , K^+ , Na^+ are removed together with iron and aluminium. This leaching is accompanied by migration and subsequent accumulation of

⁶ **Chemical weathering** is defined as decomposition of rocks by surface processes that change the chemical composition of the original material, transforming rocks and minerals into new chemical combinations.

iron and/or aluminium organo-mineral complexes in a soil horizon B called podzolic. Further description of podzols is given in Section 1.1.5.

One of the colloids' properties is strong scavenging capacities towards cations. They play a major role in the mobilization of trace elements in soils and waters affecting elemental distribution in natural systems through interfacial adsorption or complexation processes (Buffle, 1988). Quantitative modeling of migration and bioavailability of TE requires the knowledge of stability constants for complexation reactions of trace metals with colloidal organic matter. The most powerful and precise method of assessing these constants is voltammetry and potentiometry; however, their use is restricted by very low number of transition metals (Zn, Cu, Cd, Pb) and some rare earth elements (Stevenson and Chen, 1991; Johannesson et al., 2004; Chang Chien et al., 2006; Prado et al., 2006). Up to present time, large number of trace elements, including trivalent and tetravalent elements, remains unexplored and the quantification of their stability constants with natural colloidal matter is not possible. This hampers the progress in applying quantitative physico-chemical models such as WHAM (Tipping and Hurley, 1992; Tipping, 1994; Tipping, 1998; Tipping, 2002), WinHumicV based on WHAM model (Gustafsson, 1999), NICA-Donnan (Benedetti et al., 1995; Kinniburgh et al., 1999; Milne et al., 2001, 2003; Tipping, 2002) for assessing trace elements speciation in continental waters.

Generally speaking, chemical composition of the most of surface and ground waters is a result of the rain-water-rock interaction on the earth surface and especially in the soil zone (Drever, 1982). From ultrafiltration experiments in tropical environment (Cameroon), Dupré et al. (1999) demonstrated the key role of organic colloids in the transport of elements such as Al and Fe, the major constituents of the soil minerals. Experimental study of the TE speciation in waters of boreal forest landscapes performed by Dobrovolsky (1983) demonstrated an important role of complex organic compounds of metals, as well as colloidal particles. Forms of monatomic ions of iron participating in water migration in boreal zones play here a subordinate role, whereas organic complexes can constitute up to 80% of the overall soluble metals in soil. Notably, the percentage of these forms increases in more boreal landscapes, i.e., proportion of organic complexes depends on the proportion of wetlands of a territory (Laudon et al., 2004; Frey and Smith, 2005). Hence, the first goal of this thesis consists in quantitative

characterization of trace element speciation in pristine, organic-rich boreal rivers and surface waters.

1.1.3. Methods of colloids' separation

There is a whole range of currently available strategies for separation and analysis of colloids in natural water. An important progress in characterizing the behaviour of TE in aquatic environments has been done thanks to development of high resolution analytical instrumentation and techniques (Gaillardet et al., 2003). Techniques like dialysis, voltammetry, gels diffusion (DET and DGT) are routinely used to obtain *in situ* information for small colloids, whereas a combination of rapid fractionation procedures, including filtration, field-flow fractionation, split-flow lateral-transport thin (SPLITT) separation cells, and cross-flow ultrafiltration (CFF) can be used for the ex-situ characterisation of TE association with colloids.

Ultrafiltration is most often used to characterize the proportion of dissolved and colloidal forms in surficial rivers, lakes, groundwater and seawater (Hoffman et al., 1981, 2000; Guo and Santschi, 1996; Viers et al., 1997; Dupré et al., 1999; Eyrolle and Benaim, 1999; Olivié-Lauquet et al., 1999, 2000; Ingri et al., 2000, 2004; Pokrovsky and Schott, 2002; Pokrovsky et al., 2005a, 2006a, 2006b; Dia et al., 2000; Pourret et al., 2007; Pédrot et al., 2008). In contrast, only few authors used dialysis as an *in situ* technique of colloid characterization (Benes and Steiness, 1974; Borg and Andersson, 1984; Berggren, 1989; Alfaro-De la Torre et al., 2000; Gimpel et al., 2003; Nolan et al., 2003; Buschmann and Sigg, 2004; Pokrovsky et al., 2005a).

Though ultrafiltration is widely used, some artifacts of this procedure such as charge separation, clogging of the filter membrane induced by forced filtration, various sources of contamination (filter, apparatus, tubing, recipient) etc. (Viers et al., 1997; Dupré et al., 1999) make the separation and characterization of colloids in water difficult. As a result, there are several main requests raising as necessary to develop nowadays, such as sampling methods with conservation of species, rapid, simple and inexpensive methods for the assessment of TE speciation, and separation of species including *in situ* methods. In this context, the dialysis method allows a rapid and relatively inexpensive *in situ* assessment of the equilibrium distribution of solutes having a pore size less than that of the membrane. In this study we compared the size

fractionation of TE in colloids using two contrasting techniques, dialysis and ultrafiltration, and recommended an easily-available separation procedure for routine assessment of the colloidal state of TEs in boreal waters.

1.1.4. Change of trace elements speciation in the context of the global climate warming

Metals speciation in natural waters is of increasing interest and importance because toxicity, bioavailability, environmental mobility, biogeochemical behaviour, and potential risk in general are strongly dependent on the chemical species of metals (Fytianos, 2001). To allow an explanation of the diverging degrees of bioavailability and toxicity of different elements, enhanced knowledge is needed about the chemical forms in which the trace elements are present in water.

Arctic and subarctic regions are among the most fragile zones in the world due to their low resistance to the industrial impact, low productivity of terrestrial biota, limited biological activity over the year, and thus, low ability of the ecosystem for self-recovering. In view of the importance of these circumpolar zones for our understanding of ecosystems response to the global warming, detailed regional studies of trace elements geochemistry in the boreal landscapes are very timely.

Mobility of the organic carbon (OC) and associated TE during permafrost thawing caused by the climate warming is the main change happening in boreal zones and one of the principal environmental and scientific challenges nowadays. Continuous increase of the runoff of Russian arctic rivers during the last several decades (Serreze et al., 2002) together with the liberation of carbon and metals scavenged to present day by this permafrost (Guo et al., 2004) can modify fluxes of elements exported to the oceans (Hölemann et al., 2005), as well as their speciation in river water and soil solutions.

The effect of global environmental change consisting not only in rising the surface temperature but also in acidification of water reservoirs is expected to be mostly pronounced in the Arctic. Acidification of surface waters is nowadays one of the major issues of concern (Seip, 1986; Reuss, 1987; Borg et al., 1989; Moiseenko, 1995; Aggarwal et al., 2001; Evans et al., 2001; Galloway, 2001; Skjelkvåle et al., 2001, 2005; Davies et al., 2005). Naturally, the acidity of water in freshwater lakes and streams is predominantly determined by the soil and rock types of an area. However, it was shown

by Reuss et al. (1987) that waters sensitive to increased acidification typically drain areas underline by granitic or other highly siliceous bedrock covered by thin and patchy soils. In terms of anthropogenic influence, the acidification of waters is related to numerous factors, e.g., increasing acid precipitation caused by increased emissions of sulphur and nitrogen oxides, afforestation, soils acidification caused by changes in land use and depositions of compounds of anthropogenic origin (Seip, 1986). The increased content of the carbon dioxide in the atmosphere leads to uptake of CO₂ by surface waters and increase of water pH due to carbonic acid (H₂CO₃) dissociation.

Acidification of surface waters can change not only the speciation of TE, but consequently, the proportion of labile and biologically available forms of metals and thus, pollutants migration and bioavailability. In most cases the ‘bioavailable’ fraction is found to be the free metal ion (Slaveykova & Wilkinson, 2002) or labile metal species in the form of small-size organic and inorganic complexes (Mylon et al., 2003). Also, the toxicity of TE depends not only on their abundance and speciation but also on their bioavailability.

Quantitative prediction of these phenomena requires rigorous knowledge of the proportion of colloidal forms of TE in solution as a function of pH. One of the goals of this study is to develop a simple in-situ method which allows quantifying distribution coefficients and degree of TE association with organo-mineral colloids. It is anticipated that achieving this goal will allow better understanding of TE speciation and, consequently, their bioavailability in natural waters of subarctic regions.

1.1.5. Podzols in boreal zone

Podzolic soils (also known as spodosols) are characteristic for cool and humid boreal regions, notably, the taiga zone. The vegetation of podzols consists largely of coniferous trees, which are well adapted to this climate. Podzols are typically found on siliceous or silicate coarsely textured base-poor parent materials such as sands and sandy tills, often in Precambrian Shield granitic/gneissic environments (Lundström et al., 2000a). The name of these soils is derived from the Russian words *pod* (under) and *zola* (ash), because their eluvial E-horizon has a grey-ash colour.

The soil profile (Fig. 1.3) is designated by the letters O (uppermost organic horizon), A (topsoil), E (eluvial soil), B (subsoil) and C (weathered parent rock). In

some podzols, the E horizon is absent, being either masked by biological activity or obliterated by disturbance. Podzols with little or no E horizon development are often classified as brown podzolic soils. The E horizon, which is usually 4-8 cm thick, is low in Fe and Al oxides and humus. It is found under a layer of surface organic material (acidic plant litter) undergoing the process of decomposition (O horizon which is usually 5-10 cm thick). Plant material decomposition releases organic acids that mix with carbonic acid in rainwater and then percolate into the soil in the form of small size organic molecules and colloids (1-10 kDa). In the underlying mineral layer these acids cause the dissolution of silicates, removing iron and aluminium thus forming mineral Fe-Al-colloids. Cation lixiviation in this horizon leads to bleaching, whereas OM-colloids of plant litter degradation transform into Fe-Al-colloids and Fe-Al-OM-colloids often identified in interstitial soil solutions (i.e., Pokrovsky et al., 2005a). It was shown recently (Lundström et al., 2000a) that very high concentrations of dissolved organically-complexed Fe and Al are present in the organic surface layer (O horizon) in podzols. Undergoing microbiological decomposition, mobile cations are washed out of the soil, but aluminium and in the lesser degree iron are accumulated in the underlying horizon together with humus thus producing aluminium-rich solid horizon (Al(OH)_3) and large-size organo-ferric colloids (Fe-OM). These colloids contribute significantly to the trace metal load of surface waters especially when they are flushed from the upper soil layers into the stream by rising water levels during spring flood and heavy rains (Andersson et al., 2006; Björkvald et al., 2008). Other possibility of colloids formation is a Fe-oxyhydroxide phase present in boreal streams and rivers, which is formed from anoxic groundwaters reaching surface waters during the low tide in winter and summer.

Podzols in Russia were first described by Dokuchaev V.V. in 1880, and then followed by Georgievsky (1888), Glinka (1932), Ponomareva (1964), Perelman (1974). Elsewhere, the formation of podzols was described in numerous reviews and books of European researchers (e.g., Muir, 1961; Anderson et al., 1982; Buurman, 1984; Righi and Chauvel, 1987; Lundström, 1993; Courchesne and Hendershot, 1997; Lundström et al., 2000a; Buurman and Jongmans, 2005).

In northern Europe, notably, in Sweden and Finland, a number of recent works addressed mineralogical and major and trace element composition, and provided the calculation of weathering losses of podzols and spodosols developed on granite-gneiss

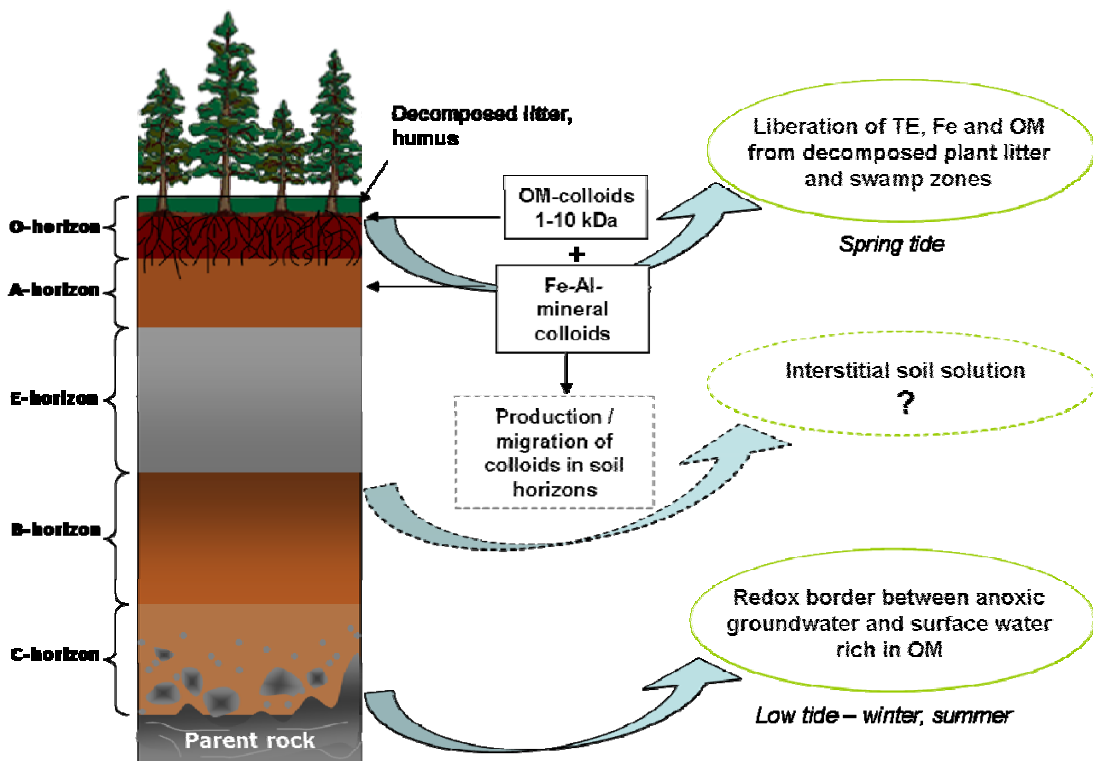


Fig. 1.3. Schematic representation of a typical podzol soil of the boreal forest.

glacial moraine deposits typical for this zone (Olsson and Melkerud, 2000; Öhlander et al., 1996, 2003; Land et al., 1999a, 1999b, 2002; Giesler et al., 2000; Land and Öhlander, 2000; Melkerud et al., 2000; Tyler, 2004; Starr and Lindroos, 2006). In particular, Lundström et al. (2000b) reported results of a multidisciplinary study combining geochemical, mineralogical, micromorphological, microbiological, hydrochemical and hydrological investigations, aimed at testing existing theories on the formation of podzols and acquiring better understanding of the fundamental mechanisms of this process. Weathering release rates of heavy metals (Cd, Cu, Ni, Pb and Zn) were calculated for a Haplic podzol in eastern Finland by Starr et al. (2003). Clay mineralogy and chemical weathering of soils in a recently deglaciated environment in Arctic-Alpine Sweden were studied by Allen et al. (2001). Also, chemical and mineralogical composition of soils developed on hard (i.e., nepheline syenite, amphibolite, metamorphized diabase) rocks influenced by granitic moraine depositions in the NW Russia was recently reported by Lesovaya et al., 2008. However, there is still a lack of studies addressing the issue of the soil formation process on mafic rocks and related river hydrochemistry in these particular environments under glacial deposits,

especially introducing a multidisciplinary approach (e.g., using mineralogical, chemical and isotope investigations).

1.1.6. Role of chemical weathering in elements transport to the oceans and associated CO₂ consumption

During two last decades, significant attention has been paid to study of major chemical composition of rivers with regard to the consumption of atmospheric CO₂ by chemical weathering of rocks. Chemical weathering of crustal rocks is considered to be one of the principal processes controlling the geochemical cycle of elements at the Earth surface (Viers et al., 2007). It controls the chemical and physical properties of the soil being the major chemical process by which soils are generated. Within the different reservoirs (continent, ocean, and atmosphere) chemical weathering is the major source of elements delivered by rivers to the oceans (Martin and Whitfield, 1983; Viers et al., 2007). This natural phenomenon involves consumption of atmospheric and/or endogenous carbon dioxide and metals leached from the rocks, these latter being released to rivers and shallow groundwaters and finally discharged into the ocean. Moreover, as chemical weathering consumes a greenhouse gas, it is likely to strongly influence the evolution of the Earth's climate over a long period of time.

Boreal regions can potentially play a major role in regulation of the CO₂ content in the atmosphere due to the chemical weathering of important surface of rocks and carbon sinks. Indeed, these zones have large territories of surfaces exposed to weathering and are covered both by organic-rich soils of the permafrost type and wetland zones which constitute an important sink of carbon (Botch et al., 1995). The circumpolar boreal biome⁷ is one of the world's largest biomes, covering $\sim 20 \times 10^6$ km², which constitutes $\sim 13\%$ of the earth's surface, and containing ~ 800 Pg (800×10^{15} g) of carbon in biomass, detritus, soil, and peat carbon pools (Apps et al., 1993; Dixon et al., 1994).

⁷ **Biome** is a climatically and geographically defined area of ecologically similar climatic conditions such as communities of plants, animals, and soil organisms, and are often referred to as ecosystems. Major terrestrial biomes include tropical rain forest, northern coniferous forest, tundra, desert, grassland, savanna, and chaparral.

In order to acquire better understanding of the process of continental erosion and evolution of climate, numerous works on chemical weathering balance and consumption of CO₂ have been conducted at the global scale (Berner et al., 1983; Meybeck, 1987; Ludwig et al., 1998; Gaillardet et al., 1999; Dessert et al., 2003), as well as at the scale of large river basins like Amazon (Gaillardet et al., 1997) or Congo (Gaillardet et al., 1995), and small catchments (Zakharova et al., 2005, 2007).

Garrels and MacKenzie (1971) have shown that only silicate rock weathering consume the atmospheric CO₂ during long-term carbon cycle. In this context, basic rocks dominated watersheds are useful to investigate since, among the rocks of volcanic origin, they are particularly important for regulating the long-term CO₂ cycle (Dessert et al., 2003). Many previous works were dedicated to the estimation of mechanical erosion, chemical weathering rates and associated atmospheric CO₂ consumption rates for basaltic rocks using river chemical composition (Louvat and Allègre, 1997, 1998; Dessert et al., 2001; Pokrovsky et al., 2005b; Rad et al., 2006). The effect of basalt rock crystallinity, secondary minerals formation, rock age, vegetative/glacial cover, and runoff on fluxes of dissolved elements to the ocean in Southwest Iceland were thoroughly studied by Gislason et al. (1996) and Stefansson and Gislason (2001).

Karelia and Kola provinces (NW Russia) considered in the present work, offer a possibility of studying the weathering of the coexisting mafic (e.g., olivinite, gabbronorite) and felsic (e.g., gneiss, granite) rocks. The region is characterised by abundant presence of glacial moraine deposits. Different genetic moraine types of a similar composition for this region were determined in Finland, and their geochemistry, mineralogy and morphology were studied in several works (Peuraniemi, 1982; Peuraniemi et al., 1997 and references therein; Sarala, 2005), e.g., ground moraine, Rogen moraine, Pulju moraine, Sevetti moraine, Kianta moraine, De Geer moraine etc. according to the classification given by Hättestrand (1997). Land et al. (1999) and Land and Öhlander (2000) estimated chemical weathering and erosion rates of granitic till in northern Sweden, and Thorn et al. (2006) calculated weathering rates of surficial pebble in this zone. Also, Akselsson et al. (2006) studied the relations between elemental content in till, mineralogy of till and bedrock mineralogy in southern Sweden in order to find a mechanism that controls the mineralogical composition of till. However, investigations devoted to weathering of mafic rocks under glacial moraine deposits in

boreal zone, as well as soil formation process on these rocks, are still poorly documented in the literature.

Thus, the third part of the present work is aimed at improving our knowledge of weathering of mafic silicate rocks in boreal climate and peculiarities of the soil forming process over these rocks influenced by glacial moraine deposits, especially in view of the importance of this type of rocks in the atmospheric CO₂ regulation. For this, we used a multidisciplinary approach combining physico-chemical, isotopic and mineralogical investigations of rocks, soils and related surface waters.

1.2. Description of the region

1.2.1. Characteristics of the boreal zone

The study of pristine river geochemistry, apart of some undeveloped tropical regions and temperate areas of the southern hemisphere, has a tendency to be more and more limited to the subarctic regions. The boreal zone's remoteness and harsh winter climate have led to much of it being sparsely populated by people. Although not completely isolated from anthropogenic influence, the subarctic environments are relatively pristine which is significant for the studies of basic biogeochemical mechanisms operating in the terrestrial biosphere.

Covering most of inland Russia (especially Siberia), Sweden, Finland, Norway, Alaska and Canada, as well as parts of the extreme northern continental United States, northern Kazakhstan and Japan (Fig. 1.4), the **taiga** or **boreal forest** is the world's largest terrestrial biome extending throughout the middle and high latitudes (from 55°N up to the North Pole Circle) (Sayre, 1994).

Taiga zone has a harsh continental climate with a very large temperature range between summer and winter varying from -50°C to 30°C throughout the whole year. Aside from the tundra and permanent ice caps, it is the coldest biome on Earth. The zone experiences relatively low precipitation throughout the year (300-850 mm annually on average), primarily as rain during the summer months, but also as fog and snow; as evaporation is also low for most of the year, precipitation exceeds evaporation and is sufficient for the dense vegetation growth (Sayre, 1994). The forests of the taiga are largely coniferous, dominated by larch, spruce, fir, and pine, but some broadleaf trees also occur, notably birch, aspen, willow, and rowan.

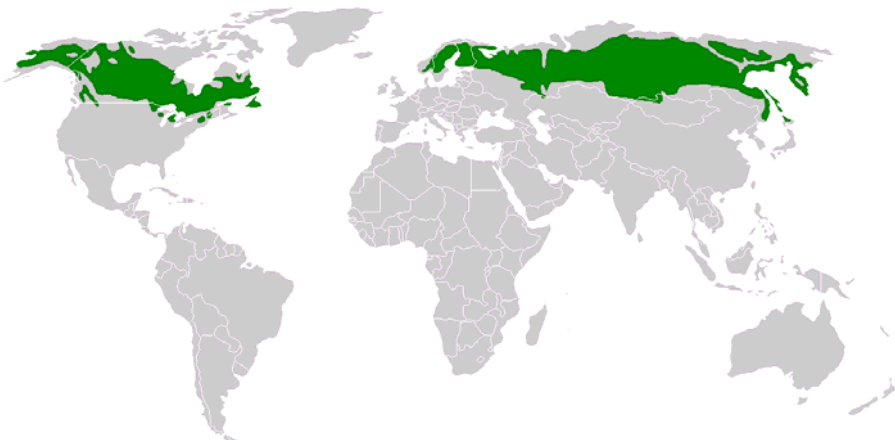


Fig. 1.4. Geographical distribution of the taiga zone (after the Köppen-Geiger climate classification world map) corresponding to “Dfc” and “Dfd” zones (<http://fr.wikipedia.org/wiki/Image:Taiga.png>).

Rocks of the NW Russia boreal zone are very heterogeneous and presented by Archean granites, basalts, ultramafic rocks. Much of the area was glaciated about 10-15 thousand years ago. As the glaciers receded, they left depressions that have since filled with water, creating lakes and bogs (especially muskeg⁸ soil). Elsewhere the rocks are covered by granitic moraine released by glaciers in retreat.

Boreal soils tend to be geologically young and poorly developed varying in depth from 30-40 cm in the north to 60-85 cm in the south and mostly presented by podzols in the European zone. They tend to be acidic due to the decomposition of organic materials (e.g., plant litter) and either nutrient-poor or have nutrients unavailable because of low temperatures (Sayre, 1994).

1.2.2. Study site

The difficult and costly access to the Central and Eastern Russian Arctic has hampered progress in understanding the geochemistry of boreal zones. Hence, the more easy accessible small catchments of the White Sea basin are of interest since they may be representative of extensive zones of the Russian Arctic.

⁸ **Muskeg** is a soil type (also a peatland or wetland type called a bog) common in arctic and boreal areas. Muskeg itself consists of dead plants in various states of decomposition (i.e., peat), ranging from fairly intact sphagnum moss, to sedge peat and highly decomposed muck.

A part of the boreal region considered in this work is situated between latitudes 67°N and 63°N and longitudes 30°E and 36°E in North-Western part of Russia around the White Sea which constitutes a part of the Arctic Ocean. Sites where sampling campaigns were held are indicated on the map (Fig. 1.5). Several series of water, soil and rock samples were taken during extensive field campaigns in summer period around a mountain range Vetreny (Windy – in English) Belt (1) and in Paanajarvi national park around the Kivakka layered intrusion zone (2).

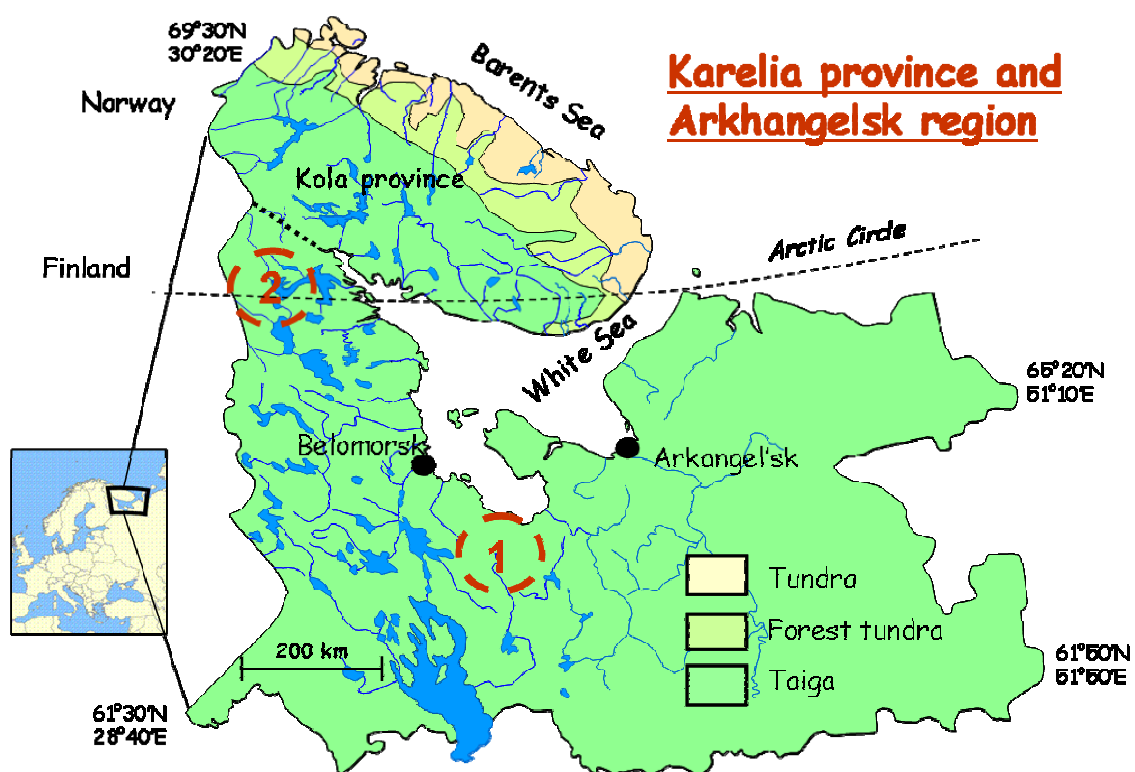


Fig. 1.5. Map of the White Sea with the studied Vetreny Belt paleorift zone (1) and Kivakka intrusion zone (2).

Four main factors were determinant for choosing the sites:

- Small Karelian rivers can be representative of the extensive zones of the Russian Arctic;
- These zones due to their limited accessibility and absence of anthropogenic load can be considered as pristine with natural levels of elements concentrations in water and soil;

-
- Karelia and Kola provinces (NW Russia) offer a possibility of studying the weathering of the geographically coexisting mafic (e.g., olivinite, gabbro-norite, peridotite) and felsic (e.g., gneiss, granite) rocks;
 - There is a strong geological and petrological background acquired by Russian colleagues of more than 20 years study of Vetreney Belt and Kivakka intrusions.

In the south-eastern part of the Baltic Shield, three large early Precambrian lithotectonic units are juxtaposed, comprising an Archean amphibolite-gneiss-migmatite and granite-greenstone unit and a Lower Proterozoic volcanic-sedimentary unit. The Archean units are volumetrically dominant. They constitute the Karelian granite-greenstone terrain, which occupies a total area of ca. 350,000 km² (Puchtel et al., 1997). The area around one of the large belts, the early Proterozoic Vetreney Belt (~2.5 Ga, Puchtel et al., 1997), situated on the territory of Arkhangelsk and south-eastern Karelian regions and composed entirely of komatiitic basalts, is the subject of this study. The belt can be traced from Lake Vyg south-eastward over a distance of more than 250 km (Kulikov, 1988).

Another studied site is situated in the northern part of Karelia in Paanajarvi national park, eastern Baltic Shield. The Polar Circle is just several kilometers from its northern boundary. Paleoproterozoic layered intrusions (~2.5 Ga, Amelin and Semenov, 1996) and associated mafic dykes occurring within granitic gneisses are widespread over this zone. The considered in this study zone is situated around the Kivakka intrusion which belongs to the Olanga group of layered peridotite-gabbro-norite intrusions hosted by migmatized biotite and amphibole gneisses, granite-gneisses, and granodiorite-gneisses of Late Archean age (Bychkova et al., 2007). More detailed geomorphological description of the chosen sites is presented in corresponding chapters.

1.3. Objectives and scope of the study

This study is aimed at improving our understanding of the weathering processes of mafic silicate rocks and trace element speciation and migration in specific conditions of a boreal environment.

The main objectives of the study are:

1. To describe the partition of elements between basic and acid rocks and soils formed after the last glaciation period, and to characterize the mechanisms governing the chemical weathering and mineral formation in subarctic zone;
2. To recognize the factors responsible for the chemical composition of surface water of boreal high latitude river basins and to assess the role of the rock lithology (granitic environment versus basaltic) in TE speciation and organo-mineral colloids formation;
3. To reveal the pH-dependence of TE speciation in order to predict possible changes in elements bioavailability in natural subarctic waters due to their acidification caused by local anthropic pressure or the global climate warming.

The main originality of the thesis is to combine, for the first time on the same natural objects, the geochemical, isotope, physico-chemical and mineralogical techniques to better understand the factors that control biogeochemical cycling of elements in the subarctic region. It is anticipated that the knowledge gained in this study should provide a basis for a possible evaluation of the impact of climate warming on boreal environments.

1.4. Thesis organisation

The manuscript is composed of the main thesis based on publications, submitted or in preparation, addressing the above mentioned objectives, and the supplementary information which comprises several extended annexes presenting analytical results.

The principal part of the manuscript comprises four chapters considering the issue of geochemical behaviour and forms of migration of elements in subarctic zone, including a comparative study of chemical alteration process in basaltic versus granitic environments and its effect on chemical fluxes of elements in surficial fluids:

- **Chapter 2: Chemical weathering of mafic rocks in boreal subarctic environment (North-West Russia) under glacial moraine deposits.** This chapter is organised in form of a manuscript (Vasyukova et al., 2008a, in preparation) and aimed at studying geochemical migration and partition of major and trace elements between rock and soil reservoirs during chemical weathering

process. Notably, we describe the soil forming process on mafic rocks under strong influence of glacier moraine, and related rivers hydrochemistry, and give characteristics of specific features for the estimation of mafic rocks weathering rates in view of the importance of weathering of these rocks in atmospheric CO₂ consumption.

- **Chapter 3: Trace elements in organic- and iron-rich surficial fluids of boreal zone: Assessing colloidal forms via dialysis and ultrafiltration.** This part contains a publication (Vasyukova et al., 2008b, submitted to *Geochimica et Cosmochimica Acta*) which is aimed at quantitative characterization of trace elements speciation in pristine, organic-rich rivers and surface waters belonging to the White Sea basin (Karelian region). The role of colloidal status of elements in their transport with water flows is addressed. In this work we compare two contrasting techniques, dialysis and ultrafiltration, both used for the assessment of the elements speciation in water, and study the role of the rock lithology (granitic environment versus basaltic) in colloids formation and their chemical nature;
- **Chapter 4: Experimental study of trace elements complexation with natural organo-mineral colloids using dialysis.** This chapter, also organised in form of a manuscript (Vasyukova et al., 2008c, in preparation), describes the results of a number of experiments conducted with natural surface waters at different pH using the equilibrium dialysis technique. In this work we evaluated the complexation of trace elements with natural organo-mineral colloids present in boreal surface waters and quantified empirical distribution coefficients of TE between dissolved (<1 kDa) and colloidal (1 kDa – 0.22 µm) pools. TE complexation with OM colloids was described using the Visual MINTEQ (NICA-Donnan) humic ion model. Quantification of proportion of trace elements in colloidal form in solution as a function of pH carried out in this study should contribute to the prediction of water acidification phenomena expected to be mostly pronounced in the Arctic due to global climate warming;
- In **Chapter 5, conclusions** of the principle results are given and **perspectives** of further research are proposed.

Chapter 2

Chemical weathering of mafic rocks in boreal subarctic environment (North-West Russia) under glacial moraine deposits



E.V. Vasyukova, P. Oliva, J. Viers, F. Martin, O.S. Pokrovsky, B. Dupré

In preparation for *Chemical Geology*

Chemical weathering of mafic rocks in boreal subarctic environment (North-West Russia) under glacial moraine deposits

E.V. Vasyukova^{1,2}, P. Oliva¹, J. Viers¹, F. Martin¹, O.S. Pokrovsky¹, B. Dupré¹

(in preparation for *Chemical Geology*)

¹ *Laboratory of Mechanisms and Transfers in Geology (LMTG, UMR 5563), University of Toulouse,
OMP-CNRS; 14, avenue Edouard Belin, 31400 Toulouse, France,*

² *Saint-Petersburg State Polytechnic University, 29, Polytechnicheskaya st., Saint-Petersburg, Russia*

Keywords: chemical weathering, mafic rocks, natural waters, boreal zones.

Abstract

This work addresses geochemical migration and the partitioning of major and trace elements between rock and soil reservoirs during chemical weathering. In particular, we investigate soil forming processes on mafic rocks under the influence of glacial moraine in the North-Western Russia (Kivakka and Vetreny Belt mafic intrusions hosted within crystalline granitic rocks). To accomplish this we analyzed 5 samples of mafic and felsic rocks, 10 soil profiles, 24 surface waters and 3 soil solutions. A multidisciplinary approach has been used, and includes major and trace element chemical analysis, Sr and Nd isotopic measurements, and mineralogical investigations. Quaternary (Pleistocene) deposits observed in the deepest horizons of some soil profiles confirm a strong moraine influence in this region. As a result, despite of the mafic nature of parent rocks, most soils show podzolic features. Furthermore, chemical and Sr isotopic analyses reveal a strong influence of moraine to the soil chemistry and mineralogy. Mineralogical studies show the presence of non-aeolian quartz and zircon in soils which are not linked to the nature of the parental rocks (i.e., mafic and felsic). At the same time, the presence of etch pit corrosion on the surface of zircons and feldspars, and a newly-formed matter adjacent to the surface of primary phases was revealed. The chemical index of alteration (CIA) showed no or weak weathering for soils in the studied region, and the use of invariant elements to quantify the weathering processes was impossible. The composition of most surface waters reflects the weathering of silicate rocks (dissolved load TDS is between 10 and 30 mg/l)

but does not allow purely granitic and purely basic source rocks to be distinguished. Relative enrichment in Na with respect to Ca and Mg in rivers compared to rocks from both granitic and basaltic watersheds is observed. This suggests that either Mg-vermiculite formation and CaMg-amphibole preservation in soils limits Ca and Mg export in waters, or that there are highly weatherable Ca- and Mg-rich minerals present in granitic rocks. Alternatively, due to the influence of granitic moraine fraction in this zone, it is also possible that it enriched the soil with Na-rich phases. Consequently, two hypotheses can be invoked to explain the soil pedogenesis and chemical weathering in the studied zone: i) weathering process occurred before the last glacier period (10-20 Ky ago) or ii) contemporary weathering mechanisms of basic rocks coupled with strong moraine influence are operating. Our results favour the second scenario.

According to our calculations, the weathering rates of ultramafic rocks are higher than those for the granitic till, but dominated moraine depositions in this region hide the evidence of a real weathering process. Values estimated for the olivinite rock appear to be lower than the weathering rates estimated on the basis of surface water fluxes for Karelian and Siberian mafic rocks in previous works. Retention of Mg and Ca in soil due to precipitation of secondary phases such as Mg-vermiculite or process of adsorption on mineral, organic or organo-mineral phases, can serve as an explanation of this discrepancy.

2.1. Introduction

Knowledge of chemical weathering is fundamental to the successful analysis of important environmental issues such as acidification of soils and global warming. Numerous works have emphasized the significant role of silicate weathering in atmospheric CO₂ consumption and climate regulation, being considered to be the principal process of removing carbon dioxide from the atmosphere on long time scales (Berner et al., 1983; Brady, 1991; Berner et al., 1992, 1995; Berner and Maasch, 1996; Boeglin and Probst, 1998; Gaillardet et al., 1999; Kump et al., 2000; Berner and Kothavala, 2001; Dessert et al., 2003; Dupré et al., 2003; Pokrovsky et al., 2006). Weathering of continental basalts, accounting for about 30% of CO₂ total consumption by the silicate weathering (Dessert et al., 2003), has been recently addressed in several studies (Gislason et al., 1996; Louvat and Allègre, 1997, 1998; Dessert et al., 2001;

Grard et al., 2005; Pokrovsky et al., 2005). In contrast, very few investigations deal with the impact of chemical weathering on soil formation and CO₂ consumption in the environment underlain by intrusive mafic rocks such as gabbros and olivinite (Schroeder et al., 2000). There are relatively few studies of comparative weathering intensity of acidic versus basic silicate rocks at the catchment scale. Notably, in Karelia and Kola provinces (NW Russia), cationic weathering fluxes estimated from river water chemical compositions and daily discharges are among the lowest in the world : TDSc = 0.33 and 2.3 t/km²/yr for granite and basaltic watershed respectively (Zakharova et al., 2007). Surprisingly for mafic rock dominated watersheds, the Baltic Shield values are only half the value calculated for central Siberian basalt (~5 t/km²/yr, Pokrovsky et al., 2005) given similar runoff but larger average annual temperature differences (+1 ± 2°C in Karelia versus -9 ± 2°C in Central Siberia). Such a disagreement does not allow reliable extrapolation of widely used “temperature – basic rocks weathering intensity” relationship (Dessert et al., 2003) to specific subarctic environments both at present and in the past. Therefore, studying the weathering mechanisms at the soil and small catchment scales is necessary to explain this difference and to reveal the factors responsible for slower weathering rates under specific environmental conditions of the NW Russia.

In contrast with the West European environments lying at the Baltic sea cost in a relatively mild climate, the understanding of the geochemistry of ecosystems situated at the Arctic sea coast, including the White sea, still remains quite poor. Karelia and Kola provinces (NW Russia) belonging to this zone, offer a possibility of studying the weathering of the coexisting mafic (e.g., olivinite, gabbro-norite) and felsic (e.g., gneiss, granite) rocks at a relative small and thus easily accessible space scale. The region is characterised by abundant presence of glacial moraine deposits. In Finland, different genetic moraine types were determined (e.g., ground moraine, Rogen moraine, Pulju moraine, Sevetti moraine, Kianta moraine, De Geer moraine etc. according to the classification given by Hättestrand (1997) and their geochemistry, mineralogy and morphology were studied in several works (Peuraniemi, 1982; Zilliacus, 1989; Peuraniemi et al., 1997 and references therein; Sarala, 2005). The chemical and mineralogical composition of moraine that covers the studied area (northern and

southern Karelia) suggest it was formed from of quaternary deposits of the Pleistocene age (Evdokimova, 1957; State Geological Map of Russian Federation, 2001).

Soil ages in this zone are supposed to be around 10 Ky. Indeed, following Thiede et al. (2001), Karelia and the Arkhangelsk region were ice sheet covered only during the late Weichselian glaciation phase (i.e., 17-15 ky). It is supposed that during this period soil erosion process was so important that almost all the soil cover disappeared, contrary to more southern regions (Salminen et al., 2008) where soil profile ages varies from 60 to 150 ky.

For cool and humid boreal regions, notably Taiga, podzolic soils are characteristic, as the conditions in this zone favour the development of an acid and deep organic surface layer. In Russia podzolisation process was first described by Dokuchaev V.V. in 1880, and then followed by Georgievsky (1888), Glinka (1932), Ponomareva (1964), Perelman (1974). Elsewhere, the formation of podzols was described in foreign reviews and books (e.g., Muir, 1961; Anderson et al., 1982; Buurman, 1984; Righi and Chauvel, 1987; Lundström, 1993; Courchesne and Hendershot, 1997, van Breemen and Buurman, 1998; Lundström et al., 2000, 2000a; Buurman and Jongmans, 2005). Podzols are typically found on coarsely textured base-poor parent materials such as sands and sandy tills, often in Precambrian Shield granitic/gneissic environments (Lundström et al., 2000). However, podzol type soil were also described in mafic and ultramafic environment under boreal climate (e.g., Lesovaya et al., 2008; Salminen et al., 2008; D'Amico et al., and references therein). The occurrence of podzol type soils over mafic rocks is also suggested in the World Reference Base for soil Resources (IUSS Working Group WRB, FAO, 2006), but, considering the most used taxonomic systems criteria, only few of those podzol type soil developed over mafic rock could be classified as true podzol. Indeed, even if the soils show a podzol like morphology (i.e., occurrence of an eluvial "albic" horizon overlying a reddish-brown illuvial "spodic" horizon), these soils pHs are usually too high compared to classic podzols (D'Amico et al., 2008). According to the last authors, in this particular case, the podzolisation processes is favoured by the occurrence of quartz-rich allochthonous material such as Aeolian deposit or till. The question of the role of moraine deposit in boreal podzol pedogenesis under granitic environment was also raised by a number of recent works devoted to the study of mineralogical and major and trace element composition (as well

as calculation of weathering losses) of podzols and spodosols developed on granite-gneiss glacial moraine deposits in northern Europe, i.e., in Sweden and Finland (Öhlander et al., 1991, 1996, 2003; Giesler et al., 2000; Melkerud et al., 2000; Olsson and Melkerud, 1989, 2000; Land and Öhlander, 2000; Land et al., 1999, 1999a, 2002; Tyler, 2004; Starr and Lindroos, 2006). Lundström et al. (2000a) reported results of a multidisciplinary study (combining geochemical, mineralogical, micromorphological, microbiological, hydrochemical and hydrological investigations) aimed at testing existing theories (adsorption/precipitation versus biodegradation mechanisms) on the formation of podzols in glacial till context. Clay mineralogy and chemical weathering of soils in a recently deglaciated environment in Arctic-Alpine Sweden was studied by Allen et al. (2001). The authors suggest that the occurrence of mixed layer minerals could be a tracer of parental rock weathering in soils affected by moraine deposits. On the contrary, Akselsson et al. (2006) found that there is no relation between elemental content and mineralogy of till and bedrock mineralogy for podzolic soil in southern Sweden and conclude that the information on the bedrock is not sufficient for prediction of the till mineralogy.

In the NW Russia, chemical and mineralogical composition of soils developed on nepheline syenite, amphibolite and metamorphized diabase affected by moraine deposition was recently studied by Lesovaya et al., 2008. These authors argued that soil profiles become thicker and show notable clay mineral transformation when allochthonous moraine material is admixed. However, despite of all those studies on soil formation and chemical weathering processes in boreal environment, there is still a lack of studies devoted to the soil forming process on mafic rocks and related river hydrochemistry under glacial moraine, especially introducing a multidisciplinary approach (e.g., using mineralogical, chemical and isotope investigations).

High concentrations of the dissolved organic matter ($<0.22\text{ }\mu\text{m}$) and colloidal status of the major part of trace elements is a particular feature of the boreal organic-rich river geochemistry (Ingri et al., 2000; Andersson et al., 2001, 2006; Pokrovsky and Schott, 2002; Dahlqvist et al., 2004, 2007; Pokrovsky et al., 2006a). It is thought to be partly the result of podzolisation processes (Giesler et al., 2000; Lundström et al., 2000a). In order to obtain more detailed information on the natural concentrations and transport of major and some trace elements in the studied region, a number of small and

medium rivers were sampled. Presented in this study data corroborate those previously published for the Karelian region (Pokrovsky and Schott, 2002; Feoksitov, 2004; Zakharova et al., 2007; Vasyukova et al., 2008, submitted). Our study is aimed to improve our understanding of mafic rocks weathering in boreal climate, especially in view of the fact that weathering of basic rocks is responsible for 30% of atmospheric CO₂ consumption. Towards this goal, we used a multidisciplinary approach which comprises study of geochemical migration and partition of major and trace elements between different reservoirs (rocks and soils), major and trace elements analyses, Sr and Nd isotopic measurements, and mineralogical investigations characterizing the rock weathering rates and related rivers hydrochemistry and peculiarities of soil forming processes on basaltic rocks in the boreal zone influenced by glacial moraine.

Our investigations were conducted on mafic and felsic rocks, soil and water samples collected within Kivakka (Olanga complex, northern Karelia) and Vetreny Belt (south-eastern Karelia) magmatic formations bounded with crystalline granitic rocks of the Archean age. The main open questions we attempted to answer in this study are: i) to which degree the presence of granite-gneissic moraine can modify the intensity of weathering of basic rocks in the boreal zone, and ii) can we assess the difference of different mafic rocks (gabbro, norites, peridotites, olivinites, and basalts) weathering features under the same environmental conditions (climate, vegetation).

2.2. Geological and geographical setting

Vetreny Belt paleorift and Kivakka layered intrusion are situated within the same geographical zone, Karelian region, with similar geological, climatic, and hydrological conditions. The main difference between two sites lays in the nature of mafic rocks: gabbro-norite (peridotite) of Kivakka and basalts with some olivinites of the Vetreny Belt.

2.2.1. Lithology, soils, and vegetation

Karelian region is situated in the north-western part of Russia, bordering Finland to the west, Lakes Ladoga and Onega to the south, and the White Sea – an extensive gulf of the Arctic Ocean – to the east. Largely a hilly plain, the region has mountains in the west with elevations up to 600 m. The lowest lands lie near the White Sea and the

many lakes that have filled the hollows scoured in the surface of the plain during the last glaciation period. The relief of Karelian zone was formed under the influence of this glaciation which occurred at least 3 times during Pleistocene (Reimann and Melezhik, 2001), and the last glacier disappeared about 20-10 thousand years ago.

The studied area is a part of the Eastern Fennoscandian Shield. A simplified map of the two chosen sites with sampling points and some geological information is given in Fig. 2.1. Quaternary deposits consist primarily of coarse-grained and sandy till or glaciofluvial deposits showing well-developed podzol profiles. Detailed information of the major and trace element composition of volcanic rocks and rock-forming minerals considered in this work was reported in numerous previous works: Amelin and Semenov, 1996; Koptev-Dvornikov et al., 2001; Bychkova, 2003; Bychkova and Koptev-Dvornikov, 2004; Bychkova et al., 2007 for the Kivakka layered intrusion; Kulikova and Kulikov, 1981; Ryabchikov, 1988; Puchtel et al., 1996, 1997; Kulikov, 1999; Kulikov et al., 2005 for the Vetryeny Belt; Lobach-Zhuchenko et al., 1986, 1993; Bibikova et al., 2005 for the Archaean granitic and tonalitic gneisses surrounding the chosen intrusions.

The main part of the studied zone belongs to the boreal taiga forest ecosystem with pine, fir, birch, ericaceous species and moss that cover more than 80% of the territory. Approximately 20% of the territory is covered by wetlands developed on a thick peat and gley-podzol soils. On well-drained territories alluvial-ferruginous-humic and alluvial-humic podzols prevail. They are developed under pine- and spruce-pine forests with moss-fruticulose cover. The soil depths in the region vary from 30-40 to 60-85 cm in the northern and southern part of Karelia, respectively. On the hill tops (100-200 m), soils depths do not exceed 10-20 cm. Ferruginous podzols are remarkable for high acidity, especially in superficial horizons (Lundström et al., 2000a and references therein).

Soils are partly developed on a glacial granite moraine which consists mainly of sand and loamy sand with gravel and boulder inclusions. The glacio-lacustrine and lacustrine as well as fluvio-glacial deposits in the form of lenses are also wide spread (Zakharova et al., 2007).

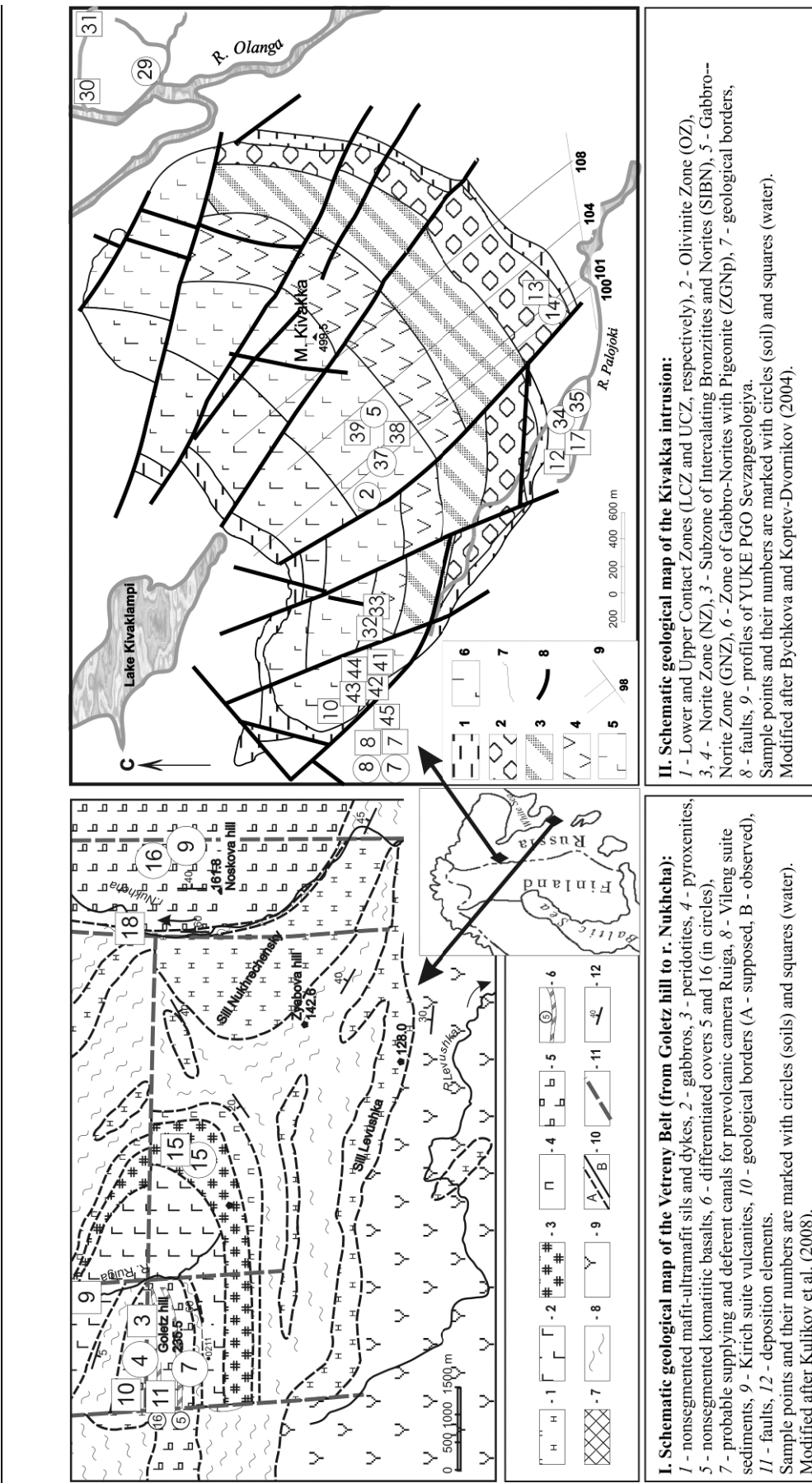


Fig. 2.1. Map of the studied areas Vetrynny Belt (left) and Kivakka intrusion (right) showing soil (circles) and water (squares) sample points and geological situation.

2.2.1.1. Vetreny Belt paleorift

Vetreny Belt ($63^{\circ}46'N - 35^{\circ}48'E$) (Fig. 2.1, left) is situated in the south-eastern part of the Baltic Shield, on the territory of the south-eastern Karelia and Arkhangelsk region. It occupies a territory of approximately 5200 km^2 and can be traced from Lake Vyg southeastward over a distance of more than 250 km. Its width increases from 15 to 85 km to the southeast, where it plunges beneath the Paleozoic cover of the Russian platform and extends further southeast (Kulikov et al., 2003). Detailed description of the Vetreny Belt suite is given by Puchtel et al. (1997) who also supposed that massifs like Kivakka layered intrusion have a related origin to the Vetreny Belt volcanic and plutonic rocks. Vetreny suite consists entirely of a thick unit of basaltic komatiites and belongs to the Sumian and younger groups in the area (Kulikov and Kulikova, 1982). The isotopic dating of the Vetreny belt yielded the following values: $2449 \pm 35 \text{ Ma}$ and $2410 \pm 34 \text{ Ma}$ (Sm-Nd), $2424 \pm 178 \text{ Ma}$ (Pb-Pb), $2437 \pm 4 \text{ Ma}$ (U-Pb) (Puchtel et al., 1997).

2.2.1.2. Kivakka layered intrusion

The Kivakka pluton ($66^{\circ}12'N - 30^{\circ}33'E$) (Fig. 2.1, right) is located in northern Karelia and belongs to the complex of layered peridotite-gabbro-norite intrusions of the Olanga group, which are hosted by migmatized biotite and amphibole gneisses, granite-gneisses, and granodiorite-gneisses of Late Archean age (Lavrov, 1979; Amelin et al., 1995). In addition to Kivakka, the group includes the Lukkulaisvaara and Tsipringa massifs (Shmygalev, 1968; Lavrov, 1979; Klyunin et al., 1994; Semenov et al., 1995; Amelin and Semenov, 1996), all of which are spatially restricted to an east-west trending regional fault zone and compose the eastern branch of an extensive belt of layered massifs, whose western branch continues across Finland (Alapieti, 1982). Detailed geological and petrological description of the Kivakka layered intrusion is given elsewhere (Koptev-Dvornikov, 2001). The isotopic dating of the massif yielded the following values: $2420 \pm 23 \text{ Ma}$ (Sm-Nd), $2445 \pm 3.4 \text{ Ma}$ (Zr) and $2444 \pm 1 \text{ Ma}$ and $2445 \pm 2 \text{ Ma}$ (Amelin and Semenov, 1990, 1996; Barkov et al., 1991; Balashov et al., 1993).

2.2.2. Climate and hydrology

The climate of the most of the territory is mild-cold, transitional between oceanic and continental, with a determinant influence of the Arctic and Northern Atlantics. Snow period lasts from October to April-May with the thickness of snow cover ranging from 70 up to 110 cm. Mean annual temperature is close to 0°C but extremes can reach +35° to -35°C in summer and winter periods, respectively. Mean precipitation amount is between 400 and 600 mm/yr.

The region has a well-developed river network that flows via a system of glacial lakes. Chemical composition of river water in Karelia is determined by the chemical weathering of silicate parent rocks of the Baltic crystalline shield and quaternary deposits, and the presence of numerous peatlands. Typical values of total discharge of solids (TDS) for this region are 15-30 mg/l (Maksimova, 1967; Zakharova et al., 2007), and the concentration of river suspended matter is very low.

The studied region can be considered as pristine, although the influence of Kola peninsula smelters can be pronounced via long-range atmospheric pollution (i.e., de Caritat et al., 2001).

2.3. Materials and methods

2.3.1. Sampling of rocks, soils, surface waters and soil pore waters

A list of soil, water and soil water samples and their bedrock composition is presented in Table 2.1. For both soils and waters, series named “V” and “K” correspond to samples taken within the Vetreny Belt paleorift, and Kivakka layered intrusion zones, respectively. Three altered rock samples – an Archean granite, basalt and peridotite – were taken within the Vetreny Belt intrusion zone, and two other basic rocks – gabbro-norite and olivinite – were taken from Kivakka layered intrusion in order to investigate the formation of secondary phase minerals in the thin sections.

Ten soil profiles, five from each studied site (Vetreny Belt and Kivakka intrusion) and five on each type of supposed parent rocks (basic or acidic), were sampled for pedological, mineralogical and chemical analysis (see Table 2.1 for description and Table 2.2 for chemical composition of soils). Most of soils exhibit podzolic features. Considering their depth and horizon succession, V-15, V-9 and K-29 can be classified as regosol (WRB, 2006). All the other soil profiles belong to podzol

(WRB, 2006) with the exception of the V-4 and K-14 soil profiles which, despite of the occurrence of an albic horizon, do not show a true spodic horizon (i.e., pH H₂O > 5.9). In the following of this work, the V-4 and K-14 soils will be named as podzol even if they do not match with the WRB criteria. The soil K-8 shows features of orstein within the spodic horizon and the deepest horizon of the K-14 soil profile is lithochromic.

Small and large rivers, as well as several wetlands and soil pore waters draining basic and granitic rocks were sampled during extensive field campaigns in July-August 2004, February 2006 and July 2006 for dissolved major and trace elements contents. Three types of water were chosen for this study: river and swamp water, and soil solutions draining both granitic and basaltic rocks (see Table 2.1 for description and Table 2.3 for chemical composition of waters).

2.3.2. Analytical techniques

2.3.2.1. Mineralogical and chemical analysis of rocks and soils

Mineralogical studies on altered rock material were made on polished consolidated thin sections using optical microscopy, scanning electron microscopy (SEM GEOL 6360LV coupled to EDS PGT SDD SAHARA) including X-ray microanalysis, and electron microprobe analysis (CAMECA SX50). Modal composition of the different altered rock samples was calculated by using structural formulae of minerals and chemical composition of parental rocks and was coupled with SEM information. Analysis of clays in the soil sample K-14 (C horizon) was performed by transmission electron microscopy (TEM) in laboratory CRMCN, UPR7251, Paul Cézanne University, Aix-Marseille III, France.

The individual composition of soil minerals was determined by SEM with EDS on soil grain thin sections. Afterwards, a structural X-ray diffraction analysis (XRD) was performed on soil clay fractions. Clay fraction (i.e., <2 µm grain size) was separated by sedimentation in water column. For further structural XRD analysis performed on INEL G3000 Cu K_{α1,α2}, oriented samples were prepared by depositing a drop of <2 µm suspension on a glass plate and drying it at room temperature. Standard treatment (H₂O, ethylene glycol, and heating at 500°C) was employed to assess the interlayer distances of clay minerals.

Table 2.1. Soils and surface waters studied and their bedrock composition. Sample series from Vetreny Belt paleorift and Kivakka intrusion are defined as "V" and "K", respectively. Samples marked with "w" correspond to surface waters and with "ss" - to soil solutions.

Sample no.	Description	Bedrock composition
Soils		
V-4	Podzol	Komatiitic basalts, glacial deposits
V-7	Podzol	Komatiitic basalts, glacial deposits
V-9	Regosol	Gneisses, glacial deposits
V-15	Regosol	Peridotites
V-16	Podzol	Gneisses, glacial deposits
K-7	Podzol	Gneisses, glacial deposits
K-8	Podzol	Gneisses, glacial deposits
K-14	Podzol	Olivinite
K-29	Regosol	Gneisses, glacial deposits
K-37	Podzol	Gabbro-norites
Waters		
V-3-w	Surface water	Basalt
V-9-w	r. Ruiga	Basalt
V-10-w	Surface water from basalt field	Basalt
V-11-w	Surface water from basalt field	Basalt
V-12-w	r. Ruiga, upstream biofilms	Basalt
V-13-w	r. Ruiga, highest upstream	Basalt
V-15-w	Creek over ultramafites	Ultramafites
V-18-w	r. Nukhcha	Basalt
K-7-w	r. Palajoki, tributary	Gneisses, glacial deposits
K-8-w	Subsurface flow (right bank of the r. Palajoki)	Gneisses, glacial deposits
K-10-w	Swamp (corresponds to K-43 and K-44)	Gabbro-norites
K-12-w	Spring from a swamp	Gneisses, glacial deposits
K-13-w	River over olivenites	Olivinite
K-17-w	Subsurface flow	Norites
K-30-w	r. Vartalambina downstream	Gneisses, glacial deposits
K-31-w	r. Vartalambina upstream, tributary	Gneisses, glacial deposits
K-32-w	Swamp	Gabbro-norites
K-33-w	Stream	Gabbro-norites
K-38-w	Swamp	Gabbro-norites
K-39-w	Swamp	Gabbro-norites
K-41-w	r. Molodilny (springing from swamp)	Gabbro-norites
K-43-w	Swamp	Gabbro-norites
K-44-w	Swamp	Gabbro-norites
K-45-w	r. Palajoki	Gneisses, glacial deposits
Soil solutions		
V-16-ss	Soil water	Peridotites, olivinites
K-5-ss	Soil solution	Gabbro-norites
K-35-ss	Soil solution	Norites

Table 2.2. Chemical analysis of the bulk fraction and Rb-Sr and Sm-Nd isotope data for soils from Vetreny Belt (V) and Kivakka layered intrusion (K). Values are expressed in wt % of oxide for major elements, and in ppm for trace elements. Here, TOC signifies total organic carbon; LOI – lost on ignition; ND – not determined; γ – granitic substratum; β – basaltic substratum; P – peridotite; Ol – olivinite; N – norite; G-n – gabbro-norite. ϵ_{Nd} is calculated using ratios $^{143}\text{Nd}/^{144}\text{Nd}=0.51264$ and $^{147}\text{Sm}/^{144}\text{Nd}=0.1966$ for present-day CHUR.

Sample	V-4	V-7		V-9		V-15
Parent rock	β	β	β	γ	P	
Horizon	E	E	B	O	A	O/A
Depth, cm	0-5	8-17	20-35	0-6	6-12	2-4
pH	6.21	4.41	4.58	3.43	4.30	5.07
% wt						
TOC	0.71	5.50	2.22	42.11	10.40	6.10
SiO ₂	82.00	68.22	68.10	2.71	55.71	40.09
Al ₂ O ₃	8.67	10.74	12.04	0.58	6.84	5.06
Fe ₂ O ₃	0.83	1.48	3.87	0.34	4.98	10.70
CaO	1.28	1.82	2.11	0.51	4.71	6.63
MgO	0.25	0.70	1.52	0.16	3.38	20.53
Na ₂ O	2.45	2.77	2.89	0.08	1.39	0.42
K ₂ O	1.61	1.88	1.85	0.15	0.54	0.10
TiO ₂	0.42	0.46	0.47	0.04	0.73	0.31
MnO	0.02	0.03	0.04	0.02	0.09	0.26
P ₂ O ₅	0.02	0.14	0.10	0.17	0.23	0.10
LOI	2.1	11.7	7.1	95.1	21.8	15.5
Total	99.6	100.0	100.1	99.9	100.4	99.7
ppm						
V	21.52	39.21	62.80	8.51	114.21	104.86
Cr	20.53	48.86	96.67	15.69	116.31	1793.80
Co	1.00	3.50	8.62	1.86	15.43	71.69
Ni	3.32	12.22	30.84	11.42	27.58	434.74
Cu	1.97	4.72	14.56	6.76	27.49	13.21
Zn	10.60	21.28	32.84	78.05	70.94	68.87
Rb	33.28	51.72	50.81	5.90	14.75	5.98
Sr	176.9	220.6	213.4	24.4	131.3	60.6
Zr	148.08	110.65	92.81	4.82	95.94	25.08
Ba	467.8	543.3	501.4	75.2	177.4	62.5
La	6.64	8.74	12.42	1.00	9.23	3.96
Ce	13.31	16.31	23.67	1.93	18.45	8.37
Pr	1.58	1.93	2.95	0.23	2.19	1.04
Nd	6.20	7.50	11.51	0.88	8.89	4.38
Sm	1.32	1.62	2.32	0.16	1.90	0.98
Eu	0.33	0.49	0.63	0.04	0.62	0.30
Gd	1.00	1.27	1.81	0.12	1.60	0.92
Tb	0.16	0.22	0.27	0.02	0.27	0.15
Dy	1.00	1.40	1.70	0.12	1.76	1.00
Ho	0.20	0.29	0.34	0.02	0.38	0.21
Er	0.63	0.89	1.00	0.08	1.13	0.62
Tm	0.10	0.14	0.15	0.01	0.17	0.09
Yb	0.67	0.91	0.96	0.07	1.13	0.57
Lu	0.11	0.14	0.15	0.01	0.18	0.09
Pb	9.15	16.24	11.58	23.34	22.59	7.98
Th	2.23	2.84	3.85	0.18	2.34	0.75
U	0.76	0.87	0.97	0.09	0.69	0.21
Eu/Eu*	0.88	1.05	0.93	0.88	1.08	0.95
⁸⁷ Rb/ ⁸⁶ Sr	0.5249	0.6542	0.6645	0.6746	0.3134	0.2754
⁸⁷ Sr/ ⁸⁶ Sr ± 2σ	0.724312 ± 9	0.724586 ± 11	0.724597 ± 8	0.720883 ± 12	0.714063 ± 11	0.708422 ± 9
¹⁴³ Sm/ ¹⁴⁴ Nd	0.1327	0.1342	0.1253	0.1125	0.1331	0.1397
¹⁴³ Nd/ ¹⁴⁴ Nd ± 2σ	0.511490 ± 9	0.511559 ± 7	0.511415 ± 10	ND	0.511709 ± 7	0.511606 ± 6
$\epsilon_{\text{Nd}}, \text{‰}$	-22.4 ± 0.2	-21.0 ± 0.1	-23.9 ± 0.2	ND	-18.1 ± 0.1	-20.1 ± 0.1

Table 2.2, continued.

Sample	V-16			K-7			K-8	
Parent rock	γ		O/A	γ		E	γ	
Horizon	E	B	0-5	E	B	15-40	E	
Depth, cm	9-34	34-82	0-5	5-15	15-40	5-15	5-15	
pH	5.90	6.60	3.68	4.90	5.25		5.30	
% wt								
TOC	0.23	0.22	34.82	0.76	0.86		0.88	
SiO ₂	80.19	76.44	ND	73.10	69.30		73.90	
Al ₂ O ₃	10.59	11.81	ND	11.85	11.45		10.90	
Fe ₂ O ₃	1.00	1.95	ND	1.98	5.78		2.54	
CaO	1.74	1.91	ND	1.46	1.92		1.58	
MgO	0.37	0.72	ND	0.72	1.47		1.01	
Na ₂ O	3.16	3.48	ND	3.87	3.37		3.39	
K ₂ O	1.87	1.86	ND	2.57	2.18		2.33	
TiO ₂	0.31	0.21	ND	0.61	0.62		0.63	
MnO	0.02	0.04	ND	0.02	0.04		0.03	
P ₂ O ₅	ND	0.05	ND	0.03	0.03		0.12	
LOI	1.0	1.4	73.2	2.36	4.06		2.9	
Total	100.3	99.9	ND	98.7	100.5		99.4	
ppm								
V	24.78	27.23	21.04	37.44	117.55		66.25	
Cr	23.44	24.96	12.06	35.34	62.50		36.15	
Co	1.72	4.87	4.31	3.00	9.72		5.15	
Ni	4.81	17.91	9.02	7.99	22.37		12.34	
Cu	1.81	2.89	5.94	1.00	5.39		1.29	
Zn	10.65	22.33	49.17	8.92	23.83		13.31	
Rb	43.65	41.47	12.69	56.00	64.84		60.40	
Sr	244.2	246.9	415.20	247.05	290.94		271.23	
Zr	94.58	47.89	59.32	163.10	117.34		128.17	
Ba	578.8	546.5	426.52	588.16	518.32		609.24	
La	6.34	6.77	9.85	10.44	12.10		11.44	
Ce	12.54	12.73	25.25	20.38	25.72		22.95	
Pr	1.52	1.50	3.35	2.28	3.00		2.65	
Nd	6.01	5.74	13.57	8.60	11.79		10.08	
Sm	1.27	1.09	2.35	1.60	2.22		1.93	
Eu	0.40	0.36	0.59	0.49	0.69		0.58	
Gd	0.98	0.81	1.66	1.32	1.89		1.58	
Tb	0.16	0.13	0.19	0.17	0.25		0.21	
Dy	0.95	0.73	0.81	0.89	1.35		1.08	
Ho	0.19	0.15	0.13	0.16	0.26		0.20	
Er	0.59	0.44	0.32	0.50	0.74		0.60	
Tm	0.09	0.06	0.04	0.08	0.11		0.09	
Yb	0.58	0.42	0.27	0.55	0.73		0.59	
Lu	0.09	0.07	0.04	0.09	0.11		0.10	
Pb	9.75	9.78	22.28	8.44	9.18		10.62	
Th	1.98	2.18	0.91	3.13	3.97		4.05	
U	0.56	0.49	0.25	0.69	0.74		0.72	
Eu/Eu*	1.10	1.18	0.91	1.03	1.03		1.01	
⁸⁷ Rb/ ⁸⁶ Sr	0.4989	0.4687	0.0853	0.6325	0.6219		0.6214	
⁸⁷ Sr/ ⁸⁶ Sr $\pm 2\sigma$	0.722969 ± 13	0.721551 ± 9	0.705476 ± 13	0.721316 ± 18	0.718244 ± 14		0.720612 ± 12	
¹⁴⁷ Sm/ ¹⁴⁴ Nd	0.1317	0.1180						
¹⁴³ Nd/ ¹⁴⁴ Nd $\pm 2\sigma$	0.511427 ± 13	0.511178 ± 6						
ϵ_{Nd} , %	-23.6 ± 0.3	-28.5 ± 0.1						

Table 2.2, continued.

Sample	K-8		K-14			K-29
Parent rock	γ		OI		γ	
Horizon	B	C	B ₁	B ₂	C	O/A
Depth, cm	15-25	45-55	5-10	10-20	20-25	0-8
pH	5.90	7.60	6.00	6.60	8.74	3.61
% wt						
TOC	3.54	0.41	0.47	1.13	0.15	37.16
SiO ₂	61.80	72.70	40.30	71.20	40.00	14.80
Al ₂ O ₃	11.15	11.50	3.12	10.15	2.27	2.80
Fe ₂ O ₃	4.17	2.83	14.95	3.62	14.10	0.46
CaO	1.76	2.28	1.56	2.19	1.59	0.95
MgO	1.10	1.44	35.80	2.78	39.00	0.15
Na ₂ O	2.80	3.53	0.36	3.08	0.14	0.89
K ₂ O	1.71	2.12	0.16	1.83	0.02	0.22
TiO ₂	0.36	0.48	0.24	0.46	0.13	0.10
MnO	0.03	0.04	0.18	0.04	0.18	0.02
P ₂ O ₅	0.13	0.04	0.07	0.03	0.03	0.14
LOI	12.85	1.99	3.22	3.2	2.26	79.4
Total	98.0	99.1	100.0	98.7	99.8	100.0
ppm						
V	59.04	52.10	61.67	62.18	43.94	10.14
Cr	51.56	46.54	450.77	202.84	511.50	3.66
Co	6.86	6.75	146.25	9.75	148.56	1.16
Ni	15.89	16.85	1 783.79	61.56	1 971.11	4.17
Cu	5.07	3.98	9.56	2.26	37.55	3.48
Zn	16.61	17.06	115.98	21.33	81.36	28.83
Rb	44.68	50.11	6.67	45.02	0.82	7.06
Sr	208.83	211.58	29.21	221.05	16.91	136.28
Zr	76.46	108.92	27.06	100.22	7.16	6.76
Ba	417.27	461.11	43.49	414.57	15.60	159.00
La	15.71	14.14	2.52	10.16	1.25	2.53
Ce	31.68	28.62	6.01	20.79	4.24	5.45
Pr	3.68	3.32	0.72	2.45	0.35	0.69
Nd	13.95	12.64	3.02	9.46	1.52	2.84
Sm	2.55	2.36	0.66	1.78	0.35	0.53
Eu	0.74	0.69	0.19	0.55	0.12	0.15
Gd	2.16	2.03	0.67	1.56	0.39	0.42
Tb	0.28	0.27	0.11	0.21	0.06	0.05
Dy	1.50	1.48	0.64	1.13	0.39	0.29
Ho	0.27	0.28	0.13	0.22	0.08	0.05
Er	0.75	0.80	0.41	0.62	0.25	0.14
Tm	0.10	0.12	0.06	0.09	0.04	0.02
Yb	0.68	0.78	0.39	0.61	0.24	0.12
Lu	0.10	0.12	0.06	0.10	0.04	0.02
Pb	6.49	7.09	1.60	7.94	0.45	15.54
Th	4.50	4.03	0.47	2.92	0.13	0.26
U	0.73	0.72	0.12	0.57	0.02	0.06
Eu/Eu*	0.96	0.96	0.87	1.01	0.99	0.97
⁸⁷ Rb/ ⁸⁶ Sr	0.5970	0.6609	0.6371	0.5683	0.1346	0.0509
⁸⁷ Sr/ ⁸⁶ Sr $\pm 2\sigma$	0.722364 ± 33		0.724569 ± 17	0.714092 ± 15	0.719148 ± 18	0.704323 ± 19
¹⁴³ Sm/ ¹⁴⁴ Nd						0.70441 ± 17
¹⁴³ Nd/ ¹⁴⁴ Nd $\pm 2\sigma$						
ε_{Nd} , %						

Table 2.2, continued.

Sample Parent rock	K-29				K-37 G-n		
	E γ	C 15-18	O 0-7	A 7-18	B ₁ 18-25	B ₂ 25-36	C 36-46
Horizon							
Depth, cm	8-15	15-18	0-7	7-18	18-25	25-36	36-46
pH	5.50	5.86	3.82	4.67	5.33	5.79	5.66
% wt							
TOC	0.91	1.62	22.16	7.73	2.41	2.66	2.52
SiO ₂	72.30	68.20	39.90	61.20	67.90	64.10	67.10
Al ₂ O ₃	13.65	14.15	6.15	10.25	10.95	12.85	12.50
Fe ₂ O ₃	1.64	2.40	2.19	3.42	4.05	3.76	2.93
CaO	3.43	3.48	1.27	1.84	2.23	2.90	2.21
MgO	0.38	0.86	1.02	1.59	1.95	2.06	1.55
Na ₂ O	4.63	4.65	1.60	2.75	3.04	3.17	3.18
K ₂ O	0.45	0.54	1.17	2.03	1.96	1.85	1.95
TiO ₂	0.41	0.42	0.32	0.50	0.45	0.39	0.32
MnO	0.03	0.04	0.02	0.03	0.04	0.04	0.03
P ₂ O ₅	<0.01	0.04	0.14	0.11	0.05	0.08	0.10
LOI	2.62	4.95	45.9	16.15	7.09	8.65	8.04
Total	99.7	99.9	99.7	100.0	99.8	100.0	100.0
ppm							
V	47.33	42.84	30.00	71.59	78.94	68.10	51.84
Cr	13.31	19.01	37.50	62.89	60.38	50.69	44.21
Co	2.31	4.61	3.41	7.24	10.32	10.73	8.23
Ni	2.45	5.74	11.48	22.31	27.84	28.08	21.86
Cu	1.05	1.36	5.95	9.90	12.66	22.41	18.27
Zn	15.84	26.26	15.28	13.71	21.60	21.99	17.52
Rb	9.95	11.21	19.72	46.43	51.36	47.94	52.87
Sr	717.60	614.21	77.82	177.57	205.99	240.05	201.19
Zr	25.91	17.64	39.74	106.16	115.56	76.43	71.32
Ba	412.15	386.03	173.51	414.39	451.54	443.78	449.69
La	13.05	12.61	3.99	8.21	11.19	12.52	11.18
Ce	27.34	25.58	8.00	16.91	25.15	26.92	24.73
Pr	3.41	3.08	0.87	1.81	2.59	2.93	2.61
Nd	13.89	12.25	3.31	6.83	10.10	11.36	9.96
Sm	2.55	2.14	0.65	1.33	1.90	2.18	1.95
Eu	0.75	0.67	0.20	0.42	0.60	0.67	0.63
Gd	2.01	1.65	0.57	1.14	1.71	1.96	1.73
Tb	0.25	0.20	0.08	0.15	0.23	0.27	0.24
Dy	1.26	0.98	0.42	0.85	1.31	1.50	1.32
Ho	0.22	0.18	0.08	0.17	0.25	0.29	0.25
Er	0.61	0.46	0.26	0.51	0.75	0.80	0.70
Tm	0.08	0.06	0.04	0.07	0.11	0.11	0.10
Yb	0.49	0.38	0.26	0.53	0.68	0.74	0.66
Lu	0.07	0.05	0.04	0.09	0.11	0.11	0.09
Pb	6.60	5.47	8.87	8.89	8.50	7.12	7.36
Th	1.47	1.42	1.43	3.10	3.40	3.01	3.00
U	0.12	0.08	0.32	0.69	0.69	0.56	0.53
Eu/Eu*	1.01	1.09	0.99	1.04	1.01	1.00	1.04
⁸⁷ Rb/ ⁸⁶ Sr	0.0354	0.1481	0.7350	0.7500	0.7027	0.5612	0.7368
⁸⁷ Sr/ ⁸⁶ Sr $\pm 2\sigma$	0.703928 \pm 13	0.706263 \pm 12	0.723565 \pm 24	0.724717 \pm 16	0.724683 \pm 19	0.720769 \pm 14	0.726039 \pm 19
¹⁴³ Sm/ ¹⁴⁴ Nd							
¹⁴³ Nd/ ¹⁴⁴ Nd $\pm 2\sigma$							
ϵ_{Nd} , %							

Table 2.3. Major, trace elements and dissolved organic carbon (DOC) concentrations, and strontium isotopic ratios ($^{87}\text{Sr}/^{86}\text{Sr}$) measured in the dissolved phase (i.e., <0.22 (0.45) μm) in river and swamp waters from Vettreny Belt and Kivakkka intrusion zone. “nm” signifies not measured; “ $<\text{dl}$ ” – below detection limit; “TDS” – total dissolved solids; “RW” – river water; “SW” – surface water; “SWW” – swamp water; “SS” – soil solution; “SS” – soil solution; “SS” – soil substratum; P – peridotite; Ol – olivine; N – norite; G-n – gabbro-norite.

	Vettreny Belt	V-9-W	V-12-W	V-13-W	V-15-W	V-18-W	V-10-W	V-11-W	V-3-W	V-16-SW
	0.22 μm µg/l	RW β	RW β	RW P	RW β	RW β	RW β	SW β	SW β	SS P
pH	5.92	5.9	6.5	5.07	7.05	5.18	5.18	5.46	7.11	
t°C	20	27	27	25	23	29	29	23	24	
DOC, mg/l	36.5	34.7	35.7	39.7	17.2	8.8	98.5	9.8	20.6	
Na ⁺	2.335	2.532	2.215	1.687	4.430	1.800	2.045	1.365	1.508	
K ⁺	514	469	407	106	224	517	304	305	651	
Mg ²⁺	2.867	2.793	6.034	3.128	2.917	425	328	544	8.023	
Ca ²⁺	1.838	1.811	1.689	837	2.943	1.296	922	1.112	516	
H ₄ SiO ₄	4.900	5.070	4.030	4.020	2.210	3.970	4.540	2.930	5.980	
Cl ⁻	1.270	nm	1.590	2.080	3.900	1.582	2.460	1.350	2.210	
SO ₄ ²⁻	750	nm	531	531	800	900	810	1.540	1.590	
NO ₃ ⁻	<dl	<dl	480	295	101	100	<dl	290	539	
F ⁻	70	<dl	<dl	39	56	28	<dl	33	<dl	
[Alk], mg/l	4.85	5.56	16.6	2.05	28	4.21	4.84	1.77	29.89	
Al	nm	537	340	319	56	264	310	244	161	
Fe	1.888	865	752	2.374	2.216	618	135	290	311	
Rb	0.52	0.59	0.53	0.38	0.48	0.85	0.41	0.56	0.76	
Sr	13.00	12.18	11.19	5.08	18.81	11.99	9.24	10.11	4.15	
TDS, mg/l	16.4	14.1	18.1	15.4	19.9	11.5	8.6	10.0	21.5	
$^{87}\text{Sr}/^{86}\text{Sr}$	0.723799 ± 20	nm	0.722741 ± 20	0.721984 ± 12	nm	nm	0.715087 ± 17	0.723249 ± 33		

Table 2.3, continued.

	Kivakkä intrusion 0.45 µm µg/l	K-7-W RW γ	K-8-W RW γ	K-12-W SW γ	K-30-W RW γ	K-31-W RW γ	K-45-W RW γ	K-13-W RW OI	K-17-W SW N	K-33-W RW G-n
pH	7.36	5.95	6.56	7.42	7.45	7.31	6.56	6.72	6.13	nm
t°C	16	6	nm	nm	nm	nm	nm	nm	nm	nm
DOC, mg/l	10.42	1.74	5.60	6.32	5.08	94.36	30.55	2.22	6.41	6.41
Na ⁺	1 667	1 379	2 161	2 732	1 714	1 652	1 378	2 044	1 164	1 164
K ⁺	502	315	64	386	907	370	374	72	38	38
Mg ²⁺	2 106	674	1 451	3 898	7 874	1 821	13 002	1 218	570	570
Ca ²⁺	9 745	2 047	4 891	10 596	17 435	7 219	1 901	7 385	2 328	2 328
H ₄ SiO ₄	3 210	3 990	3 760	4 880	3 290	2 390	7 310	4 560	3 200	3 200
Cl ⁻	568	576	295	393	495	526	453	534	400	400
SO ₄ ²⁻	1 498	3 650	2 300	351	688	1 922	432	3 576	736	736
NO ₃ ⁻	<dl	<dl	<dl	<dl	139	<dl	<dl	<dl	<dl	<dl
F ⁻	<dl	<dl	<dl	<dl	<dl	<dl	<dl	<dl	<dl	<dl
[AlK], mg/l	27.38	8.28	22.76	39.42	80.20	28.32	40.21	26.17	9.59	9.59
Al	26.34	32.30	51.74	7.48	9.76	32.97	191.38	20.07	125.24	125.24
Fe	2 589.87	5.59	116.64	115.31	246.79	2 124.46	391.96	3.33	270.26	270.26
Rb	1.23	0.99	0.17	0.78	1.79	1.06	1.53	0.20	0.15	0.15
Sr	50.89	9.94	12.55	17.20	15.91	36.96	14.26	14.79	8.50	8.50
TDS, mg/l	19.30	12.63	14.92	23.24	32.54	15.90	24.85	19.39	8.44	8.44
⁸⁷ Sr/ ⁸⁶ Sr	0.721067 ± 15	0.725299 ± 15	0.716615 ± 15	nm	nm	0.721102 ± 12	0.717867 ± 21	0.713467 ± 19	nm	nm

Table 2.3, continued.

	Kivakkä intrusion 0.45 µm µg/l	K-41-w RW G-n	K-10-w SWW γ	K-43-w SWW G-n	K-44-w SWW G-n	K-32-w SWW G-n	K-38-w SWW G-n	K-39-w SWW G-n	K-5ss SS N	K-35-ss SS G-n
pH	7.17	4.94	5.85	5.41	4.56	4.65	5.03	4.94		nm
t°C	nm	24	16	21	nm	19	nm	6		nm
DOC, mg/l	4.96	29.46	nm	31.59	16.65	11.60	5.28	3.43	40.34	
Na ⁺	1 871	1 031	1 094	1 068	1 399	845	743	569	1 102	
K ⁺	89	58	32	50	190	249	133	77	178	
Mg ²⁺	1 068	832	1 327	1 055	384	217	165	114	674	
Ca ²⁺	3 166	2 065	3 707	2 382	909	644	674	520	1 305	
H ₄ SiO ₄	3 700	1 930	2 780	2 250	2 470	490	760	2 520	4 540	
Cl ⁻	374	725	726	841	1 252	1 180	742	217	1 414	
SO ₄ ²⁻	1 610	494	255	235	332	220	599	1 853	1 868	
NO ₃ ⁻	<dl	<dl	<dl	<dl	<dl	<dl	<dl	862	595	
F ⁻	<dl	<dl	<dl	<dl	<dl	<dl	<dl	<dl	<dl	
[Al] ¹ , mg/l	16.61	453.75	302.11	386.37	163.85	179.22	224.63	274.24	440.35	
Al	42.69	3 876.17	10 507.70	4 778.12	164.02	180.11	237.39	913.91	41.37	
Fe	36.68	0.10	0.13	0.08	0.51	0.45	0.24	0.29	0.65	
Rb	0.17	12.93	16.71	14.19	4.09	4.02	5.31	3.65	10.44	
Sr	11.56	11.88	11.5	20.7	13.0	7.3	4.2	7.9	12.2	
TDS, mg/l	0.713984 ± 13	nm	0.721347 ± 46	nm	nm	nm	nm	nm	nm	
⁸⁷ Sr/ ⁸⁶ Sr										

After crushing, pulverization, and homogenization, soil samples were digested in H₂O₂ at 25°C during 24 h and then in HF-HNO₃-HCl on a hot plate at 60-120°C in Teflon beakers in a clean room. Validity of total chemical analysis for soils was verified by applying the same procedure for international geostandards BE-N (i.e., basalt), GA and AC-E (i.e., granites) for rocks, and LKSD-1 (i.e., lake sediment) for soils. Trace elements in rocks and soils were analysed by ICP-MS with an uncertainty < 10% for the elements presented in this study. Indium and rhenium were used as internal standards. Major elements in soils were analysed by ICP-AES method in SARM laboratory (Nancy, France) and ALS Chemex laboratory (Vancouver, Canada). The analytical error of these measurements was in the range 5-10 %.

Total organic carbon (TOC) was analysed in dried soils by Horiba carbon/sulphur analyzer EMIA-320V with an uncertainty better than 10%. pH measurements were performed using a combined Schott-Geräte electrode calibrated against NIST buffer solutions (pH = 4.00 and 6.86 at 25 °C). Soil pH was measured in deionised water suspension according to international ISO norms for measuring soil pH (AFNOR, 1996, ISO 10390). The accuracy of measurements was ± 0.05 pH units.

2.3.2.2. Chemical analysis of river, surface swamp and soil pore waters

Physico-chemical parameters of unfiltered water samples (pH, temperature ($\pm 0.2^\circ\text{C}$), and electrical conductivity) were measured in the field. The pH was measured using a combined Schott-Geräte electrode calibrated against NIST buffer solutions (pH = 4.00 and 6.86 at 25 °C), with an accuracy of ± 0.02 pH units. Samples were collected from near the middle of the flow channel, using 1-l high-density polyethylene (HDPE) containers held out from the beach on a non-metallic stick. Plastic gloves were always used during handling of the samples. The water samples were immediately filtered through sterile, single-use Minisart® filter units (Sartorius, acetate cellulose filter) with pore sizes of 0.45 and 0.22 µm. The first 200 ml of the filtrate was systematically discarded. Filtered solutions for cations, trace element and Sr isotope analyses were acidified (pH = 2) with ultrapure double-distilled HNO₃ and stored in HDPE bottles previously washed with ultrapure 0.1 M HCl and rinsed with MilliQ deionized water. Filtered water samples for anions were not acidified and stored in HDPE bottles previously washed according to the above-described procedure as for cations. Samples

for dissolved organic carbon (DOC) were collected in pyrolysed (550°C) Pyrex test tubes.

Soil pore waters were extracted from humid soil horizons in the field using a Ti pressure device. This titanium vessel has a 50 mm diameter, 150 mm length, and a special thread allowing it to reach 20 000 kg/cm² pressure. Depending on saturation state of soil samples, 10 to 50 mL of solution was collected and filtered through a 0.45 or 0.22 µm cellulose filter. After each extraction, the vessel and its compartments were thoroughly washed by river water, and afterward, by 100 to 200 mL of distilled water. Before and after fieldwork, blank samples were run by filling the pressure system with MilliQ water at neutral pH and letting it to react for 24h. No detectable contamination of major and trace elements and DOC was observed.

Major anion concentrations (Cl, SO₄, F, NO₃, PO₄) were measured by ion chromatography (HPLC, Dionex 2000i) with an uncertainty of 2%. Calcium, magnesium, sodium, and potassium concentrations were determined using an atomic absorption spectrophotometry (AAS) Perkin-Elmer 5100PC spectrometer with an uncertainty of 2%. Aqueous silica concentration was determined by standard colorimetry (molybdate blue method) with an uncertainty of 2% using Technicon automated analyzer. Alkalinity was measured by potentiometric titration with HCl to pH = 4.2 using Gran method with detection limit of 10⁻⁵ M and an uncertainty of 2%. DOC was analyzed using a Carbon Total Analyzer (Shimadzu TOC 5000A) with a detection limit of 0.1 µg/l and an uncertainty better than 3%.

Trace elements (TE) were measured without preconcentration by ICP-MS (Elan 6000, Perkin Elmer and 7500ce, Agilent Technologies). Indium and rhenium were used as internal standards. The international geostandard SLRS-4 (Riverine Water Reference Material for Trace Metals certified by the National Research Council of Canada) was used to check the validity and reproducibility of each analysis. A good agreement between our replicated measurements of SLRS-4 and the certified values was obtained (relative difference < 5%).

2.3.2.3. Isotope analysis of surface waters and soils

Strontium and neodymium isotopic ratios were measured by thermal ionization mass spectrometry (Finnigan Mat 261) preceded by chemical separation, involving the

dissolution of the sample and chemical extraction of Rb and Sr, and Sm and Nd by ion exchange chromatography using three chromatographic materials Sr.Spec, TRU.Spec and Ln.Spec, and HF, HNO₃ and HCl acids in a clean room. Data correction was based on the systematic analysis of the NBS 987 standard for Sr and standard La Jolla for Nd. During this work, the average ⁸⁷Sr/⁸⁶Sr for NBS 987 standard was 0.710250 ± 0.000010 (4 measurements) and 0.511834 ± 0.000006 for ¹⁴³Nd/¹⁴⁴Nd (1 measurement).

2.4. Results

2.4.1. Bedrock mineralogy and chemistry

The chemical composition of studied altered minerals and rocks, assessed from electron microprobe analysis of thin sections of several basic rocks and one granite collected in the zone of Kivakka and Vetreny Belt mafic intrusions is presented in Table A-1 of the Annex A. Major and trace elements composition of unweathered parent rocks considered in this study was taken from data reported in the literature. Trace elements composition for unweathered basalts from Ruiga and Goletz hills of the Vetreny Belt paleorift is given in Table A-2 of the Annex A.

Using the oxide data in Table A-1, the data have been recast into structural formulae for the assemblage minerals of (gabbro)-norite, olivinite, peridotite, basalt and Archean granite. For gabbro-norite, structural formulae of the clynopyroxene, orthopyroxene and plagioclase are $\text{Si}_{1.94}\text{Al}_{0.06}\text{O}_6\text{Mg}_{0.9}\text{Ca}_{0.9}\text{Fe}_{0.2}$ (augite), $\text{Si}_{1.97}\text{Al}_{0.03}\text{O}_6\text{Mg}_{1.5}\text{Ca}_{0.1}\text{Fe}_{0.4}$ (bronzite) and An₆₉-An₇₈ (bytownite), respectively. In addition to the primary minerals, rocks show notable amounts of amphibole (i.e., hornblende type with variable composition), epidote, talc, as well as serpentine, chalcopyrite, pyrite and iron oxide which were observed by scanning electronic microscopy (SEM).

Olivinite shows an olivine with chromic spinel ($\text{Fe}_{0.3}\text{Mg}_{1.7}\text{SiO}_4$, 18% Fe), plagioclase (An₅₇-An₆₅ (labrador)), orthopyroxene ($\text{Si}_2\text{O}_6\text{Mg}_{1.6}\text{Fe}_{0.3}$ (bronzite)), and clynopyroxene ($\text{Si}_2\text{O}_6\text{Mg}_{1}\text{Fe}_{0.2}\text{Ca}_{0.7}$ (augite)) mineral assemblage. Hornblende and epidote are mainly present in altered zones and correspond to post magmatic hydrothermal alteration producing secondary mineral assemblages.

Peridotite shows a pyroxene ($\text{Ca}_{0.4}\text{Mg}_{1.3}\text{Fe}_{0.3}\text{Si}_2\text{O}_6$ (pigeonite)), amphibole ($\text{Ca}_{1.4}\text{Mg}_{4.9}\text{Fe}_{0.7}\text{Si}_{7.4}\text{O}_{22}$ (actinolite)), plagioclase ($\text{Ca}_{0.6}\text{Na}_{0.4}\text{Al}_{1.6}\text{Si}_{2.4}\text{O}_8$ (plagioclase

labradorite), An_{60-63}), olivine ($\text{Fe}_{0.5}\text{Mg}_{1.5}\text{SiO}_4$ (33% of Fe)) and chlorite ($\text{Mg}_{4.3}\text{Al}_{1.6}\text{Fe}_{0.5}\text{Si}_{3.3}\text{O}_{10}(\text{OH})_8$) mineral assemblage. Serpentine ($\text{Mg}_{2.8}\text{Fe}_{0.2}\text{Si}_2\text{O}_5(\text{OH})_4$), spinel ($\text{Ti}_{0.1}\text{Fe}_{1.7}\text{Al}_{0.4}\text{Cr}_{0.8}\text{O}_4$), hematite and ilmenite are present as secondary mineral assemblages.

For basalt, structural formulae of the amphibole, pyroxene and feldspar are $\text{Ca}_{1.3}\text{Mg}_{4.1}\text{Fe}_{1.2}\text{Al}_{0.4}\text{Si}_{7.6}\text{O}_{22}(\text{OH})_2$, $\text{Al}_{0.1}\text{Ca}_{0.8}\text{Mg}\text{Fe}_{0.2}\text{Si}_{1.9}\text{O}_6$ and $\text{Ca}_{0.6}\text{Na}_{0.4}\text{Al}_{1.6}\text{Si}_{2.4}\text{O}_8$ (labrador), respectively. Minor minerals like ilmenite, spinel and talc are present in addition to primary minerals.

For an Archean granite mineral assemblage is represented by oligoclase ($\text{Ca}_{0.2}\text{Na}_{0.6}\text{K}_{0.2}\text{Al}_{1.2}\text{Si}_{2.8}\text{O}_8$ (An_{22-25})) and biotite ($\text{K}_{1.9}\text{Al}_{0.4}\text{Mg}_{2.3}\text{Fe}_{2.6}\text{Ti}_{0.4}\text{Si}_{5.6}\text{Al}_{2.4}\text{O}_{20}(\text{OH})_{3.7}\text{F}_{0.3}$).

2.4.2. Soil mineralogy

Mineral composition of solid material was further characterized by structural X-ray analyses of fine (<0.1 μm , 0.1-2 μm and >2 μm) and bulk fractions of 10 soil profiles: samples V-4, V-7 (basalts), V-9, V-16 (gneisses), V-15 (peridotites, olivinites) and K-7, K-29 (gneisses), K-14 (olivinites), K-37 (gabbro-norites). Clay mineralogy results presented in this study were obtained on soil samples having enough fine fraction for analysis. However, in boreal podzols, the clay fraction is generally known to be <5% (Melkerud et al., 2000; Mokma et al, 2004; Allen et al., 2001). Although peak intensities in the diffractograms varied somewhat as a function of depth, the <2 μm fractions from soils developed on basic rocks indicated that quartz (all samples except K-14-C and V-15-O/A), feldspar (all samples except K-14-B₁ and -C and V-15-O/A), amphibole (all samples except K-14-B₁), illite (all samples), chlorite (all samples except K-37-A, V-16-E and -B, V-9-A and V-15-O/A), vermiculite (K-7, K-14, K-37-B₁ and -B₂, V-16-B, V-15), as well as interstratified layers illite/vermiculite (K29-O/A), smectite (K-37-B₁, V-4-E and V-15-O/A) and amorphous phases (K-29, V-16, V-7 and V-9) were the major clay-fraction constituents (Table 2.4). Amorphous aluminosilicates (i.e., imogolite), chlorite, regular interstratified layer mica/vermiculite (25 Å) were found in soil profile K-29 developed on granite-gneiss which is comparable to the clay fraction composition of podzols developed on granite-gneissic rocks in southern Sweden described by Schweda et al. (1991) and in northern Sweden described by

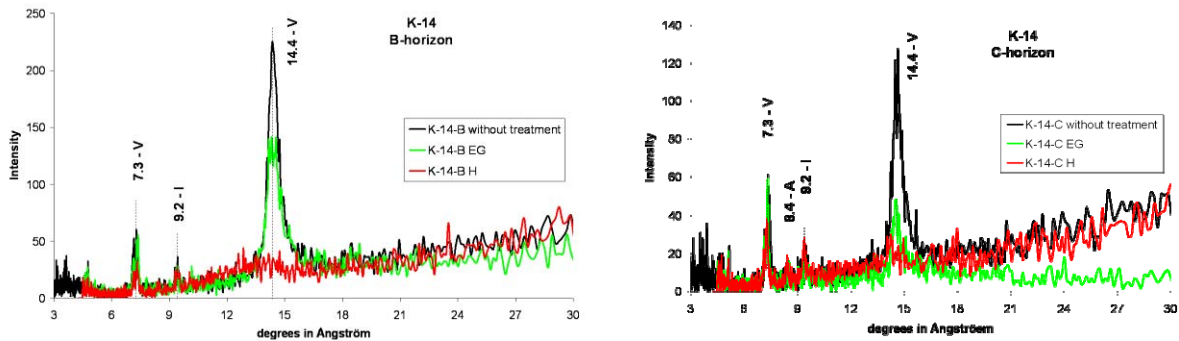
Table 2.4. Mineralogical composition of studied soils. Number of “+” signs indicates the different degree of presence of a mineral in soil, “Tr.” stands for “traces”.

Mineral composition	Quartz	Feldspar	Amphibole	Illite	Vermiculite	Chlorite	Hydrobiotite	Amorphous phases	Interlayered Mica/Vermiculite	Smectite	Talc
K-7-B	+	++	+	+	++	Tr.					
K-14-B1	Tr.			+	+++	+					
K-14-C			+	+	+++	+					Tr.
K-29-O/A	++	++	+	++		Tr.	++	+	+		
K-29-E	++	++	Tr.	++		Tr.	++	+			
K-37-A	++	++	++	++							
K-37-B1	++	++	+	+	++	+					+
K-37-B2	++	+	+	+	+	+					
V-16-E	++	++	++	+					++		
V-16-B	++	++	+	+	+				+		
V-4-E	++	+	Tr.	Tr.			+				++
V-7-B	++	+	+	+	+	++			+		
V-9-A	++	+	+						+		
V-15-O/A			+	+	++						++

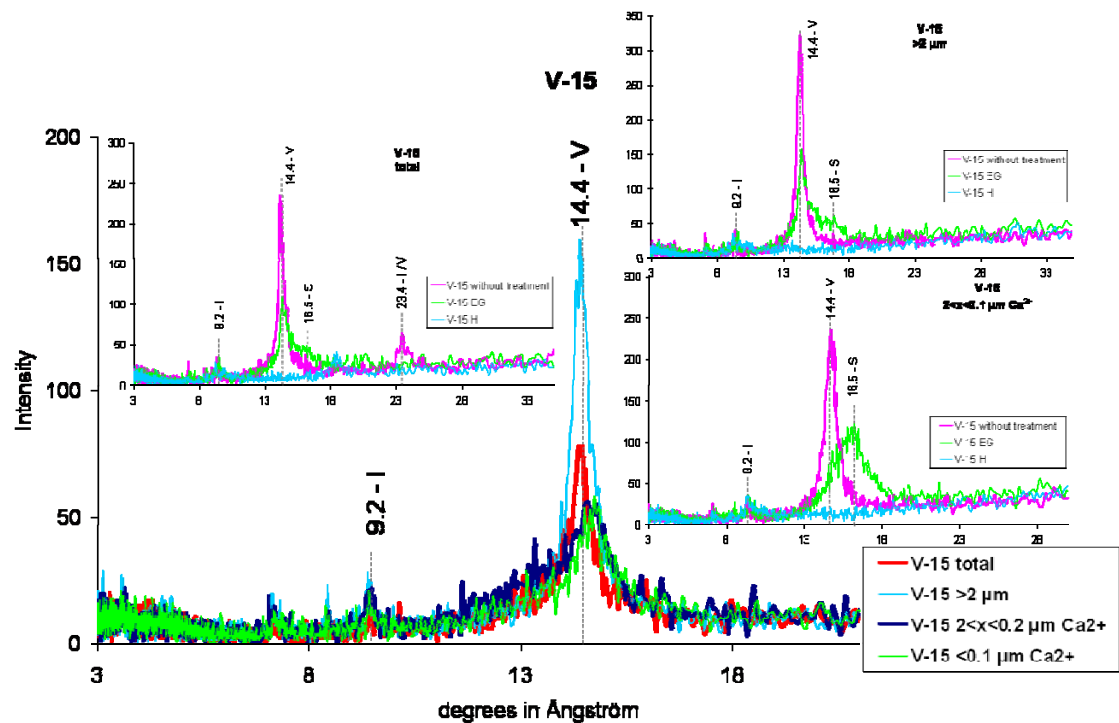
Land et al. (1999). Hydrobiotite, mineral containing regularly interstratified layers of biotite and vermiculite (Sawhney, 1989, Murashkina et al., 2007), was indicated by a peak at 12 Å in granitic soil K-29.

Our observations are consistent with the observations of Lesovaya et al. (2008) who reported the presence of hydrobiotite, amorphous phase, smectite (explained as the degradation of hydrobiotite) and K-feldspar in mountainous tundra soils (NW Russia) over nepheline syenite in horizons C and B₂, as well as quartz and plagioclase in horizons B₁ and E. Our results are also comparable with the clay fraction composition of soil developed on glacial moraine in Finland (gneissic moraine material) (Melkerud et al., 2000; Mokma et al., 2004) which includes quartz, plagioclase, K-feldspar, amphibole, chlorite, illite, mixed layer illite/vermiculite and allophanes. Observed mixed layer chlorite/vermiculite is reported as a product of degradation of chlorite.

Fig. 2.2 shows representative clay mineral XRD patterns from within the olivinitic profile K-14 and A horizon of the ultramafic soil V-15 exposed to heating (at 500°C), ethylene glycol treatment, and Ca²⁺ saturation procedures. The analysis of the



a



b

Fig. 2.2. Representative X-ray diffractograms of soil profiles K-14 (a) and V-15 (b). Minerals: I – illite, I/V – interstratified layers of illite and smectite, S – smectite, V – vermiculite. EG – ethylene-glycol saturation, H – heating, Ca²⁺ – calcium saturation.

clay fraction in K-14 indicates the presence of vermiculite (occurrence of a 14.4 Å (7.3 Å) peak on the air-dried pattern, expandable on the ethylene-glycol pattern and collapsed on the heated pattern), illite (10 Å) and amphibole (8.4 Å). The analysis of V-15 (peridotite) shows the presence of both of expandable vermiculite and smectite (vermiculite predominant), and an interstratified layer illite/vermiculite (23.4 Å). Supplementary TEM investigations on the K-14 sample over olivinite from the Kivakka intrusion allowed acquiring detailed information on the nature of vermiculite formed in the C horizon of this soil. These results confirm the presence of a Mg-vermiculite together with a chlorite and amphibole, which also contain Mg.

Further optical and SEM observations on consolidated thin sections of structurally preserved soil samples from different horizons revealed the presence of quartz and feldspar almost in all studied soil profiles developed on basic rocks: gabbro-norite, olivinite, peridotite, except for the C horizon of K-14 (soil over olivinite) and the O/A horizon of V-15 (soil over basalt). Zircon was found in soils developed on granite-gneisses (K-7, B horizon; K-29, C horizon) and, surprisingly, on soil over peridotites (V-16, E horizon). Morphological observations of soils by SEM carried out during this study reveal the presence of etch pits corrosion on the surface of zircon and feldspar (Fig. 2.3 a, b) together with newly-formed matter visible as a coating on quartz, plagioclase and pyroxene surfaces (Fig. 2.3 c).

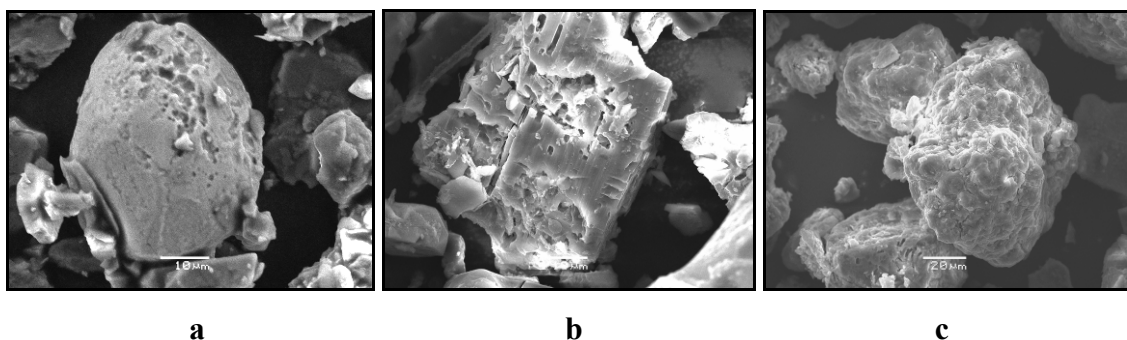


Fig. 2.3. SEM images of minerals found in soils illustrating neo-formed material and erosion on the surface of minerals: a – altered zircon in podzol V-16 over granite; b – altered feldspar in regosol K-29 over granite; c – quartz covered with aluminous coating in podzol K-37 over gabbro-norite.

2.4.2.1. Evolution of the soil chemical composition as a function of depth

The total major and trace chemical composition, pH and total organic carbon (TOC) concentrations for each type of studied soil are given in Table 2.2. Pictures of podzols V-4, K-14 and K-37 developed on basalt, olivinite and gabbro-norite, respectively, and regosol K-29 over granite-gneiss are presented in the Fig. 2.4. pH (H_2O) of soils developed on granitic rocks varies between 3.43 and 7.60, and those on basic rocks between 3.82 and 8.74, being the most acid in the surface organic rich soil horizons. The high pH found for V-4 and K-14 soils could be attributed to the mafic nature of the parental rock. Podzolisation process is favoured within low pH environment which is usually the consequence of pedogenesis on acid rocks under deep and acid litter. In this context, the pH (H_2O) measured for the V-16-B and K-8-B

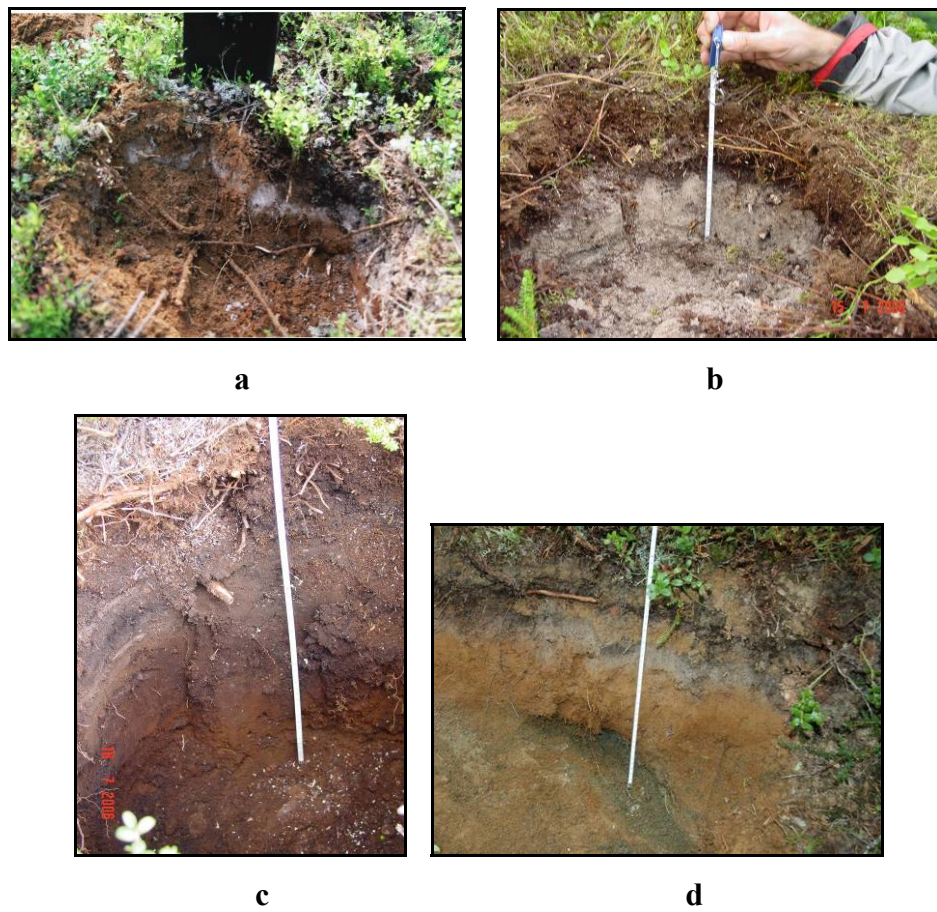


Fig. 2.4. Photos: a - podzol V-4 developed on komatiitic basalts from the Goletz hill of Vetreny Belt; b – regosol K-29 under heather and bilberry bushes developed on granito-gneiss from the Kivakka intrusion zone; c – podzol K-37 developed on gabbro-norite rock of the Kivakka intrusion; d – podzol K-14 developed on olivinite rock of the Kivakka intrusion.

samples are problematic (pH is too basic for a podzol type soil). TOC concentration ranges from 7.7 to 42.1 %wt in organic surface horizons (O/A), and from 0.15 to 3.5 %wt for deeper horizons (E, B and C).

Chemical analysis of soils was performed on bulk fractions (including gravel). Observations of elements concentrations along the soil profiles (see graphical illustration in Fig. A-1 of the Annex A) show that all soils developed on granitic rocks exhibit higher content in Si, K (except K-29), Al (except K-7) and Na, and lower content in Ca (except K-29), Fe and Mg with respect to their parent rock. Podzol V-7 developed on basic rocks show relatively higher content in Si, Al, Na and K than its parent rock similarly to the soils developed on granitic rocks (V-9, K-8, K-29). K-14 and K-37 exhibit low Si, Al and Na content compared to olivenite or gabbro-norite. Higher content in K in the surface horizon compared to the parental rock is observed for all soils except K-14, K-29 and V-15. Almost all soils developed on basic rocks show lower content in Fe (except K-14) and Mg (except V-9 and V-15) compared to their respective parent rock.

2.4.3. Hydrochemistry

Measured water parameters (pH and temperature), dissolved organic carbon (DOC) concentration, major and some trace elements concentrations (Al, Fe, Sr and Rb), as well as $^{87}\text{Sr}/^{86}\text{Sr}$ isotopic ratios for some selected samples are presented in Table 2.3 for both Kivakka intrusion and Vetreny Belt zones.

The studied waters are essentially neutral with pH varying from 6 to 7.5. However, some surface organic rich waters and swamp waters are more acidic with pH decreasing to 4.5-5.5. Bicarbonate ion concentration ranges from 1.8 to 40.2 mg/l for rivers draining basic rocks and from 8.3 to 80.2 mg/l for those draining granitic rocks. In surface wetlands and interstitial waters from soils developed on basalts, the alkalinity ranges from 2.2 to 8.0 and from 1.8 to 29.9 mg/l, respectively. The majority of surficial fluids exhibit high concentrations of dissolved organic carbon, from 5 to 40 mg/l.

The composition of the dissolved load of most rivers reflects the weathering of silicate rocks because the total dissolved solids (TDS) expressed as a sum of major inorganic species concentrations (Na, Ca, K, Mg, Al, Fe, H_4SiO_4 , Cl, NO_3 , and SO_4) is low (between 10-30 mg/l). These measurements are comparable with previous results

on Karelia region (Feoksitov, 2004, Zakharova et al., 2007). Rivers analyzed in the present work have an average H_4SiO_4 concentration around 4 mg/l (3.6 ± 0.9 mg/l for rivers draining granitic rocks, 4.3 ± 1.3 mg/l for the basaltic) which constitutes only 30% of the TDS. Calcium and sodium dominate among cations in these waters, except in the olivinite zone where Mg dominates. Negative charge of inorganic species is mainly represented by bicarbonate and sulfate. The inorganic anions (Cl^- and SO_4^{2-}) content is in the same range for both studied sites 200-3900 $\mu\text{g/l}$, similar to that reported for Karelian granites and basalts (Pokrovsky and Schott, 2002; Zakharova et al., 2007).

The concentration of the major dissolved cations in surface (river and swamp) water both for Vetreny Belt and Kivakka intrusion zones (average values in $\mu\text{mol/l}$ are given in brackets) follows the order Ca (336) > Mg (116) > Na (77) > K (16) for waters draining acidic rocks and Mg (95) > Ca (77) = Na (77) > K (7) for those draining basic rocks. Potassium and sodium values (16 $\mu\text{mol/l}$ and 90 $\mu\text{mol/l}$, respectively) are comparable with those reported by Ingri et al. (2005) for a pristine boreal Kalix river draining a mixed granitic and carbonate-shale environment, whereas calcium content in our case is higher than that of the Kalix river (149 $\mu\text{mol/l}$). We can not detect any systematic difference in Mg concentration between granitic and basaltic catchments; its concentration varies from 400 to 8000 $\mu\text{g/l}$ within the Vetreny belt zone and from 100 to 13000 $\mu\text{g/l}$ within the Kivakka intrusion zone. Within the basic rocks catchments, we could not detect any significant difference between waters draining rocks of different composition: gabbro-norites, olivinite, basalts.

2.5. Discussion

2.5.1. Moraine influence over the full depth of soil profile

2.5.1.1. Major elements

The occurrence of corroded zircon and feldspar and the evidence of clay mineral formation in those soils witness similar weathering processes on all types of parental rock. Etch-pitting of zircon is usually related to intense weathering processes, generally in tropical environment (e.g., Oliva et al., 1999). However, the lack of kaolinite neoformation and the persistence of amphibole and plagioclase feldspar in soils suggest not very intense weathering processes, in accordance with a start of pedogenesis about 10 Ky ago.

Using ratios of invariant elements (i.e., Zr, Ti, Al, Th having the lowest mobility) in soils and in rocks, we have calculated the theoretical concentrations of major elements in soil profile assuming that no weathering occurs. The comparison of these theoretical concentrations with the measured ones allows us to estimate depletion or enrichment of elements in soils samples compared to unaltered rocks. According to our calculations, the theoretical concentrations of major elements in soil profiles were systematically higher than in the parental rock for Na and/or K except for the B₁ and C-horizons of samples K-14 (soil over olivinite, Kivakka intrusion) and V-15 (soil over peridotite, Vetreny Belt). Moreover, the Zr/Ti ratio is not constant along the soil profiles (observed depletion in Zr in O and A horizons and slight enrichment in B horizons). This may suggest that Zr was not initially homogeneously distributed in soils or that Ti is not invariant in these profiles. Indeed, elevated mobility of Ti in organic-rich soil has been earlier reported for tropical soil solutions from Cameroon and Amazonia and explained by organic or mineral colloids (Viers et al., 1997; Cornu et al., 1999).

Similar results were observed when using Al and Th as invariants. We believe that the main reason for this discrepancy is unusually high mobility of tetravalent elements in the form of large-size organo-mineral ferric colloids whose presence is unambiguously demonstrated in surficial waters of Karelian zone (Pokrovsky and Schott, 2002; Vasyukova et al., 2008, submitted).

Major element percentage allows calculation of Chemical Index of Alteration (CIA; Nesbitt and Young, 1982; Fedo et al., 1995). CIA indicates the degree of weathering of the source rock calculated, using molar proportion, as follows:

$$\text{CIA} = (\text{Al}_2\text{O}_3 / (\text{Al}_2\text{O}_3 + \text{CaO} + \text{Na}_2\text{O} + \text{K}_2\text{O})) \cdot 100$$

Basic rocks exhibit average CIA values of 42 and 36 for Kivakka layered intrusion and Vetreny Belt paleorift, respectively. Soils developed on basic rocks exhibit close CIA values: from 42 to 52 for soils from Kivakka intrusion (average 49), and from 28 to 53 for soils from the Vetreny Belt (average 46). Archean granite has a CIA = 50. Soils developed on granite-gneiss have the chemical index of alteration 45-54 (average 49) and 32-51 (average 43) for Kivakka intrusion and Vetreny Belt, correspondingly. The ratio CIA_{soil sample}/CIA_{parent rock} indicates the weathering degree of soil (Fig. 2.5 a, b). It can be seen that the CIA index of soils is not always higher than that of their parent rocks. Indeed some samples (V-15, V-9, K-8-E, K-8-C, all the K-29

samples) show $\text{CIA}_s/\text{CIA}_r$ lower than 1. Since the CIA calculation involves aluminium which is thought to be rather mobile during podzolisation, and potassium which is a nutrient highly recycled by vegetation, several hypothesis can explain this value of CIA ratio: 1) the loss of Al during weathering of K-feldspars; 2) the removal (or accumulation?) of K by the buried organic matter in the form of plant litter and uppermost organic-rich soil horizons, and 3) the input of K, Al, Ca and Na from allochthonous sources.

Al loss during podzolisation usually affects O, A and E horizons (Melkerud et al., 2000; Olsson et al., 2000; Giesler et al., 2000); K incorporation may affect O horizon and the effect of the addition of allochthonous material depends on its origin (e.g., aeolian, morainic) and composition. Indeed, the incorporation of allochthonous material may lead to a “dilution” effect thus giving the underestimation of element content in the soil profile. As a result, even at zero level of chemical weathering intensity, the presence of moraine or aeolian material can lead to an underestimation or an overestimation of the CIA. Except a few samples mentioned above, most soils developed on mafic rocks show $\text{CIA}_s/\text{CIA}_r > 1$ which is higher than soils over granitic formation ($\text{CIA}_s/\text{CIA}_r \sim 1$). However, the dilution effect of the moraine is more important for basic rocks compared to acidic rocks because of the gneissic dominant nature of the moraine.

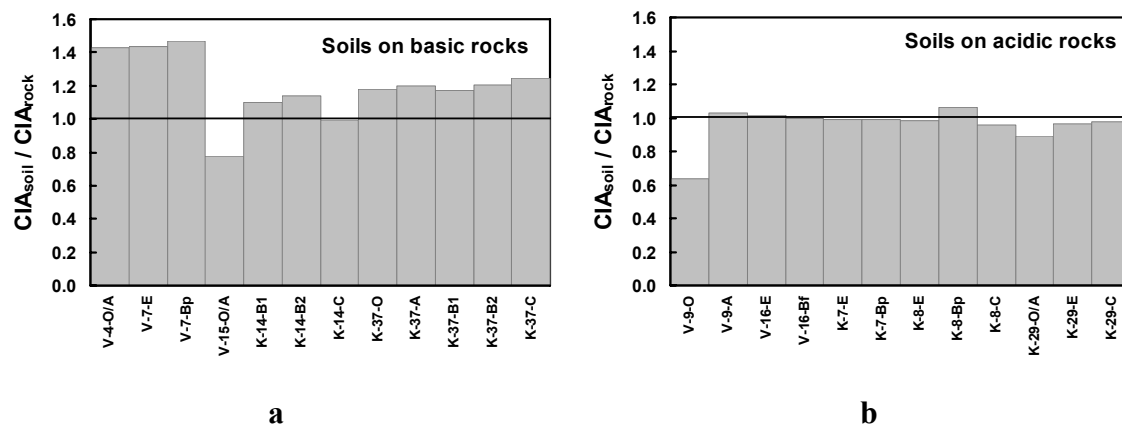


Fig. 2.5. Ration of Chemical Index of Alteration (CIA) of soils to that of rocks for soils developed on basic rocks (a) and on acidic rocks (b) from Vetreny Belt and Kivakka intrusion

Mineralogical studies performed on soils samples show ubiquitous quartz (and in some soils, zircon) independent on the nature of the parental rocks (i.e., mafic and felsic). The size of quartz grains varies from 10 to 450 µm and from 50 to 200 µm in soils developed on basic and granitic rocks, respectively, which precludes an aeolian origin of these quartz grains. In contrast, quaternary (Pleistocene) deposits observed even in the deepest horizons of some soil profiles (Fig. 2.6) confirm a strong moraine influence in this region.

2.5.1.2. REE upper crust normalized diagrams

The upper crust (Taylor and McLennan, 1985) normalized REE patterns for selected soil samples are plotted in Fig. 2.7. REE patterns of five horizons of a soil developed on gabbro-norites (sample K-37 from the Kivakka intrusion, Fig. 2.7 a) are different from those of the parent rock. We observe enrichment in LREE and depletion in HREE relative to the source rock. Enrichment in LREE was also observed by Öhlander et al. (1996) in B-horizons of spodosols developed on granitic till in northern Sweden, whereas E-horizons were depleted in all REE, with LREE being more depleted than HREE. According to this author, this secondary enrichment in B-horizons could be caused by adsorption on secondary oxy-hydroxides, on clay minerals or organic material, or by precipitation of secondary LREE enriched phosphates. Note that the higher affinity of LREE to adsorb on oxy(hydr)oxides and the tendency of HREE to form more stable dissolved complexes than LREE in solution (Bau, 1999) is in agreement with these tendencies.



Fig. 2.6. Photo of a podzol (K-7) developed on granito-gneiss from the Kivakka intrusion zone. Full scale quaternary (Pleistocene) deposits can be observed in the deepest horizon confirming a strong moraine influence in this region.

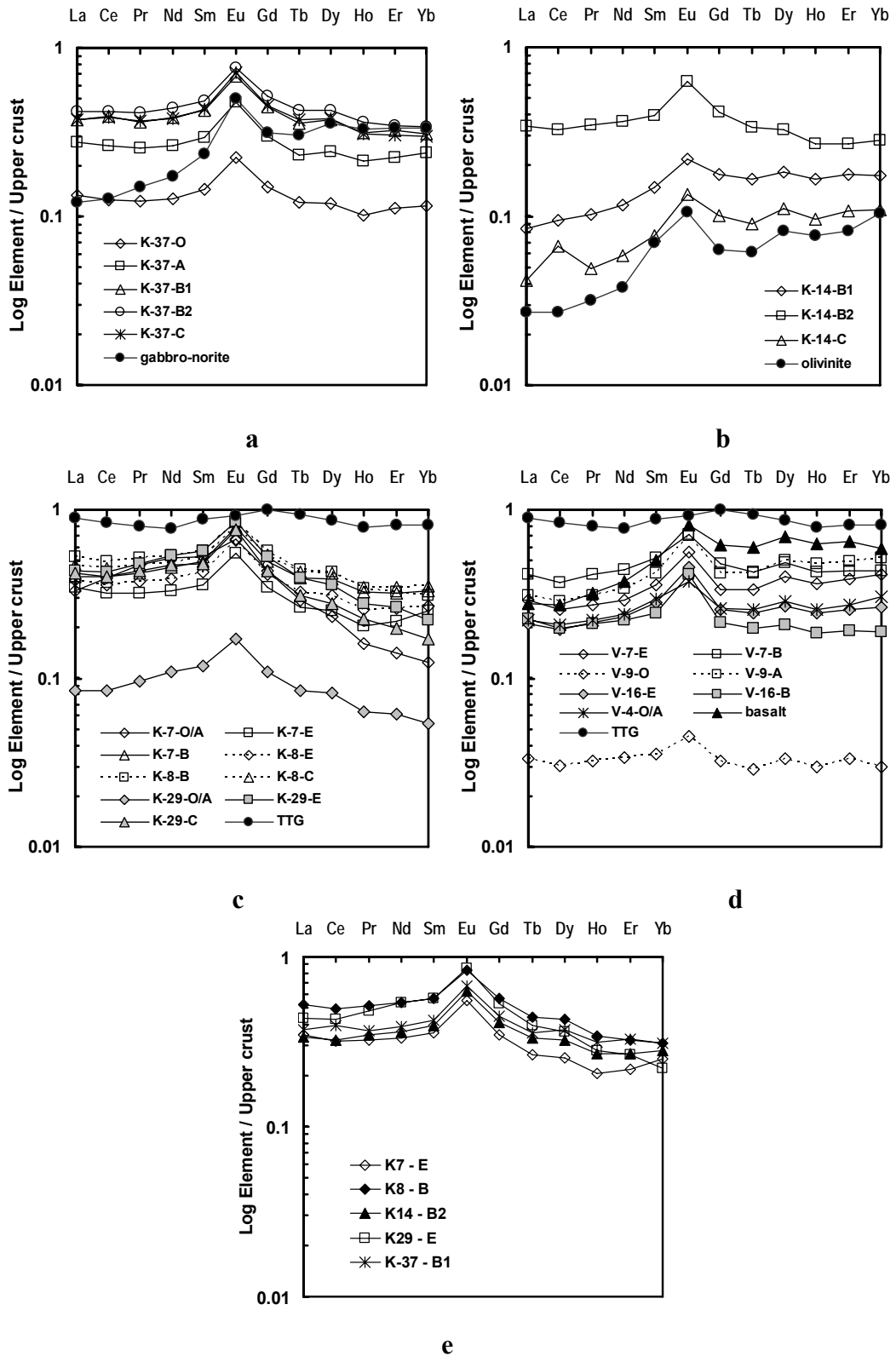


Fig. 2.7. Upper crust normalized REE patterns for soils from Kivakka intrusion (a, b, c), Vetreny Belt (d), and a mixed diagram on which E and B horizons of different soils are plotted (e). Average composition of the continental crust is taken from Taylor and MacLennan (1985); REE data on rocks of the Kivakka intrusion are from N. Krivolutskaya (unpublished data).

Olivinite rock is enriched in HREE, and the sample K-14 from the Kivakka intrusion (Fig. 2.7 b) is enriched in all REE relative to its parent rock for all horizons of the soil profile. On the contrary, soils developed on granitic rocks (samples K-7, K-8, K-29 from Kivakka intrusion, Fig. 2.7 c) have inverted REE concentrations with respect to the parent granite, all horizons being depleted in REE relative to the source rock. On the Fig. 2.7 d REE patterns of soils developed both on basic and granitic rocks in the Vetreny Belt zone are plotted. Soils developed on basalt (samples V-4 and V-7) are depleted in REE with respect to the parent rock except the B horizon of V-7 which is slightly enriched in LREE. Soils over granitic rock are also and more significantly depleted in all REE relative to the source TTG. However, it can be seen that the patterns of soils which have different origin (mafic or felsic) are quite similar. This is further illustrated in Fig. 2.7 e on which E or B horizons of different soils developed both on felsic (K-7, K-8, K-29) and mafic (K-14, K-37) rocks are plotted. It demonstrates that the REE fractionation in intermediate horizons in all studied soils is identical irrespective of the underlying rock. This is in agreement with observations of Lesovaya et al. (2008) on podzols and podzolized podburs on mafic substrates under influence of glacial moraine deposits in the mountainous taiga area in the northwest Russia. According to this author, the mineralogical effect of the admixture of gneiss-derived material is, in general, most pronounced in the E horizon.

Slight positive europium anomaly observed in majority of soil horizons is likely to be related to the presence of feldspar in the soil-rock system. Eu/Eu* (Table 2.2) is calculated using the formula (Condie, 1993):

$$\text{Eu/Eu}^* = \text{Eu}_N / (\text{Sm}_N \cdot \text{Gd}_N)^{1/2}$$

were $\text{Gd} = (\text{Sm} \cdot \text{Tb}^2)^{1/3}$. The ratio is within the range 0.87-1.05 for soils on basic rocks for both Vetreny Belt and Kivakka intrusion, and 0.88-1.18 and 0.91-1.09 for soils on granitic rocks for Vetreny Belt and Kivakka intrusion, correspondingly. It can be seen that the ratios are quite similar for granitic and basaltic soil-rock systems, again confirming the influence of exterior moraine deposits.

2.5.1.3. Extended upper crust normalized diagrams

The extended upper crust normalized patterns for the whole set of elements in studied samples are presented in Fig. 2.8: for soils both of granitic and basic origin from

the Kivakka intrusion site (samples K-7, K-8, K-29 and K-37, Fig. 2.8 a) and for soils from the Vetreny Belt site (samples V-7, V-9, V-16, V-4 and V-15, Fig. 2.8 b). It can be seen that all soils from the Kivakka intrusion zone (Fig. 2.8 a) exhibit quite similar upper-crust normalized trace elements patterns independent on their parent rock. The soils are generally depleted in most elements compared to the upper crust: Li, Sc, Mn, Co, Ni, Cu, Zn, As, Rb, Y, Zr, Nb, Mo, Cd (except surface horizons O/A of soils K-7, K-29 and K-37), Sb, Cs, Hf, Ta, W, Tl, Pb, Th, U. For these elements surface horizons O/A appear to be more depleted than the deeper ones. Olivinitic soil K-14 (not shown) exhibits a slightly different pattern, being less depleted in the above mentioned elements relative to the upper crust and enriched in Cr, Co, Zn and Ni, in accord with these elements elevated concentration in the source rocks. For some soil samples a slight enrichment in V (samples K-7-B, V-9-A, V-15-O/A), Cr (K-37 all horizons, V-15-O/A (significantly enriched), V-9-A, V-7-B), Sr (K-29, E and C horizons), Cd (K-7-O/A, K-37-O, V-9, O and A horizons, V-7-E) and Sb (K-7-O/A, K-29-O/A, V-9-O) relative to the upper crust can be observed. The last observation is also true for V-15 sample developed on ultramafic rocks.

The soils from the Vetreny Belt zone (Fig. 2.8 b) exhibit similar pattern independent on their parent rocks, and most of them are depleted in Sc, Ti, Co, Ni, Cu, Zn, Ge, Rb, Sr, Y, Zr, Nb, Cs, Hf, Ta, Th, U and significantly in Pb compared to the upper crust. The surface horizons O/A are depleted in V, Cd and Sb. A-horizon of soil V-9 and V-15 are enriched in Sc, V, Cr, Co, Ni, Cd, and all soils are significantly enriched in Tl with respect to the upper crust.

Overall, results on TE partitioning in soils corroborate the previous conclusion on the dominant role of glacial deposits on soil chemistry both on mafic and felsic rocks.

2.5.2. Actual weathering processes: waters versus soils and rocks

The degree of chemical weathering in studied systems can be illustrated using ternary diagram plotted in Al-K-(Ca+Na) molar coordinates (Fig. 2.9). The data for soils and rocks from boreal (Northern Europe: Melkerud et al., 2000; Tyler, 2004), temperate (Central Pyrenees, Estibère mountain zone: Oliva et al., 2004; Remaury et al., 2002; Debon et al., 1995) and tropical zones (Cameroon: Oliva et al., 1999; Braun et al.,

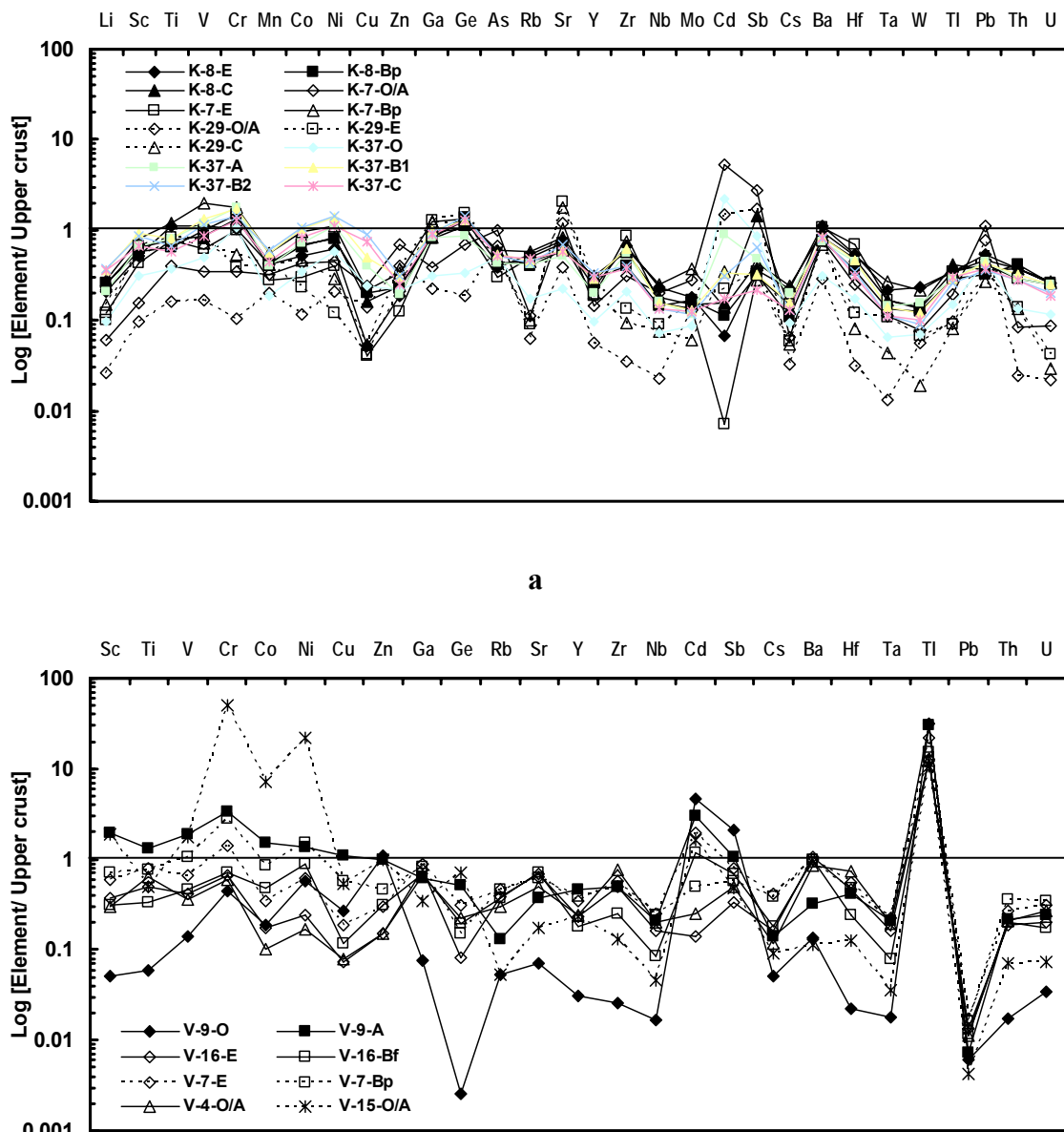


Fig. 2.8. Upper crust (Taylor and MacLennan, 1985) normalized extended elements patterns for soils developed on both granitic and basic rocks from the Kivakka intrusion zone (a) and Vetreny Belt zone (b).

1998) were also included in this diagram. In general, it can be seen that the composition of rocks and soils developed either on mafic rocks or on acidic does not differ much as it could be expected, even in comparison to soils and rocks of boreal zone, which are more altered and situated in the same zone on the diagram as a weathered granitic rock in tropical environment (Cameroon) and podzolic soils in mountain temperate zone

(Estibère). As demonstrated from previous mineralogical observations, this stems from the strong influence of the moraine glacial deposits on the chemical composition of soil profile irrespective of the parent rock composition. The direction of weathering process is similar to that in tropical and temperate systems (depletion in Ca and Na and enrichment in Al). For some samples, the slight K enrichment can be attributed to the “moraine addition” (i.e., K-feldspar).

A binary logarithmic diagram of the molar Ca/Na versus Mg/Na ratios is presented in Fig. 2.10. We reported here all data on rocks, soils and waters. Data on atmospheric precipitation in Karelian region are from Lozovik and Potapova, 2006. Carbonate, silicate and evaporite end-members are taken from Gaillardet et al. (1999). It can be seen in this diagram that the Ca/Na ratio ranges from 0.2 to 8.6 and 0.25 to 5.8 for soils and waters, respectively. The Mg/Na ratio varies between 0.15 and 8.9 for waters, and between 0.1 and 1.9 for soils with the highest ratio of 76.5 and 214.3 for the soil K-14 on olivinite (B_1 and C horizons, respectively). There is a good correlation between Ca/Na and Mg/Na ratios in soils and rocks, and in surface waters and rocks. The majority of samples from Kivakka intrusion and Vetreny Belt, except soils K-29 (horizon E) and K-14 (horizons B_1 and C) which drop out of the tendency, are located on the mixing line between silicate and carbonate end-members although no clear evidence of carbonate phases was previously described neither for rocks, nor for soils.

Lower Ca/Na and Mg/Na ratio for soils compared to rocks is consistent with the chemical weathering process, as calcium-rich phases usually weather more rapidly than sodium-rich phases in silicate environment. In this regard, the addition of moraine material enriched in Na (Na-K feldspar) can also explain this tendency. Lesovaya et al. (2008) observed the presence of moraine admixtures in mafic rock-soil systems, expressed in the lower content of calcium in podbur soils (in the middle taiga zone of Karelia) which, according to the author, can be due to the admixture of stable K-Na feldspars.

Stream waters are known to have higher Ca/Na molar ratio than rocks, and soils should exhibit lower Ca/Na ratio compared to the parent rocks (Gaillardet et al., 1999; Oliva et al., 2004). We observe different tendencies of the water composition: is the surface waters are situated either in the same region or shifted towards Ca or Mg enrichment compared to soils in the case of the Vetreny Belt rock-soil-water system.

For the case of Kivakka intrusion system, the surface fluids are located in between the soil and rock reservoirs reflecting the preferential mobilisation of sodium relative to calcium or magnesium in these surface waters in comparison to rocks. The waters from Vetreny Belt mafic rocks exhibit higher Mg/Na and lower Ca/Na ratios compared to Kivakka basic massif and surrounding felsic rocks which is in agreement with higher Mg concentrations in basalts of the Vetreny Belt (up to 20-25% MgO in spinifex-like structures, see Kulikov et al., 2005).

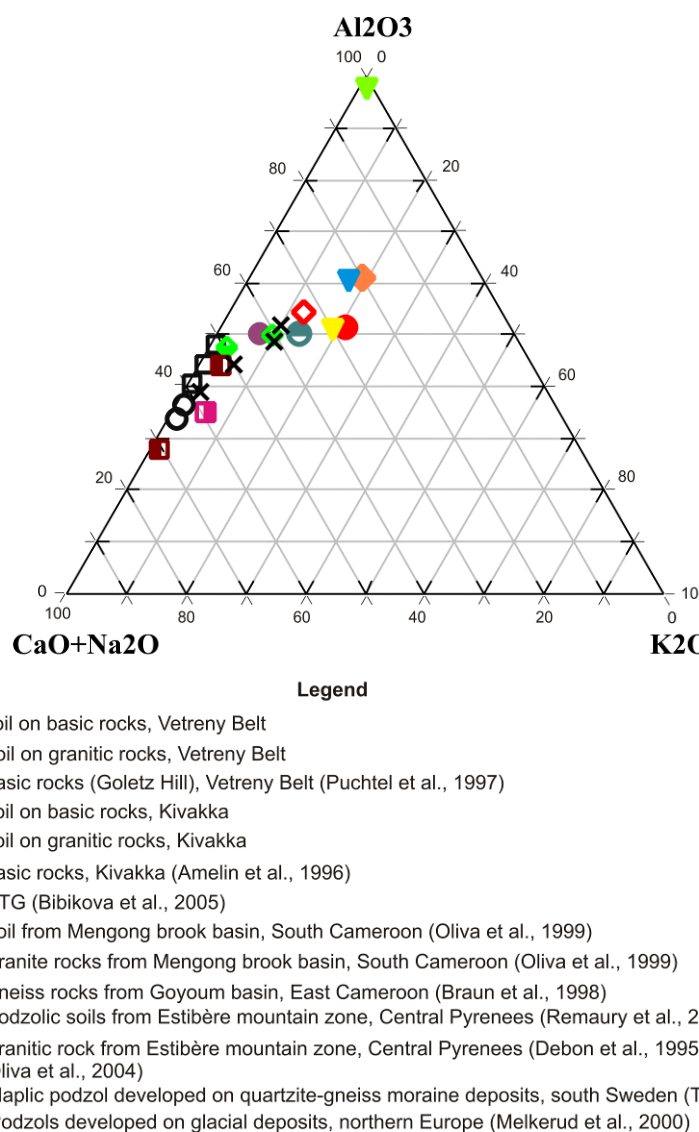


Fig. 2.9. Ternary molar diagram with rock and soil composition for the studied sites. Published elsewhere major cations data for soils and rocks from boreal (Melkerud et al., 2000; Tyler, 2004), temperate (Central Pyrenees, Estibère mountain zone: Oliva et al., 2004; Remaury et al., 2002; Debon et al., 1995) and tropical zones (Cameroon: Oliva et al., 1999; Braun et al., 1998) were taken for comparison.

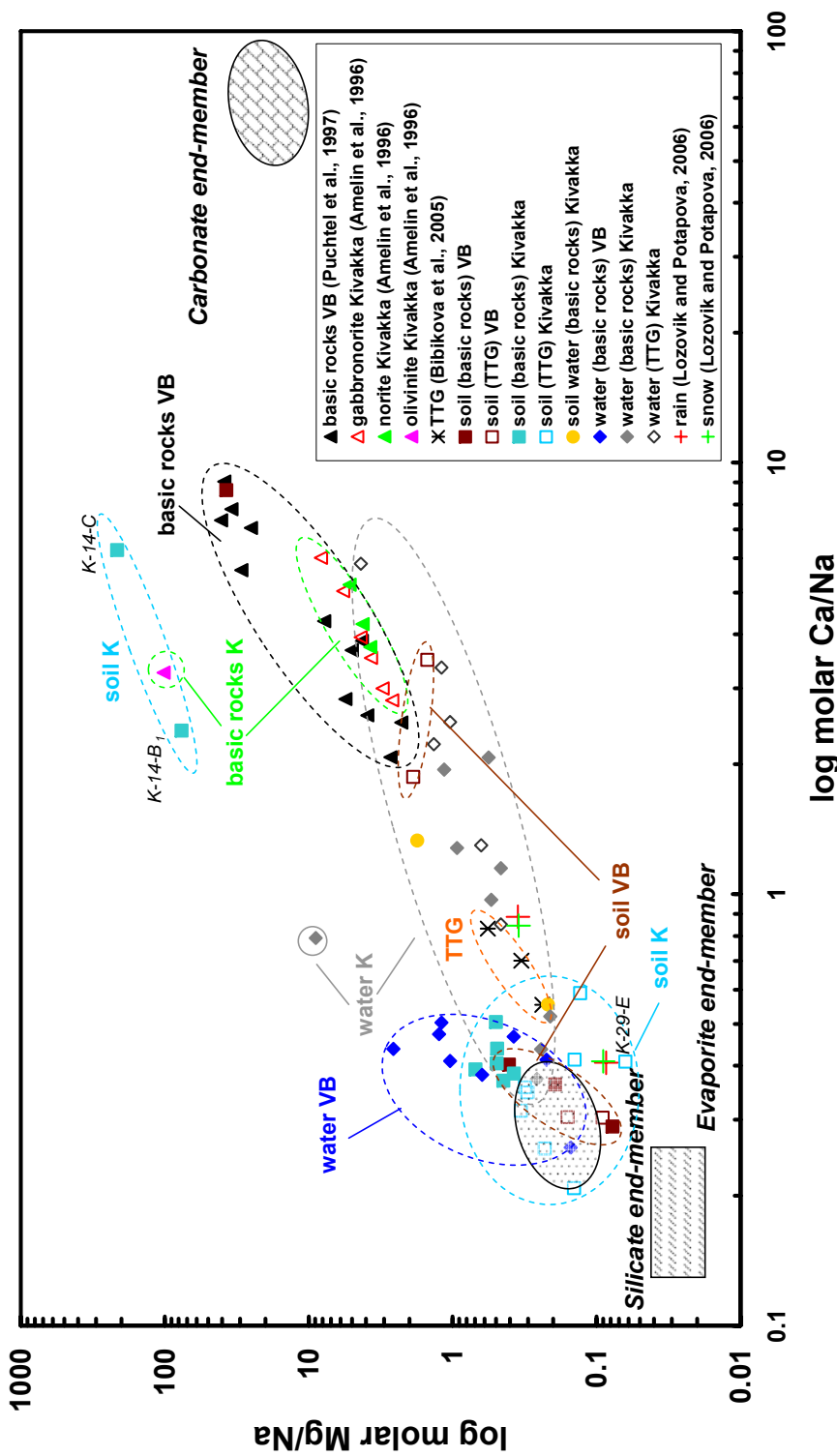


Fig. 2.10. Ca/Na molar ratios vs. Mg/Na molar ratios showing different materials (soils, rocks and waters) from Kivakka intrusion and Vetryny Belt (VB) zones. The carbonate, silicate, and evaporate end-members are taken from Gaillardet et al. (1999). Atmospheric signatures are calculated from the data reported by Lozovik and Potapova (2006). “VB” and “K” on the diagram stand for Vetryny Belt and Kivakka intrusion zones, respectively. Note that the scale of axes is different.

Unexpectedly, surface waters draining felsic environment show higher Ca/Na and Mg/Na molar ratios than waters draining mafic rocks. This relative enrichment in Na with respect to Ca and Mg in rivers from basaltic watersheds compared to granitic watershed may be explained by higher mobility of sodium compared to Ca and Mg during weathering process and the retention of Mg and Ca during secondary phases forming. It is possible that Ca and Mg, unlike Na, participate in secondary minerals formation in soils; for example, Mg-vermiculite. Some Ca and Mg rich phases (i.e., CaMg-amphibole) can also weather less rapidly than Na rich phase (i.e., feldspar) (Salminen et al., 2008).

The soil K-14 over olivinite (B and C horizons) exhibits a clear tendency of enrichment in Mg and Ca compared to Na during basic rock weathering. This is consistent with the presence of Mg-vermiculite and CaMg-amphibole in the clay fraction. The persistence of Ca-amphibole in such soil has been also observed by Lesovaya et al. (2008).

2.5.6. Isotope study

Another peculiar feature of soil and water geochemistry in considered zones is large variation of their Sr isotopic composition. Concentrations of Rb, Sr, Sm and Nd, and $^{87}\text{Sr}/^{86}\text{Sr}$ and $^{143}\text{Nd}/^{144}\text{Nd}$ isotopic ratios for soils from Vetreny Belt and Kivakka intrusion are listed in Table 2.2. Fig. 2.11 (a, b) presents a plot of $^{87}\text{Sr}/^{86}\text{Sr}$ versus $^{87}\text{Rb}/^{86}\text{Sr}$ isochrone for whole rocks, individual minerals, soil and water samples from the Vetreny Belt site and Kivakka intrusion site. Data for parent rocks and rock minerals for the Vetreny Belt are taken from Vasiliev (2006), for the Kivakka intrusion from Amelin and Semenov (1996) and Revyako et al. (2007). For the Kivakka intrusion (Fig. 2.11 a), soils developed on olivinite (K-14, the deepest horizon) and TTG (K-29) have lower $^{87}\text{Sr}/^{86}\text{Sr}$ ratios similar to the parent rock isotope ratios (Amelin and Semenov, 1996). The opposite tendency is obtained for other soils developed on basic and granitic rocks. The high $^{87}\text{Sr}/^{86}\text{Sr}$ ratios of “granitic” soils K-8 and K-7 (except the surface O/A horizon) are consistent with the high $^{87}\text{Rb}/^{86}\text{Sr}$ ratios of their parent rock granite-gneiss (Rb/Sr ratio for TTG was calculated from data reported in Bibikova et al., 2005). At the same time, the $^{87}\text{Sr}/^{86}\text{Sr}$ ratios of the samples K-7 and K-37 developed on gabbro-norites are similar to those of “granitic” K-8 being enriched in Rb, and having the same

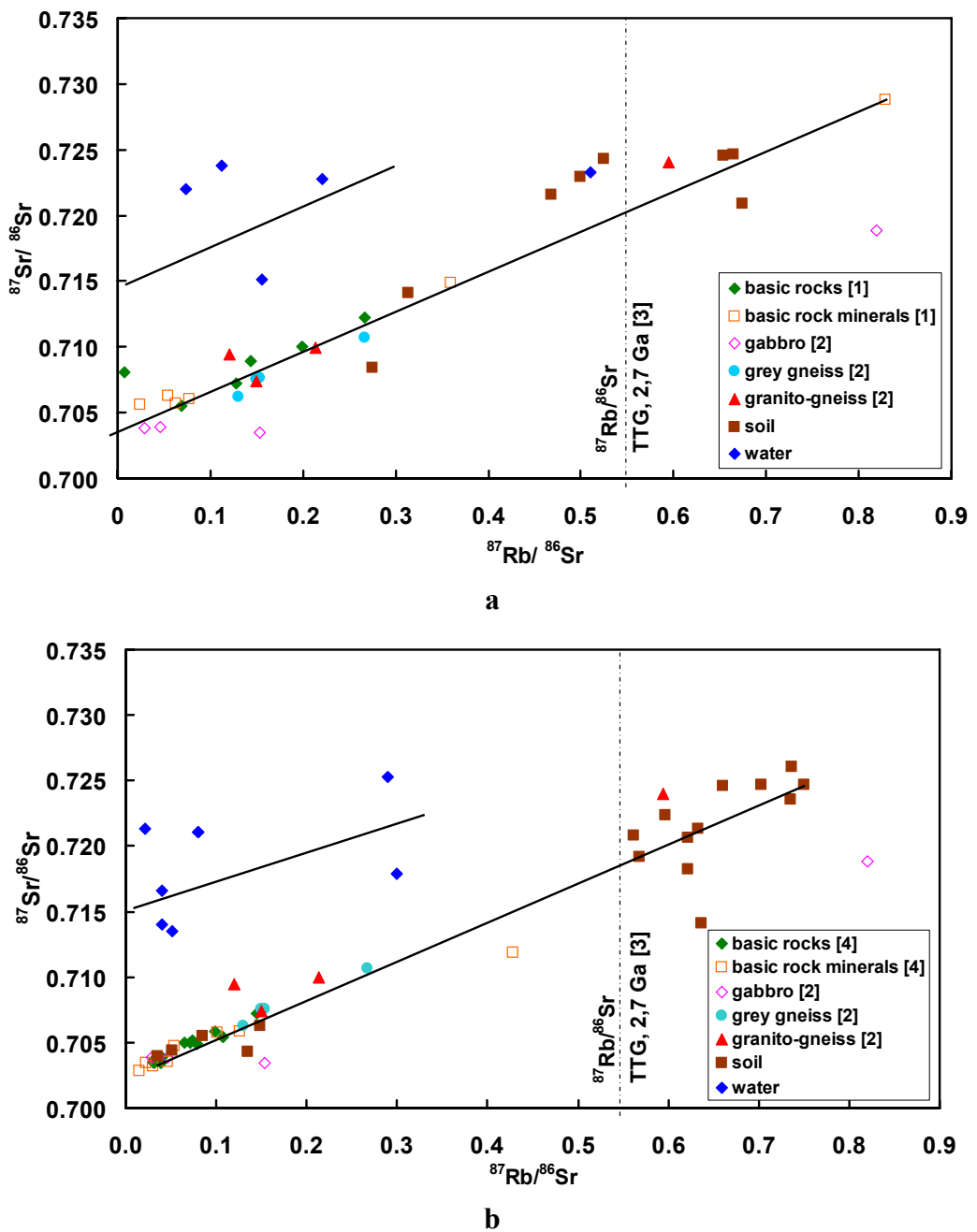


Fig. 2.11. Scatter diagram of $^{87}\text{Sr}/^{86}\text{Sr}$ vs. $^{87}\text{Rb}/^{86}\text{Sr}$ for the whole set of rocks, rock minerals, soils and waters: a – Kivakka intrusion, b – Vetryeny belt. $^{87}\text{Rb}/^{86}\text{Sr}$ isotope ratio for TTG showed as a vertical dotted line is calculated from data reported by Bibikova et al. (2005). Numbers in square brackets refer to: [1] Vasiliev M.V. (2006); [2] Revyako et al. (2007); [3] Bibikova et al. (2005); [4] Amelin and Semenov (1996).

$^{87}\text{Sr}/^{86}\text{Sr}$ ratio as estimated by Land et al. (2000) for podzols developed on Quaternary till of granitic composition in northern Sweden (0.721-0.727). Furthermore, soil horizons B₂ and C of ultramafic K-14, and B₂ of mafic K-37 have similar pedological characteristics to those of the B horizon of granitic K-7, and quite close isotope ratio ($^{87}\text{Sr}/^{86}\text{Sr} \sim 0.718$ and $^{87}\text{Rb}/^{86}\text{Sr} \sim 0.6$). This unambiguously suggests the strong influence of external (moraine) deposits. Surface waters have a more radiogenic signature ($^{87}\text{Sr}/^{86}\text{Sr}$ of waters = 0.714-0.725) than their parent rocks and primary minerals for “basic rock derived” samples, which is lower than that reported by Land et al. (2000) for stream waters (~ 0.74) draining felsic rocks in northern Sweden within the Kalix river watershed.

The soils developed on mafic rocks from Vetreny Belt zone (Fig. 2.11 b) exhibit close behaviour having $^{87}\text{Sr}/^{86}\text{Sr}$ and $^{87}\text{Rb}/^{86}\text{Sr}$ isotope ratios higher than their source rocks. Obviously, both for Kivakka intrusion and Vetreny Belt, all soils and rocks lie on a mixing line between two isotopically distinct endmembers, basic and granitic, rushing towards the granitic one.

Concerning isotopic composition of surface waters, the diagrams demonstrate two similar tendencies for both sites: *i*) waters show higher Sr isotopic ratios (between 0.715 and 0.730) compared to rocks and rock minerals (between 0.705 and 0.713) within the same range of $^{87}\text{Rb}/^{86}\text{Sr}$ ratios (from 0 to 0.4); *ii*) Sr isotope ratios of waters are in the same range as soils (except the soil V-15 from Vetreny Belt site) although soils have higher $^{87}\text{Rb}/^{86}\text{Sr}$ ratios (0.3-0.75) than water (< 0.3).

Overall, our results demonstrate high Sr and low Rb mobility in waters which is consistent with chemical preferential weathering of Sr-rich phases. This may be also due to the process of secondary minerals formation with Rb being incorporated into the clay minerals. Isotope signatures of waters draining mafic environment do not reflect the weathering of primary phases but rather more radiogenic minerals.

Note that the “apparent” age of soil material both on basic and granitic rocks from Kivakka intrusion calculated from the slope of the best fit line of $^{87}\text{Rb}/^{86}\text{Sr}$ isochrone is 2027 ± 166 My which corresponds to the age of rocks and rock minerals (2420 ± 23 and 2444 ± 1 My) reported elsewhere (Amelin and Semenov, 1990, 1996; Barkov et al., 1991). This implies the local nature of the moraine and the absence of aeolian input to the soil.

Our results invoke two hypothesis of the development of the soil-rock system:

1) During different stages of weathering, easily weatherable and less radiogenic minerals were strongly consumed throughout the full depth of examined soil profile. This provided to most of soils developed on mafic rocks a more radiogenic Sr isotopic signature compared to that of the parent rocks as it is especially pronounced in the surface horizons. In both cases of Kivakka intrusion and Vetreny Belt, we observe a shift of $^{87}\text{Sr}/^{86}\text{Sr}$ from ~ 0.705 (rocks) to 0.715-0.725 (soils). The same behaviour was observed for soils developed over mafic rocks in Central Siberia (Viers, personal communication);

2) All the granitic moraine influence in Karelian region has a more radiogenic signature than the studied rocks, but the exact chemical and isotopic composition of this moraine remains unknown.

2.5.7. Chemical weathering rates

In general, it can be seen that the composition of surface waters does not reflect a purely granitic or basic source being similar in all waters, except one Mg-rich surface water draining olivinite environment of the Kivakka intrusion (sample K-13-w). Saturation indices of surface waters draining both Kivakka and Vetreny Belt region demonstrate strong oversaturation with respect to $\text{Al}(\text{OH})_3$, boehmite, gibbsite, halloysite, imogolite, kaolinite, ferrihydrite (factor 10 to 10^6), undersaturation with respect to amorphous silica, and saturation index close to zero for quartz. Apparently, the amorphous, organic-rich Al and Fe oxyhydroxides and silicates constitute the major part of secondary phases in soils as it is well known for boreal zone (Lundström et al., 2000, Giesler et al., 2000). The particular feature of the soil K-14 is the occurrence of Mg-vermiculite and a high pH. Processes usually occurring in podzolic soils are rock dismantling, Al- and Fe-organic complexes forming, organic matter modification, oxidation of iron bearing primary phases, and amorphous alumino-silicate forming. However, podzolisation process is poorly known for its importance in the clay mineral formation which is relatively absent (Mokma et al., 2004). The K-14-C soil sample is the only sample which is not affected by moraine deposit, and thus, the only one which can be used for calculation of weathering rates of basic rocks. For comparison, calculations were also made for horizons K-14-B₂ (with respect to the parent rock) and

K-37-A and -B₁ (with respect to its C horizon). Our results give a long term TDS weathering rate of 1184 eq/ha/yr for olivinite rock, which is 4 times higher than the long term base cation flux (360 eq/ha/yr) and about 2 times higher than the actual TDS weathering rate (~700 eq/ha/yr) estimated by Land et al. (1999) for granitic till in northern Sweden. This value gives a long term weathering rate of ~1.5 t/km²/yr which is lower than the present day weathering rate estimated by Zakharova et al. (2007) and Pokrovsky et al. (2005b) for Karelian and Siberian mafic rocks, respectively. The same calculation for the horizon K-14-B₂ exhibit a TDS weathering rate about 3456 eq/ha/yr, but from the previous results, we know that this sample was affected by moraine depositions. Thus, if we do not consider moraine influence, this calculated value shows that weathering rates are significantly underestimated in this case. Calculations similar to those performed by Land et al. (1999) were performed for the soil K-29 (on granitic till). Calculation of weathering fluxes were conducted for A and B₁ horizons, and give the values 364 eq/ha/yr and 148 eq/ha/yr which are consistent with the fluxes reported by Land et al. (1999) for the granitic till.

These calculations demonstrate that the weathering rates of ultramafic rocks are higher than those for the granitic till, but dominated moraine depositions in this region hide the evidence of a real weathering process. Therefore, values estimated for the olivinite rock in this study appear to be lower than weathering rates estimated on the basis of surface water fluxes (Pokrovsky et al., 2005b; Zakharova et al., 2007). Retention of Mg and Ca in soil due to precipitation of secondary phases such as Mg-vermiculite or process of adsorption on mineral, organic or organo-mineral phases, can serve as an explanation of this discrepancy.

2.6. Conclusions

(1) Traces of chemical corrosion on the surface of zircons and feldspars along with the presence of new-formed amorphous matter on the surface of quartz, plagioclases and pyroxenes witness similar weathering processes on all types of parental rock. However, the lack of kaolinite neoformation and the persistence of amphibole and plagioclase feldspar in soils suggest not very intense weathering processes, in accordance with a start of pedogenesis about 10 Ky ago.

(2) The presence of quartz and zircons in soils developed on basic rocks, similarity of REE patterns of intermediate and deep soil horizons both for felsic and mafic rocks, as well as isotopic signature of soils on gabbro-norite and olivenite close to that of granodiorites raise a question of polycyclic nature of these soils (soil developed on fragments of already pre-existing soil), and assume their “contamination” with exterior deposits (e.g., granitic moraine).

(3) The relative enrichment in Na with respect to Ca and Mg in rivers from both granitic and basaltic watersheds raises the possibility of contribution to the river chemistry of other sources than primary silicate weathering reactions. We suggest that either Mg-vermiculite and Ca, Mg-amphibole formation in soils limits Ca and Mg export in waters, or there are highly weatherable Ca- and Mg-rich minerals present in granitic rocks. These specific features should be taken into account in the estimation of mafic rocks weathering rates and calculations of atmospheric CO₂ consumption by weathering in such a particular environment.

(4) In the cold subarctic climate, even thin deposits of glacial till moraine are capable of protecting mafic rocks to direct chemical weathering. In addition, over 10-15,000 years of exposure after last glaciation, full weathering soil profile on basic rocks could not be established.

(5) According to the calculations, the weathering rates of ultramafic rocks are higher than those for the granitic till, but dominated moraine depositions in this region hide the evidence of a real weathering process. Therefore, values estimated for the olivinite rock in this study appear to be lower than the weathering rates estimated on the basis of surface water fluxes for Karelian and Siberian mafic rocks in previous studies. Retention of Mg and Ca in soil due to precipitation of secondary phases such as Mg-vermiculite or process of adsorption on mineral, organic or organo-mineral phases, can serve as an explanation of this discrepancy.

References

- AFNOR (1996) *Qualité des sols. Recueil de normes Françaises*, Association Française de Normalisation, Paris.
- Akselsson, C.; Holmqvist, J.; Kurz, D. & Sverdrup, H. (2006), 'Relations between elemental content in till, mineralogy of till and bedrock mineralogy in the province of Småland, southern Sweden', *Geoderma* 136, 643-659.
- Alapieti, T. & Tuomo (1982), 'The Koillismaa layered igneous complex, Finland : its structure, mineralogy and geochemistry, with emphasis on the distribution of chromium', *Bull. Geol. Surv. Finl.* 319, 116.
- Allen, C.; Darmody, R.; Thorn, C.; Dixon, J. & Schlyter, P. (2001), 'Clay mineralogy, chemical weathering and landscape evolution in Arctic-Alpine Sweden', *Geoderma* 99, 277-294.
- Amelin, Y. & Semenov, V. (1990), 'On the age and sources of magmas for the early Proterozoic layered intrusions of Karelia (abstracts of papers)', *Isotopic dating of endogenic ore associations*, Tbilisi, 40-42.
- Amelin, Y. V.; Heaman, L. & Semenov, V. (1995), 'U-Pb geochronology of layered mafic intrusions in the eastern Baltic Shield: implications for the timing and duration of Paleoproterozoic continental rifting', *Precambrian Res.* 75, 31-46.
- Amelin, Y. V. & Semenov, V. S. (1996), 'Nd and Sr isotopic geochemistry of mafic layered intrusions in the eastern Baltic shield: implications for the evolution of Paleoproterozoic continental mafic magmas', *Contrib. Mineral. Petrol.* 124, 255-272.
- Anderson, H.; Berrow, M.; Farmer, V.; Hepburn, A.; Russell, J. & Walker, A. (1982), 'A reassessment of podzol formation processes', *J. Soil Sci.* 33, 125-136.
- Andersson, P. S.; Porcelli, D.; Gustafsson, O.; Ingri, J. & Wasserburg, G. J. (2001), 'The importance of colloids for the behavior of uranium isotopes in the low-salinity zone of a stable estuary', *Geochim. Cosmochim. Acta* 65(1), 13-25.
- Andersson, K.; Dahlqvist, R.; Turner, D.; Stolpe, B.; Larsson, T.; Ingri, J. & Andersson, P. (2006), 'Colloidal rare earth elements in a boreal river: Changing sources and distributions during the spring flood', *Geochim. Cosmochim. Acta* 70, 3261-3274.
- Balashov, Y. A.; Bayanova, T. B. & Mitrofanov, F. P. (1993), 'Isotope data on the age and genesis of layered basic-ultrabasic intrusions in the Kola Peninsula and northern Karelia, northeastern Baltic Shield', *Precambrian Res.* 64, 197-205.
- Barkov, A.; Gannibal, L.; Ryunginen, G. & Balashov, Y. (1991), 'Zircon dating of the Kivakka layeres massif, Northern Karelia. Abstracts of papers', *All-Union seminar on methods of isotopic geology, Zvenigorod, 21-25 October 1991*, St.

Petersburg, 21-23.

- Bau, M. (1999), 'Scavenging of dissolved yttrium and rare earths by precipitating iron oxyhydroxide: Experimental evidence for Ce oxidation, Y-Ho fractionation, and lanthanide tetrad effect', *Geochim. Cosmochim. Acta* 63, 67-77.
- Berner, R. A.; Lasaga, A. C. & Garrels, R. M. (1983), 'The carbonate-silicate geochemical cycle and its effect on atmospheric carbon dioxide over the past 100 million years', *American Journal of Science* 283, 641-683.
- Berner, R. (1992), 'Weathering, plants, and the long-term carbon cycle', *Geochim. Cosmochim. Acta* 56(8), 3225-3231.
- Berner, R. (1995), 'Chemical weathering and its effect on atmospheric CO₂ and climate', *Reviews in mineralogy and geochemistry* 31(1), 565-583.
- Berner, R. A. & Maasch, K. A. (1996), 'Chemical weathering and controls on atmospheric O₂ and CO₂: Fundamental principles were enunciated by J. J. Ebelmen in 1845', *Geochim. Cosmochim. Acta* 60(9), 1633-1637.
- Berner, R. A. & Kothavala, Z. (2001), 'Geocarb III: a revised model of atmospheric CO₂ over phanerozoic time', *American Journal of Science* 301, 182-204.
- Bibikova, E.; Skiodl, T.; Bogdanova, S.; Gorbatschev, R. & Slabunov, A. (2001), 'Titanite-rutile thermochronometry across the boundary between the Archaean Craton in Karelia and the Belomorian Mobile Belt, eastern Baltic Shield', *Precambrian Res.* 105, 315-330.
- Bibikova, E. V.; Samsonov, A. V.; Petrova, A. Y. & Kirnozova, T. I. (2005), 'The Archean geochronology of Western Karelia', *Stratigraphy and Geological Correlation* 13(5), 459-475.
- Boeglin, J. & Probst, J. (1998), 'Physical and chemical weathering rates and CO₂ consumption in a tropical lateritic environment: the upper Niger basin', *Chem. Geol.* 148(3-4), 137-156.
- Brady, P. V. (1991), 'The Effect of Silicate Weathering on Global Temperature and Atmospheric CO₂', *Journal of Geophysical Research* 96(B11), 18101-18106.
- Braun, J.; Viers, J.; Dupré, B.; Polve, M.; Ndam, J. & Muller, J. (1998), 'Solid/ liquid REE fractionation in the lateritic systems of the Goyoum, East Cameroon: The implication for the present dynamics of the soil covers of the humid tropical regions', *Geochim. Cosmochim. Acta* 62(2), 273-299.
- van Breemen, N. & Buurman, P. (1998), *Soil Formation*, chapter Podzolization, pp. 245-270.
- Buurman, P. (1984), *Podzols*. Van-Nostand Reinhold Soil Science Series. ISBN-0-442-21129-5. Campbell, I.B., Claridge, G.G., 1987. *Antartica-Soils, Weathering Process and Climate*. Elsevier, New York.

-
- Buurman, P. & Jongmans, A. (2005), 'Podzolisation and soil organic matter dynamics', *Geoderma* 125(1-2), 71-83.
- Bychkova, Y. V. (2003), 'Autoref: Zakonomernosti stroeniya kontrastnoi pitmicheskoi rassloennosti v Kivakkskom intruzive', PhD thesis, MGU, Geologicheskogo f-t.
- Bychkova, Y. & Koptev-Dvornikov, E. (2004), 'Rhythmic layering of Kivakka type: geology, petrology, petrochemistry, hypothesis of formation (in Russian)', *Petrology* 12(3), 281-302.
- Bychkova, Y. V.; Koptev-Dvornikov, E. V.; Kononkova, N. N. & Kameneva, E. E. (2007), 'Composition of rock-forming minerals in the Kivakka layered massif, Northern Karelia, and systematic variations in the chemistries of minerals in the rhythmic layering subzone', *Geochemistry International* 45(2), 131–151.
- de Caritat, P.; Reimann, C.; Bogatyrev, I.; Chekushin, V.; Finne, T. E.; Halleraker, J. H.; Kashulina, G.; Niskavaara, H.; Pavlov, V. & Ayras, M. (2001), 'Regional distribution of Al, B, Ba, Ca, K, La, Mg, Mn, Na, P, Rb, Si, Sr, Th, U and Y in terrestrial moss within a 188,000 km² area of the central Barents region: influence of geology, seaspray and human activity', *Appl. Geochem.* 16, 137-159.
- Condie, K. C. (1993), 'Chemical composition and evolution of the upper continental crust: Contrasting results from surface samples and shales', *Chem. Geol.* 104(1-4), 1-37.
- Cornu, S.; Lucas, Y.; Lebon, E.; Ambrosi, J. P.; Luizão, F.; Rouiller, J.; Bonnay, M. & Neal, C. (1999), 'Evidence of titanium mobility in soil profiles, Manaus, central Amazonia', *Geoderma* 91(3-4), 281-295.
- Courchesne, F. & Hendershot, W. (1997), 'Essai. La Genèse des podzols', *Geogr. Phys. Quarter.* 51, 235-250.
- Dahlqvist, R.; Benedetti, M. F.; Andersson, K.; Turner, D.; Larsson, T.; Stolpe, B. & Ingri, J. (2004), 'Association of calcium with colloidal particles and speciation of calcium in the Kalix and Amazon rivers', *Geochim. Cosmochim. Acta* 68(20), 4059-4075.
- Dahlqvist, R.; Andersson, P.; Ingri, J. & Porcelli, D. (2006), 'Vertical REE profiles in water and DGT in the central Arctic Ocean', *Goldschmidt Conference Abstracts*.
- Dahlqvist, R.; Andersson, K.; Ingri, J.; Larsson, T.; Stolpe, B. & Turner, D. (2007), 'Temporal variations of colloidal carrier phases and associated trace elements in a boreal river', *Geochim. Cosmochim. Acta* 71, 5339-5354.
- D'Amico, M.; Julitta, F.; Previtali, F. & Cantelli, D. (2008), 'Podzolization over ophiolitic materials in the western Alps (Natural Park of Mont Avic, Aosta Valley, Italy)', *Geoderma* 146, 129-137.
- Darmody, R.; Thorn, C.; Harder, R.; Schlyter, J. & Dixon, J. (2000), 'Weathering implications of water chemistry in an arctic-alpine environment, northern

-
- Sweden', *Geomorphology* 34, 89-100.
- Debon, F.; Enrique, P. & Autran, A. (1995), 'Magmatisme Hercynien', *Synthèse géologique et géophysique des Pyrénées. Edt BRGM 1*, Cycle Hercynien (eds. A. Barnolas and J. C. Chiron), 361-499.
- DePaolo, D. & Wasserburg, G. (1976), 'Inferences about magma sources and mantle structure from variations of $^{143}\text{Nd}/^{144}\text{Nd}$ ', *Geophys. Res. Lett.* 3, 249-252.
- DePaolo, D. J. (1981), 'Neodymium isotopes in the Colorado Front Range and crust-mantle evolution in the Proterozoic', *Nature* 291, 193-196.
- DePaolo, D. (1988), *Neodimium isotope geochemistry*, Springer-Verlag, New York.
- Dessert, C.; Dupré, B.; Francois, L. M.; Schott, J.; Gaillardet, J.; Chakrapani, G. & Bajpai, S. (2001), 'Erosion of Deccan Traps determined by river geochemistry: impact on the global climate and the $^{87}\text{Sr}/^{86}\text{Sr}$ ratio of seawater', *Earth Planet. Sci. Lett.* 188, 459-474.
- Dessert, C.; Dupré, B.; Gaillardet, J.; François, L. M. & Allègre, C. J. (2003), 'Basalt weathering laws and the impact of basalt weathering on the global carbon cycle', *Chem. Geol.* 202, 257– 273.
- Dokuchaev, V. (1880), 'O podzole', *Trudy Volnogo ekonomicheskogo obschestva* 1(2).
- Dupré, B.; Gaillardet, J.; Rousseau, D. & Allègre, C. J. (1996), 'Major and trace elements of river-borne material: The Congo Basin', *Geochim. Cosmochim. Acta* 60(8), 1301-1321.
- Dupré, B.; Dessert, C.; Oliva, P.; Godderis, Y.; Viers, J.; Francois, L.; Millot, R. & Gaillardet, J. (2003), 'Rivers, chemical weathering and Earth's climate', *C. R. Geoscience* 335, 1141–1160.
- Fedo, C. M.; Nesbitt, H. W. & Young, G. M. (1995), 'Unraveling the effects of potassium metasomatism in sedimentary rocks and paleosols, with implications for paleoweathering conditions and provenance', *Geology* 23(10), 921-924.
- Feoktistov, V. M. (2004), 'Water Chemical Composition of Karelian Rivers and Their Dissolved Chemical Discharge into the White Sea', *Water Resour.* 31(6), 631-638.
- Gaillardet, J.; Dupré, B.; Louvat, P. & Allègre, C. (1999), 'Global silicate weathering and CO₂ consumption rates deduced from the chemistry of large rivers', *Chem. Geol.* 159, 3-30.
- Georgievsky, A. (1888), 'K voprosu o podzole', *Materialy po izucheniu russkikh pochv* 4.
- Giesler, R.; Ilvesniemi, H.; Nyberg, L.; van Hees, P.; Starr, M.; Bishop, K.; Kareinen, T. & Lundström, U. (2000), 'Distribution and mobilization of Al, Fe and Si in three podzolic soil profiles in relation to the humus layer', *Geoderma* 94, 249-

- Gislason, S. R.; Arnorsson, S. & Armannsson, H. (1996), 'Chemical weathering of basalt in Southwest Iceland; effects of runoff, age of rocks and vegetative/glacial cover', *American Journal of Science* 296, 837-907.
- Glinka, K. (1932), *Pochvovedenie*, M.-L.: Selhozgiz.
- Goldstein, S.; O'Nions, R. & Hamilton, P. (1984), 'A Sm-Nd study of atmospheric dusts and particulates from major river system', *Earth Planet. Sci. Lett.* 70, 221-236.
- Grard, A.; François, L.; Dessert, C.; Dupré, B. & Goddériss, Y. (2005), 'Basaltic volcanism and mass extinction at the Permo-Triassic boundary: Environmental impact and modeling of the global carbon cycle', *Earth Planet. Sci. Lett.* 234(1-2), 207-221.
- Hättestrand, C. (1997), 'Ribbed moraines in Sweden distribution pattern and palaeoglaciological implications', *Sedimentary Geology* 111, 41-56.
- Ingri, J.; Widerlund, A.; Land, M.; Gustafsson, O.; Andersson, P. S. & Öhlander, B. (2000), 'Temporal variations in the fractionation of the rare earth elements in a boreal river; the role of colloidal particles.', *Chem. Geol.* 166, 23-45.
- Ingri, J.; Widerlund, A. & Land, M. (2005), 'Geochemistry of Major Elements in a Pristine Boreal River System; Hydrological Compartments and Flow Paths', *Aquatic Geochemistry* 11, 57-88.
- Jacobsen, S. B. & Wasserburg, G. (1980), 'Sm-Nd isotopic evolution of chondrites', *Earth Planet. Sci. Lett.* 50(1), 139-155.
- Kempton, P. D.; Downes, H.; Neymark, L. A.; Wartho, J. A.; Zartman, R. E. & Sharkov, E. V. (2001), 'Garnet granulite xenoliths from the northern Baltic Shield—the underplated lower crust of a palaeoproterozoic large igneous province?', *J. Petrol.* 42(4), 731-763.
- Klyunin, S.; Grokhovskaya, T.; Zakharov, A. & Solov'eva, T. (1994), 'Geology and platinum-bearing potential of the Olanga group of massifs, Northern Karelia', *Geologiya i genesis mestorozhdenii platinovykh metallov (Geology and genesis of PGE deposits)*, Nauka, Moscow, 111-126.
- Koptev-Dvornikov (2001), 'Distribution of cumulative mineral assemblages, major and trace elements over the vertical section of the Kivakka intrusion, Olanga group of intrusions, Northern Karelia', *Petrology* 9(1), 3-27.
- Kulikov, V. & Kulikova, V. (1982), 'On the summary section of the early Precambrian of the Vetreny belt (in Russian)', *Geology and Stratigraphy of the Karelian Precambrian Rocks. Petrozavodsk, Year Book Information*, 21-26.
- Kulikov, V. (1999), 'Komatiitic Basalts of the Vetreny Belt (Karel. Nauch. Tsentr, Petrozavodsk) (in Russian)', *Selected Works of the Karelian Scientific Center of*

Russian Academy of Sciences, 60-61.

- Kulikov, V.; Kulikova, V.; Bychkova, Y. & Zudin, A. (2003), 'Sumiiskii riftovyi vulkanizm paleoproterozooya yugo-vostochnoi chasti Karel'skogo kratona', *Materialy II Vserossiiskogo simpoziuma po vulkanologii i paleovulkanologii "Vulkanizm i geodinamika"*, Ekaterinburg, 99-104.
- Kulikov, V.; Bychkova, Y.; Kulikova, V.; Koptev-Dvornikov, E. & Zudin, A. (2005), 'Role of deep-seated differentiation in formation of Paleoproterozoic Sinegorie lava plateau of komatiite basalts, southeastern Fennoscandia', *Petrology* 13(5), 469-488.
- Kulikova, V. V. & Kulikov, V. S. (1981), 'New Data on Archean Peridotitic Komatiites in East Karelia', *Dokl. Akad. Nauk SSSR* 259(3), 693-697.
- Kump, L. R.; Brantley, S. L. & Arthur, M. A. (2000), 'Chemical weathering, atmospheric CO₂, and climate', *Annu. Rev. Earth Planet. Sci. Lett.* 28, 611-667.
- Land, M.; Ingri, J. & Öhlander, B. (1999a), 'Past and present weathering rates in northern Sweden', *Appl. Geochem.* 14, 761-774.
- Land, M.; Öhlander, B.; Ingri, J. & Thunberg, J. (1999b), 'Solid speciation and fractionation of rare earth elements in a spodosol profile from northern Sweden as revealed by sequential extraction', *Chem. Geol.* 160, 121-138.
- Land, M.; Ingri, J.; Andersson, P. S. & Öhlander, B. (2000), 'Ba/Sr, Ca/Sr and ⁸⁷Sr/⁸⁶Sr ratios in soil water and groundwater: implications for relative contributions to stream water discharge', *Appl. Geochem.* 15, 311-325.
- Land, M. & Öhlander, B. (2000), 'Chemical weathering rates, erosion rates and mobility of major and trace elements in a boreal granitic till', *Aquat. Geochem.* 6, 435-460.
- Land, M.; Thunberg, J. & Öhlander, B. (2002), 'Trace metal occurrence in a mineralised and a non-mineralised spodosol in northern Sweden', *J. Geochem. Explor.* 75, 71-91.
- Lavrov, M. (1979), 'Giperbazity i rassloennye peridotite-gabbro-noritovye intruzii dokembriya Severnoi Karelii (Ultramafics and layered peridotite-gabbro-norite intrusions in the Precambrian of Northern Karelia)', *Nauka, Leningrad*.
- Lesovaya, S.; Goryachkin, S.; Pogozhev, E.; Polekhovskii, Y.; Zavarzin, A. & Zavarzina, A. (2008), 'Soils on hard rocks in the Northwest of Russia: Chemical and mineralogical properties, genesis, and classification problems', *Eurasian Soil Science* 41(4), 363-376.
- Lobach-Zhuchenko, S.; Levchenkov, O.; Cherulaev, V. & Krylov, I. (1986), 'Geological evolution of the Karelian granite-greenstone terrain', *Precambrian Res.* 33(1-3), 45-65.

-
- Lobach-Zhuchenko, S.; Chekulayev, V.; Sergeev, S.; Levchenkov, O. & Krylov, I. (1993), 'Archaean rocks from southeastern Karelia (Karelian granite greenstone terrain)', *Precambrian Res.* 62(4), 375-397.
- Lobach-Zhuchenko, S.; Arrestova, N.; Chekulaev, V.; Levsky, L.; Bogomolov, E. & Krylov, I. (1998), 'Geochemistry and petrology of 2.40-2.45 Ga magmatic rocks in the north-western Belomorian Belt, Fennoscandian Shield, Russia', *Precambrian Res.* 92, 223-250.
- Louvat, P. & Allègre, C. J. (1997), 'Present denudation rates on the island of Réunion determined by river geochemistry: Basalt weathering and mass budget between chemical and mechanical erosions', *Geochim. Cosmochim. Acta* 61(17), 3645-3669.
- Louvat, P. & Allègre, C. J. (1998), 'Riverine erosion rates on Sao Miguel volcanic island, Azores archipelago', *Chem. Geol.* 148(3-4), 177-200.
- Lozovik, P. & Potapova, I. (2006), 'Input of chemical substances with atmospheric precipitation onto the territory of Karelia', *Water Resour.* 33(1), 104-111.
- Lundström, U. (1993), 'The role of organic acids in soil solution chemistry in a podzolized soil', *J. Soil Sci.* 44, 121-133.
- Lundström, U. S.; van Breemen, N. & Bain, D. (2000a), 'The podzolization process. A review.', *Geoderma* 94, 91-107.
- Lundström, U. S.; van Breemen, N.; Bain, D. et al. (2000b), 'Advances in understanding the podzolization process resulting from a multidisciplinary study of three coniferous forest soils in the Nordic Countries', *Geoderma* 94(2-4), 335-353.
- Maksimova, M. (1967), 'Inorganic and organic composition of major ions in rivers of Karelian coast of the White Sea (in Russian)', *Gidrobiologicheskie issledovaniya na Karel'skom poberezh'ye Belogo morya. Nauka, Leningrad*, 9-20.
- Melkerud, P.; Bain, D.; Jongmans, A. & Tarvainen, T. (2000), 'Chemical, mineralogical and morphological characterization of three podzols developed on glacial deposits in Northern Europe', *Geoderma* 94, 125-148.
- Millot, R.; Gaillardet, J.; Dupré, B. & Allègre, C. J. (2003), 'Northern latitude chemical weathering rates: Clues from the Mackenzie River basin, Canada', *Geochim. Cosmochim. Acta* 67(7), 1305-1329.
- Mokma, D.; Yli-Halla, M. & Lindqvist, K. (2004), 'Podzol formation in sandy soils of Finland', *Geoderma* 120, 259-272.
- Muir, A. (1961), 'The podzol and podzolic soils', *Advances in Agronomy* 13, 1-56.
- Murashkina, M.; Southard, R. & Pettygrove, G. (2007), 'Silt and fine sand fractions dominate K fixation in soils derived from granitic alluvium of the San Joaquin Valley, California', *Geoderma* 141, 283-293.

-
- Nesbitt, H. W. & Young, G. M. (1982), Early Proterozoic climates and plate motions inferred from major element chemistry of lutites: *Nature* 299, 715-717.
- Öhlander, B.; Ingri, J. & Ponter, C. (1991), 'Geochemistry of till weathering in the Kalix River Watershed, northern Sweden. Reports in Forest Ecology and Forest Soils, Swedish University of Agricultural Sciences', In: *Chemical Weathering Under Field Conditions* (ed. K. Rosén). Report 63, 1-18.
- Öhlander, B.; Land, M.; Ingri, J. & Widerlund, A. (1996), 'Mobility of rare earth elements during weathering of till in northern Sweden', *Appl. Geochem.* 11, 93-99.
- Öhlander, B.; Thunberg, J.; Land, M.; Hoglund, L. O. & Quishang, H. (2003), 'Redistribution of trace metals in a mineralized spodosol due to weathering, Liikavaara, northern Sweden', *Appl. Geochem.* 18, 883-899.
- Oliva, P.; Viers, J.; Dupré, B.; Fortune, J. P.; Martin, F.; Braun, J.; Nahon, D. & Robain, H. (1999), 'The effect of organic matter on chemical weathering: Study of a small tropical watershed: Nsimi-Zoétélé site, Cameroon', *Geochim. Cosmochim. Acta* 63(23/24), 4013-4035.
- Oliva, P.; Dupré, B.; Martin, F. & Viers, J. (2004), 'The role of trace minerals in chemical weathering in a high-elevation granitic watershed (Estibère, France): Chemical and mineralogical evidence', *Geochim. Cosmochim. Acta* 68(10), 2223-2244.
- Olsson, M. T. & Melkerud, P. (2000), 'Weathering in three podzolized pedons on glacial deposits in northern Sweden and central Finland', *Geoderma* 94, 149-161.
- Perelman, A. (1974), 'Pochva kak biokosnaya sistema zemnoi kory"Trudy X Mezhdunarodnogo kongressa pochvovedov', M.: Nauka.
- Peuraniemi, V. (1982), 'Geochemistry of till and mode of occurrence of metals in some moraine types in Finland', *Geol. Surv. Finland Bull.* 322, 75.
- Peuraniemi, V.; Aario, R. & Pulkkinen, P. (1997), 'Mineralogy and geochemistry of the clay fraction of till in northern Finland', *Sedimentary Geology* 111, 313-327.
- Pokrovsky, O. & Schott, J. (2002), 'Iron colloids/organic matter associated transport of major and trace elements in small boreal rivers and their estuaries (NW Russia)', *Chem. Geol.* 190, 141-179.
- Pokrovsky, O.; Schott, J.; Kudryavtsev, D. I. & Dupré, B. (2005b), 'Basalt weathering in Central Siberia under permafrost conditions', *Geochim. Cosmochim. Acta* 69(24), 5659-5680.
- Pokrovsky, O. S.; Schott, J. & Dupré, B. (2006a), 'Trace element fractionation and transport in boreal rivers and soil porewaters of permafrost-dominated basaltic terrain in Central Siberia', *Geochim. Cosmochim. Acta* 70, 3239-3260.

-
- Pokrovsky, O.; Schott, J. & Dupré, B. (2006b), 'Basalt weathering and trace elements migration in the boreal Arctic zone', *J. Geochem. Explor.* 88, 304-307.
- Ponomareva, V. (1964), *Teoria podzoloobrazovatel'nogo processa (Theory of podzol-formation process)*, M.-L.: Nauka (in Russian).
- Puchtel, I.; Hofmann, A.; Mezger, K.; Shchipansky, A.; Kulikov, V. & Kulikova, V. (1996), 'Petrology of a 2.41 Ga remarkably fresh komatiitic basalt lava lake in Lion Hills, central Vetreny Belt, Baltic Shield', *Contrib. Mineral. Petrol.* 124(3-4), 273-290.
- Puchtel, I. S.; Haase, K. M.; Hofmann, A. W.; Chauvel, C.; Kulikov, V. S.; Garbe-Schonberg, C. & Nemchin, A. A. (1997), 'Petrology and geochemistry of crustally contaminated komatiitic basalts from the Vetreny Belt, southeastern Baltic Shield: Evidence for an early Proterozoic mantle plume beneath rifted Archean continental lithosphere', *Geochim. Cosmochim. Acta* 61(6), 1205-1222.
- Reimann, C. & Melezhik, V. (2001), 'Metallogenic provinces, geochemical provinces and regional geology - what causes large-scale patterns in low density geochemical maps of the C-horizon of podzols in Arctic Europe?', *Appl. Geochem.* 16(7-8), 963-983.
- Remaury, M.; Oliva, P.; Guillet, B.; Martin, F.; Toutain, F.; Dagnac, J.; Belet, J.; Dupré, B. & Gauquelin, T. (2002), 'Nature and genesis of spodic horizons characterized by inverted color and organic content in a subalpine podzolic soil (Pyrenees Mountains, France)', *Bulletin de la Société Géologique de France* 172(1), 77-86.
- Revyako, N.; Bychkova, Y. & Kostitsyn, Y. (2007), 'Isotope evidence of the interaction of basic melt with crust rocks on the example of Kivakka layered intrusion (Karelia) (in Russian)', *Proceding of the International conference "Ultrabasic-basic complexes of fold regions". Irkutsk, 2007*, 487-490.
- Righi, D. & Chauvel, A. (1987), 'Podzols and Podzolization', *Assoc. Franc. Etude Sol. INRA, Plaisir et Paris, Paris..*
- Ryabchikov, I.; Suddaby, P.; Girnis, A.; Kulikov, V.; Kulikova, V. & Bogatikov, O. (1988), 'Trace-element geochemistry of Archaean and Proterozoic rocks from eastern Karelia, USSR', *Lithos* 21, 183-194.
- Salminen, R.; Gregorauskiene, V. & Tarvainen, T. (2008, in press), 'The normative mineralogy of 10 soil profiles in Fennoscandia and north-western Russia', *Appl. Geochem..*
- Sarala, P. (2005), 'Till geochemistry in the ribbed moraine area of Peräpohjola, Finland', *Appl. Geochem.* 20, 1714-1736.
- Sawhney, B. L. (1989), *Minerals in soil environments*, Soil Science Society of America, chapter Chapter 16: Interstratification in layer silicates, pp. 789-828.
- Schroeder, P. A.; Melear, N. D.; West, L. T. & Hamilton, D. A. (2000), 'Meta-gabbro

-
- weathering in the Georgia Piedmont, USA: implications for global silicate weathering rates', *Chem. Geol.* 163, 235-245.
- Schweda, P.; Araujo, P. D. R. & Sjoeberg, L. (1991), 'Soil chemistry, clay mineralogy and noncrystalline phases in soil profiles from southern Sweden and Gårdsjön.', In: Rosén, K. (Ed.), *Chemical weathering under field conditions, Reports in Forest Ecology and Forest Soils*. Swedish University of Agricultural Sciences Report 63, 49-62.
- Semenov, V.; Koptev-Dvornikov, E.; Berkovskii, A.; Kireev, B.; Pchelintseva, N. & Vasil'eva, M. (1995), 'Layered troctolite-gabbro-norite Tsipinga intrusion, Northern Karelia: Geologic structure and petrology', *Petrology* 3(6), 588-610.
- Shmygalev, V. (1968), 'Mafic and ultramafic intrusions of the Olanga group', *Proterozoic volcanic and ultramafic complexes of Karelia, Petrozavodsk* 1, 209-219.
- Starr, M.; Lindroos, A.; Ukonmaanaho, L.; Tarvainen, T. & Tanskanen, H. (2003), 'Weathering release of heavy metals from soil in comparison to deposition, litterfall and leaching fluxes in a remote, boreal coniferous forest', *Appl. Geochem.* 18, 607-613.
- State Geological Map of Russian Federation, 2001. Sheet Q-(35)-37. In: Bogdanov, Yu.B. (Ed.), Explication Note. Ministry of Natural Resources, St-Petersbourg. VSEGEI.
- Taylor, S. & McLennan, S. (1985), *The continental crust: its composition and evolution*, Blackwell Scientific Publications, Oxford.
- Thiede, J.; Bauch, H. A.; Hjort, C. & Mangerud, J. (2001), 'The late Quaternary stratigraphy and environments of northern Eurasia and the adjacent Arctic seas - new contributions from QUEEN', *Global and Planetary Change* 31(1-4), vii-x.
- Thorn, C. E.; Dixon, J. C.; Darmody, R. G. & Allen, C. E. (2006), 'A 10-year record of the weathering rates of surficial pebbles in Kärkevagge, Swedish Lapland', *Catena* 65, 272-278.
- Tyler, G. (2004), 'Vertical distribution of major, minor, and rare elements in a Haplic Podzol', *Geoderma* 119, 277-290.
- Vasiliev, M. V. (2006), 'Osobennosti intruzivnyh sistem Vetrenogo poyasa (in russian) (Specific features of intrusive systems of the Vetryny Belt paleorift)', Master's thesis, Geologicheskii f-t MGU.
- Vasyukova, E.; Pokrovsky, O.; Viers, J.; Oliva, P.; Dupré, B.; Martin, F. & Candaudap, F., 'Trace elements in organic- and iron-rich surficial fluids of boreal zone: Assessing colloidal forms via dialysis and ultrafiltration', *Geochim. Cosmochim. Acta* (submitted).
- Viers, J.; Dupré, B.; Braun, J.; Deberdt, S.; Angeletti, B.; Ngoupayou, J. N. & Michard,

-
- A. (2000), 'Major and trace element abundances, and strontium isotopes in the Nyong basin rivers (Cameroon): constraints on chemical weathering processes and elements transport mechanisms in humid tropical environments', *Chemical Geology* 169, 211–241.
- World Reference Base for soil Resources (IUSS Working Group WRB, FAO)', 2006.
- Zakharova, E.; Pokrovsky, O. S.; Dupré, B.; Gaillardet, J. & Efimova, L. (2007), 'Chemical weathering of silicate rocks in Karelia region and Kola peninsula, NW Russia: Assessing the effect of rock composition, wetlands and vegetation', *Chem. Geol.* 242, 255-277.
- Zilliacus, H. (1989), 'Genesis of De Geer moraines in Finland', *Sedimentary geology* 62(2-4), 309-317.

Chapter 3

**Trace elements in organic- and iron-rich surficial
fluids of boreal zone: Assessing colloidal forms
via dialysis and ultrafiltration**



E.V. Vasyukova, O.S. Pokrovsky, J. Viers, P. Oliva, B. Dupré, F. Martin and F. Candaudap

Submitted to *Geochimica et Cosmochimica Acta*

Preface

Soil is a complex heterogeneous system which consists of solid phases containing minerals and organic matter, and fluid phases. These phases interact with each other, as well as absorb elements such as metal ions which enter the soil system with aqueous solution. Inorganic colloids such as clays, metal oxides and hydroxides, metal carbonates and phosphates, as well as organic colloidal matter, i.e., humic and fulvic acids originating from decomposing plant litter are important interfaces for metal adsorption.

Soil forming process is based on mechanical and chemical weathering of underlying rocks, which are, in its turn, initiated by a joint action of physical processes and dissolution of minerals under the influence of water and dissolved substances which it contains. During these processes, some chemical elements remain *in situ* in the form of newly-formed minerals, and constitute a soil together with primary minerals. Other elements are exported with water flows in dissolved (< 0.22 or 0.45 µm) or particulate (> 0.22 or 0.45 µm) form. There is a growing understanding of the importance of colloidal fluxes, which can represent an essential part of the total flux for many usually insoluble elements (Viers et al., 2007). This colloidal transport is especially important for the boreal regions of the world, where rivers contain high concentration of dissolved organic matter and iron. It was shown recently (Lundström et al., 2000) that very high concentrations of dissolved organically-complexed Fe and Al are present in the organic surface layer (O horizon) in podzols of the boreal zone. Undergoing microbiological decomposition, mobile cations are washed out of the soil, but aluminium and in the lesser degree iron are accumulated in the underlying horizon together with humus thus producing aluminium-rich solid horizon (Al(OH)_3) and large-size organo-ferric colloids (Fe-OM). These colloids contribute significantly to the trace metal load of surface waters especially when they are flushed from the upper soil layers into the stream by rising water levels during spring flood and heavy rains (Andersson et al., 2006; Björkvald et al., 2008).

There is a large amount of previous studies which addressed the speciation and transport of trace elements in water in tropical (Viers et al., 1997; Braun et al., 1998; Dupré et al., 1999), temperate (Dia et al., 2000; Johannesson et al., 2004; Pokrovsky et al., 2005a; Pédrot et al., 2008) and boreal zones (Ingri et al. 2000; Dahlqvist et al., 2004,

2007; Björkvald et al., 2008). Qualitative estimation of fluxes of dissolved matter exported with water flows is essential to acquire better understanding of the process of continental weathering. However, despite the increasing interest to boreal permafrost-dominated areas among aquatic geochemists, these particular zones remain much less investigated. The following two chapters are devoted to qualitative and quantitative assessment of the speciation of trace elements in boreal rivers and surface waters of the White Sea basin. The important role of organo-mineral colloids in scavenging of trace elements will be shown based both on *in-situ* size fractionation procedure and *ex-situ* laboratory experiments, and the possible effect of underlying rock lithology on TE colloidal speciation will be assessed.

Trace elements in organic- and iron-rich surficial fluids of the boreal zone: Assessing colloidal forms via dialysis and ultrafiltration

E.V. Vasyukova^{1,2}, O.S. Pokrovsky¹, J. Viers¹, P. Oliva¹, B. Dupré¹, F. Martin¹
and F. Candaudap¹

(submitted to *Geochimica et Cosmochimica Acta*, November 18, 2008)

¹ *Laboratory of Mechanisms and Transfers in Geology (LMTG, UMR 5563), University of Toulouse,
OMP-CNRS; 14, avenue Edouard Belin, 31400 Toulouse, France,*

² *Saint-Petersburg State Polytechnic University, 29, Polytechnicheskaya st., Saint-Petersburg, Russia*

Keywords: trace element, colloids, ultrafiltration, dialysis, speciation, lithology, boreal zones

Abstract

The high concentration of Dissolved Organic Matter (DOM), and hence the colloidal form of most of the trace elements (TE), is an important characteristic feature of the TE geochemistry of surface waters in the European Russian Arctic zone. To obtain a first-order understanding of the colloidal transport and speciation of TE in this region, on-site size fractionation of about 40 major and trace elements was performed on waters from boreal small rivers and their estuaries in the Karelia region of North-West Russia around the “Vetreny Belt” mountain range and Paanajärvi National Park (Northern Karelia). Samples were filtered in the field using a progressively decreasing pore size (5 µm, 2.5 (3) µm, 0.22 (0.45) µm, 100 kDa, 10 kDa and 1 kDa) by means of frontal filtration and ultrafiltration techniques and employing *in-situ* dialysis with 10 kDa and 1 kDa membranes followed by ICP-MS analysis. Most rivers exhibit high concentrations of dissolved iron (0.1 – 8.6 mg/l), aluminium (0.01 – 0.75 mg/l), manganese (0.3 – 155 mg/l) and organic carbon (5 – 150 mg/l), as well as many trace elements usually considered as immobile during weathering (Ti, Zr, Th, Al, Ga, Y, REE and Pb). Two methods of colloid separation (ultrafiltration and dialysis) were tested to assess the proportion of colloidal forms. For most samples, dialysis yields a

systematically higher (factor of 2 to 5) proportion of colloidal forms compared to ultrafiltration.

Fe and OC are poorly correlated in the (ultra)filtrates and dialysates: iron concentration gradually decreases with filtration from 5 (2.5) μm to 1 kDa, whereas most of the OC is concentrated in the < 1 kDa and 10 kDa – 0.22 μm fractions. Similar to previous studies in European subarctic zones, this reflects the presence of two pools of colloids composed of organic-rich and Fe-rich particles. All major anions and silica are present as dissolved species (or solutes) passing through the 1-kDa membrane. Several groups of elements can be distinguished according to their behaviour during filtration and association with these two types of colloids: (i) species very weakly affected or unaffected by ultrafiltration, which are present as truly dissolved inorganic species or weak organic complexes (Ca, Mg, Li, Na, K, Cs, Si, B, As, Sr, Ba, W, Sb and Mo); (ii) elements present in the fraction smaller than 1–10 kDa, which are liable to form strong organic complexes (Ni, Zn, Cu, Cd and, in some rivers, Sr and Cr), and (iii) elements strongly associated with colloidal iron in all ultrafiltrates and dialysates, with up to 95% concentrated in large colloidal particles (> 10 kDa) (Mn, Al, Ga, REEs, Pb, V, Cr, Ti, Zr, Th, U, Co, Y, Hf and Bi).

The effect of rock lithology (acidic vs. basic) on the colloidal speciation of TE is seen solely in the increase of Fe (and some accompanying TE) concentrations in catchment areas dominated by basic rocks. Neither the ultrafiltration pattern nor the relative proportions of colloidal versus dissolved TE are affected by the lithology of the underlying rocks: within $\pm 10\%$ uncertainty, the three colloidal pools show no difference in TE distribution between two types of bedrock lithology.

3.1. Introduction

Boreal zones of the Russian Arctic are likely to play a crucial role in the regulation of trace element (TE) input into the ocean at high latitudes. In view of the importance of these circumpolar zones for our understanding of ecosystem response to global warming, it is very timely to carry out detailed regional studies of trace elements geochemistry in boreal landscapes. In contrast to our good knowledge of Western European Arctic environments located in a relatively warm climate on the Baltic Sea coast in areas subject to anthropogenic influence, we still have an extremely poor

understanding of the geochemistry of small pristine catchments situated to the east of Scandinavia, on the coast of the Arctic Ocean and adjoining seas. In these regions, the nature of dissolved organic matter, iron and aluminium colloids, as well as the estuarine behaviour of TE, may be very different from that observed in the “model” Kalix river, which has been very thoroughly studied over the past decades (Pontér et al., 1990, 1992; Ingri and Widerlund, 1994; Öhlander et al., 1996, 2000; Ingri et al., 1997, 2000, 2005, 2006; Land and Öhlander, 1997, 2000; Porcelli et al., 1997; Andersson et al., 1998, 2001; Land et al., 1999, 2000; Dahlqvist et al., 2004, 2005, 2007). The difficult and costly access to the Central and Eastern Russian Arctic has hampered progress in understanding the geochemistry of these zones. Hence, the more easy accessible small catchments of the White Sea basin are of interest since they may be representative of extensive zones of the Russian Arctic. Therefore, the present study is aimed at quantitative characterization of trace element speciation in pristine, organic-rich rivers and surface waters of the White Sea basin sampled during the base flow in summer.

The second main issue addressed here is the role of bedrock lithology in controlling the formation and nature of colloids (granites versus basalts). In contrast to the large amount of information on the effect of rock lithology on the fluxes and geochemical behaviour of major elements in dissolved and particulate matter ($> 0.45 \mu\text{m}$) from various climatic zones (Bluth and Kump, 1994; Gaillardet et al., 1997; Zakharova et al., 2005, 2007), the colloidal transport of major and trace elements remains poorly understood. The composition and redox conditions of river water (Zakharova et al., 2007) and groundwater (Dia et al., 2000), as well as the composition of the colloids present (Degueldre et al., 2000), are likely to be strongly influenced by the chemical and mineralogical composition of the bedrock. In this regard, the basic rocks and granites that are both present in the Karelian region offer a rigorous and straightforward possibility of assessing the control of lithology on colloid formation in surface waters. For this purpose, we directly compared the colloidal speciation of TE in fluids sampled from basic and granitic catchments as well as swamp zones.

The third motivation behind this study was to compare the size fractionation of TE in colloids using two contrasting techniques, dialysis and ultrafiltration. The first method allows an *in situ* assessment of the equilibrium distribution of solutes having a pore size less than that of the membrane (Alfaro-De la Torre et al., 2000; Gimpel et al.,

2003). Ultrafiltration, which is more widely used in assessing the state of TEs and organic ligands in natural waters (Buffle et al., 1978; Hoffmann et al., 1981; Dai et al., 1995; Dai and Martin, 1995; Sholkovitz, 1995; Eyrolle et al., 1996; Viers et al., 1997; Porcelli et al., 1997; Pham and Garnier, 1998; Dupré et al., 1999; Guo et al., 2001), may involve various potential artefacts such as charge separation, filter clogging etc. (Viers et al., 1997; Dupré et al., 1999). In the present study, we performed both UF and dialysis on the same samples in the field, using on-site separation procedures of similar design.

Therefore, we attempt to answer two open questions concerning the geochemistry of trace elements in the present-day Arctic: i) what kind of easily-available separation procedure can be recommended for routine assessment of the colloidal state of TEs in boreal waters? and ii) is there a difference in TE speciation and size distribution of colloids, as well as the chemistry of their carriers, depending on the lithology of the underlying rocks? Addressing these issues will hopefully allow us to define the source of major and trace elements and organic carbon. In this way, we should be able to develop environmentally-friendly policies for the use of water resources and predict the response of Arctic and subarctic ecosystems to on-going environmental changes on the scale of small and large catchments.

3.2. Sample area

The studied area is located in north-western Russia and is situated within three large geological structures: the Kola and Karelia Provinces, and the Belomorian belt. Figure 3.1 presents a simplified map of the sites along with sampling points and geological setting. The investigated sites are situated around a paleorift belonging to the Vetreny (Windy in English) Belt ($63^{\circ}46'N - 35^{\circ}48'E$) on the south-west coast of the White Sea (Puchtel et al., 1996, 1997; Kulikov et al., 2005), as well as in the Paanajärvi National park ($66^{\circ}12'N - 30^{\circ}33'E$), where basic intrusions crop out in the Kivakka-Tsipringa zone of northern Karelia (Amelin et al., 1995). The ~2.45 Ga-old Vetreny Belt formation is represented by ultramafic komatiitic rocks displaying spinifex structure, with high MgO (up to 24%), and low Al₂O₃ and TiO₂ contents (Puchtel et al., 1997). The Kivakka and Tsipringa intrusions (~2.44 Ga) (Balashov et al., 1993; Amelin and Semenov, 1996) belong to the Olanga group of peridotite-gabbro-norite layered

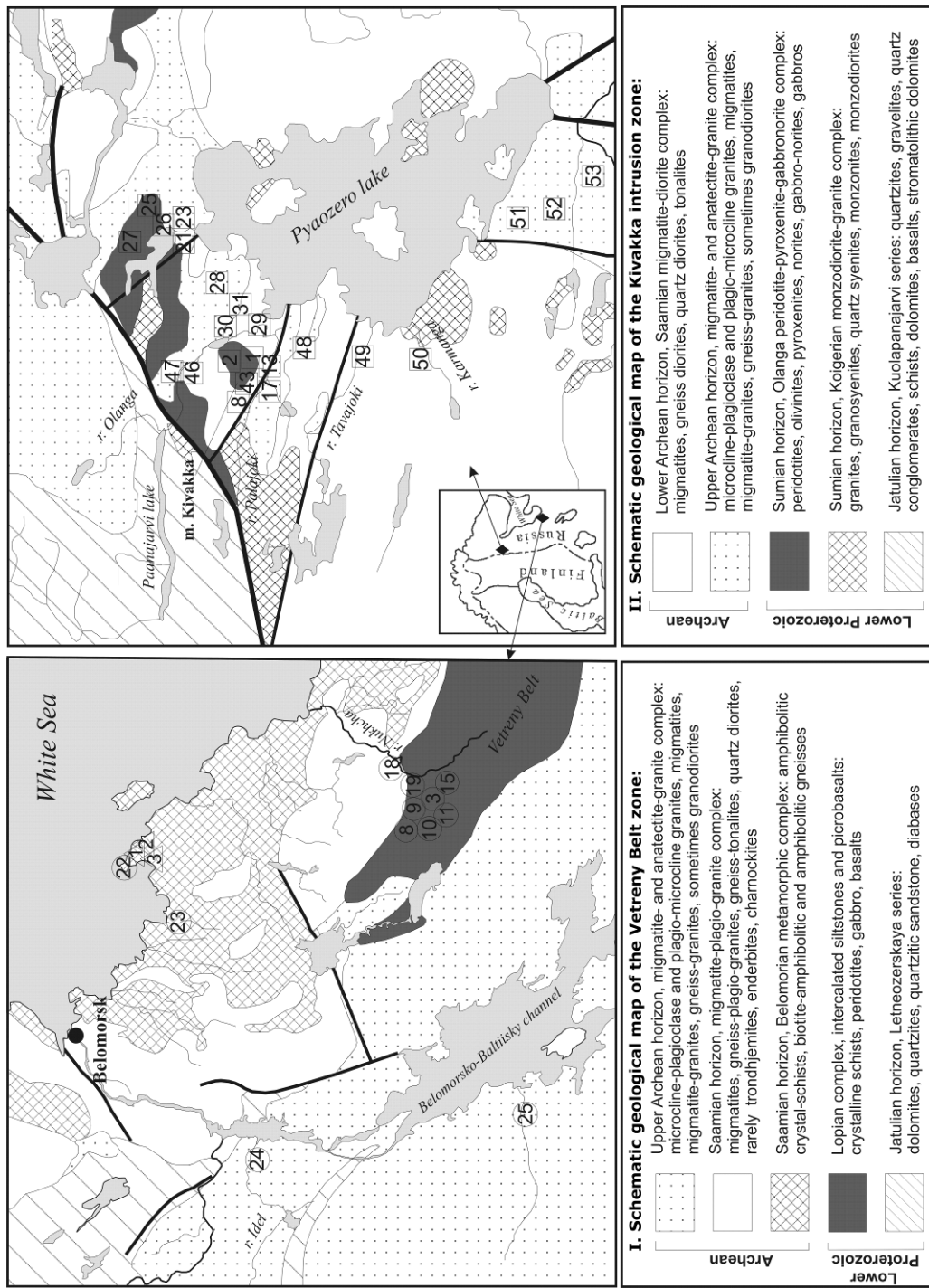


Fig. 3.1. Map of the studied area showing main geomorphological regions and sampling locations in the Vetryny Belt zone ("No." series, numbers in circles), the White Sea coast ("Y" series, numbers in triangles) and the Kivakka intrusion zone ("K" series, numbers in squares).

intrusions, which are hosted by migmatized biotite and amphibole gneisses, granite-gneisses and granodiorite-gneisses of Late Archean age (Bychkova et al., 2007).

Selected zones can be considered as pristine environments with natural concentrations of elements in rivers because of the absence of any industrial or agricultural activity and the limited accessibility. The list of sampled waters and their bedrock compositions are presented in Table 3.1. For this study, we selected two types of catchment: with predominantly granite/granite-gneiss acidic rocks and with predominantly basic rocks. For mixed, granitic-gneiss and basic bedrock lithologies, the discriminant criterion between these two types of catchment was taken as 50% coverage by basic or acidic rocks.

In most areas, podzol is the main soil type, with soil depths varying from 15 to 50 cm, while very thin horizons (15-20 cm) are typical of more elevated areas (> 200 m above sea level) (Evdokimova, 1957). Tundra brown soils are typical of the upper part of the Kivakka and Vetryeny Belt intrusions, where they exhibit a shallow profile (10-20 cm) with high proportions of organic detritus. Peat gley soils occur in valleys, wide plains, gentle slopes and local depressions. The vegetation is represented by typical taiga species: spruce and pine forests mixed with some birch trees that cover more than 80% of the terrain. Large areas of peatland, located in glacial depressions, yield high concentrations of dissolved organic carbon (DOC) in surface waters.

3.3. Materials and methods

3.3.1. Sampling, filtration and dialysis

Different series of streams, large rivers and swamps were sampled during extensive field campaigns in July-August 2004, February 2006 and July 2006 only during the summer and winter base-flow period because of the difficult access to the studied sites during spring-flood period. Water temperature and pH were measured in the field. The pH was measured using a combined Schott-Geräte electrode calibrated against NIST buffer solutions (pH = 4.00 and 6.86 at 25 °C), with an accuracy of ± 0.02 pH units. Samples were collected from near the middle of the flow channel, using 1-l high-density polyethylene (HDPE) containers held out from the beach on a non-metallic stick. Plastic gloves were always used during handling of the samples. The water samples were immediately filtered through sterile, single-use Minisart® filter units

Table 3.1. Studied samples from rivers, lakes and swamps, with their bedrock composition. “No.” and “K” series correspond to samples taken from Vetryny Belt and Kivakka intrusion zones, respectively (summer period), and “Y” to samples from the White sea coast (winter period).

Sample no.	Description	Bedrock composition of the catchment
No.6	r. Maksimova	Gneisses, glacial deposits
No.8	Surface water	Basalt
No.9	r. Ruiga	Basalt
No.10	Surface water from basalt field	Basalt
No.11	Surface water from basalt field	Basalt
No.12	r. Ruiga, upstream biofilms	Basalt
No.13	r. Ruiga, highest upstream	Basalt
No.15	Creek over ultramafites	Ultramafites
No.18	r. Nukchcha	Basalt
No.22	r. Yukova at low tide	Gneisses, glacial deposits
No.23	r. Ladreka	Gneisses, glacial deposits
No.24	r. Idel	Gneisses, amphibolites, quartzites
No.25	r. Pezega	Granites, leucogranites, tonalite-trondhjemites
K-1	Lake on the top of Kivakka intrusion	Gabbro-norites
K-3	Lake	Gabbro-norites, basic dyke
K-4	Lake	Gabbro-norites
K-7	Tributary of r. Palajoki	Gneisses, glacial deposits
K-8	Subsurface flow (south-bank tributary of r. Palajoki)	Gneisses, glacial deposits
K-10	Swamp (corresponds to K-43 and K-44)	Gabbro-norites
K-11	Lake (source of r. Palajoki)	Gneisses, glacial deposits
K-12	Spring from a swamp	Gneisses, glacial deposits
K-13	River over olivinites	Olivinite
K-15	Swamp	Pyroxenites and peridotites
K-17	Subsurface flow	Norites
K-21	Lake Tsipringa (water canal from lake Pyaozero)	Gneisses, glacial deposits
K-22	Swamp on lake Tsipringa coast	Peridotites
K-23	Swamp on lake Tsipringa coast	Peridotites
K-23-A	Swamp on lake Tsipringa coast	Peridotites
K-23-B	Swamp on lake Tsipringa coast	Peridotites
K-24	Subsurface flow at lake Tsipringa	Peridotites
K-25	Lake Liukulampi	Gneisses, glacial deposits
K-26	Spring	Gneisses, glacial deposits
K-27	Swamp	Gneisses, glacial deposits
K-28	Creek	Gneisses, glacial deposits
K-30	r. Vartalambina downstream	Gneisses, glacial deposits
K-31	r. Vartalambina upstream, tributary	Gneisses, glacial deposits
K-32	Swamp	Gabbro-norites
K-33	Stream	Gabbro-norites
K-38	Swamp	Gabbro-norites
K-39	Swamp	Gabbro-norites
K-40	Small pond on the top of Kivakka mountain	Gabbro-norites
K-41	r. Molodilny (spring from swamp)	Gabbro-norites
K-43	Swamp	Gabbro-norites
K-44	Swamp	Gabbro-norites
K-45	r. Palajoki	Gneisses, glacial deposits
K-46	r. Olanga	Gneisses, glacial deposits
K-47	r. Siltyoki (right-bank tributary of r. Olanga)	Gneisses, glacial deposits
K-48	r. Nuris	Gneisses, glacial deposits
K-49	r. Tavajoki	Gneisses, glacial deposits
K-50	r. Karmanga	Gneisses, glacial deposits
K-51	r. Kolo	Gneisses, glacial deposits
K-52	r. Varaka, right-bank tributary (spring from swamp)	Gneisses, glacial deposits
K-53	r. Keret	Gneisses and amphibolites; tonalites and trondhjemites
Y-1	r. Yukova (spring from swamp)	Gneisses, glacial deposits
Y-3	Spring, subsurface flow	Gneisses, glacial deposits
Y-5	Ice formed from soil solutions under granite boulders	Gneisses, glacial deposits

(Sartorius, acetate cellulose filter) with pore sizes of 5, 0.45 and 0.22 µm. The first 200 ml of the filtrate was systematically discarded. Only filtered (0.45 or 0.22 µm) samples were used in the ultrafiltration steps, which involved a series of decreasing pore size (100 kDa, 10 kDa and 1 kDa).

Frontal ultrafiltration (UF) was performed in the field using a 50-ml polycarbonate cell (Amicon 8050) equipped with a suspended magnet stirring bar located beneath the filter to prevent clogging during filtration. The major advantage of this procedure over the more commonly used tangential filtration technique is the very small size of the filter and low amount of pore space, which minimizes the adsorption inside the filter during filtration. Argon pressure (3 bars) was provided by a portable bottle. Filtration was performed with 100, 10, and 1 kDa membranes (Amicon, regenerated cellulose, 200-µm thickness, 44.5-mm diameter). Before each filtration, the system was cleaned by flushing MilliQ water, then ~0.1 M ultrapure HNO₃, and finally, MilliQ water again. Preliminary experiments demonstrated that flushing 50 ml of MilliQ water through an Amicon UF cell with a membrane is sufficient to decrease the blank of OC and all TEs to analytically acceptable values. During filtration, the first 50 ml of sample solution were discarded, thus allowing saturation of the filter surface prior to recovery of the filtrate. Each filter was washed in MQ water before the experiment and used only once. This greatly decreased the probability of cross-contamination during sample filtration, while improving the OC blank. It also provided identical conditions of filtration for all samples and allowed a high recovery of colloidal particles. Discussions of this technique and precautions against possible filtration artefacts are given in Viers et al. (1997), Dupré et al. (1999), Pokrovsky and Schott (2002), Pokrovsky et al. (2005, 2006).

Dialysis experiments were performed using 20-50 ml precleaned dialysis bags placed in i) 2-litre polypropylene containers filled with river water (*ex-situ* dialysis), and ii) directly in the river or swamp water (*in-situ* dialysis). The duration of this dialysis procedure was between 24 and 72h. Pokrovsky et al. (2005) showed in laboratory experiments that, for both 1 and 6-8 kDa membranes, an equilibrium distribution is attained within 6 h, in agreement with the manufacturer's specifications. For dialysis experiments, EDTA-cleaned trace-metal pure Spectrapor 7® dialysis membranes made of regenerated cellulose and having pore sizes of 100, 10 and 1 kDa were thoroughly

washed in 0.1 M double-distilled HNO₃, ultrapure water, filled with ultrapure MQ deionized water and then placed into natural water. The efficiency of the dialysis procedure was evaluated by comparing major anion concentrations (e.g., Cl⁻ and SO₄²⁻) or neutral species (H₄SiO₄⁰) not associated with colloids between the dialysis bag and the external solution. These concentrations were always identical to within ± 10%, suggesting an equilibrium distribution of dissolved components. The crucial requirements for successful dialysis separation are i) a high external solution/dialysate ratio, and ii) constant concentration of dissolved and colloidal components in the external solution over the entire dialysis procedure. The first condition was satisfied by frequently changing the external solution in the polypropylene containers in such a way that the volume ratio of river water to dialysis compartment was higher than 100. For the *in-situ* dialysis procedure used in river or swamp waters, this ratio was > 100. The second condition was met for most experiments described here, as corroborated by the analysis of organic carbon (OC), major and trace elements in < 0.45 µm filtrate of external solution before and after dialysis. The concentrations remained constant to within ± 10 % for OC and major elements including Fe, and ± 20 % for trace metals.

3.3.2. Analysis

Filtered or dialysed solutions for cations and trace element analyses were acidified (pH = 2) with ultrapure double-distilled HNO₃ and stored in HDPE bottles previously washed with ultrapure 0.1 M HCl and rinsed with MilliQ deionized water. The preparation of sampling bottles was performed in a clean bench room. The samples for OC analyses were collected in a pyrolysed sterile Pyrex glass tube. Filtration through 0.45 or 0.22 µm pore size provided fully sterile solutions without bacterial development as tested by inoculation on nutrient agar media. Therefore, it was unnecessary to add conservants for DOC analysis. Blanks were performed to check the level of pollution produced by sampling and filtration. The organic carbon blanks of filtrate and ultrafiltrates never exceeded 0.1 mg/l, which is quite low for the organic-rich rivers sampled in this study (i.e., 5-20 mg/l OC). For all major and most trace elements, concentrations in blanks were below detection limits. In several cases, however, clear contamination by Zn, Cu and Pb was detected in the 10 and 1 kDa ultrafiltrates. These samples were not considered in the analysis of results.

Aqueous silica concentrations were determined colorimetrically (molybdate blue method) using a Technicon autoanalyzer II, with an uncertainty of 2%. In the ultrafiltrates, the total dissolved silica was also analysed by ICP-MS. No difference was found within the analytical uncertainty. Alkalinity was measured by potentiometric titration with HCl by automated titrator (Metrohm 716 DMS Titrino) using a Gran method with a detection limit of 10^{-5} M and an uncertainty of 2%. DOC was analysed using a Carbon Total Analyzer (Shimadzu TOC 5000) with an uncertainty better than 3%. Major anion concentrations (Cl, SO₄, F, NO₃ and PO₄) were measured by ion chromatography (HPLC, Dionex ICS 2000) with an uncertainty of 2%. Calcium, magnesium, sodium, and potassium concentrations were determined with an uncertainty of 1-2% using a Perkin-Elmer 5100PC atomic absorption spectrometer. High concentrations of dissolved iron (i.e., > 0.5 mg/l) were measured by flame AAS, whereas lower concentrations were analysed by ICP-MS (Elan 6000, Perkin-Elmer and Agilent 7500). Trace elements (TE) were determined without preconcentration by ICP-MS. Indium and rhenium were used as internal standards, and corrections for oxide and hydroxide ions were made for REEs and metals (Ariés et al., 2000). The international geostandard SLRS-4 (Riverine Water Reference Material for Trace Metals certified by the National Research Council of Canada) was used to check the accuracy and reproducibility of each analysis (Yeghicheyan et al., 2001). We obtained a good agreement between replicated measurements of SLRS-4 and the certified values (relative difference < 10%), except for B and P (30%).

3.4. Results and discussion

Measured major and trace elements concentration in various filtrates and dialysates are reported in the Annex B (Table B-1). In the following section, we discuss the behaviour of major and trace elements during ultrafiltration and dialysis separation experiments.

3.4.1. Comparison between dialysis and ultrafiltration

A quantitative comparison between ultrafiltration and dialysis was performed for the following samples: i) two rivers – the Ruiga (No.9), draining basic rocks, and the Palajoki (K-7), draining granite-gneisses and glacial deposits; ii) two surface streams on

basaltic (No.8) and ultramafic rocks (No.15); iii) an oligotrophic lake on the top of Kivakka mountain (K-1); and iv) two swamps developed on peridotite and gabbro-norite (K-23 and K-43, respectively). For almost 30 elements affected by the size-separation procedure, ultrafiltrates and dialysates concentrations exhibit differences (Table B-1), with ultrafiltrates being generally enriched in major and trace elements compared to dialysates by a factor of 2 to 3. Note that dialysates and ultrafiltrates exhibit similar concentrations of neutral species ($\text{H}_4\text{SiO}_4^\circ$) and anions (Cl^- , SO_4^{2-}) that are not associated with the colloidal fraction. By plotting the concentrations of elements in 1 kDa dialysates versus 1 kDa ultrafiltrates, we can see a systematic enrichment in ultrafiltrates which correspond to rivers, creeks and lakes (No.9, K-7, No.15, and K-23) (Fig. 3.2). It is possible that various UF artefacts such as charging of the membrane could be responsible for generally higher concentrations of TE and some major elements in the filtrates compared to the dialysates.

The swamp water sample K-43 yields higher concentrations of elements and, consequently, a lower proportion of colloidal TE in dialysates compared to filtrates, and has a high concentration of Fe (10.5 mg/l, which is 2 to 5 times higher than in the other samples). The divalent iron present in this sample could be partially subject to oxidation during ultrafiltration. Trace elements may be scavenged by Fe hydroxides and remain on the filter. This would lead to higher concentrations of TE in *in-situ* dialysates compared to filtrates.

Although the dialysis procedure is able to provide rapid *in-situ* separation of colloidal and dissolved components, it yields systematically lower concentrations in membrane-passed fractions compared to the ultrafiltrates, and thus gives a higher proportion of colloidal forms for all trace elements and some major components (Ca, Mg and DOC). In addition to problems remain present for the UF procedure, using dialysis prevents such artefacts as clogging of the filter membrane due to forced filtration and contamination from the filter, apparatus or tubing recipient. This is especially important for potentially “unstable” samples subject to the oxidation or photodegradation of OM. However, for consistency with previous studies, we consider below the major and trace elements in (ultra)filtrates in order to evaluate the proportion of colloids in various size fractions.

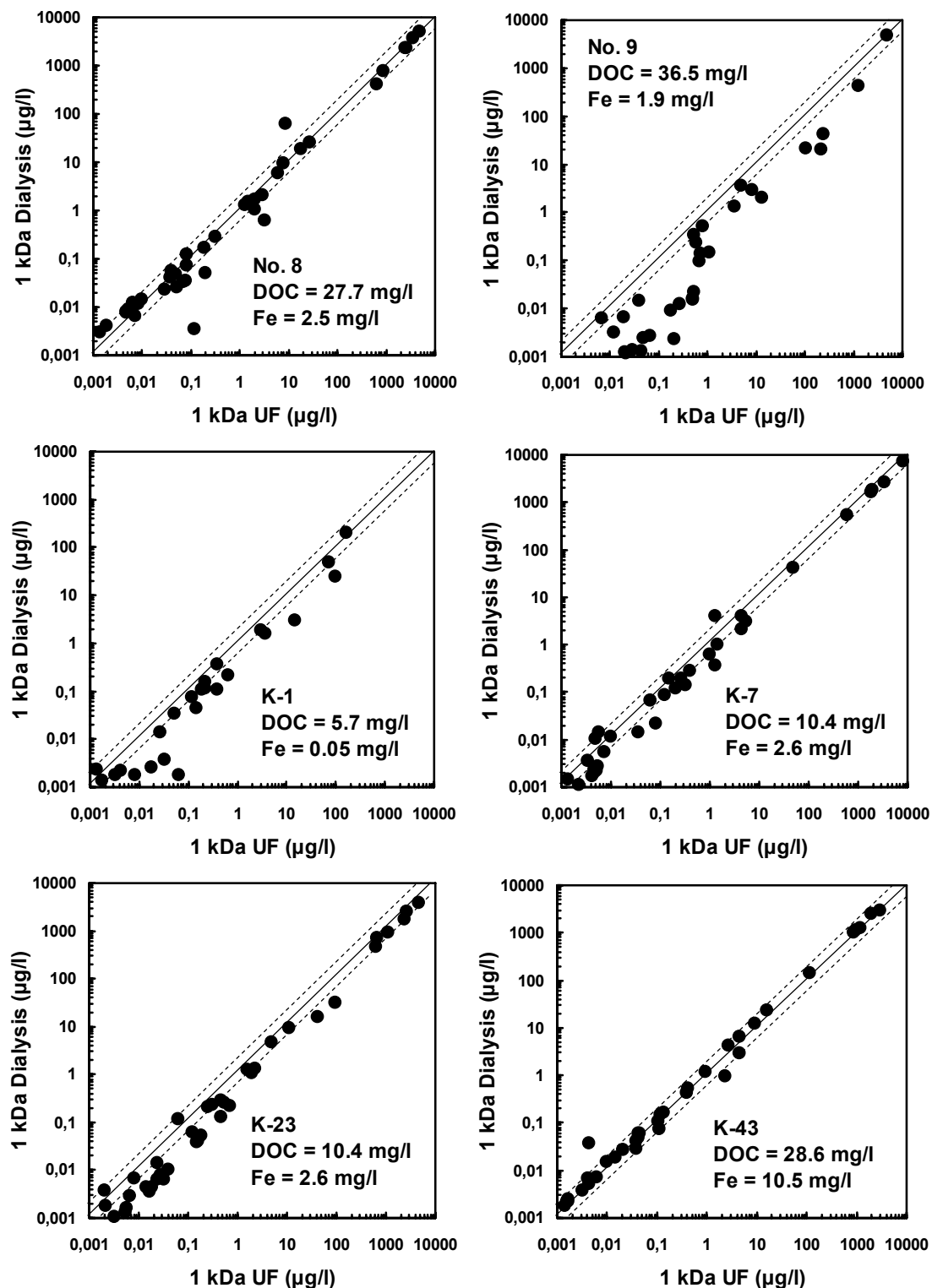


Fig. 3.2. Concentrations of elements in 1 kDa dialysates versus 1 kDa ultrafiltrates. Log scale is given for both axes. The solid line represents a 1:1 dialysates/ultrafiltrates ratio, the dotted line represents a 10% discrepancy between UF and dialysates. Note systematic enrichment in rivers No.8, No.9 and K-7, lake K-1 and swamp K-23, with ultrafiltrates being enriched in most of the elements. Sample K-43 (swamp water) exhibits lower or almost the same concentrations in ultrafiltrates comparing to dialysates.

3.4.2. Major and trace element speciation

3.4.2.1. Organic Carbon and Iron

The studied waters are essentially neutral with pH varying from 6 to 7. No difference can be detected between the pH values of filtrates and ultrafiltrates within ± 0.1 pH. The inorganic non-balanced charge ($(\Sigma^+ - \Sigma^-)/\Sigma^+$) calculated for most samples is ≤ 0.1 . Only the organic-rich river waters exhibit an important non-balanced anion deficit, with $(\Sigma^+ - \Sigma^-)/\Sigma^+ = 0.2-0.6$, which correlates with the concentration of organic carbon in filtrates and ultrafiltrates as illustrated in Fig. 3.3. Almost all rivers exhibit very high concentrations of dissolved organic carbon, ranging from 10 to 150 mg/l, which is typical of rivers draining peatland areas. Figure 3.4 shows the typical OC distributions in filtrates passing through various pore sizes. Generally speaking, up to 90% of OC is concentrated in the < 10 kDa fraction, with about 40-60% of OC being in the < 1 kDa fraction (except for K-7 and K-23). This is consistent with the presence of small-size polymers of fulvic nature (Pokrovsky and Schott, 2002). Similar to lakes and streams in Finland and Sweden (Pontér et al., 1990; Ingri and Widerlund, 1994; Ingri et al., 1997, 2000; Land and Öhlander, 1997; Porcelli et al., 1997; Andersson et al., 1998; Åström and Corin, 2000; Åström, 2001; Björkvald et al., 2008), the dissolved iron concentration in Karelian rivers is around 1-5 mg/l, rising to 14 mg/l in some peatlands (sample K-43).

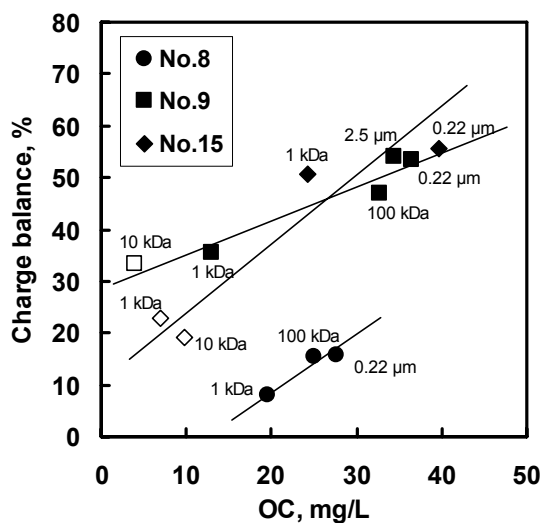


Fig. 3.3. Correlation between charge balance and OC in successive filtrates and dialysates from 2.5 μ m to 1 kDa. Solid symbols correspond to filtrates and ultrafiltrates, empty symbols indicate dialysates.

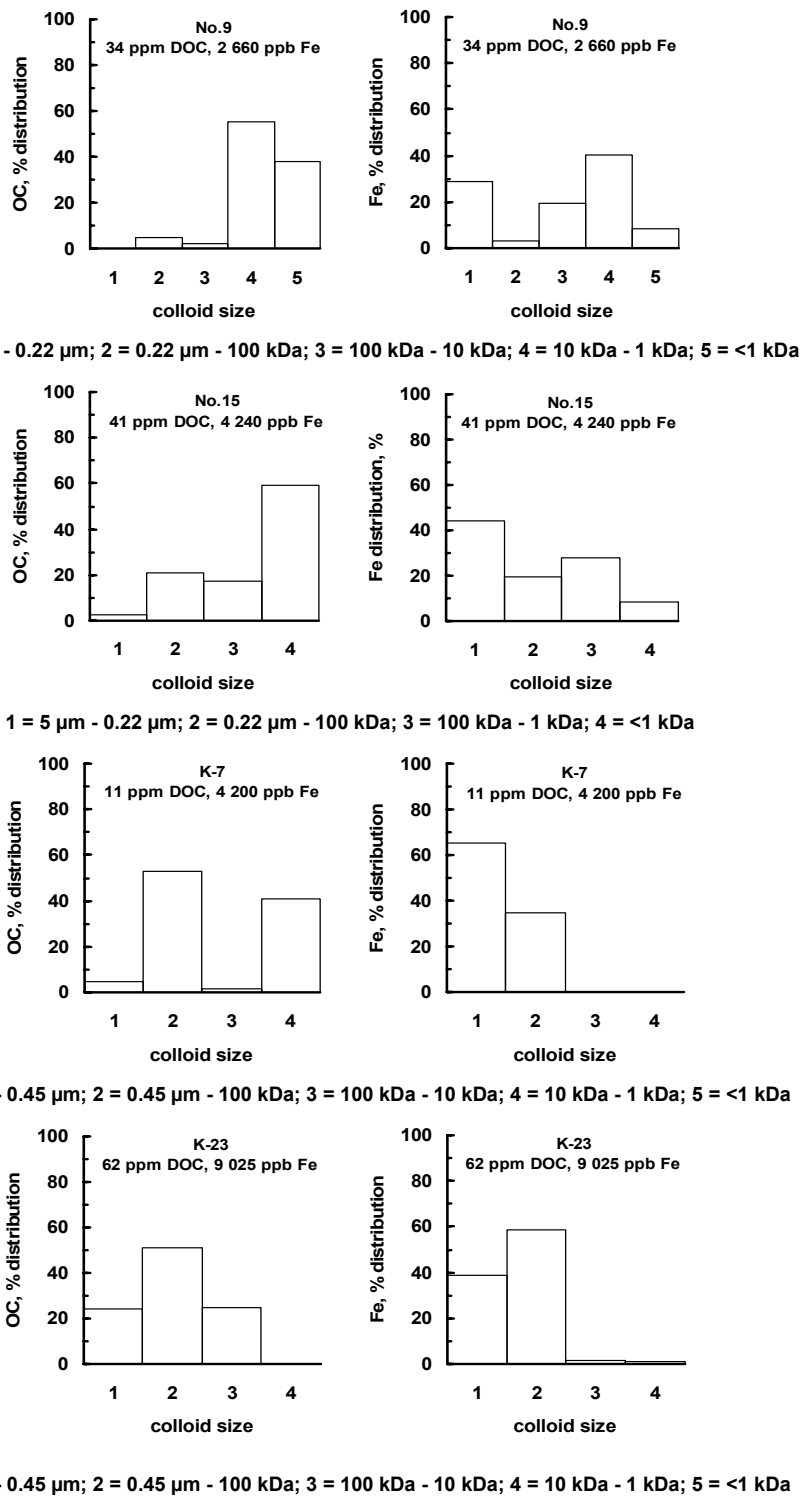


Fig. 3.4. Distribution of OC and Fe among filtrates in various pore size classes. Concentrations reported on the top of figures are measured in 5 μm (2.5 μm) filtrates. There is an important difference between the distributions of Fe and OC for a given river. This suggests the existence of two colloidal pools. Most of the OC is concentrated in small colloidal particles (1-10 kDa) and conventionally dissolved pools (< 1 kDa), whereas a significant amount of Fe is contained in the 0.22 (5) μm – 100 (10) kDa fraction representing large colloidal particles.

In most filtrates and ultrafiltrates, we find only a very poor correlation between Fe and OC (Fig. 3.5). The only exception is swamp water draining basic rocks (K-23 and K-43, not shown), where the correlation coefficient in ultrafiltrates is 0.93-0.98. Let us assume that Fe and OC behave independently during the ultrafiltration (UF), thus representing two different pools of colloids. We can define these colloids as iron-rich and fulvic(humic)-rich, and the following discussion shows how different elements follow Fe or OC colloids during the filtration and ultrafiltration procedures.

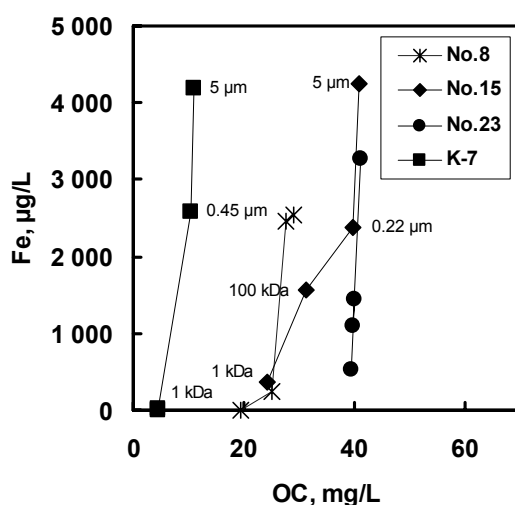


Fig. 3.5. Correlation between Fe and OC concentrations in various filtrates. For each filtration experiment, the first (upper) symbol corresponds to 5 or 2.5 µm pore size and the last (lower) one corresponds to 1 kDa. Samples: surface water (No.8), creek over ultramafic rocks (No.15), r. Ladreka (No.23), r. Palajoki (K-7).

Unlike OC, Fe is in most cases strongly affected by the filtration procedure, as shown in Fig. 3.4. It is very often present in large-size colloids (0.22 – 5 µm), and is almost completely removed from solution before filtration through 10 and 1 kDa membranes. This is illustrated in Fig. 3.6, where we plot the ratio of [Fe] to [Organic Carbon] in filtrates and ultrafiltrates for different samples as a function of filter pore size. This ratio decreases with decrease of filter pore size demonstrating the enrichment of OC vs. Fe in small-size colloids.

3.4.2.2. Alkali Metals, Alkaline Earths, Divalent Transition and Heavy Metals

Na, Mg, Ca, K, Li, Rb, Cs, Sr and Ba are mostly present in the truly dissolved phase, with 1 to 40% being present in the colloidal fraction (1 kDa – 0.45 µm).

However, organic-rich and surface swamp waters (No.8, No.9, No.15, No.22, K-23, K-44) show that colloids exert a clear control on Ca, Mg, Sr, Ba and Cs since the concentrations of these elements are decreased by a factor 2-3 upon filtration from 5 μm to 1 kDa, with 44 to 97% being in colloidal form (notably, 50-77% for Ca, not shown here). This is in agreement with Dahlqvist et al. (2004), who have shown that some Amazonian rivers and the boreal Kalix river have between 1% and 25% of their total dissolved Ca load present in the colloidal fraction.

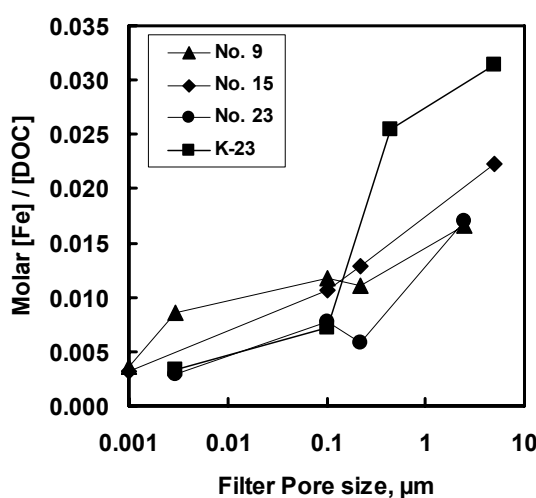


Fig. 3.6. [Fe] to [Organic Carbon] ratio in filtrates and ultrafiltrates for different samples.

No direct correlation is observed between either Mn or Fe and OC in 0.22 (0.45) μm filtrates (not shown) for basic catchments ($r^2 = 0.18$), whereas, for granitic catchments, the correlation is more pronounced between Mn and both Fe and OC ($r^2 = 0.94$ and $r^2 = 0.74$, respectively). Upon filtration, Mn concentration decreases and shows a correlation with iron (but not OC), suggesting that 25-60% of the Mn is associated with iron colloids. In some rivers (Ruiga No.9, Ladreka No.23, Palajoki K-7 and a creek over ultramafites No.15) up to 90% of the Mn is concentrated in iron colloids (Fig. 3.7).

We observe a positive correlation between Co and OC ($r^2 = 0.22$) or Fe ($r^2 = 0.83$ and 0.40 for basic and granitic catchments, respectively) (Fig. 3.8 a, b), indicating a possible mobilization of this element by both iron and organic colloids. This is backed up by results of ultrafiltration showing that, on average, 50-60% of total Co is in a truly dissolved form (< 1 kDa). In some Fe- and OC-rich rivers (Ruiga No.9, Nukhcha No.18,

Ladreka No.23 and Palajoki K-7) and swamp waters (K-23 and K-44), up to 90% of the Co is in colloidal form (Table B-2).

Cu and Zn are not appreciably affected by the presence of iron or organic colloids, since their concentrations are not correlated with Fe or OC. However, Ni exhibits a good correlation with both OC and Fe in 0.22 (0.45) μm filtrates whatever the parent rock (Fig. 3.8 c, d). Ni, Cu and Zn concentrations show almost no change on filtration from 5 μm to 1 kDa, except for the stream over ultramafites (No.15) and swamp water (K-23) which show a strong complexation with colloidal iron.

In most studied rivers, dissolved Pb concentrations are about 10 times higher than the values reported by Rember and Trefry (2004) for arctic rivers, by Shiller (1997) for the Mississippi river, and world river average (0.079 $\mu\text{g/l}$, Gaillardet et al., 2003), which is probably related to the colloidal state of this element, as first noted in the NW of Russia (Pokrovsky et al., 2002). Indeed, during filtration, Pb is associated with Fe rather than OC in most samples (Fig. 3.9) and exhibits 50-99% in colloidal form.

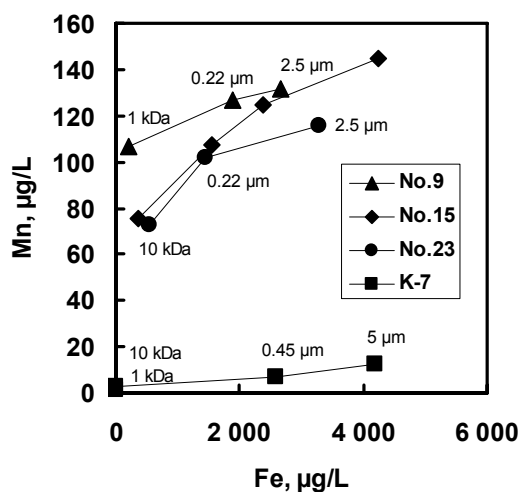


Fig. 3.7. Correlation between Mn and Fe concentration in various filtrates.

3.4.2.3. Trivalent Metals: Al, Ga, Y and REE

Aluminium concentrations range from 20 to 340 $\mu\text{g/l}$ in rivers on basic rocks, while attaining the highest levels (400-750 $\mu\text{g/l}$) in small creeks in swamp areas (No.9 and K-24) as well as in swamp waters (K-10 and K-43), but falling to between 1 and 50 $\mu\text{g/l}$ in rivers on granitic rocks. [Al] correlates better with [OC] in waters draining

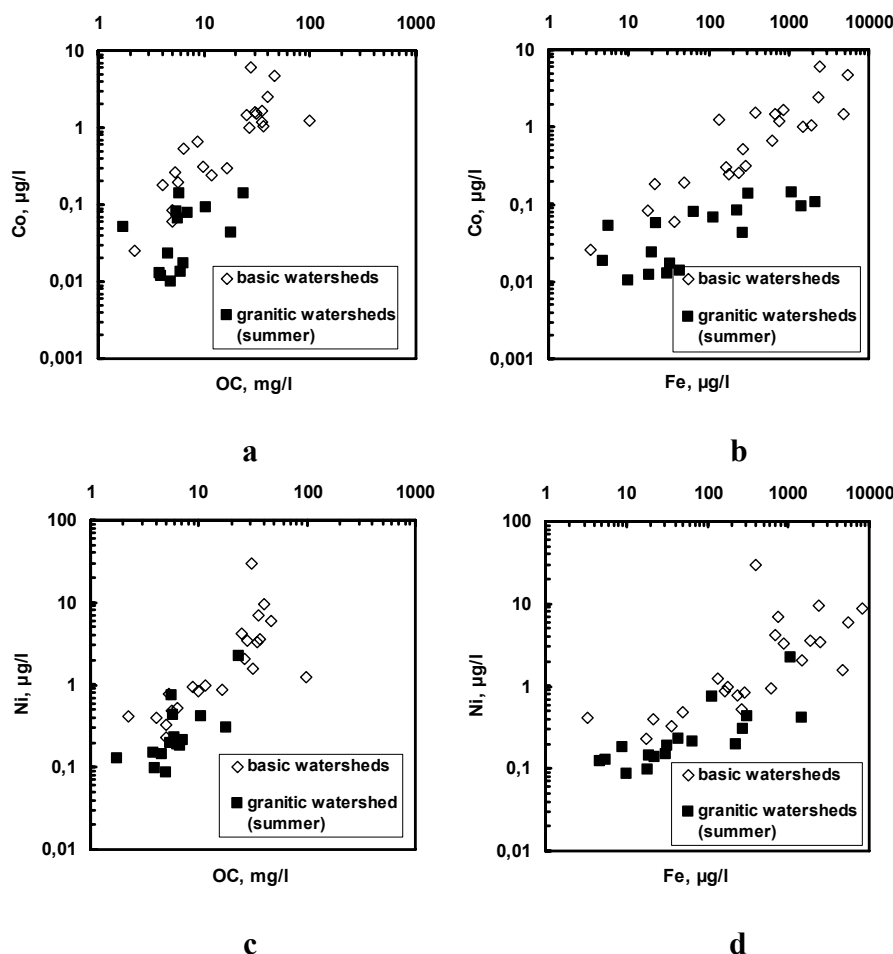


Fig. 3.8. Cobalt (a, b) and nickel (c, d) correlations with organic matter and iron in 0.22 (0.45) μm filtrates for rivers draining different rocks. Log scale is used for both axes.

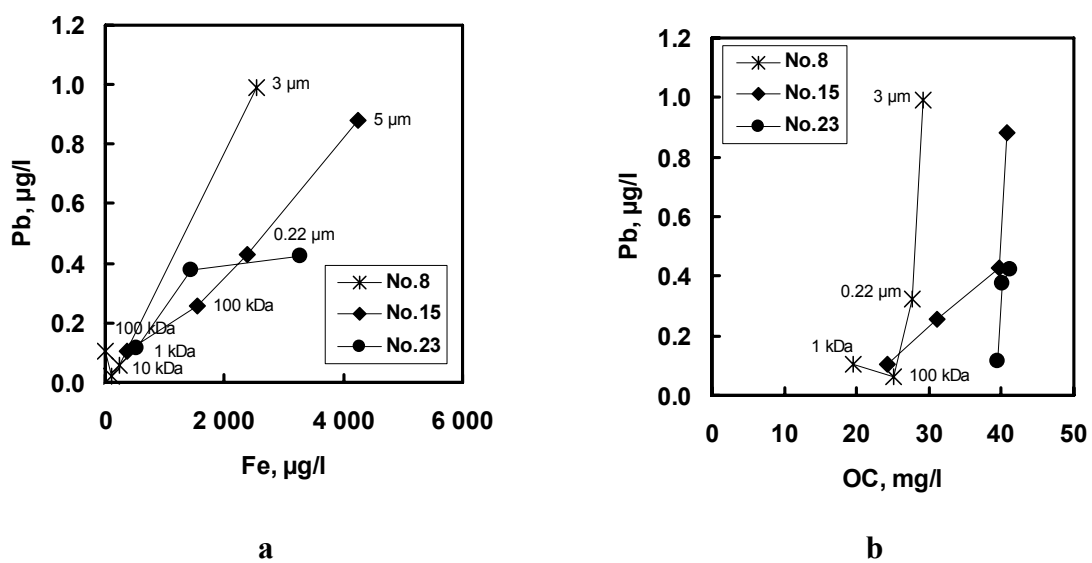


Fig. 3.9. Pb concentration as a function of Fe (a) and OC (b) concentrations in successive filtrates from 5 μm to 1 kDa.

granitic rocks and with [Fe] in basic catchments ($r^2 = 0.28$ and 0.70 for [OC] vs. [Al]) and $r^2 = 0.47$ and 0.06 for [Fe] vs. [Al] in basic and granitic catchments, respectively, Fig. 3.10). The Al concentration in rivers is strongly affected by the size separation procedure, since 80-95% of the total Al is essentially bound to Fe colloids (Fig. 3.11 a). The correlation between Al and OC in filtrates and ultrafiltrates is much less pronounced, suggesting that organic colloids play a less important role in Al speciation in the studied rivers (not shown). Ga follows closely Al, since it is controlled by iron colloids. The concentration of Ga strongly decreases with decreasing Fe concentration in the filtrates (Fig. 3.11 b). The percentage of colloidal Ga (20-90% in 1 kDa – $0.22\text{ }\mu\text{m}$ fraction) does not depend on rock lithology and season, but rather correlates with total [Fe] and [OC] (see discussion below).

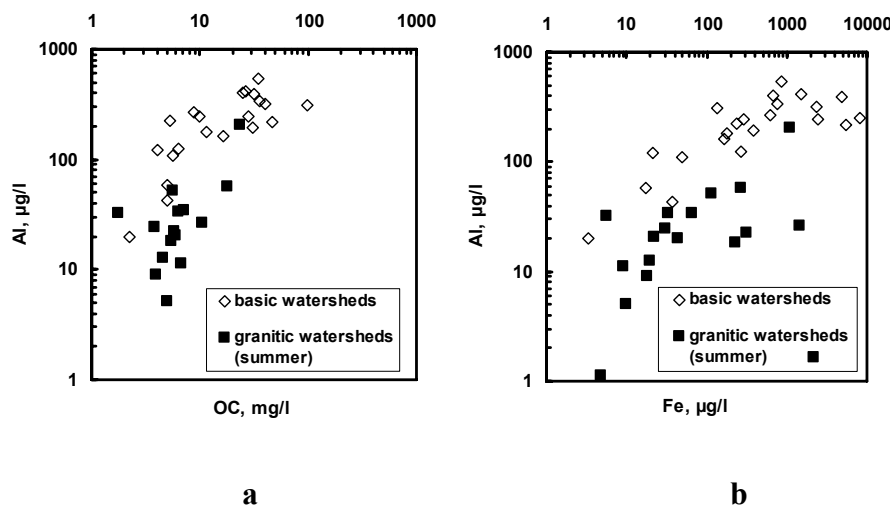


Fig. 3.10. Aluminium correlations with organic matter (a) and iron (b) in 0.22 (0.45) μm filtrates for rivers draining different rocks. Log scale is used for both axes.

La and Ce concentrations in samples waters range from 0.01 to $0.8\text{ }\mu\text{g/l}$ and from 0.05 to $4\text{ }\mu\text{g/l}$, respectively, which is similar to values reported for tropical (Dupré et al., 1996; Viers et al., 1997), temperate (Johannesson et al., 2004) and boreal (Ingri et al., 2000; Pokrovsky and Schott, 2002; Pokrovsky et al., 2006) organic-rich rivers. Dissolved ($< 0.45\text{ }\mu\text{m}$) Y and REEs concentrations are correlated with both Fe and OC in basic rather than in granitic catchments ($r^2(\text{Fe}) = 0.90$ and 0.10 , and $r^2(\text{OC}) = 0.30$ and 0.60 for basic and granitic catchments, respectively, see Fig. 3.12). We observe no systematic enrichment in light or heavy REEs in the sampled waters, as illustrated from crust-normalized REE patterns (Fig. 3.13). This is in agreement with the ultrafiltration

experiments of Viers et al. (1997), who obtained flat patterns from organic-rich rivers of the Cameroun, as well as similar shapes of patterns for the 0.22 µm and 5 kDa fractions. For certain samples (No.6, No.8, No.15, No.18, K-1, K-7, K-22, K-23 and K-24), we observe a negative Ce anomaly in ultrafiltrates or dialysates, or in both types of solution. This fractionation can be explained by preferential oxidation of Ce during the coprecipitation/adsorption of REEs onto Fe hydroxides or colloids from aqueous solution as supported by laboratory experiments (Bau, 1999), and has also been observed in boreal surface waters (Pokrovsky et al., 2006).

Yttrium and REEs are strongly affected by the size-separation procedure and, in most cases, are completely removed from solution by filtration through 1 kDa. In ultrafiltrates, Y and all the REE are associated with iron colloids rather than organic matter, except for the river Ruiga on basic rocks (No.9) and a stream over ultramafic rocks (No.15), where OC colloids are equally important. This is illustrated in Fig. 3.14 for cerium (a, b) and ytterbium (c, d). More than 90% of Y and REE are complexed with large-size colloids (10 kDa – 0.22 µm), the only exception being the swamp water K-23 where 90% of Y and ~70% of REE are present in the 1-10 kDa colloidal fraction.

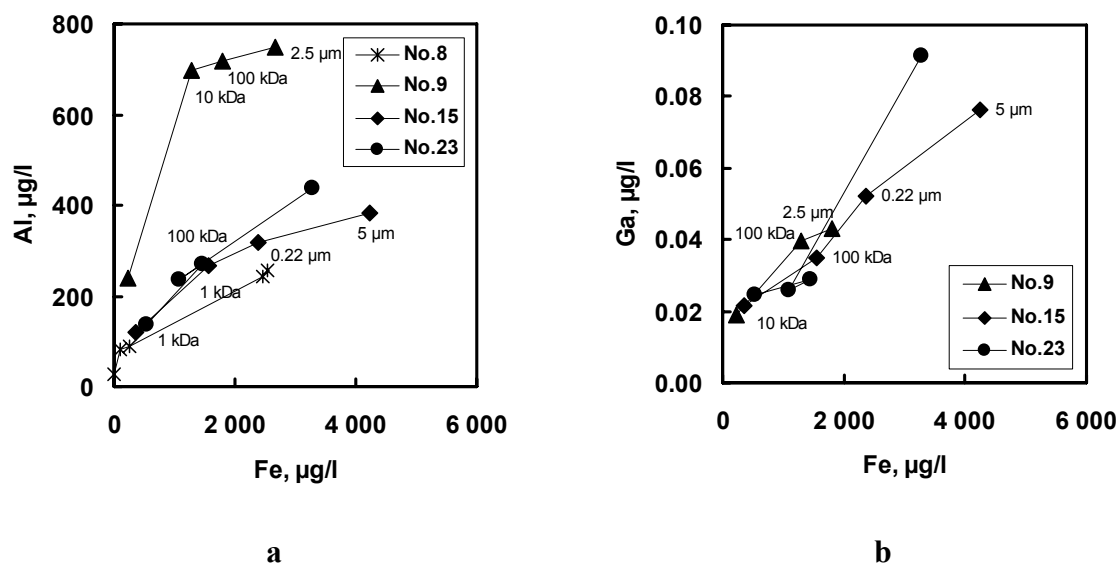


Fig. 3.11. Al (a) and Ga (b) concentration as a function of Fe concentration in successive filtrates from 5 µm to 1 kDa.

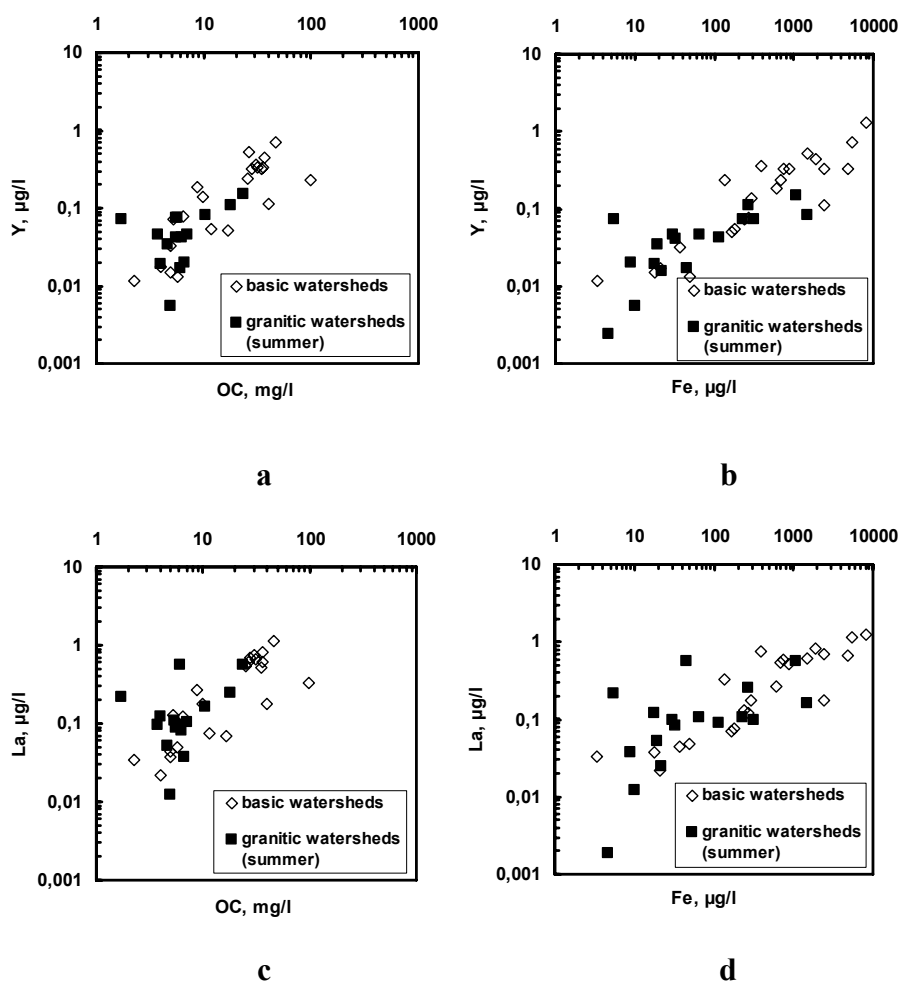


Fig. 3.12. Ytterbium (a, b) and La (c, d) correlations with organic matter and iron in 0.22 (0.45) μm filtrates for rivers draining different rocks. Log scale is used for both axes.

3.4.2.4. Tetravalent Metals: Ti, Zr, Hf and Th

Ti concentrations in the studied fluids range from 0.2 to 3.5 $\mu\text{g/l}$ on basalt catchments, but reach ~8 $\mu\text{g/l}$ on the basic catchment of the organic-rich Ruiga river (No.9) and the stream draining olivinite rocks (K-13). In rivers draining granite-gneisses, the Ti concentration is much lower (0.03-1.3 $\mu\text{g/l}$). Ti is positively correlated with both [Fe] and [OC] in < 0.22 μm filtrates, forming two distinct but close trends for waters draining basic and granitic rocks (Fig. 3.15). However, the results of filtration and ultrafiltration experiments demonstrate the dominant role of iron colloids in Ti speciation: in ultrafiltrates of river waters from granitic catchments, we observe positive correlations of Ti against Fe and OC, with $r^2 = 0.97$ and 0.88, respectively, (Fig. 3.16 a).

The range of Zr, Hf, and Th concentrations measured in Karelian rivers and streams is an order of magnitude higher than for average world rivers (Gaillardet et al., 2003). While total dissolved ($< 0.45 \mu\text{m}$) Zr, Hf and Th concentrations are positively correlated with both Fe and OC (not shown), inorganic Fe colloids are essentially responsible for the high concentrations of these three elements as illustrated in Fig. 3.16 (b, c, d) that reports the results of ultrafiltration and dialysis experiments.

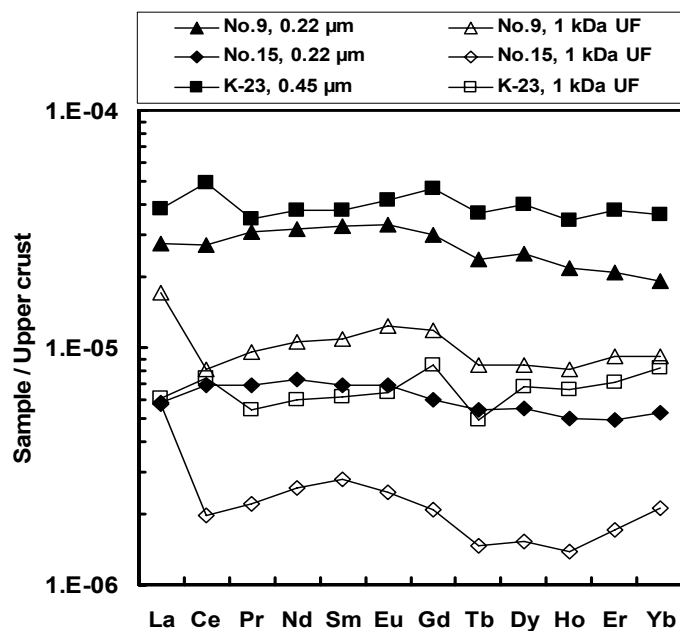


Fig. 3.13. Upper-crust normalized REE pattern (Taylor and McLennan, 1985) of 0.22 (0.45) μm and 1 (10) kDa (ultra)filtrates for Ruiga river (No.9), creek over ultramafites (No.15) and swamp water (K-23).

3.4.2.5. Other Trace Elements: V, Cr, Mo, W, As, Sb, Sn, Nb and U

V, Cr, Mo and W concentrations are slightly higher in rivers and streams draining basic rocks (0.15-0.4, 0.15-3.8, 0.001-0.5 and 0.001-0.02 $\mu\text{g/l}$, respectively) compared to acid-rock dominated catchments (0.05-0.8, 0.08-0.8, 0.005-0.36 and 0.001-0.012 $\mu\text{g/l}$, respectively). Among these elements, only Cr and V on granitic catchments show a clear correlation with dissolved Fe and OC in the 0.22- μm filtrates ($r^2 = 0.88$). Cr concentration is affected by ultrafiltration in all the studied waters, with 40-94% being present in the 1 kDa – 0.22 μm colloidal fraction. Between 36 and 97% of the vanadium is associated with OC or Fe colloids (1 kDa – 0.22 μm) in samples No.6,

No.8, No.18, K-7, K-23, K-43 and K-44, while its concentration falls sharply with decreasing pore size from 5 μm to 1 kDa (Fig. 3.17 a).

Molybdenum and tungsten are mostly present as MoO_4^{2-} and WO_4^{2-} ions unaffected by ultrafiltration or dialysis. However, Mo is present in colloidal form in organic- and Fe-rich swamp waters on basic rocks (60%, samples K-23 and K-43) as well as in some rivers on granitic catchments (70-87% in Ladreka No.23 and Palajoki K-7).

Although arsenic is not associated with either Fe or organic colloids in most rivers, its concentration nevertheless decreases by factor of 1.5 upon filtration and

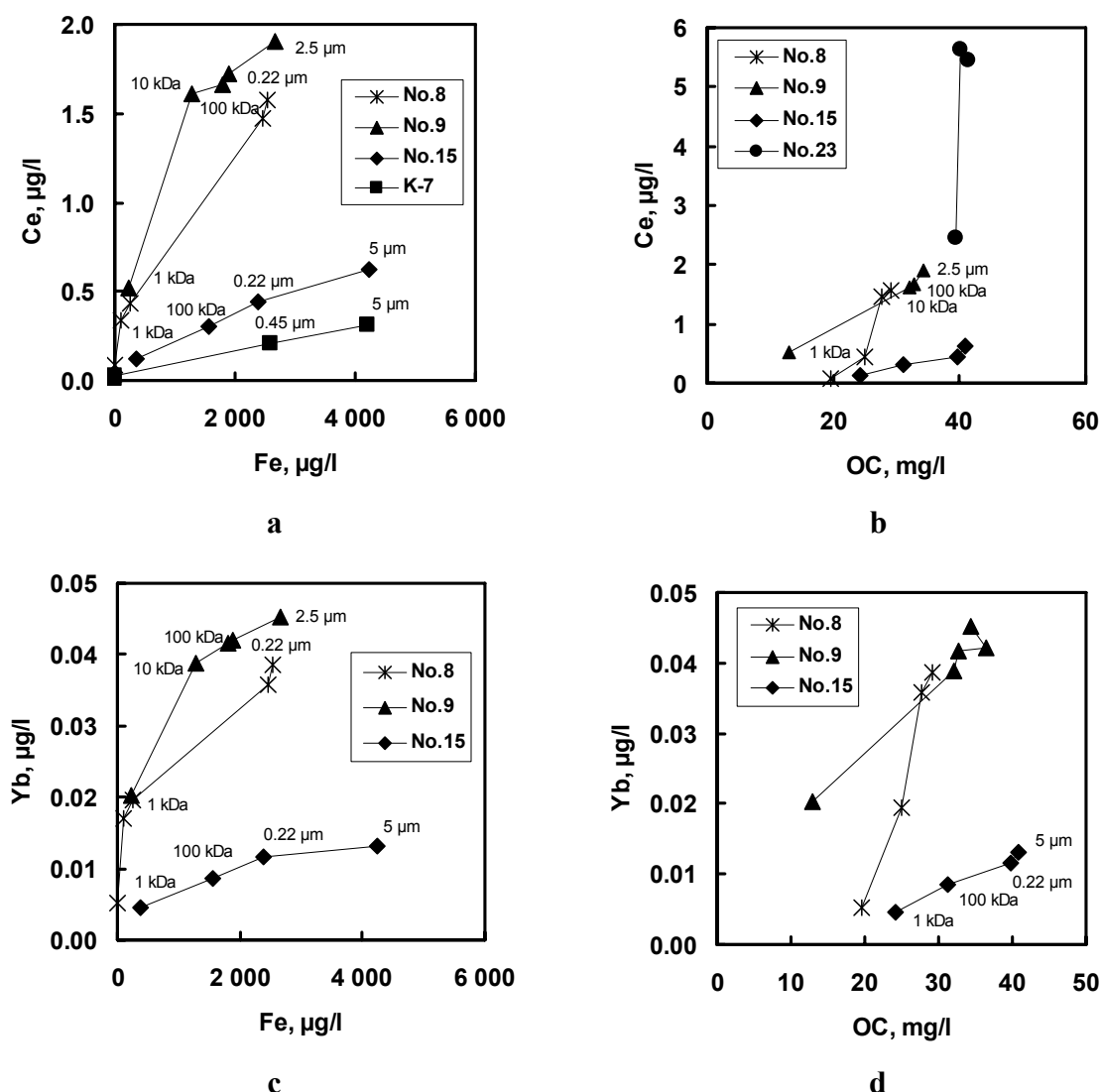


Fig. 3.14. Ce and Yb concentrations as a function of Fe (a, c) and OC (b, d) in successive filtrates from 5 μm to 1 kDa.

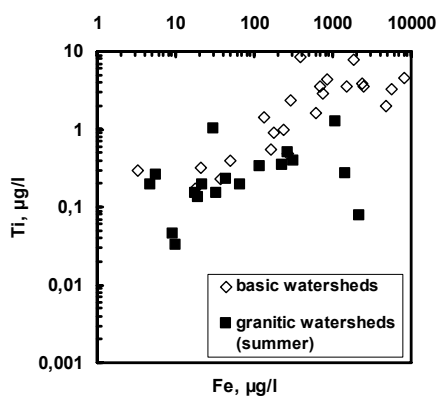


Fig. 3.15. Titanium-Fe correlation in 0.22 (0.45) μm filtrates for rivers draining different rocks. Log scale is used for both axes.

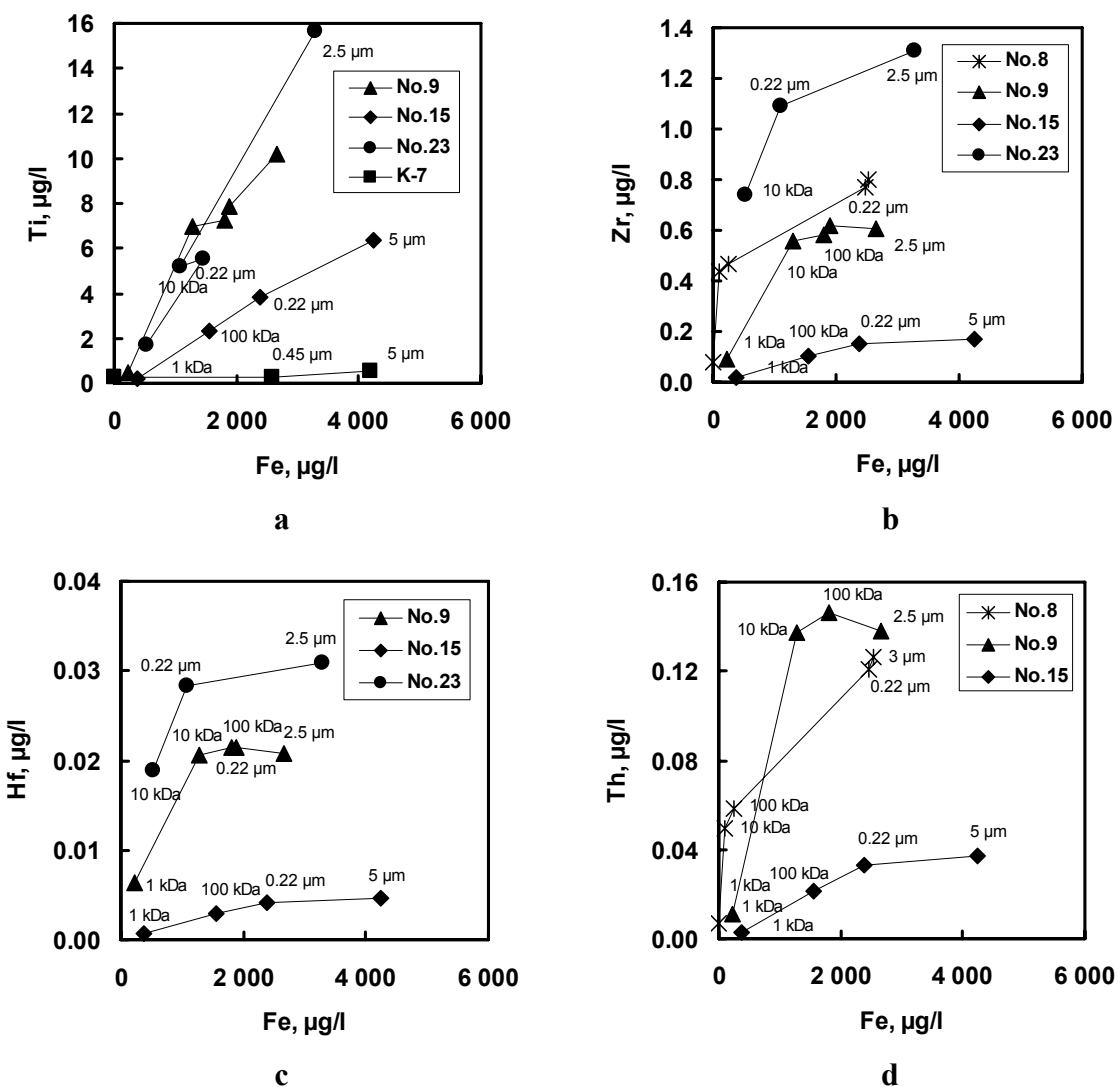


Fig. 3.16. Ti (a), Zr (b), Hf (c), and Th (d) concentrations as a function of Fe concentration in successive filtrates from 5 μm to 1 kDa.

ultrafiltration of samples from organic-rich rivers (Ruiga No.9 and Ladreka No.23) and a stream over ultramafic rocks (No.15) (Fig. 3.17 b). Both As and Sb are essentially present in truly dissolved form (< 1 kDa), with only 20-30% concentrated in small colloidal particles (1 to 10 kDa) in Fe- and organic-rich rivers (Ruiga No.9, Ladreka No.23, stream over ultramafic rocks No.15). In contrast, we fail to observe any correlation between Sb and Fe or OC concentrations in the 0.22- μm filtrates, and Sb concentration shows no change during ultrafiltration experiments, even in samples No. 9 and No. 23.

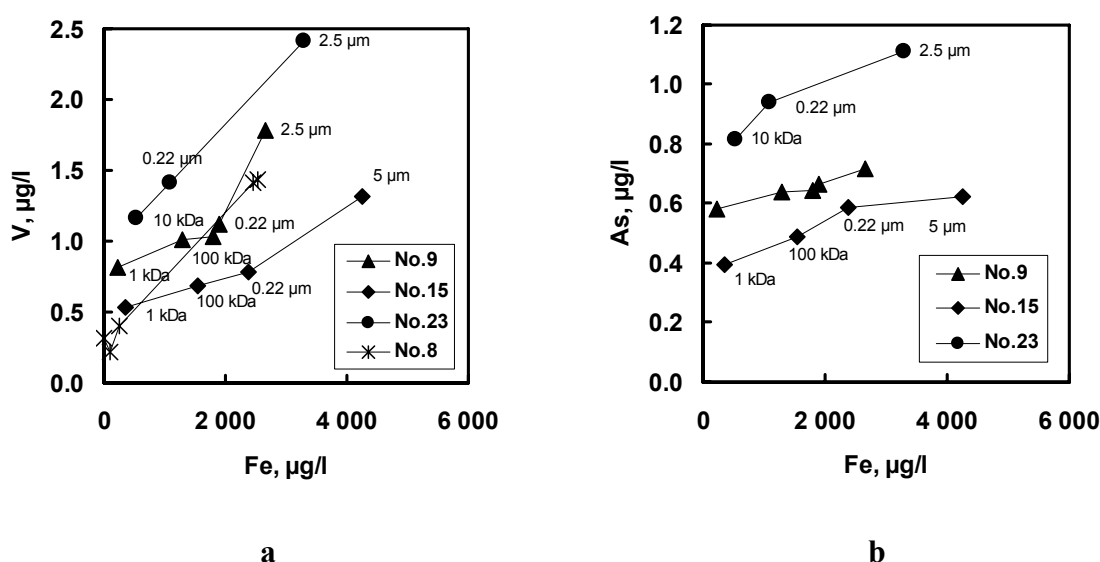


Fig. 3.17. V (a) and As (b) concentration as a function of Fe concentration in successive filtrates from 5 μm to 1-10 kDa.

Nb is essentially present in the large colloidal particles (98% is in the 10 kDa – 0.22 μm fraction in samples No.9, No.15 and K-43). This element is strongly affected by filtration and ultrafiltration, being completely removed from solution in the < 1 kDa fraction. Large-sized colloids also dominate the speciation of uranium, with ca. 80% being incorporated in the 10 kDa – 0.22 μm fraction.

3.4.3. Effect of lithology on element distribution among various types of colloid

The total dissolved concentrations (in samples filtered to < 0.22 or 0.45 μm) of TE are systematically higher for rivers draining basic compared with granitic

catchments; this difference ranges from 15-30% (e.g., for Cu, Cd, REE, Mo, As and Sn) to 50-70% (e.g., for Ti, Zr, Hf, Nb, Ni, Al and Zn) (see Table B-1). At the same time, the concentrations of DOC and Fe, which represent the main TE carriers, are higher in waters from basaltic catchments.

Table B-2 of the Annex B reports the TE distribution between three colloidal pools (< 1 kDa, 1 kDa – 10 kDa and 10 kDa – 0.22 µm) for acidic- and basic rock-dominated catchments (average of five and nine samples, respectively), while Fig. 3.18 presents the results for Fe, Al, Ca, V, Co, La, Th and U. The first important conclusion is that, within ±10% uncertainty, there is no difference in TE distribution within the dissolved and two colloidal pools between the two types of lithology. Though our data do not allow straightforward discrimination, we consider that this conclusion is consistent with three possible pathways of colloid formation, i.e., i) via TE, Fe and OM release from decomposing plant litter in the uppermost surface horizon (Viers et al., 2005; Pokrovsky et al., 2005, 2006), ii) in interstitial soil solutions via production/migration of colloids between soil horizons or iii) at the redox front between Fe(II)-bearing anoxic groundwaters and surficial OM-rich waters of the riparian zone (Pokrovsky and Schott, 2002). Furthermore, it seems very likely that colloids can be formed in riparian zones which are often “suspended” over the lithological substrate. From this point of view, even though the parent rocks differ (mafic or felsic), it is possible that their signature is not pronounced in colloidal speciation of TE.

The second important feature of TE speciation in colloids is the existence of a significant pool of large colloidal particles (10 kDa – 0.22 µm) which account for 10 to 40% of the major cations (solely Ca, Mg and Na for samples No.8, No.22, No.24 and K-44; K for samples No.8 and No.9) and other divalent alkaline-earth elements (Sr and Ba) which are usually considered as being truly dissolved. For most elements significantly affected by the presence of colloids (> 70% of Al, Ti, Y, REEs, Zr, Th and U contained in the 1 kDa – 0.22 µm fraction), the fraction of small colloidal particles (1 to 10 kDa) accounts for only a minor proportion (10 to 20%) compared with large colloidal particles (10 kDa to 0.22 µm, from 50 to 90%).

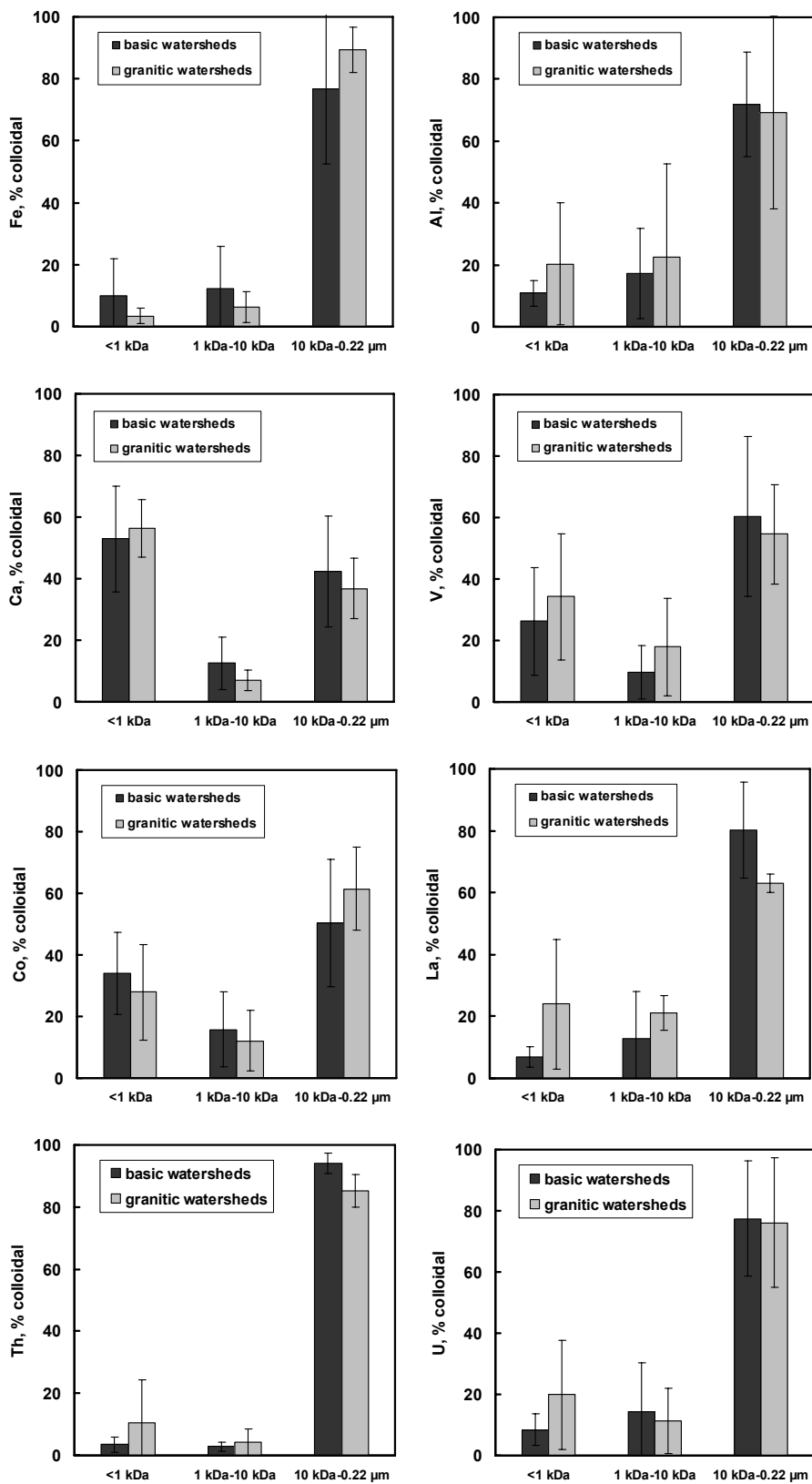


Fig. 3.18. TE distribution between dissolved matter ($< 1 \text{ kDa}$) and two colloidal pools ($1 \text{ kDa} - 10 \text{ kDa}$ and $10 \text{ kDa} - 0.22 \mu\text{m}$) both for acidic- and basic rock-dominated catchments (average of 9 and 5 samples for basic and granitic catchments, respectively) for Fe, Al, Ca, V, Co, La, Th and U.

Thirdly, the transition metals (Cu, Zn, Ni and Co) known to be strongly complexed with organic matter (Benedetti et al., 1996; Bradl, 2004; Tyler, 2004; Dahlqvist et al., 2007; Pédrot et al., 2008) are present in both colloidal and dissolved form, with similar proportions in each of the three pools (< 1 kDa, 1 – 10 kDa and 10 kDa – 0.22 µm). Overall, the effect of rock lithology on TE distribution within different pools of colloids is not pronounced.

3.4.4. Thermodynamic analysis

To improve our understanding of the effect of OM versus Fe oxy(hydr)oxides on TE interaction with different groups of colloids, we made use of available computer codes to carry out a thermodynamic analysis of TE complexation with natural organic matter. Element speciation is assessed here using the Visual MINTEQ computer code, implementing a database for the binding of metals to discrete carboxylic sites (Allison and Perdue, 1994). This calculation is performed here assuming a constant content of 10 µeq COO⁻ per mg DOC (Oliver et al., 1983). Figure 3.19 shows the results of vMINTEQ speciation calculations at pH 5.07-7.50 for Al, Ba, Ca, Na, Cd, Ce, Co, Cu, Dy, Eu, Fe, La, Mn, Nd, Ni, Pb, Sr, Th, U, Y, Yb and Zn in samples No.15, No.23, No.24 and K-43. The proportion of organic complexes increases in the following order by groups of elements: Na-K (2-3%) < Ca-Mg-Sr-Ba (20-40%) < transition and heavy metals Mn-Co-Al-Ni-Zn-Cd-Fe-Pb-Cu (40-90%) ≤ REE-Th-U (70-100%).

This result generally agrees with the speciation of elements in the colloidal fraction obtained by the UF or dialysis procedure (cf. Fig. 3.18 and Table B-2). However, there is some discrepancy for Cd, Pb, Cu whose calculated complexation with organic colloidal matter is overestimated by 10-60%, compared to experimental measurement. In addition, significant proportion of elements is concentrated in large-size (10 kDa – 0.22 µm) colloidal fraction which is not accounted for by vMINTEQ model. There are two main reasons for this discrepancy: i) organic ligands that complex trace elements are smaller than the minimal cut-off (1 kDa) of dialysis/UF used in this study, as recently shown by Pédrot et al. (2008), so these ligands are not detectable by the size-separation procedure, and ii) the speciation of TE in colloids is controlled by interaction with Fe oxy(hydr)oxides rather than DOC. In cases of TE complexation with organic ligands, the main controlling factor is expected to be the surface area of

colloids, which defines the number of functional groups available for chemical reaction. For many trace elements (Ti, Cr, Co, Ni, Pb, REE, Th, U, etc.) strongly associated with large colloidal particles (< 30% in 1 – 10 kDa and 60-99% in 10 kDa – 0.22 µm), it turns out that the total surface area of 10 kDa – 0.22 µm iron hydroxide colloids is insufficient to accommodate all the TE carried by the colloidal matter. This conclusion corroborates the results of Pokrovsky and Schott (2002) and Pokrovsky et al. (2006). Therefore, we should consider trace elements are incorporated within the colloids rather than adsorbed onto their surface or complexed with OM.

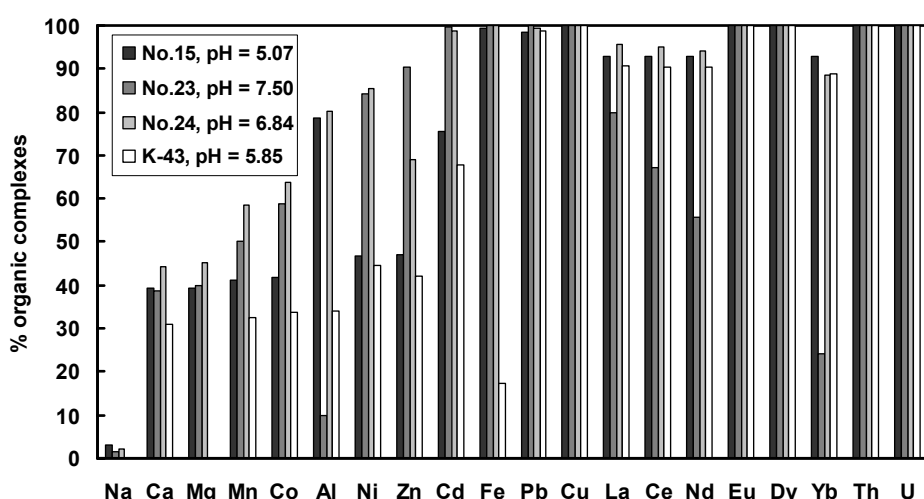


Fig. 3.19. Calculated proportions of organic complexes for Na, Ca, Mg, Mn, Co, Al, Ni, Zn, Cd, Fe, Pb, Cu, REEs, Th and U in four samples in 0.22 µm fraction (No.15, No.23, No.24 and K-43).

To obtain a quantitative assessment of parameters describing the incorporation of TE into the bulk of large colloids via coprecipitation, we calculate the iron-normalized TE partition coefficient between “dissolved” (< 1 kDa) and colloidal (1 kDa to 0.22 µm) fractions, which is defined as follows:

$$K_d = (\text{TE}/\text{Fe})_{\text{colloidal}} / (\text{TE}/\text{Fe})_{\text{dissolved}}$$

Iron-normalized K_d values range from 0.01-0.1 to 1-2 (Table B-3 of the Annex B), being highest for trivalent and tetravalent elements. Note a systematic decrease of K_d from La to Lu, in agreement with the tendency of LREEs to adsorb/coprecipitate with Fe hydroxide and HREEs to form stable aqueous complexes in solution (Bau, 1999). Highly soluble elements exhibiting only weak affinity for colloids (V, Mn, Co, Ni, Cu, Zn, As, Mo, Sn and Sb) have K_d values between 0.001 and 0.3 (except for swamp water

K-43, which yields the highest K_d values) due, probably, to the artifacts of UF procedure raised from Fe^{2+} oxidation (see Section 3.4.1).

3.5. Conclusions

For almost 30 elements affected by size separation during filtration, dialysis yields a 2 to 3 times higher proportion of colloidal forms (1 kDa – 0.22 µm) compared to frontal ultrafiltration. Nevertheless, dialysis is able to provide a fast and artefact-free *in-situ* separation of colloidal and dissolved components. Its main advantages over the more widely used ultrafiltration technique are i) the absence of charge separation; ii) no clogging of the filter membrane induced by forced filtration, and iii) a reduction in the various sources of contamination (filter, apparatus, tubing and recipient) provided the constant chemical composition and colloidal stability of the external pool is maintained.

Within $\pm 10\%$ uncertainty, there is no difference in TE distribution between truly dissolved forms (< 1 kDa) and two colloidal pools (1 kDa – 10 kDa and 10 kDa – 0.22 µm) in surface waters draining acidic and basic rocks. We also note the existence of a significant pool of large colloidal particles (10 kDa – 0.22 µm) that accounts for 10 to 40% of major cations (Ca, Mg and Na) and other divalent alkaline-earth elements (Sr and Ba) that are usually considered as being in truly dissolved forms. The transition metals (Cu, Zn, Ni and Co), which are known to be strongly complexed with organic matter, are present in both colloidal and dissolved form, with similar proportions in each fraction (< 1 kDa, 1 – 10 kDa and 10 kDa – 0.22 µm) pools. Finally, for most elements significantly affected by the presence of colloids (Al, Ti, Y, REEs, Zr, Th and U) more than 70% is contained in the 1 kDa – 0.22 µm fraction, while the small colloidal particles (1 – 10 kDa) account for only a minor proportion (10 to 20%) compared to large colloidal particles (10 kDa – 0.22 µm, from 50 to 90%).

Geochemical modelling of the complexation of several TE with natural organic matter provides a general agreement with the experimental results although it does not allow us to reproduce quantitatively the distribution of all colloidal versus dissolved forms. This is consistent with a previous hypothesis that the TEs are associated with the inorganic (Fe-bearing) part of the colloids, and not just complexed with humic or fulvic acids. Our observations are compatible with three possible pathways of colloid formation, i.e., i) in the uppermost surface horizon via the release of dissolved TE, Fe

and organic matter from decomposing plant litter, ii) in interstitial soil solutions via production/migration of colloids between soil horizons and iii) at the redox front between Fe(II)-bearing anoxic groundwaters and surficial OM-rich waters of the riparian or wetland zone. Indeed, since we did not investigate the flood period, the influence of decomposing plant litter is difficult to assess and its contribution is low during the base flow. Though our data do not allow straightforward discrimination, we consider the third process is more likely to contribute to colloids origin during the summer time. The only exception is mire zone around river Palajoki (samples K-43 and K-44) where the grass/mosses degradation occurs in small ponds/reservoirs directly linked to the river channel.

Further stable-isotope (Ca, Cu, Fe) geochemical studies and experimental modelling of colloid formation are required to ascertain the mechanism of TE interaction with organo-mineral colloids of the boreal zone.

Acknowledgements. This work was supported by the French National Programme INSU (EC2CO, Environnement Côtier PNEC), GDR TRASS, and by European Associated Laboratory “LEAGE”. We thank Jacques Schott for his help in the field and useful discussions. Michael Carpenter post-edited the English style.

References

- Alfaro-De la Torre M. C., Beaulieu P. Y. and Tessier A. T. (2000) In situ measurement of trace metals in lakewater using the dialysis and DGT techniques. *Anal. Chim. Acta* **418**, 53–68.
- Allison J. D. and Perdue E. M. (1994) Modeling metal-humic interaction with Minteqa2. In *Humic Substances in the Global Environment and Implications on Human Health*, Senesi N., Miano T.M. (Eds.). Elsevier Science B.V., Amsterdam. pp. 927-942.
- Amelin Yu. V., Heaman L. and Semenov V. (1995) U-Pb geochronology of layered mafic intrusions in the eastern Baltic Shield: implications for the timing and duration of Paleoproterozoic continental rifting. *Precambrian Res.* **75**, 31-46.
- Amelin Yu. V. and Semenov V. S. (1996) Nd and Sr isotopic geochemistry of mafic layered intrusions in the eastern Baltic shield: implications for the evolution of Paleoproterozoic continental mafic magmas. *Contrib. Mineral. Petrol.* **124**, 255-272.
- Andersson P. S., Porcelli D., Wasserburg G. J. and Ingri J. (1998) Particle transport of $^{234}\text{U}/^{238}\text{U}$ in the Kalix river and in the Baltic Sea. *Geochim. Cosmochim. Acta* **62**(3), 385-392.
- Andersson P. S., Dahlqvist R., Ingri J. and Gustafsson Ö. (2001) The isotopic composition of Nd in a boreal river: A reflection of selective weathering and colloidal transport. *Geochim. Cosmochim. Acta* **65**(4), 521-527.
- Ariés S., Valladon M., Polvé M. and Dupré B. (2000) A routine method for oxide and hydroxide interference corrections in ICP-MS chemical analysis of environmental and geological samples. *Geostandards Newsletter* **24**, 19-31.
- Åström M. and Corin N. (2000) Abundance, sources and speciation of trace elements in humus-rich streams affected by acid sulphate soils. *Aquat. Geochem.* **6**(3), 367-383.
- Åström M. (2001) The effect of acid soil leaching on trace element abundance in a medium-sized stream, W. Finland. *Appl. Geochem.* **16**, 387-396.
- Balashov Yu. A., Bayanova T. B. and Mitrofanov F. P. (1993) Isotope data on the age and genesis of layered basic-ultrabasic intrusions in the Kola Peninsula and northern Karelia, northeastern Baltic Shield. *Precambrian Res.* **64**, 197-205.
- Bau M. (1999) Scavenging of dissolved yttrium and rare earths by precipitating iron oxyhydroxide: Experimental evidence for Ce oxidation, Y-Ho fractionation, and lanthanide tetrad effect. *Geochim. Cosmochim. Acta* **63**, 67-77.
- Benedetti M. F., van Riemsdijk W. H., Koopal L. K., Kinniburgh D. G., Goodyd D. C. and Milne C. J. (1996) Metal ion binding by natural organic matter: From the model to the field. *Geochim. Cosmochim. Acta* **60**(14), 2503-2513.

-
- Björkvald L., Buffam I., Laudon H. and Mörth C. (2008) Hydrogeochemistry of Fe and Mn in small boreal streams: The role of seasonality, landscape type and scale. *Geochim. Cosmochim. Acta* **72**(12), 2789-2804.
- Bluth G. J. S. and Kump L. R. (1994) Lithologic and climatologic controls of river chemistry. *Geochim. Cosmochim. Acta* **58**(10), 2341-2359.
- Bradl H. B. (2004) Adsorption of heavy metal ions on soils and soils constituents. *J. Colloid Interface Sci.* **277**, 1-18.
- Buffle J., Deladoey P. and Haerdi W. (1978) The use of ultrafiltration for the separation and fractionation of organic ligands in fresh waters. *Anal. Chim. Acta* **101**, 339-357.
- Bychkova Ya. V., Koptev-Dvornikov E. V., Kononkova N. N. and Kameneva E. E. (2007) Composition of rock-forming minerals in the Kivakka layered massif, northern Karelia, and systematic variations in the chemistries of minerals in the rhythmic layering subzone. *Geochem. Int.* **45**(2), 131-151.
- Dahlqvist R., Benedetti M. F., Andersson K., Turner D., Larsson T., Stolpe B. and Ingri J. (2004) Association of calcium with colloidal particles and speciation of calcium in the Kalix and Amazon rivers. *Geochim. Cosmochim. Acta* **68**(20), 4059-4075.
- Dahlqvist R., Andersson P. S. and Ingri J. (2005) The concentration and isotopic composition of diffusible Nd in fresh and marine waters. *Earth Planet. Sci. Lett.* **233**, 9-16.
- Dahlqvist R., Andersson K., Ingri J., Larsson T., Stolpe B. and Turner D. (2007) Temporal variations of colloidal carrier phases and associated trace elements in a boreal river. *Geochim. Cosmochim. Acta* **71**, 5339-5354.
- Dai M. and Martin J. (1995) First data on trace metal level and behaviour in two major Arctic river-estuarine systems (Ob and Yenisey) and in the adjacent Kara Sea, Russia. *Earth Planet. Sci. Lett.* **131**(3-4), 127-141.
- Dai M., Martin J. and Cauwet G. (1995) The significant role of colloids in the transport and transformation of organic carbon and associated trace metals (Cd, Cu and Ni) in the Rhône delta (France). *Mar. Chem.* **51**, 159-175.
- Degueldre C., Triay I., Kim J., Vilks P., Laaksoharju M. and Miekeley N. (2000) Groundwater colloid properties: a global approach. *Appl. Geochem.* **15**, 1043-1051.
- Dia A., Gruau G., Olivié-Lauquet G., Riou C., Molénat J. and Curmi P. (2000) The distribution of rare earth elements in groundwaters: Assessing the role of source-rock composition, redox changes and colloidal particles. *Geochim. Cosmochim. Acta* **64**(24), 4131-4151.
- Dupré B., Gaillardet J., Rousseau D. and Allègre C. J. (1996) Major and trace elements of river-borne material: The Congo Basin. *Geochim. Cosmochim. Acta* **60**(8), 1301-1321.

-
- Dupré B., Viers J., Dandurand J.-L., Polvé M., Benezeth P., Vervier Ph. and Braun J.-J. (1999) Major and trace elements associated with colloids in organic-rich river waters: ultrafiltration of natural and spiked solutions. *Chem. Geol.* **160**, 63-80.
- Evdokimova T. (1957) Soil formation process on metamorphic rocks of Karelia. *Pochvovedenie (Soviet Soil. Sci.)* **9**, 60-69.
- Eyrolle F., Benedetti M. F., Benaim J. Y. and Février D. (1996) The distributions of colloidal and dissolved organic carbon, major elements, and trace elements in small tropical catchments. *Geochim. Cosmochim. Acta* **60**(19), 3643-3656.
- Gaillardet J., Dupré B., Allègre C. J. and Négrel P. (1997) Chemical and physical denudation in the Amazon River Basin. *Chem. Geol.* **142**, 141-173.
- Gaillardet J., Viers J. and Dupré B. (2003) Treatise on Geochemistry, **5** (eds. H.D. Holland and K.K. Turekian). In *Surface and Ground Water, Weathering, and Soils* (ed. J. I. Drever). Elsevier-Pergamon, Oxford. pp. 225-272.
- Gimpel J., Zhang H., Davison W. and Edwards A. (2003). In situ trace metal speciation in lake surface waters using DGT, dialysis, and filtration. *Environ. Sci. Technol.* **37**(1), 138-146.
- Guo L., Hunt B. J. and Santschi P. H. (2001) Ultrafiltration behavior of major ions (Na, Ca, Mg, F, Cl, and SO₄) in natural waters. *Wat. Res.* **35**(6), 1500-1508.
- Hoffman M. R., Yost E. C., Eisenreich S. J. and Maier W. J. (1981) Characterization of soluble and colloidal-phase metal complexes in river water by ultrafiltration. A mass-balance approach. *Environ. Sci. Technol.* **15**(6), 655-661.
- Ingri J. and Widerlund A. (1994) Uptake of alkali and alkaline-earth elements on suspended iron and manganese in the Kalix River, northern Sweden. *Geochim. Cosmochim. Acta* **58**(24), 5433-5442.
- Ingri J., Torssander P., Andersson P. S., Mört C. and Kusakabe M. (1997) Hydrogeochemistry of sulfur isotopes in the Kalix River catchment, northern Sweden. *Appl. Geochem.* **12**, 483-496.
- Ingri J., Widerlund A., Land M., Gustafsson Ö., Andersson P. S. and Öhlander B. (2000) Temporal variations in the fractionation of the rare earth elements in a boreal river, the role of colloidal particles. *Chem. Geol.* **166**, 23-45.
- Ingri J., Widerlund A. and Land M. (2005) Geochemistry of major elements in a pristine boreal river system, Hydrological compartments and flow paths. *Aquatic Geochemistry* **11**, 57-88.
- Ingri J., Malinovsky D., Rodushkin I., Baxter D. C., Widerlund A., Andersson P., Gustafsson Ö., Forsling W. and Öhlander B. (2006) Iron isotope fractionation in river colloidal matter. *Earth Planet. Sci. Lett.* **245**, 792-798.
- Johannesson K. H., Tang J., Daniels J. M., Bounds W. J. and Burdige D. J. (2004) Rare

-
- earth element concentrations and speciation in organic-rich blackwaters of the Great Dismal Swamp, Virginia, USA. *Chem. Geol.* **209**, 271-294.
- Kulikov V., Bychkova Ya., Kulikova V., Koptev-Dvornikov E. and Zudin A. (2005) Role of deep-seated differentiation in formation of Paleoproterozoic Sinegorie lava plateau of komatiite basalts, southeastern Fennoscandia. *Petrology* **13**(5), 469-488.
- Land M. and Öhlander B. (1997) Seasonal variations in the geochemistry of shallow groundwater hosted in granitic till. *Chem. Geol.* **143**, 205-216.
- Land M., Ingri J. and Öhlander B. (1999) Past and present weathering rates in northern Sweden. *Appl. Geochem.* **14**, 761-774.
- Land M., Ingri J., Andersson P. S. and Öhlander B. (2000) Ba/Sr, Ca/Sr and $^{87}\text{Sr}/^{86}\text{Sr}$ ratios in soil water and groundwater: implications for relative contributions to stream water discharge. *Appl. Geochem.* **15**, 311-325.
- Land M. and Öhlander B. (2000) Chemical weathering rates, erosion rates and mobility of major and trace elements in a boreal granitic till. *Aquat. Geochem.* **6**, 435-460.
- Öhlander B., Land M., Ingri J. and Widerlund A. (1996) Mobility of rare earth elements during weathering of till in northern Sweden. *Appl. Geochem.* **11**, 93-99.
- Öhlander B., Ingri J., Land M. and Schoberg H. (2000) Change of Sm-Nd isotope composition during weathering of till. *Geochim. Cosmochim. Acta* **64**(5), 813-820.
- Oliver B., Thurman E. and Malcolm R. (1983) The contribution of humic substances to the acidity of colored natural waters. *Geochim. Cosmochim. Acta* **47**, 2031-2035.
- Pédrot M., Dia A., Davranche M., Coz M. B., Henin O. and Gruau G. (2008) Insights into colloid-mediated trace element release at the soil/water interface. *J. Colloid Interface Sci.* **325**, 187-197.
- Pham M. H. and Garnier J. (1998) Distribution of trace elements associated with dissolved compounds ($< 0.45 \mu\text{m} - 1 \text{ nm}$) in freshwater using coupled (frontal cascade) ultrafiltration and chromatographic separations. *Environ. Sci. Technol.* **32**(4), 440-449.
- Pokrovsky O. and Schott J. (2002) Iron colloids/organic matter associated transport of major and trace elements in small boreal rivers and their estuaries (NW Russia). *Chem. Geol.* **190**, 141-179.
- Pokrovsky O. S., Dupré B. and Schott J. (2005) Fe-Al-organic colloids control of trace elements in peat soil solutions. *Aquat. Geochem.* **11**, 241-278.
- Pokrovsky O. S., Schott J. and Dupré B. (2006) Trace element fractionation and transport in boreal rivers and soil porewaters of permafrost-dominated basic terrain in Central Siberia. *Geochim. Cosmochim. Acta* **70**, 3239-3260.
- Pontér C., Ingri J., Burmann J. and Boström K. (1990) Temporal variations in dissolved

-
- and suspended iron and manganese in the Kalix River, northern Sweden. *Chem. Geol.* **81**, 121-131.
- Pontér C., Ingri J. and Boström K. (1992) Geochemistry of manganese in the Kalix River, northern Sweden. *Geochim. Cosmochim. Acta* **56**, 1485-1494.
- Porcelli D., Andersson P. S., Wasserburg G. J., Ingri J. and Baskaran M. (1997) The importance of colloids and mires for the transport of uranium isotopes through the Kalix River watershed and Baltic Sea. *Geochim. Cosmochim. Acta* **61**(19), 4095-4113.
- Puchtel I., Hofmann A., Mezger K., Shchipansky A., Kulikov V. and Kulikova V. (1996) Petrology of a 2.41 Ga remarkably fresh komatiitic basalt lava lake in Lion Hills, central Vetreny Belt, Baltic Shield. *Contrib. Mineral. Petrol.* **124**(3-4), 273-290.
- Puchtel I. S., Haase K. M., Hofmann A. W., Chauvel C., Kulikov V. S., Garbe-Schonberg C. and Nemchin A. A. (1997) Petrology and geochemistry of crustally contaminated komatiitic basalts from the Vetreny Belt, southeastern Baltic Shield: Evidence for an early Proterozoic mantle plume beneath rifted Archean continental lithosphere. *Geochim. Cosmochim. Acta* **61**(6), 1205-1222.
- Rember R. D. and Trefry J. H. (2004) Increased concentrations of dissolved trace metals and organic carbon during snowmelt in rivers of the Alaskan Arctic. *Geochim. Cosmochim. Acta* **68**(3), 477-489.
- Shiller A. M. (1997) Dissolved trace elements in the Mississippi River: Seasonal, interannual, and decadal variability. *Geochim. Cosmochim. Acta* **61**(20), 4321-4330.
- Sholkovitz E. R. (1995) The aquatic chemistry of rare earth elements in rivers and estuaries. *Aquat. Geochem.* **1**, 1-34.
- Tyler G. (2004) Vertical distribution of major, minor, and rare elements in a Haplic Podzol. *Geoderma* **119**, 277-290.
- Taylor S. and McLennan S. (1985) *The continental crust: its composition and evolution*. Blackwell Scientific Publications, Oxford.
- Viers J., Dupré B., Polvé M., Dandurand J. and Braun J. (1997) Chemical weathering in the drainage basin of a tropical watershed (Nsimi-Zoetele site, Cameroon): comparison between organic-poor and organic-rich waters. *Chem. Geol.* **140**, 181-206.
- Viers J., Barroux G., Pinelli M., Seyler P., Oliva P., Dupré B. and Boaventura G. R. (2005) The influence of the Amazonian floodplain ecosystems on the trace element dynamics of the Amazon River mainstem (Brazil). *Sci. Total Environ.* **339**, 219-232.
- Yeghicheyan D., Carignan J., Valladon M., Bouhnik Le Coz M., Le Corne F., Castrec-Rouelle M., Robert M., Aquilina L., Aubry E., Churlaud C., Dia A., Deberdt S., Dupré B., Freydier R., Gruau G., Hénin O., de Kersabiec A. M., Macé J., Marin L.,

-
- Morin N., Petitjean P. & Serrat E. (2001) A compilation of silicon and thirty one trace elements measured in the natural river water reference material SLRS-4 (NRC-CNRC). *Geostandards Newsletter* **25**(2-3), 465-474.
- Zakharova E., Pokrovsky O. S., Dupré B. and Zaslavskaya M. B. (2005) Chemical weathering of silicate rocks in Aldan Shield and Baikal Uplift: insights from long-term seasonal measurements of solute fluxes in rivers. *Chem. Geol.* **214**, 223-248.
- Zakharova E., Pokrovsky O. S., Dupré B., Gaillardet J. and Efimova L. (2007) Chemical weathering of silicate rocks in Karelia region and Kola peninsula, NW Russia: Assessing the effect of rock composition, wetlands and vegetation. *Chem. Geol.* **242**, 255-277.

Chapter 4

Experimental measurement of trace elements association with natural organo-mineral colloids using dialysis



Vasyukova E.V., Pokrovsky O.S., Viers J., Dupré B.

In preparation for *Environmental Science and Technology*

Experimental measurement of trace elements association with natural organo-mineral colloids using dialysis

Vasyukova E.V.^{1,2}, Pokrovsky O.S.¹, Viers J.¹, Dupré B.¹

(in preparation for *Environmental Science and Technology*)

¹ *Laboratory of Mechanisms and Transfers in Geology (LMTG, UMR 5563), University of Toulouse,
OMP-CNRS; 14, avenue Edouard Belin, 31400 Toulouse, France,*

² *Saint-Petersburg State Polytechnic University, 29, Polytechnicheskaya st., Saint-Petersburg, Russia*

Keywords: trace element, colloids, dialysis, speciation, humic acid, boreal zones

Abstract

Equilibrium dialysis procedure was used to assess the distribution coefficients of more than 50 major and trace elements between colloidal (1 kDa – 0.22 µm) and dissolved (< 1 kDa) forms. For this, Spectra Pore 7® dialysis membranes filled by deionized water were placed in large volume of natural filtered water and the pH of solution was varied between 3 and 8. After achieving equilibrium (typically after 24 hours), concentrations of trace elements were measured both inside the dialysis bag and in the external solution using ICP-MS. These measurements allowed quantification of both the TE distribution coefficients and the proportion of colloidal forms as a function of solution pH. Two groups of elements can be distinguished according to their behaviour during dialysis: i) those exhibiting significant increase of proportion of colloidal forms with pH increase (Mn, Cr, Co, Ni, Cu, Zn, Sr, Y, Cd, Ba, REEs, U, Pb, Ga, Hf, U) and strongly associated with colloids (Al, Fe, Th, Zr), and ii) elements that are weakly associated with colloids and whose distribution coefficients are not significantly affected by solution pH (Li, B, Na, K, Ca, Mg, B, Si, Ti, V, Ge, Rb, Nb, As, Mo, Sn, Sb, Cs, W, Tl). Element speciation was assessed using the Visual MINTEQ computer code with an implemented NICA-Donnan humic ion binding model and database. The model reproduces quantitatively the pH-dependence of colloidal form proportion for divalent metals (Mn, Co, Ni, Cd, Sr, Ca, Pb) whereas for other elements

(i.e., U, Cu) the decrease of stability constants by several orders of magnitude was necessary to fit the experimental data. However, reproducing the experimental pH-dependence of colloidal proportion for trivalent and tetravalent elements (Fe, Al, REEs, Th) was not possible even by decreasing their stability constants with humic and fulvic acids by many orders of magnitude. It was suggested that Fe colloids dissolution that incorporates coprecipitated trace metals is responsible for the pH-dependent pattern of colloids distribution. The main significance of this work is that it allows direct empirical prediction of most TE speciation in natural organic and Fe-rich boreal waters under condition of aquifers acidification induced by global warming.

4.1. Introduction

Quantification of the association between trace elements and colloids in natural waters is one of the major issues for modeling of trace elements migration and bioavailability in continental waters (Buffle and van Leeuwen, 1992). At present, there is little doubt that in continental waters, most trace elements are not present in the form of ionic species but rather associated with organic and organo-mineral colloids (Ingri et al., 2000). This is especially true for boreal regions, where the presence of wetlands, abundant precipitation and sufficient plant production creates favourable conditions for formation of organic rich soils and provides high concentrations of organic matter in surficial waters.

Quantitative modeling of migration and bioavailability of trace elements requires the knowledge of stability constants for complexation reactions of trace metals with colloidal organic matter. The most powerful and precise method of assessing these constants is voltammetry and potentiometry; however, their use is restricted by very low number of transition metals (Zn, Cu, Cd, Pb) and some rare earth elements (Stevenson and Chen, 1991; Chang Chien et al., 2006; Prado et al., 2006; Johannesson et al., 2004). Up to present time, large number of trace elements, including trivalent and tetravalent elements, remains unexplored and the quantification of their stability constants with natural colloidal matter is not possible. This hampers the progress in applying quantitative physico-chemical models such as WHAM (Tipping and Hurley, 1992; Tipping, 1994; Tipping, 1998; Tipping et al., 2002), WinHumicV based on WHAM model (Gustafsson, 1999) or NICA-Donnan (Benedetti et al., 1995; Kinniburgh et al.,

1999; Milne et al., 2001; Milne et al., 2003) for assessing trace elements speciation in continental waters. This work is aimed at filling this gap by suggesting a new method for quantifying the complexation of multiple trace elements with natural colloids.

Another difficulty in characterization of TE speciation in natural waters lays in extremely variable and multiple chemical nature of colloidal matter: usually, one can distinguish organic colloids (humic and fulvic acids, microbial exudates, polysaccharides) and organo-mineral entities (Fe and Al hydroxide stabilized by organic matter) (Allard, 2006; Allard and Derenne, 2007; Dahlqvist et al., 2004, 2007; Viers et al., 1997; Ingri and Widerlund, 1994; Gustafsson and Gschwend, 1997; Gustafsson et al., 2000; Andersson et al., 2001; Pokrovsky et al., 2005, 2006). Whereas the complexation of TE with organic colloids, notably with standard specially purified and thoroughly characterized humic and fulvic acids, is fairly well known, organo-mineral and mineral (Fe, Al) colloids stabilized by adsorbed OM do not exist in commercial ready-to-use form and experimental works with such synthetic or purified standard colloids are very limited. In this regard, direct experiments on natural samples may shed new lights on TE complexation with organo-mineral colloids. The present study is focused on acquiring apparent distribution coefficients of TE between conventionally dissolved (< 1 kDa) and colloidal fraction (1 kDa – 0.22 µm) as a function of solution pH that should allow further modeling of TE speciation using thermodynamic approaches with available computer codes.

Arctic and subarctic regions are among the most fragile zones in the world due to their low resistance to industrial impact, low productivity of terrestrial biota and limited biological activity over the year. At the same time, the effect of global warming consisting not only in rising the surface temperature but also acidification of water reservoirs is expected to be mostly pronounced in the Arctic (Reuss et al., 1987). Acidification is likely to change the speciation of many TE, proportion of labile and biologically available forms and thus can influence pollutants migration and bioavailability. Quantitative prediction of these phenomena requires rigorous knowledge of the proportion of colloidal forms of TE in solution as a function of pH. Equilibrium dialysis through 1-kDa membrane, comparable with the pore size of cell protein/lipid membranes, developed in this study, should allow tracing these changes at almost in-situ conditions using relatively inexpensive and straightforward technique.

Therefore, the goals of the present study are the following: 1) develop simple in-situ method for characterization of colloidal status of TE in natural waters depending on solution pH; 2) quantify distribution coefficients and degree of TE association with organo-mineral colloids found in several typical boreal waters; 3) test existing thermodynamic models for description of TE speciation as a function of pH in solutions containing complex organo-mineral colloids of poorly defined structure. It is anticipated that achieving these goals will allow better understanding of TE speciation and, consequently, their bioavailability in natural waters of subarctic regions.

4.2. Materials and methods

4.2.1. Sampling

Series of samples were collected during field campaigns in July-August 2004, February 2006 and July 2006 during summer and winter base flow period. Surface waters were collected from typical small creeks, medium size rivers and swamp zones belonging to watersheds of various lithology of the White Sea basin and located in the North-Western part of Russia, Fig. 4.1. Detailed geographical, geological and climate description of the region was given elsewhere (Pokrovsky and Schott, 2002; Zakharova et al., 2007; Vasyukova et al., 2008, submitted). Brief description of samples and chemical composition of water are given in Table 4.1. Three groups of samples corresponding to different lithology, pH, dissolved organic carbon (DOC) and Fe concentration were considered. Samples No.12 (r. Ruiga draining basalts, within the Vetreny Belt basic intrusion zone in southern Karelia) and M-1 (r. Palajoki draining glacial deposits and basic rocks, near Kivakka gabbro-norite layered intrusion in northern Karelia) correspond to permanently flowing rivers with watershed of ~ 20-50 km². The sample No.15 is a small creek draining basic and ultramafic rocks within the swamp zone and feeding the Ruiga (No.12) river; K-23 and K-43 are surface swamp waters (N Karelia) at the glacial till covering gabbro-norites, which belong to the river Palajoki watershed. Sample S-32 (r. Peschanaya) corresponds to small temporary coastal creek originated in the swamp zone and discharging to the sea and sample S-40 (peat water) is stagnant peat soil water in the swamp coastal zone of the North White Sea (Arkhangelsk region) underlain by sedimentary clay and carbonate deposits. The studied waters are essentially neutral with pH varying from 6 to 7.7, except swamp

creeks (samples No.15, S-32 and S-40) that have pH between 4 and 5. All studied samples exhibit high concentration of dissolved organic carbon, from 15 to 45 mg/l, and Fe concentration from 0.35 to 13.5 mg/L, which is typical for waters draining peatland areas of the European subarctic (Andersson et al., 1998; Ingri et al., 1997, 2000; Land and Öhlander, 1997; Pontér et al., 1990; Porcelli et al., 1997).

In the field, several litres of river water were collected into acid-washed containers. Samples were filtered a few hours later using 0.45 µm cellulose acetate filters and stored in the refrigerator in acid-washed dark polypropylene Nalgene bottles.

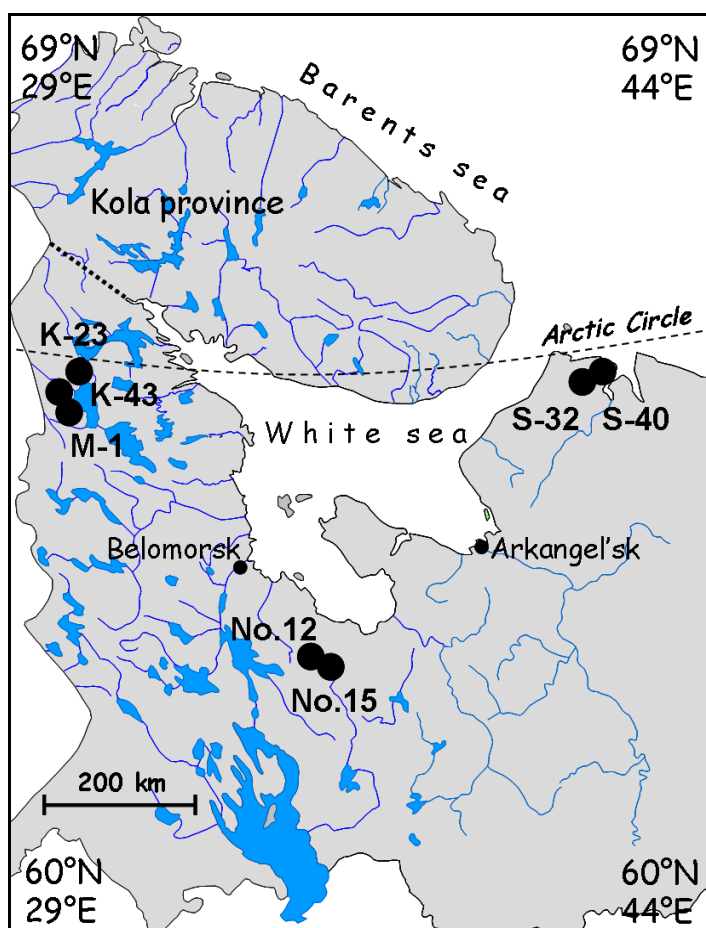


Fig. 4.1. Map of the studied region showing sampling points location.

Table 4.1. Surface waters studied, their bedrock and chemical composition.

Sample no.	Description	Bedrock composition of the catchment	pH	Concentration in < 0.22 µm fraction, mg/l								
				DOC	HCO ₃	Ca	Mg	Na	K	Cl	SO ₄	
No.12 (1)	r. Ruiga, upstream biofilms, Vetryny Belt paleorift zone (South Karelia)	Basalts	6,2	35	5,6	1,81	2,79	2,53	0,47	1,45	0,34	
No.15 (2)	Creek over ultramafites, Vetryny Belt paleorift Ultramafites zone (South Karelia)	5,1	38	2,1	0,84	3,13	1,69	0,11	2,08	0,53	2,37	
K-23 (3)	Swamp near the lake Tsipringa coast (North Karelia)	6,0	35	20,0	9,20	3,26	1,06	0,52	0,27	0,07	5,50	
K-43 (4) M-1 (5)	Swamp (North Karelia) r. Palajoki (North Karelia)	Gabbro-norites Gneisses, glacial deposits	5,9 7,3	25 15	8,1 28,3	3,71 7,22	1,33 1,82	1,09 1,65	0,03 0,37	0,73 0,53	0,25 1,92	13,50 0,90
S-32 (6)	r. Peschanaya, coastal creek issued from peat swamp, Abramzhevsky coast (Arkhangelsk region)	Clays, carbonates, glacial and marine deposits	4,2	45	nd	1,31	9,52	nd	0,04	7,40	0,19	
S-40 (7)	Soil peat water, Abramzhevsky coast (Arkhangelsk region)	Clays, carbonates, glacial and marine deposits	4,4	40	nd	1,06	1,15	nd	0,09	10,23	0,30	
											0,19	

4.2.2. Dialysis procedure and analyses

Equilibrium dialysis procedure was used to assess the distribution coefficients of ~50 major and trace elements between colloidal (1 kDa – 0.22 µm) and dissolved (< 1 kDa) forms. For this, EDTA-cleaned, trace-metal pure Spectra Pore 7® dialysis membranes made of regenerated cellulose and having 1-kDa pore size were thoroughly washed in 0.1 M bidistilled HNO₃, ultrapure water, filled with 10 mL ultrapure MQ deionized water (18 MOhm Element) and placed in 250 mL acid-cleaned polypropylene containers with natural filtered water (see the schematic representation of dialysis experiment given in Fig. 4.2). Sample pH was varied between 3 and 8 via addition of ultra-pure HNO₃ and NaOH. It remained stable within ±0.2 pH units during the full duration (72-160 hrs) of dialysis procedure. Pokrovsky et al. (2005) showed in laboratory experiments that, for 1-kDa membranes, the equilibrium distribution is achieved after 6-12 h, in agreement with specifications given by the manufacturer.

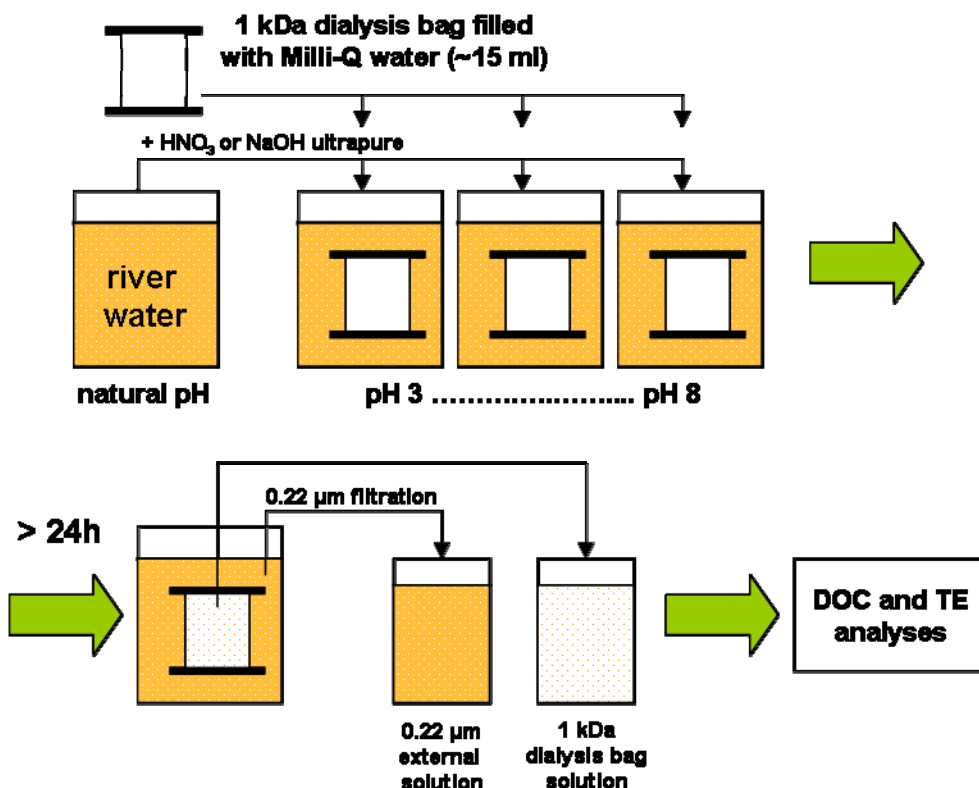


Fig. 4.2. Schematic representation of dialysis experiment procedure.

The efficiency of dialysis procedure was evaluated in the field by comparison of concentration of major anions (i.e., Cl^- , SO_4^{2-}) or neutral species ($\text{H}_4\text{SiO}_4^\circ$) not associated with colloids in the dialysis bag and in the external solution. After 12-24 hrs of exposure, these concentrations were always identical within $\pm 10\%$ suggesting equilibrium distribution of truly dissolved components. The external solution was filtered through sterile, single-used filter units Minisart[®] (Sartorius, acetate cellulose filter) having a diameter of 25 mm and pore size 0.22 μm . Each filter was washed in MQ water before the experiment and used only once. The first 20-30 ml of the filtrate was systematically rejected.

After sampling, concentrations of trace elements and dissolved organic carbon were measured both inside the dialysis bag and in the external solution (inner and outer compartments). All manipulations were carried out in clean bench rooms class A 10000. The pH in water was measured both before and after the dialysis procedure using a combined Schott-Geräte electrode calibrated against NIST buffer solutions (pH = 4.00 and 6.86 at 25°C). The accuracy of pH measurements was ± 0.02 pH units. Analysis of dissolved organic carbon (DOC) was performed immediately using Shimadzu TOC 6000 with the uncertainty of 5%. Trace elements (TE) were measured in 2% HNO_3 by inductively coupled plasma-mass spectrometry (ICP-MS, Agilent 7500, with indium and rhenium as internal standards and a precision better than $\pm 5\%$). The international geostandard SLRS-4 (Riverine Water Reference Material for Trace Metals certified by the National Research Council of Canada) was used to check the validity and reproducibility of each analysis (Yeghicheyan et al., 2001). A good agreement between our replicated measurements of SLRS-4 and the certified values was obtained (relative difference $< 10\%$).

4.3. Results

Measured major and trace elements concentrations in filtrates (0.22 μm) and dialysates (1 kDa) are reported in the Annex C (Table C-1). In the following section we will discuss the behaviour of elements depending on pH during dialysis separation experiments.

4.3.1. Methodology of dialysis at different pH

The stability of initial filtered solution with respect to colloids coagulation during experiment was tested via measurement of [DOC] and [Fe] as a function of pH. The concentrations of organic carbon and Fe in 0.22 µm fractions of all seven natural waters measured after 2 days exposure at different pH are plotted in Fig. 4.3. These concentrations remain stable for 5 samples among 7. The less stable samples K-43 and No.12 probably have some amount of divalent iron which undergoes oxidation in circumneutral and neutral solutions thus leading to decrease of ~70-80% [Fe] (<0.22 µm) concentration with pH increase. Other possibility, although this is possible only partially from the mass balance point of view, is that large amounts of Fe-oxyhydroxides are present in these samples at ambient pH (pH of the original water sample) and are subsequently dissolved to Fe(II) during lowering of pH.

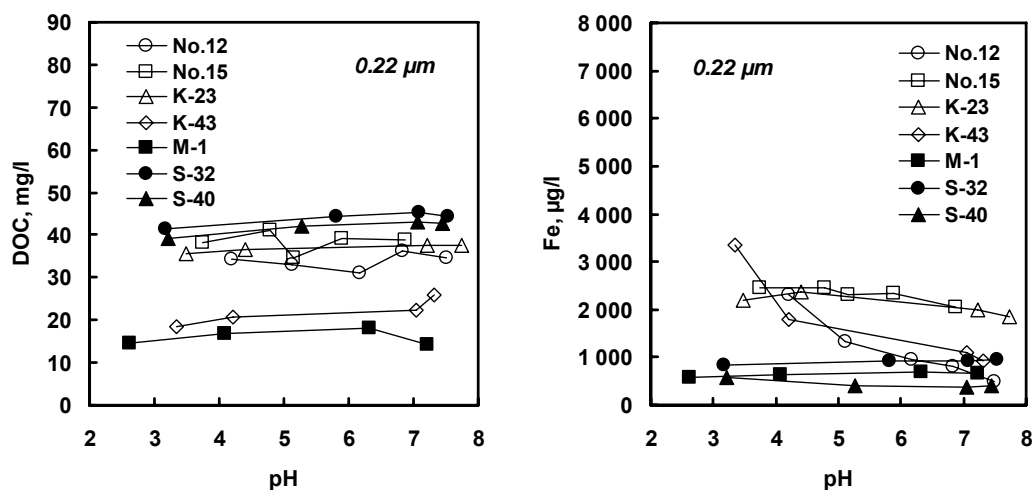


Fig. 4.3. DOC (a) and Fe (b) concentrations in 0.22 µm fraction as a function of pH for seven natural waters. Concentrations of OC and Fe of all samples were measured after 2 days exposure at different pH.

4.3.2. The pH-dependence of the percentage of dissolved form of trace elements

In all samples, between 30 and 55% of OC is concentrated in the < 1 kDa fraction (except the samples K-43 having 15% and sample S-32 having 77% of OC in < 1 kDa fraction) consistent with the presence of small-size polymers of fulvic nature (Pokrovsky and Schott, 2002). The average percentage of colloidal Fe and OC are depicted as a function of pH in Fig. 4.4. It can be seen that the proportion of colloidal

organic carbon decreases with pH increase in a much slower rate than that of iron. It was shown elsewhere (Pokrovsky and Schott, 2002; Vasyukova et al., submitted) that Fe is very often present in large-size colloids ($1 \text{ kDa} - 0.22 \mu\text{m}$) and is almost completely removed from solution before passing through 1-kDa membrane at natural pH. This is illustrated in Fig. 4.5 (a, b), where we plot the ratio of [Fe] to [Organic Carbon] in $0.22 \mu\text{m}$ filtrates and 1 kDa dialysates for different samples. In filtrates, [Fe]/[OC] ratio almost does not depend on pH except for r. Ruiga No.12 and swamp water K-43 where proportion of Fe decreases with pH increase (Fig. 4.5 a). In 1 kDa fraction of all studied samples we observe gradual decrease of the [Fe]/[OC] ratio with the pH increase indicating the highest proportion of Fe colloids in circumneutral and neutral solutions (Fig. 4.5 b). The increase of Fe at lower pH in the 1 kDa fraction could be explained by the dissolution of Fe oxyhydroxide colloids.

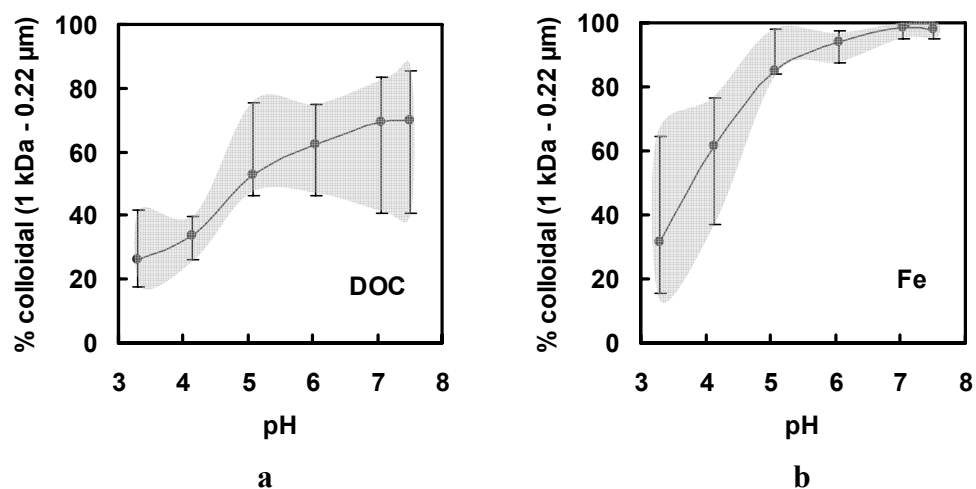


Fig. 4.4. Dependence of colloidal organic carbon (a) and Fe (b) on pH in all studied samples. The solid line is for guiding purpose. Symbols correspond to the median and the error bars reflect minimum and maximum obtained values among all samples. Solid line is for guiding purpose.

The TE distribution between dissolved ($< 1 \text{ kDa}$) and colloidal ($1 \text{ kDa} - 0.22 \mu\text{m}$) pools for seven studied waters at different pH is given in Table C-2 of the Annex C and average values at different pHs are illustrated in the stack diagram (Fig. 4.6). In this diagram, one can distinguish several groups of elements whose behaviour is illustrated in Figs. 4.7, 4.8 and 4.9:

(i) elements whose colloidal state is strongly dependent on solution pH with 40-100% being in truly dissolved form at pH = 3- 3.5 and only 0-40% being in the fraction of < 1 kDa at pH = 7 – 7.5: DOC, Fe, Ni, Cu, Sr, Ba, Mn, Cr, Co, Cd, Zn, Y, Zr, Pb, REEs, Th, U (Fig. 4.7). Most of these elements exhibit good correlation between their percentage content in colloidal fraction and that of Fe and organic carbon ($r^2 = 0.6$ -0.85 and 0.6 – 0.9, respectively).

(ii) elements whose colloidal status is not subjected to pH variation: Li, Na, K, Mg, Ca, B, Rb, Si, Cs, V, Ti, Mo, Nb, As, Sb, Sn, Ge, Tl, W (Fig. 4.8). Their percentage in dissolved form remains high (> 50%) and varies within ± 10 -15% at pH from 3 to 7. Most of these elements exhibit correlation neither with Fe, nor with OC in colloidal fraction ($r^2 < 0.4$),

(iii) elements whose percentage in dissolved form decreases gradually or remains stable between pH 3 and pH 6, then rises sharply at pH = 6-7: Al, Ga, Hf (Fig. 4.9).

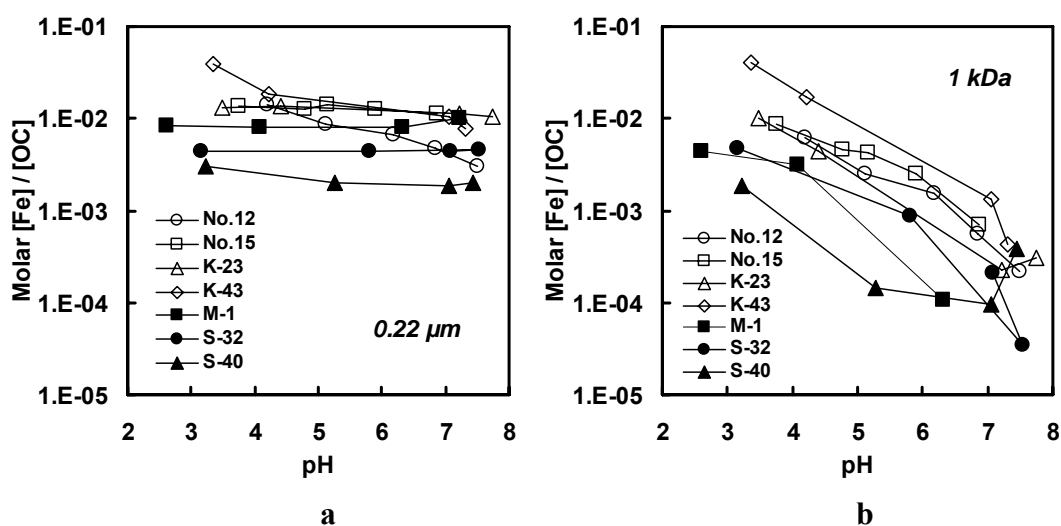


Fig. 4.5. Molar [Fe] to [Organic Carbon] ratio in 0.22 μm filtrates and 1 kDa dialysates for studied samples (in Log scale). In filtrates (a), [Fe]/[OC] ratio almost does not depend on pH except for r. Ruiga No.12 and swamp water K-43 where proportion of Fe decreases with pH increase. In 1 kDa fraction (b) of all studied samples we observe gradual decrease of the [Fe]/[OC] ratio with the pH increase indicating the highest proportion of Fe colloids in circumneutral and neutral solutions.

The attribution of some elements to one or another group depends on the sample, and apparently, on the nature of organo-mineral colloids that control their speciation. For example, Cr belongs to the first group in samples No.12, No.15, K-23, but to the second group in all other samples; Hf belongs to the first group in samples S-32 and No.12, and to the third groups in all others; Cs belongs to the third group in samples S-40, K-24 and K-43, and to the second group in all other samples; Ti belongs to the second group except for the samples K-23 and K-32; As belongs to the second group except for the samples S-40, K-23 and S-32; Ca belongs to the second group in all samples except for S-32 and S-40 which belong to the first group; Cu belongs to the third group in samples M-1, S-40 and S-32, and to the first group in all other samples.

4.3.3. Thermodynamic modeling of metal complexation with dissolved organic matter

The weak dependence of organic carbon and iron concentration on pH in 0.22 μm filtrates (Fig. 4.3) suggests that the concentration of main ligand that complex dissolved metals, fulvic and humic organic acids, remains constant in the full range of pH. It is known that the separation through 1-kDa membrane was used to assess the proportion of conventionally colloidal (i.e., > 1 kDa, Buffle and van Leeuwen, 1992) forms compared to total dissolved (< 0.22 μm) content of trace metals. One can suggest that all the humic and fulvic acids are present as conventionally colloidal substances. According to Thurman (1985), 70 to 90% of DOC in wetland areas is constituted by humic substances. In all our samples, we checked by HPLC analysis that the concentrations of low molecular weight organic acids (formic, acetic acids, etc.) were negligible. Therefore, complexation of metals with humic and fulvic acids assessed via available speciation codes can be compared with TE speciation in colloids measured by dialysis in the laboratory. For this, we used geochemical program Visual MINTEQ (Gustafsson, 1999), version 2.52 for Windows, a recent adaption of the original code written by Allison et al. (1991) (see Unsworth et al. (2006) for vMINTEQ application example) in conjunction with a database and the NICA-Donnan humic ion binding model (Benedetti et al., 1995; Kinniburgh, 1999; Milne et al., 2003). Speciation calculations were performed for Al, Fe, Ca, Mg, V, Mn, Co, Ni, Cu, Zn, Sr, Zr, Cd, Ba, La, Ce, Nd, Yb, Pb, Th and U for all seven samples at pH of 3-8.

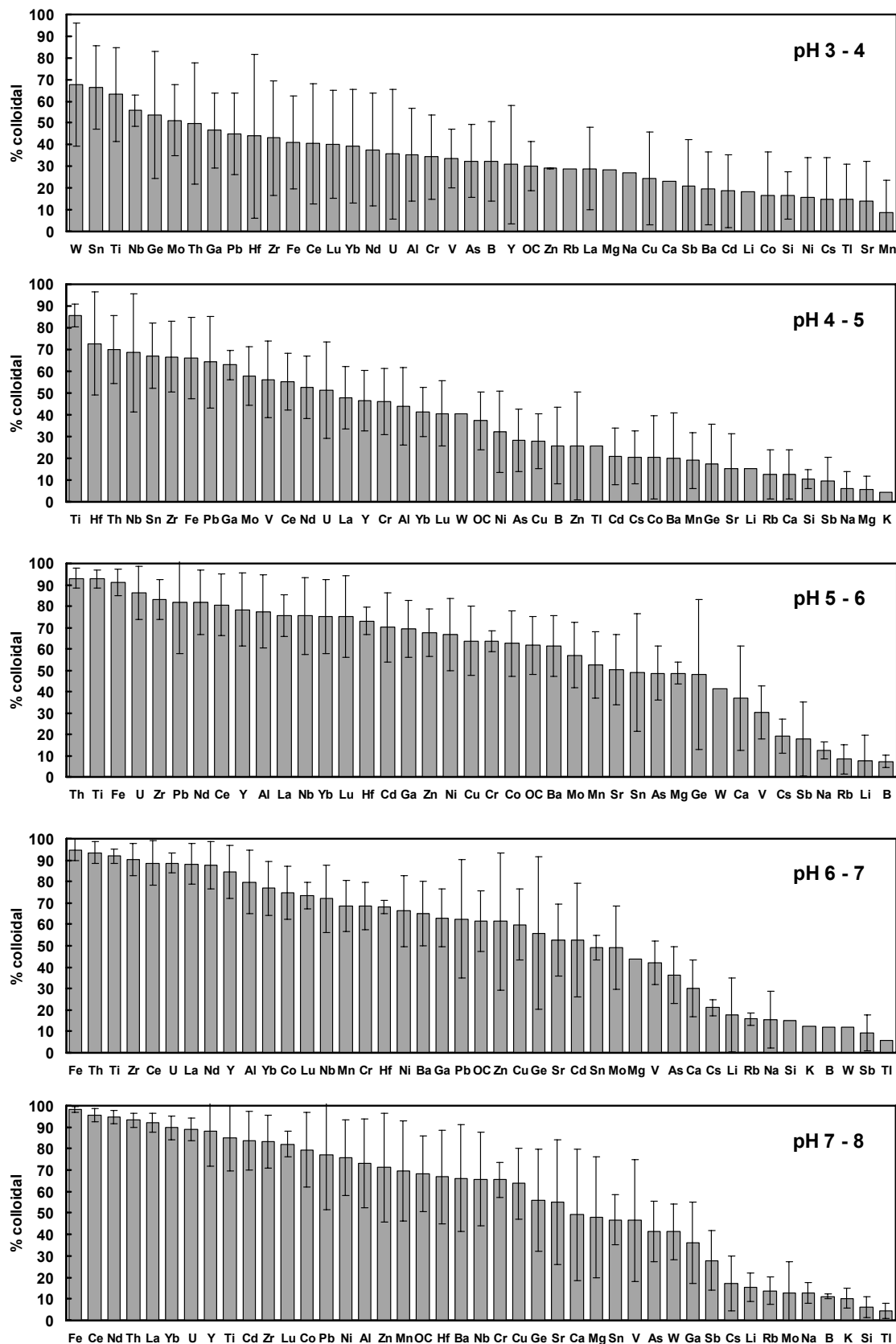


Fig. 4.6. Percentage of colloidal forms (1 kDa – 0.22 μ m) in all samples (average). The error bars represent the 2σ uncertainty.

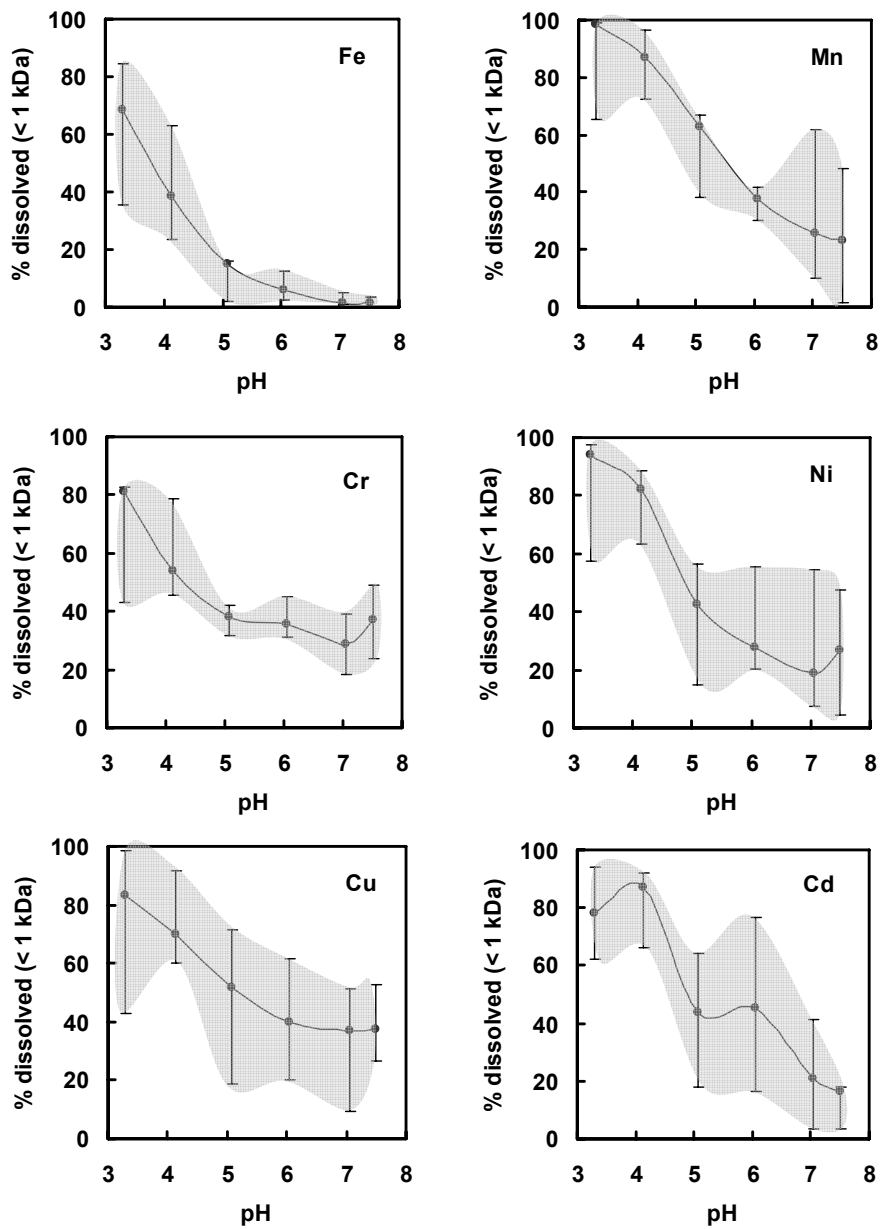


Fig. 4.7. Dependence of Fe, Mn, Ni, Cd, Cr, Cu, Y, La, Ce and U in colloidal (< 1 kDa) form on pH in seven studied samples. The diagrams are representative for the first group of elements whose colloidal state is strongly dependent on solution pH with 40-100% being in dissolved form at pH = 3- 3.5 and only 0-10% being in the fraction of <1 kDa at pH = 7-7.5. The solid line is for guiding purpose. Symbols correspond to the median and the error bars reflect minimum and maximum obtained values among all samples.

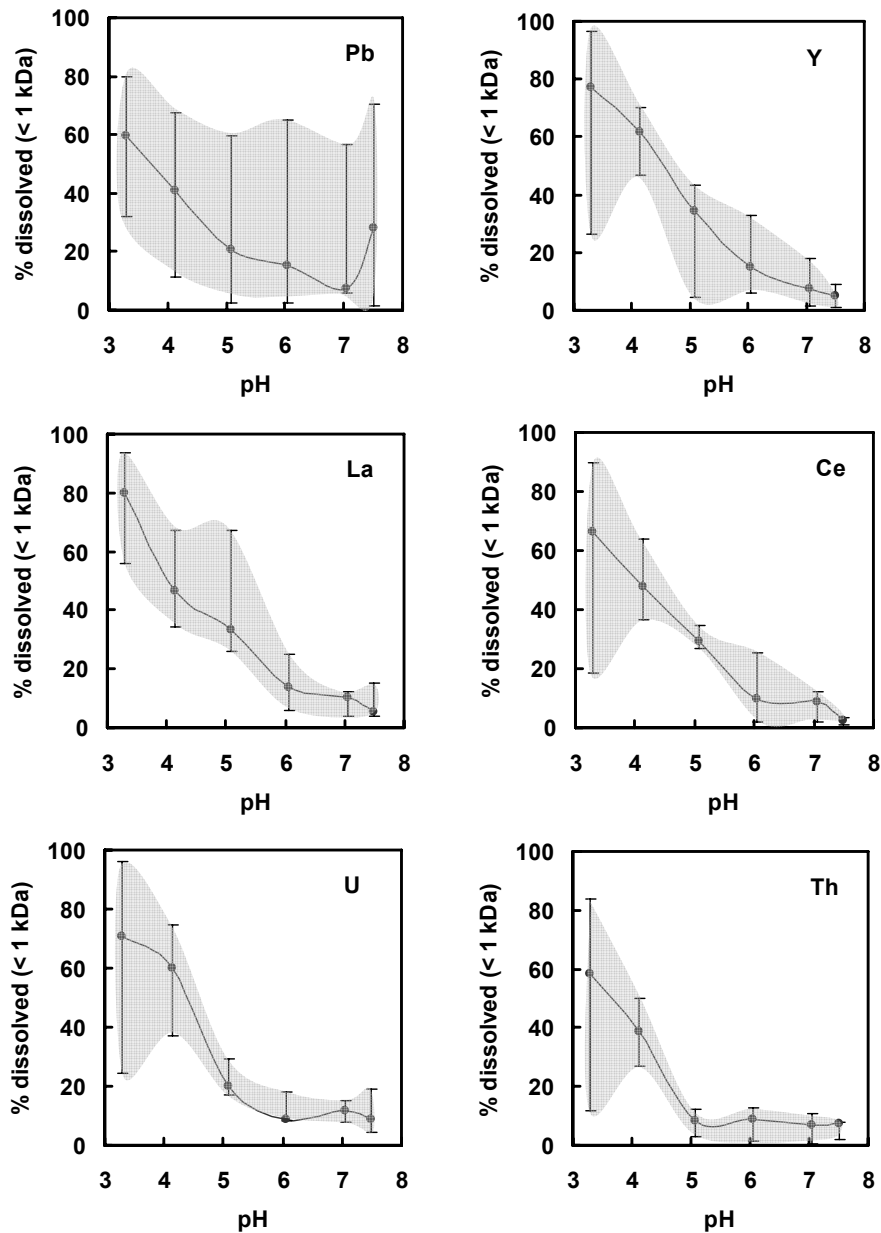


Fig. 4.7, continued.

Results of speciation calculation are presented in Figures 4.10 and 4.11 and described below according to different groups of elements. These calculations could be performed only for the elements whose stability constants with natural organic matter are available from the database in the vMINTEQ code. For most elements (Ca, Mg, Sr, Ba, Mn, Co, Cd, Ni, Pb), the model predicts gradual increase of colloidal (1 kDa – 0.22 μm) forms proportion with pH increase in all samples (Fig. 4.10). For most samples, the agreement between experimental proportion of colloidal form and predicted percentage of HA, FA- complexed metal is remarkable given totally different methods were used to

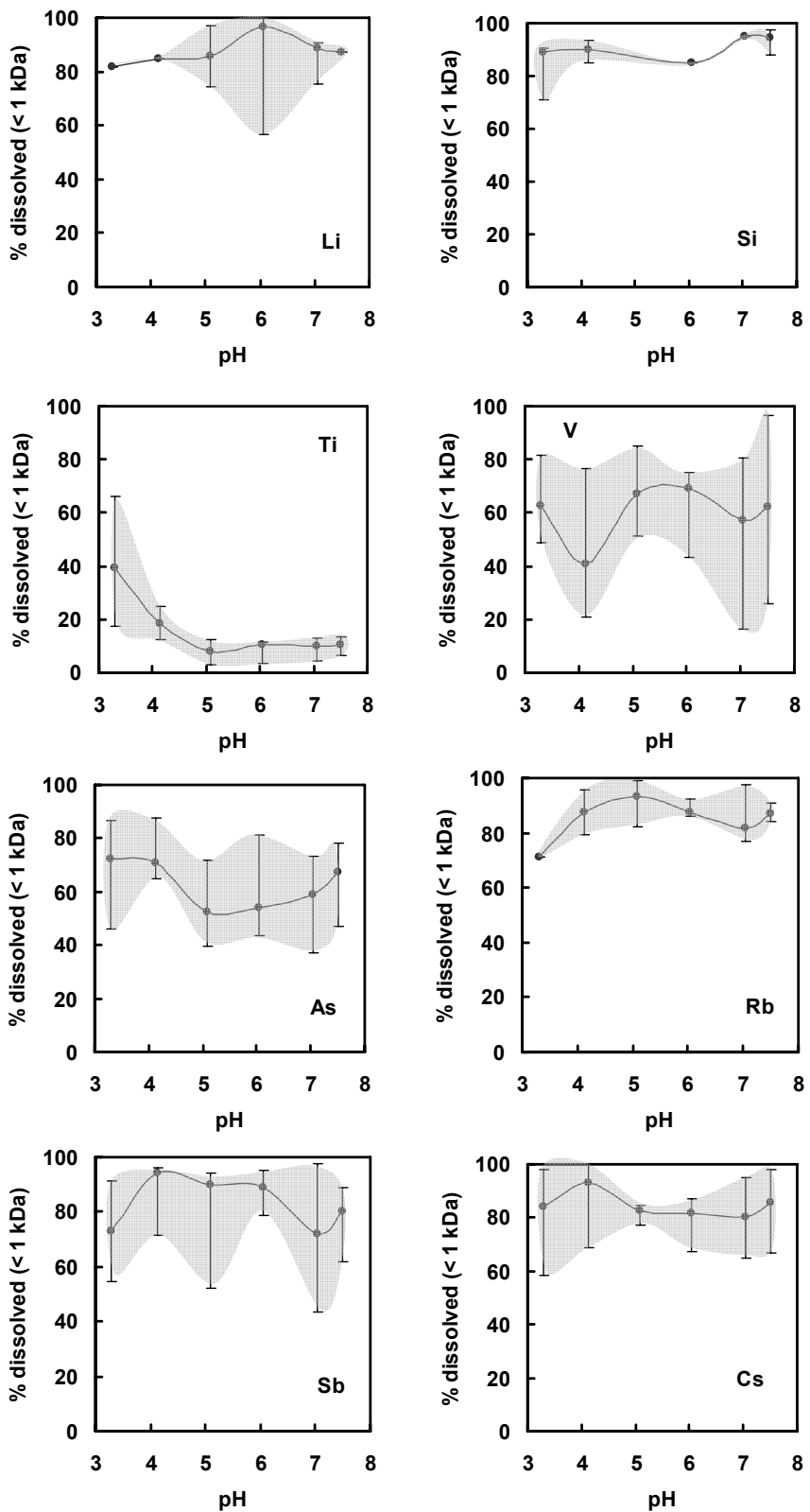


Fig. 4.8. Dependence of Li, Si, Ti, V, As, Rb, Sb and Cs in dissolved (< 1 kDa) form on pH in seven studied samples. The percentage of dissolved form weakly depends on pH. The solid line is for guiding purpose. Symbols correspond to the median and the error bars reflect minimum and maximum obtained values among all samples.

measure Me-HA(FA) stability constants for reactions in the vMINTEQ database (voltammetry or potentiometry) and Me-colloids association by dialysis in this study. The model slightly overestimates the percentage of complexed metals for coastal acidic peat waters (samples S-32, S-40). For Al, Fe, Cu, Y, all REEs, V, Th and U, the model strongly overestimates the proportion of bounded metals at pH below 5-6 (samples M-1, K-23 and K-43) or in the full range of pH (No.12, No.15, S-32 and S-40) compared to experimental proportion of colloidal fraction (Fig. 4.11).

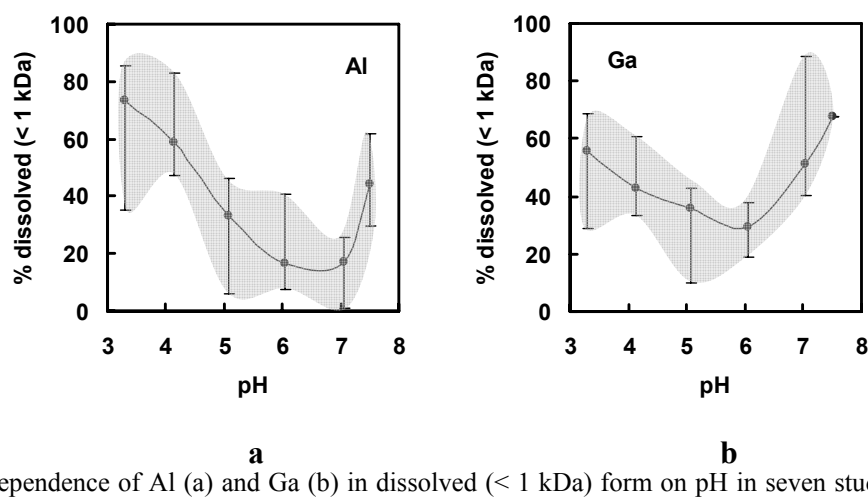


Fig. 4.9. Dependence of Al (a) and Ga (b) in dissolved ($< 1 \text{ kDa}$) form on pH in seven studied samples. These elements represent the first group of elements whose percentage in dissolved form decreases gradually or it is stable between pH 3 and pH 6, but then rises sharply at pH = 6-7. The error bars correspond to maximum and minimum obtained values among all samples. The solid line is for guiding purpose.

In order to achieve a better description of the experimental data by the model for these metals, we decreased the stability constants of metal-humic and metal-fulvic complexes in the vMINTEQ database. A decrease of each of Cu-humate and Cu-fulvate complexes by 4 orders of magnitude was necessary to fit the experimental proportion of colloidal organic Cu complexes (Fig. 4.12). For REEs (Eu and Dy), decreasing of each Me-L stability constant even by 20 orders of magnitude does not allow to reproduce the experimental dependence of colloids proportion in some samples (Fig. 4.13). For iron, the required decrease was by 3, and for Al by 3-8 orders of magnitude, but still with very poor agreement with experimental data for most samples (Fig. 4.14 a, b). For uranium, stability constants should be decreased up to 6-8 orders of magnitude to approach the experimental data (Fig. 4.14 c), while for thorium, even 20-30 orders of magnitude decrease did not produce a reasonable fit (Fig. 4.14 d).

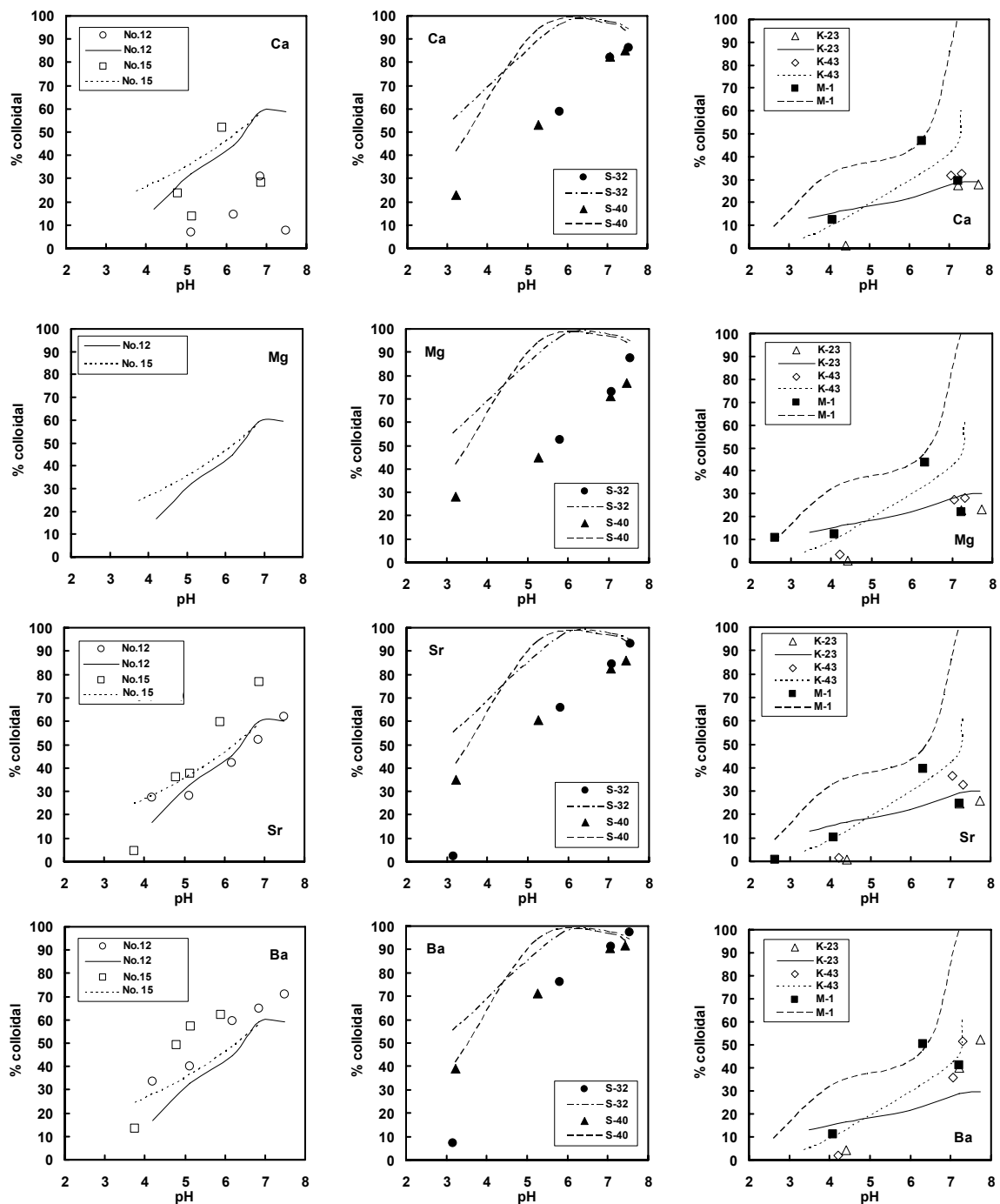


Fig. 4.10. Results of vMINTEQ speciation calculation for Ca, Mg, Sr, Ba, Mn, Co, Ni, Cd, Pb. Experimental data are shown by symbols, and model calculations are shown by smooth lines for three group of samples depending on their natural origin: Vetryny Belt zone (samples No.12 and No.15), Southern coast of the White Sea (S-32 and S-40), and Kivakka layered intrusion zone (K-23, K-43 and M-1). There are no experimental data for Mg in samples No.12 and No.15.

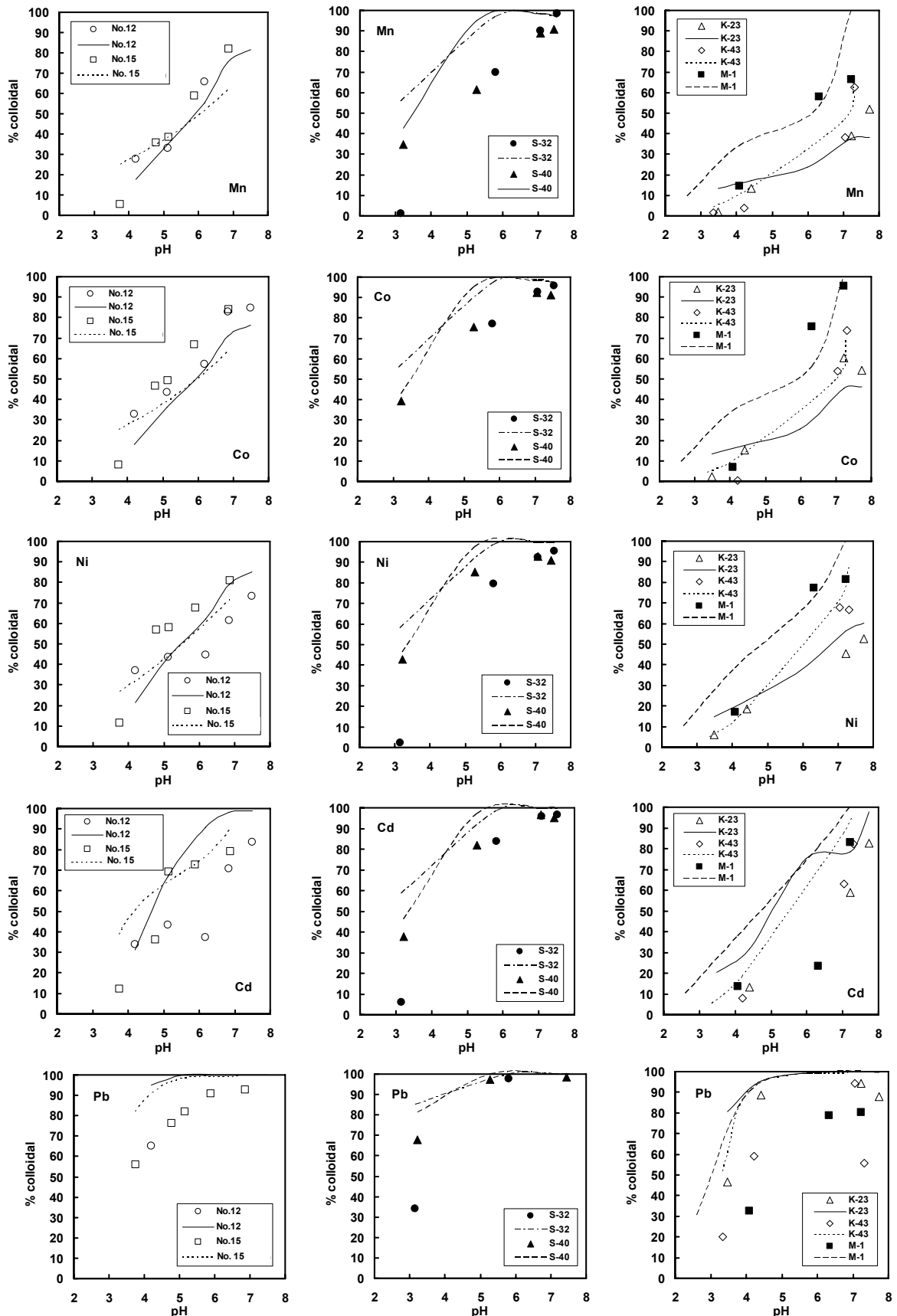


Fig. 4.10, continued.

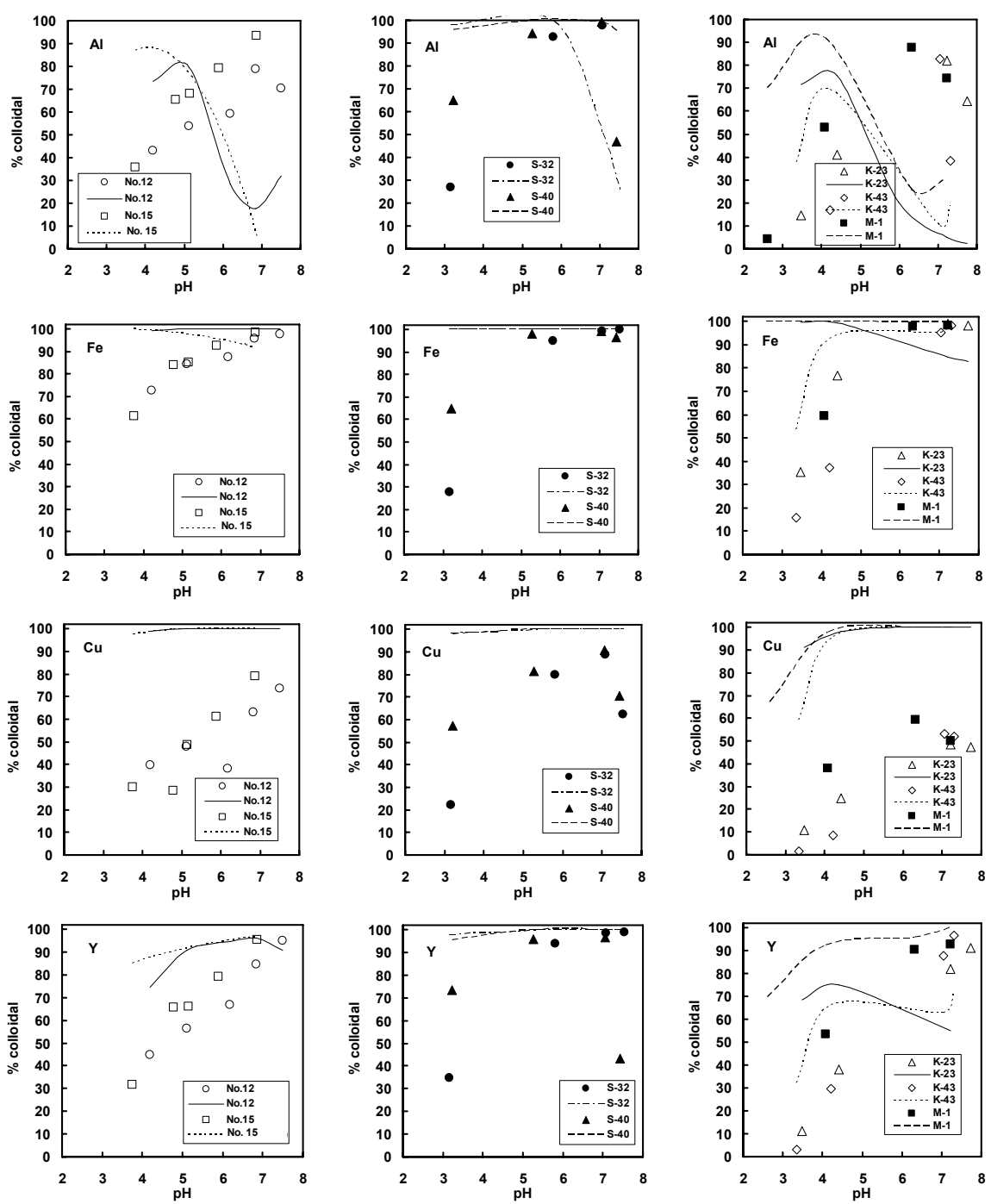


Fig. 4.11. Results of vMINTEQ speciation calculation for Al, Fe, Cu, Y, V, La, Th, U. Experimental data are shown by symbols, and model calculations are shown by smooth lines for three groups of samples depending on their geographical location: Vetreny Belt zone (samples No.12 and No.15), Southern coast of the White Sea (S-32 and S-40), and Kivakka layered intrusion zone of Northern Karelia (K-23, K-43 and M-1).

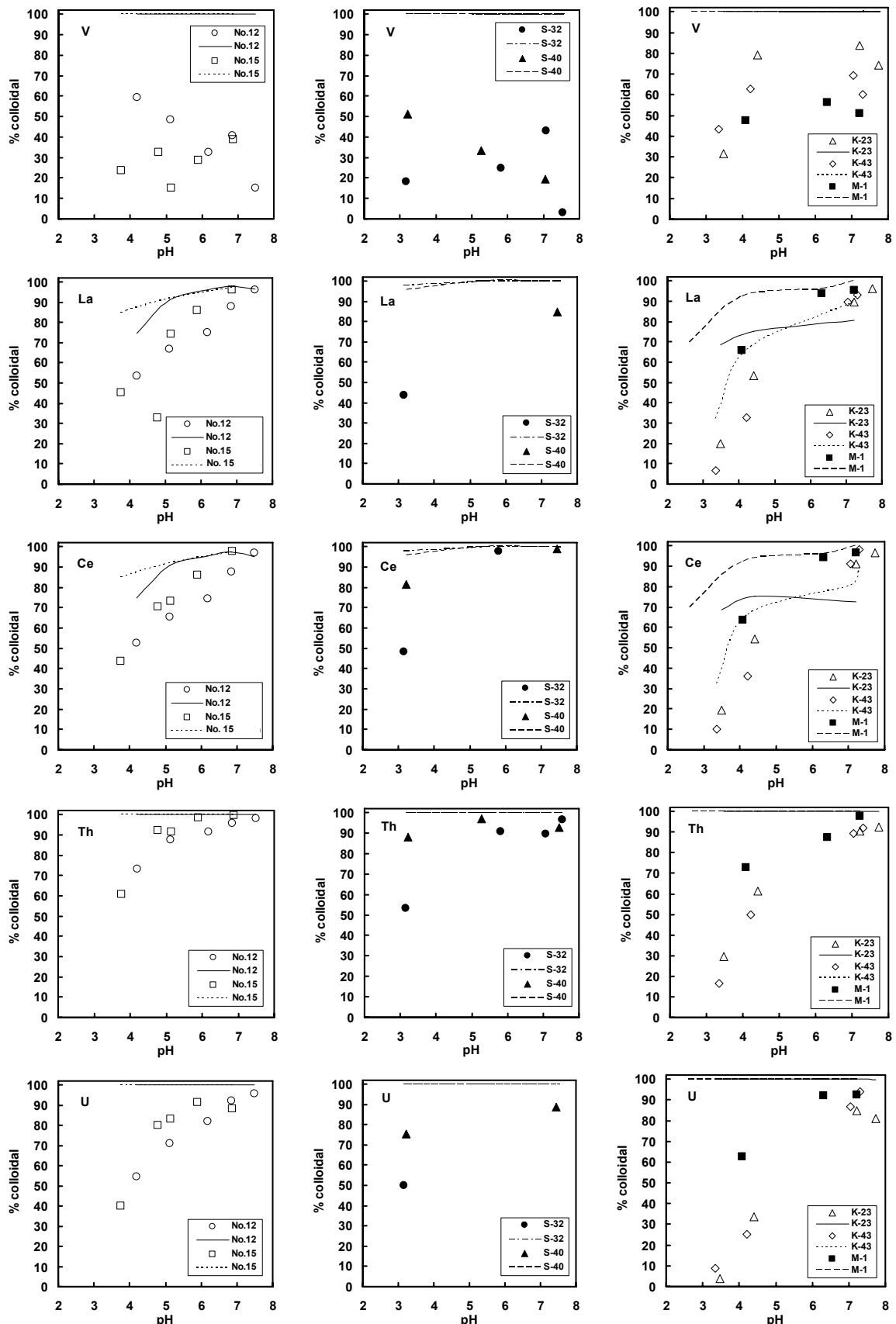


Fig. 4.11, continued.

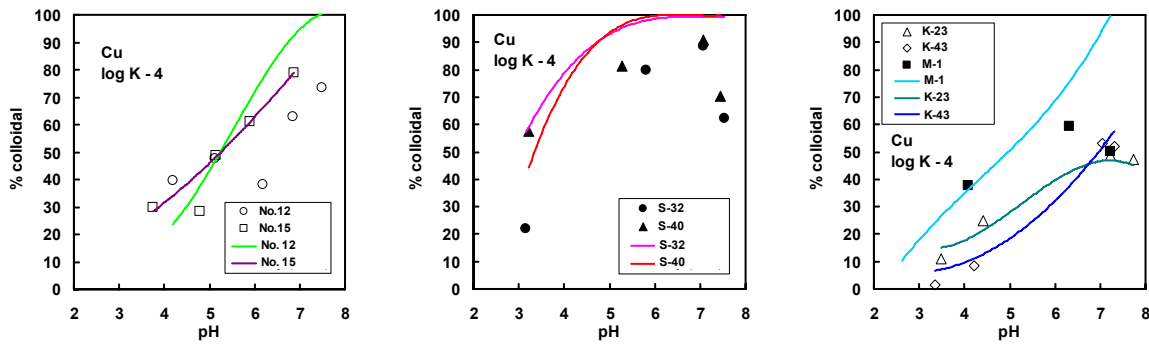


Fig. 4.12. Results of vMINTEQ speciation calculation for Cu with adjusted stability constants of Cu-humate and Cu-fulvate complexes. Symbols represent the experimental data and the solid lines correspond to fitted model calculation for three groups of samples depending on their natural origin: Vetreny Belt zone (samples No.12 and No.15), Southern coast of the White Sea (S-32 and S-40) and Kivakka layered intrusion zone (K-23, K-43 and M-1). Adjustment of all four stability constants by 4 orders of magnitude is necessary to fit the experimental proportion of colloidal organic Cu complexes.

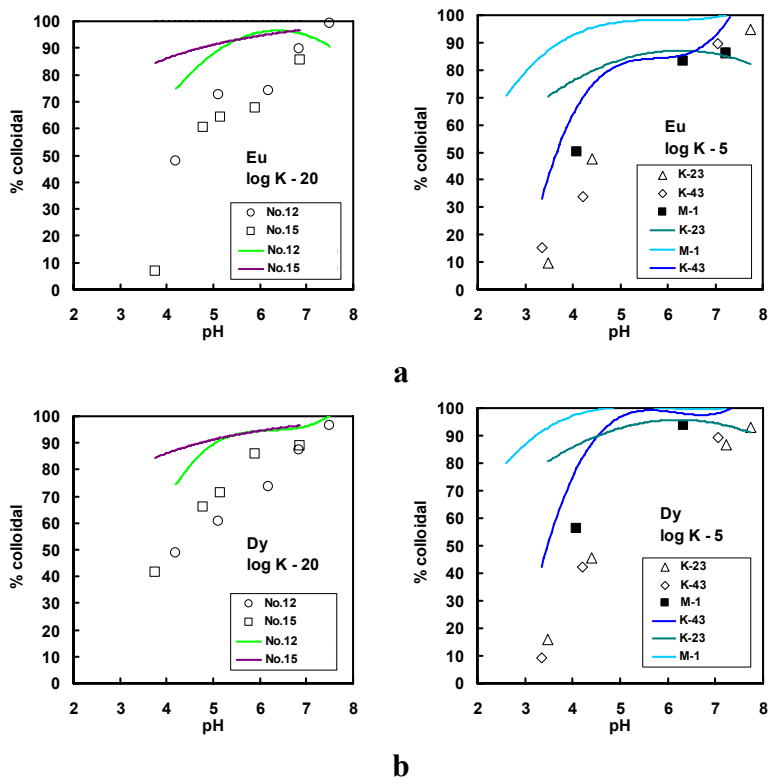


Fig. 4.13. Results of vMINTEQ speciation calculation for Eu (a) and Dy (b) with adjusted stability constants of metal-humate and metal-fulvate complexes. Symbols represent the experimental data and the solid lines correspond to fitted model calculation for three groups of samples depending on their natural origin: Vetreny Belt zone (samples No.12 and No.15) and Kivakka layered intrusion zone of Northern Karelia (K-23, K-43 and M-1). Adjustment by ≥ 5 orders of magnitude is necessary to approach the experimental proportion of colloidal organic metal complexes.

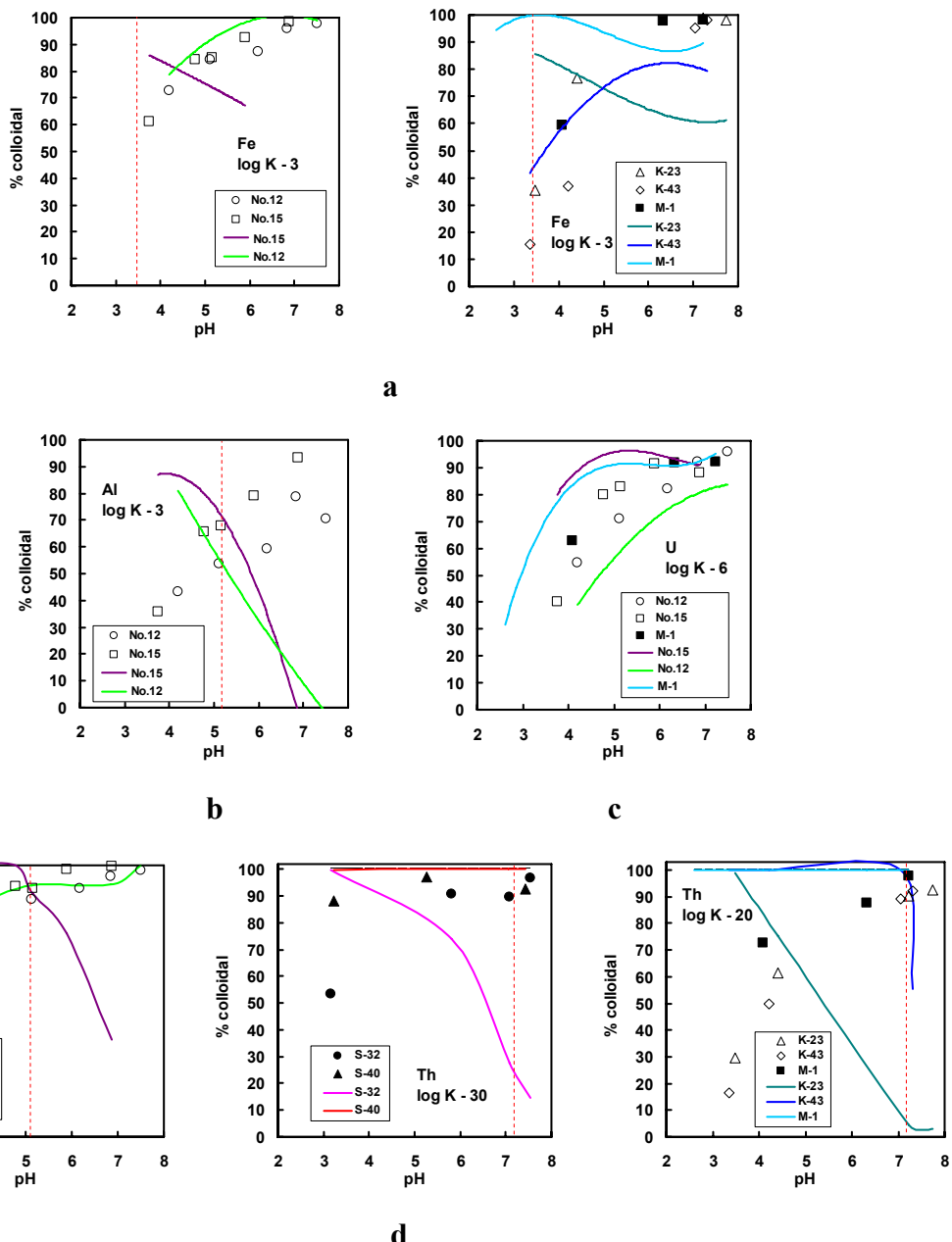


Fig. 4.14. Results of vMINTEQ speciation calculation for Fe (a), Al (b), U (c) and Th (d) with adjusted stability constants of metal-humate and metal-fulvate complexes. Symbols represent the experimental data and the solid lines correspond to fitted model calculation for three groups of samples depending on their natural origin: Vetreny Belt zone (samples No.12 and No.15), Southern coast of the White Sea (S-32 and S-40), and Kivakka layered intrusion zone of Northern Karelia (K-23, K-43 and M-1). Decrease even by 3-5 orders of magnitude for Fe and Al, 6-8 for U and 20-30 for Th, does not allow approaching the experimental proportion of colloidal organic metal complexes. The vertical dash line represents the saturation with respect to iron and thorium hydroxides.

It is important to note that all experimental solutions become oversaturated with respect to iron hydroxides at $\text{pH} \geq 3.4$, to aluminium hydroxides at $\text{pH} \geq 5.2$, while for Th hydroxide oversaturation is achieved at $\text{pH} \geq 5.2$ for the sample No.15 and at $\text{pH} \geq 7.2$ for other samples. This can explain the disagreement between model description of the percentage of OM-bound form and experimental proportion of colloids. Iron and thorium hydroxides may form colloidal precipitates that will be retained by 1-kDa membrane.

4.4. Discussion

4.4.1. Possible artifacts of dialysis procedure and colloids aggregation

After filtration of natural water and its storage in the refrigerator, major changes of colloidal distribution may occur. Indeed, metal speciation in natural waters is governed by dynamic processes of colloids formation and dissociation thus providing the pseudo steady-state. Removal of a volume of water from such a system isolates it from potential metal sources and sinks inevitably changing the distribution of element between different colloidal and dissolved fractions (i.e., Gimpel et al., 2003). In this work, we kept isolated 1-2 litres volume of filtered river and soil water in the refrigerator during 6-12 months before the laboratory dialysis procedure. During this period of storage, only little or no coagulation occurred as proven by periodic sampling, filtration and analysis for DOC and TE. Thus, we anticipate tha the colloidal fraction is stable during storage of 0.22 μm filtered water. Furthermore, in previous methodological experiments of bacteria culturing on rich nutrient media we demonstrated that 0.45 μm filtered organic-rich water (in particular, sample M-1) remains sterile over long period of time (Shirokova et al., unpublished). Therefore, we do not anticipate strong microbial degradation of OM in our samples during storage.

The colloidal distribution of elements measured via 1-kDa dialysis in-situ (in the field) and ex-situ (in the laboratory) for the same pH in sample No.15 yielded quite similar results, with values in-situ being only 10-30% higher than those for ex-situ dialysis. In sample K-23 and K-43, colloidal coagulation occurred as evidenced by 30 and 50% concentration decrease of filtered samples during storage compared to initial sample. Overall we anticipate that the long-term storage of filtered samples before the experiment allowed higher stability of organo-mineral colloids, their internal re-

equilibration between different colloidal and dissolved pools and thus identical initial conditions for all samples before the experimental pH adjustment. Concerning the stability of experimental solutions in the full range of pH, it has been argued that organic matter begins to precipitate below a pH of 3 during flocculation experiments of river water/sea water mixing (Sholkovitz, 1976). However, in our study, the colour of the solution remained uniform, [DOC] was stable (Fig. 4.3) and we did not observe flocculants after several days of exposure at different pH during dialysis.

4.4.2. Relative role of organic matter vs. adsorption or coprecipitation of trace elements with Fe-rich colloids

While for Ca, Mg, Sr, Ba, Mn, Co, Ni, Cd, Pb the model prediction of colloidal fraction as a function of pH agrees reasonably well with the experiments, significant adjustment of metal-OM stability constants was necessary for Cu, REE, and U. For Fe, Al and Th, even tremendous change of OM-metal complexes stability constant does not allow approaching the experimental pH-dependence of colloidal proportion. We see two possible explanations for such a discrepancy. To date, very few metal-humate stability constants have been determined from experimental methods. Most of them are 'conditional' or 'apparent' stability constants since they were determined at given pH and ionic strength. These constants were determined using different experimental techniques (potentiometric titration, ion exchange equilibrium, cation exchange resin) and with humic acids of different nature (extracted from the soil or the river). As a result, the values reported in the literature are often inconsistent, and, for example, the Cu^{2+} -humate stability constants vary by several orders of magnitude (Morel, 1983). The stability constant values for Fe^{3+} and Th^{4+} were often approximated from a linear correlation between the logarithm of the metal-humate stability constant and the logarithm of the first hydrolysis constant available for other elements. Recently, it has been demonstrated that the metal speciation in freshwaters assessed using various in-situ techniques and model predictions of free ion activities generally do not agree with measurements (Sigg et al., 2006; Unsworth et al., 2006). The present work offers a simple and straightforward method of metal-organic matter stability constant evaluation via fitting the experimental data on colloidal fraction proportion with pH using modified values of complexation constants. The degree to which the modification of stability

constants are necessary, for example, 4 orders of magnitude for Cu-OM complexation are within the range of the values measured in the literature.

Another possible reason for the observed discrepancy between experimental proportion of colloidal form and calculated Metal-OM complexation is that, in addition and in competition to humic and fulvic acids, the important carriers of many trivalent and tetravalent elements (Al, Y, REEs, Ti, Zr, Hf, Th) and uranium in boreal waters are iron-rich, OM-stabilized mineral colloids (Ingri et al., 2000; Pokrovsky and Schott, 2002; Allard et al., 2004; Pokrovsky et al., 2006). Indeed, there is a positive correlation ($r^2 = 0.4\text{--}0.9$) between the relative proportion of Fe and trace elements such as Al, Ti, Y, REEs, Hf, Th, U in colloidal fraction of studied natural waters in the full range of pH (Fig. 4.15).

The correlation with iron can be explained by *i*) the release of TE incorporated in the bulk of Fe particles in circumneutral and acidic solution due to the dissolution of Fe oxyhydroxides and/or *ii*) desorption of TE from the surface of colloidal Fe oxy(hydr)oxides. The second process is less likely to occur since the calculated adsorption capacity of large Fe-rich colloids are normally not sufficient to accommodate all associated trace elements (i.e., Pokrovsky et al., 2002; Vasyukova et al., 2008, submitted). In addition, the localization of TE on the surface of Fe colloids suggests metal-organic matter complexation reaction or the presence of ternary surface complexes. These complexes would greatly increase the model predicted degree of TE binding to colloids compared to experimental data, whereas we observe the opposite tendency. Therefore, since Fe is a major component of studied samples, we suggest that the major part of considered trivalent and tetravalent elements and uranium is located in the bulk of Fe-rich OM-stabilized colloids.

For quantitative assessment of TE distribution in the bulk of colloids, we calculated the iron-normalized TE partition coefficient between dissolved (< 1 kDa) and colloidal (1 kDa – 0.22 μm) fractions defined as:

$$K_d = (\text{TE/Fe})_{\text{colloidal}} / (\text{TE/Fe})_{\text{dissolved}}$$

The average values for all seven samples are illustrated in Fig. 4.16 as a function of pH (see Table C-3 of the Annex C for K_d values). There is a decrease of K_d with pH increase for Ti and Th, but no systematic variations for REEs and U. Note that the distribution coefficients calculated from our data for U, Pb, and REE are close to that of

coprecipitation of these elements with solid Fe(OH)_3 in seawater: average K_d is 0.58, 0.87 and 0.44 for U, Pb and REEs, respectively (Savenko, 1995, 2001), whereas K_d of Al, Cu, Zn, Co, Ni, Cr, V and Th are two-three times lower than those for the seawater (Savenko, 1996, 1999a, 1999b, 2001; Savenko and Pokrovsky, 2007).

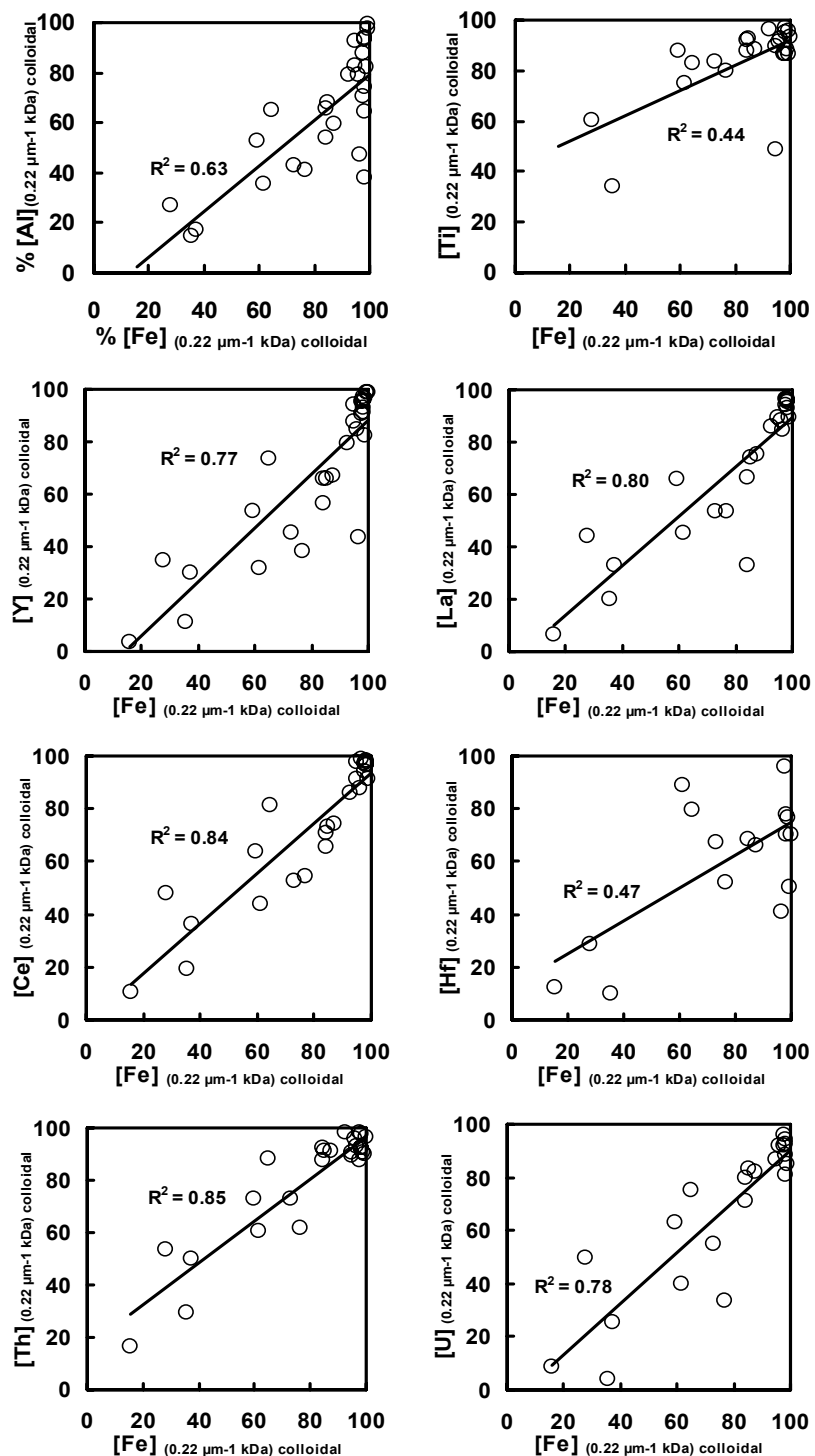


Fig. 4.15. Correlation between the concentration of Fe and trace elements in colloidal fraction of studied natural waters for Al, Ti, Y, La, Ce, Hf, Th, U.

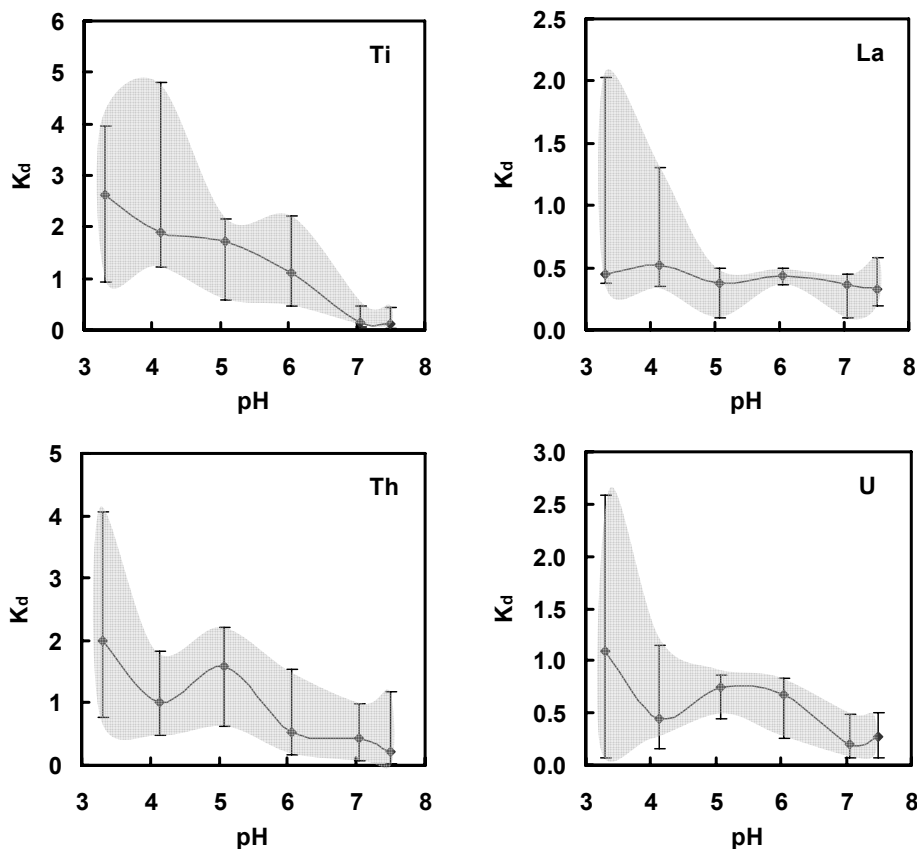


Fig. 4.16. Iron-normalized TE partition coefficient K_d (average values for seven samples) vs. pH for Ti, La, Th and U.

4.5. Conclusions and implications: Change of trace elements speciation and bioavailability during acidification of surface waters

In this work, we measured the complexation of trace elements with natural colloids present in boreal surface waters ubiquitous in the subarctic region of the NW Russia. Ex-situ dialysis through 1-kDa membrane of natural filtered waters conducted at various pH in the laboratory allows straightforward evaluation of the degree of trace metal binding to natural colloids. Use of available speciation code (vMINTEQ with implemented NICA-Donnan model for ion binding humic acid) allows reasonable description of the proportion of colloidal Ca, Mg, Sr, Ba, Mn, Co, Ni, Cd, Pb forms measured in the experiment at pH from 3 to 8 assuming that all colloidal metal is bound to humic and fulvic acid. The degree of binding of Al, Fe, REEs, Th and U is strongly overestimated by the model and decrease of humic (HA) and fulvic (FA) binding constant by at least 3-5 orders of magnitude is necessary to approach the experimental

pH-dependence. While for Cu (and probably U) such a modification is consistent with large variation of stability constants reported in literature, such significant modification for Al, Fe, REEs and Th binding with HA and FA are unlikely. In fact, even significant modification of HA, FA – metal binding constant does not allow approaching the shape of experimental pH-dependency of colloidal species proportion. Therefore, an alternative explanation for this discrepancy could be the association of trivalent and tetravalent elements with the bulk of Fe-rich (mineral) colloids, as it was already reported in previous works (Dia et al., 2000; Ingri et al., 2000; Andersson et al., 2006).

The method of estimation the proportion of colloidal forms proposed in this study can be used to assess the possible change in metal speciation induced by environmental changes such as acidification of surface waters which is one of the major issues of concern (Seip, 1986; Reuss, 1987; Borg et al., 1989; Moiseenko, 1995; Aggarwal et al., 2001; Evans et al., 2001; Galloway, 2001; Skjelkvåle et al., 2001; Davies et al., 2005). According to our results, the decrease of pH from 6 to 5 will bring about two to three-fold increase in the proportion of non-colloidal (< 1 kDa) forms of most potentially toxic metals (Al, Cu, Cd, Co, Ni, Pb, Th, U see Fig. 4.7). These conventionally dissolved species are potentially bioavailable since the pore sizes of cell wall transport channels (10-30 Å in bacteria; 35-50 Å in plant cells, Carpita et al., 1979; Colombini, 1980; Trias et al., 1992) and that of 1 kDa dialysis membrane (1-3 nm) are comparable. Therefore, significant increase in the bioavailability of trace metals may occur upon acidification of natural waters induced by local anthropogenic pressure or the global warming (atmospheric CO₂ increase, see Orr et al., 2005; Erlandsson et al., 2008). From the other hand, increase of DOC concentration in surface waters due to global warming as it is observed in Nordic Countries, British Isles, and Northern and Eastern United States (by approx. 10% over 10 years, Evans et al., 2005) may as well increase the proportion of metals bounded to colloidal organic matter thus compensating for the effect of acidification.

In perspective, study of natural colloidal samples subjected to different treatment (H₂O₂ to remove the OM, Fe³⁺ or Al³⁺ addition to bind possible binding sites of organics) will be necessary to assess the relative role of organic and mineral part in TE complexation with colloids.

References

- Aggarwal, S. G.; Chandrawanshi, C. K.; Patel, R. M.; Agarwal, S.; Kamavisdar, A. & Mundhara, G. L. (2001), 'Acidification of surface waters in Central India', *Water, Air and Soil Pollution* 130, 855-862.
- Allard, B. (2006), 'A comparative study on the chemical composition of humic acids from forest soil, agricultural soil and lignite deposit Bound lipid, carbohydrate and amino acid distributions', *Geoderma* 130(1-2), 77-96.
- Allard, B. & Derenne, S. (2007), 'Oxidation of humic acids from an agricultural soil and a lignite deposit: Analysis of lipophilic and hydrophilic products', *Org. Geochem.* 38, 2036-2057.
- Allard, T.; Menguy, N.; Salomon, J.; Calligaro, T.; Weber, T.; Calas, G. & Benedetti, M. F. (2004), 'Revealing forms of iron in river-borne material from major tropical rivers of the Amazon Basin (Brazil)', *Geochim. Cosmochim. Acta* 68(14), 3079-3094.
- Allison, J. D.; Brown, D. S. & Novo-Gradac, K. J. (1991), 'MINTEQA2/PRODEFA2, A geochemical assessment model for environmental systems: version 3.0 user's manual', (EPA/600/3-91/021), 115.
- Andersson, P. S.; Dahlqvist, R.; Ingri, J. & Gustafsson, O. (2001), 'The isotopic composition of Nd in a boreal river: A reflection of selective weathering and colloidal transport', *Geochim. Cosmochim. Acta* 65(4), 521-527.
- Andersson, P.; Porcelli, D.; Wasserburg, G. & Ingri, J. (1998), 'Particle transport of $^{234}\text{U}/^{238}\text{U}$ in the Kalix river and in the Baltic Sea', *Geochim. Cosmochim. Acta* 62(3), 385-392.
- Åström, M. & Corin, N. (2000), 'Abundance, sources and speciation of trace elements in humus-rich streams affected by acid sulphate soils', *Aquat. Geochem.* 6(3), 367-383.
- Åström, M. (2001), 'The effect of acid soil leaching on trace element abundance in a medium-sized stream, W. Finland', *Appl. Geochem.* 16, 387-396.
- Benedetti, M.; Milne, C.; Kinniburgh, D.; van Riemsdijk, W. & Koopal, L. (1995), 'Metal ion binding to humic substances: Application of the non ideal competitive adsorption model', *Environ. Sci. Technol.* 29, 446-457.
- Borg, H.; Andersson, P. & Johansson, K. (1989), 'Influence of acidification on metal fluxes in Swedish forest lakes', *Sci. Total Environ.* 87-88, 241-253.
- Buffle, J. & van Leeuwen, H. (1992), *Environmental particles*, Lewis Publishers.
- Carpita, N.; Sabularse, D.; Montezinos, D. & Delmer, D. (1979), 'Determination of the

-
- pore size of cell walls of living plant cells', *Science* 205(4411), 1144-1147.
- Chang Chien, S.; Wang, M. & Huang, C. (2006), 'Reactions of compost-derived humic substances with lead, copper, cadmium, and zinc', *Chemosphere* 64, 1353-1361.
- Colombini, M. (1980), 'Pore size and properties of channels from mitochondria isolated from *Neurospora crassa*', *J. Membrane Biol.* 53, 1432-1424.
- Dahlqvist, R.; Andersson, K.; Ingri, J.; Larsson, T.; Stolpe, B. & Turner, D. (2007), 'Temporal variations of colloidal carrier phases and associated trace elements in a boreal river', *Geochim. Cosmochim. Acta* 71, 5339-5354.
- Dahlqvist, R.; Benedetti, M. F.; Andersson, K.; Turner, D.; Larsson, T.; Stolpe, B. & Ingri, J. (2004), 'Association of calcium with colloidal particles and speciation of calcium in the Kalix and Amazon rivers', *Geochim. Cosmochim. Acta* 68(20), 4059-4075.
- Davies, J.; Jenkins, A.; Monteith, D.; Evans, C. & Cooper, D. (2005), 'Trends in surface water chemistry of acidified UK Freshwaters, 1988-2002', *Environmental Pollution* 137, 27-39.
- Dupré, B.; Viers, J.; Dandurand, J.; Polvé, M.; Bénézeth, P.; Vervier, P. & Braun, J. (1999), 'Major and trace elements associated with colloids in organic-rich river waters: ultrafiltration of natural and spiked solutions', *Chem. Geol.* 160, 63-80.
- Erlandsson, M. (2008), 'Credible acidification assessments in a changeable environment', PhD thesis, Swedish University of Agricultural Sciences.
- Evans, C.; Cullen, J.; Alewell, C.; Kopácek, J.; Marchetto, A.; Moldan, F.; Prechtel, A.; Rogora, M.; Veselý, J. & Wright, R. (2001), 'Recovery from acidification in European surface waters', *Hydrology and Earth System Sciences* 5(3), 283-297.
- Evans, C.; Monteith, D. & Cooper, D. (2005), 'Long-term increases in surface water dissolved organic carbon: observations, possible causes and environmental impacts', *Environ. Pollut.* 137, 55-71.
- Galloway, J. N. (2001), 'Acidification of the world: natural and anthropogenic', *Water, Air and Soil Pollution* 130, 17-24.
- Gimpel, J.; Zhang, H.; Davison, W. & Edwards, A. (2003), 'In situ trace metal speciation in lake surface waters using DGT, dialysis, and filtration', *Environ. Sci. Technol.* 37(1), 138-146.
- Gustafsson, J., 'A Windows version of MINTEQA2',
<http://www.lwr.kth.se/English/OurSoftware/vminteq/index.htm>.
- Gustafsson, J. (1999), 'WinHumicV For Win95/98/NT'
(<http://amov.ce.kth.se/people/gustafjp/winhumicv.htm>).
- Gustafsson, O. & Gschwend, P. M. (1997), 'Aquatic colloids: Concepts, definitions, and

-
- current challenges', *Limnol. Oceanogr.* 42(3), 519-528.
- Gustafsson, O.; Widerlund, A.; Andersson, P. S.; Ingri, J.; Roos, P. & Ledin, A. (2000), 'Colloid dynamics and transport of major elements through a boreal river — brackish bay mixing zone', *Mar. Chem.* 71, 1-21.
- Ingri, J. & Widerlund, A. (1994), 'Uptake of alkali and alkaline-earth elements on suspended iron and manganese in the Kalix River, northern Sweden', *Geochim. Cosmochim. Acta* 58(24), 5433-5442.
- Ingri, J. & Widerlund, A. (1994), 'Uptake of alkali and alkaline-earth elements on suspended iron and manganese in the Kalix River, northern Sweden', *Geochim. Cosmochim. Acta* 58(24), 5433-5442.
- Ingri, J.; Torssander, P.; Andersson, P. S.; Morth, C. & Kusakabe, M. (1997), 'Hydrogeochemistry of sulfur isotopes in the Kalix River catchment, northern Sweden', *Appl. Geochem.* 12, 483-496.
- Ingri, J.; Widerlund, A.; Land, M.; Gustafsson, O.; Andersson, P. S. & Öhlander, B. (2000), 'Temporal variations in the fractionation of the rare earth elements in a boreal river; the role of colloidal particles.', *Chem. Geol.* 166, 23–45.
- Johannesson, K. H.; Tang, J.; Daniels, J. M.; Bounds, W. J. & Burdige, D. J. (2004), 'Rare earth element concentrations and speciation in organic-rich blackwaters of the Great Dismal Swamp, Virginia, USA', *Chem. Geol.* 209, 271-294.
- Kinniburgh, D. G.; van Riemsdijk, W. H.; Koopal, L. K.; Borkovec, M.; Benedetti, M. F. & Avena, M. J. (1999), 'Ion binding to natural organic matter: competition, heterogeneity, stoichiometry and thermodynamic consistency', *Colloids and Surfaces. A: Physicochemical and Engineering Aspects* 151, 147-166.
- Land, M. & Öhlander, B. (1997), 'Seasonal variations in the geochemistry of shallow groundwater hosted in granitic till', *Chem. Geol.* 143, 205-216.
- Milne, C. J.; Kinniburgh, D. G. & Tipping, E. (2001), 'Generic NICA-donnan model parameters for proton binding by humic substances', *Environ. Sci. Technol.* 35(10), 2049-2059.
- Milne, C. J.; Kinniburgh, D. G.; van Riemsdijk, W. H. & Tipping, E. (2003), 'Generic NICA-donnan model parameters for metal-ion binding by humic substances', *Environ. Sci. Technol.* 37(5), 958-971.
- Moiseenko, T. (1995), 'Critical loads of SO₄ for surface waters in the Kola region of Russia', *Water, Air and Soil Pollution* 85, 469-473.
- Morel, F. (1983), *Principles of aquatic chemistry*, Wiley.
- Orr, J.; Fabry, V.; Aumont, O.; Bopp, L.; Doney, S. & et al., R. F. (2005), 'Anthropogenic ocean acidification over the twenty-first century and its impact on calcifying organisms', *Nature* 437, 681-686.

-
- Pokrovsky, O. & Schott, J. (2002), 'Iron colloids/organic matter associated transport of major and trace elements in small boreal rivers and their estuaries (NW Russia)', *Chem. Geol.* 190, 141-179.
- Pokrovsky, O. S.; Dupré, B. & Schott, J. (2005), 'Fe-Al-organic colloids control of trace elements in peat soil solutions', *Aquatic Geochemistry* 11, 241–278.
- Pokrovsky, O. S.; Schott, J. & Dupré, B. (2006), 'Trace element fractionation and transport in boreal rivers and soil porewaters of permafrost-dominated basaltic terrain in Central Siberia', *Geochim. Cosmochim. Acta* 70, 3239–3260.
- Pontér, C.; Ingri, J.; Burmann, J. & Bostrom, K. (1990), 'Temporal variations in dissolved and suspended iron and manganese in the Kalix River, northern Sweden', *Chem. Geol.* 81, 121-131.
- Porcelli, D.; Andersson, P. S.; Wasserburg, G. J.; Ingri, J. & Baskaran, M. (1997), 'The importance of colloids and mires for the transport of uranium isotopes through the Kalix River watershed and Baltic Sea', *Geochim. Cosmochim. Acta* 61(19), 4095-411.
- Prado, A. G.; Torres, J. D.; Martins, P. C.; Pertusatti, J.; Bolzon, L. B. & Faria, E. A. (2006), 'Studies on copper(II)- and zinc(II)-mixed ligand complexes of humic acid', *Journal of Hazardous Materials* B136, 585-588.
- Reuss, J.; Cosby, B. & Wright, R. (1987), 'Chemical processes governing soil and water acidification', *Nature* 329, 27-32.
- Savenko A.V. (1995) Coprecipitation of uranium with iron oxyhydroxide (III) formed in sea water during oxidation of iron (II) (in Russian). *Geochemistry*. 10, 1472-1479.
- Savenko A.V. (1996) Aluminium behaviour during mixture of submarine hydrothermal solutions with sea water: experimental modelling data (in Russian). *Oceanology*. 36(5), 735-740.
- Savenko A.V. (1999a) Experimental modelling of oxianions coprecipitation (PO_4^{3-} , VO_4^{3-} , CrO_4^{2-} , AsO_3^{3-} , AsO_4^{3-}) with iron oxyhydroxide in submarine hydrothermal plumes (in Russian). *Geochemistry*. 3, 281-288.
- Savenko A.V. (1999b) Role of hydrothermal iron oxyhydroxides in accumulation of cobalt and nickel in metal-bearing ocean sediments (experimental modelling data) (in Russian). *Lithology and fossil minerals*. 4, 432-438.
- Savenko A.V. (2001) Coprecipitation of manganese, copper, zinc, lead and cadmium with iron hydroxide in hydrothermal plumes (laboratory modelling data) (in Russian). *Oceanology*. 41(4), 527-532.
- Savenko A.V. and Pokrotsky O.S. (2007) Coprecipitation of hydrolyzate elements with iron (III) hydroxide in submarine hydrothermal plumes. *Proceedings of XVII*

International scientific conference (School) on marine geology "Geology of seas and oceans". November 12-16, 2007. Vol. II, Moscow, GEOS, 74-76.

- Seip, H. M. (1986), 'Surface water acidification', *Nature* 322, 118.
- Sholkovitz, E. (1976), 'Flocculation of dissolved organic and inorganic matter during the mixing of river water and seawater', *Geochim. Cosmochim. Acta* 40(7), 831-845.
- Sigg, L.; Black, F.; Buffle, J.; Cao, J.; Cleven, R.; Davison, W.; Galceran, J.; Gunkel, P.; Kalis, E.; Kistler, D.; Martin, M.; Noël, S.; Nur, Y.; Odzak, N.; Puy, J.; Riemsdijk, W. V.; Temminghoff, E.; Tercier-Waeber, M.; Toepperwien, S.; Town, R. M.; Unsworth, E.; Warnken, K. W.; Weng, L.; Xue, H. & Zhang, H. (2006), 'Comparison of analytical techniques for dynamic trace metal speciation in natural freshwaters', *Environ. Sci. Technol.* 40(6), 1934-1941.
- Skjelkvåle, B. L.; Stoddard, J. L. & Andersen, T. (2001), 'Trends in surface water acidification in Europe and North America (1989-1998)', *Water, Air and Soil Pollution* 130, 787-792.
- Stevenson, F. & Chen, Y. (1991), 'Stability constants of copper(II)-humate complexes determined by modified potentiometric titration', *Soil Science Society of America Journal* 55, 1586-1591.
- Thurman, E. M. (1985), *Organic geochemistry of natural waters*, Martinus Nijhoff/Dr W. Junk Publishers: Boston.
- Tipping, E. & Hurley, M. (1992), 'A unifying model of cation binding by humic substances', *Geochim. Cosmochim. Acta* 56(10), 3627-3641.
- Tipping, E. (1994), 'WHAM - A chemical equilibrium model and computer code for waters, sediments, and soils incorporating a discrete site/electrostatic model of ion-binding by humic substances', *Computers & Geosciences* 20(6), 973-1023.
- Tipping, E. (1998), 'Humic ion-binding model VI: an improved description of the interactions of protons and metal ions with humic substances', *Aquatic Geochemistry* 4, 3-48.
- Tipping, E.; Rey-Castro, C.; Bryan, S. E. & Hamilton-Taylor, J. (2002), 'Al(III) and Fe(III) binding by humic substances in freshwaters, and implications for trace metal speciation', *Geochim. Cosmochim. Acta* 66(18), 3211-3224.
- Trias, J.; Jarlier, V. & Benz, R. (1992), 'Porins in the cell wall of mycobacteria', *Science* 258(5087), 1479-1481.
- Unsworth, E. R.; Warnken, K. W.; Zhang, H.; Davison, W.; Black, F.; Buffle, J.; Cao, J.; Cleven, R.; Galceran, J.; Gunkel, P.; Kalis, E.; Kistler, D.; Leeuwen, H. P. V.; Martin, M.; Noël, S.; Nur, Y.; Odzak, N.; Puy, J.; Riemsdijk, W. V.; Sigg, L.; Temminghoff, E.; Tercier-Waeber, M.; Toepperwien, S.; Town, R. M.; Weng, L. & Xue, H. (2006), 'Model predictions of metal speciation in freshwaters'

compared to measurements by in situ techniques', *Environ. Sci. Technol.* 40(6), 1942-1949.

Vasyukova, E.; Pokrovsky, O.; Viers, J.; Oliva, P.; Dupré, B.; Martin, F. & Candaudap, F. (2008), 'Trace elements in organic- and iron-rich surficial fluids of boreal zone: Assessing colloidal forms via dialysis and ultrafiltration', *Geochim. Cosmochim. Acta* (*submitted*).

Viers, J.; Dupré, B.; Polve, M.; Dandurand, J. & Braun, J. (1997), 'Chemical weathering in the drainage basin of a tropical watershed (Nsimi-Zoetele site, Cameroon): comparison between organic-poor and organic-rich waters', *Chem. Geol.* 140, 181-206.

Yeghicheyan, D.; Carignan, J.; Valladona, M.; Coz, M. B. L.; Cornec, F. L.; Castrec-Rouelle, M.; Robert, M.; Aquilina, L.; Aubry, E.; Churlaud, C.; Dia, A.; Deberdt, S.; Dupré, B.; Freydier, R.; Gruau, G.; Hénin, O.; de Kersabiec, A.; Macé, J.; Marin, L.; Morin, N.; Petitjean, P. & Serrat, E. (2001), 'A compilation of silicon and thirty one trace elements measured in the natural river water reference material SLRS-4 (NRC-CNRC)', *Geostandards Newsletter* 25(2-3), 465-474.

Zakharova, E.; Pokrovsky, O. S.; Dupré, B.; Gaillardet, J. & Efimova, L. (2007), 'Chemical weathering of silicate rocks in Karelia region and Kola peninsula, NW Russia: Assessing the effect of rock composition, wetlands and vegetation', *Chem. Geol.* 242, 255-277.

Chapter 5

Conclusions and perspectives



5.1. Conclusions

Following conclusions emerge from this study:

- First part of this thesis was aimed at characterizing the mechanisms governing the chemical weathering and mineral formation in subarctic zone, and description of the partition of elements between basic and acid rocks and soils formed after the last glaciation period. In the cold subarctic climate, even thin deposits of glacial till moraine are capable of protecting mafic rocks to direct chemical weathering. Traces of chemical corrosion observed on the surface of zircons and feldspars along with the presence of new-formed amorphous matter on the surface of quartz, plagioclases and pyroxenes reveal an already pronounced weathering process in spite of a relatively short postglacial period (10-20 Ky). However, over 10-15,000 years of exposure after the last glaciation, full weathering soil profile on basic rocks could not be established. Observations like presence of quartz and zircons in soils developed on basic rocks, similarity of REE patterns of intermediate and deep soil horizons both for felsic and mafic rocks, as well as isotopic signature of soils on gabbro-norite and olivenite close to that of granodiorites raise a question of polycyclic nature of these soils (soil developed on fragments of already pre-existing soil), and assume their “contamination” with granitic moraine admixture.

The index of chemical alteration degree (CIA) showed no or weak weathering for soils in the studied region, and the use of invariant element to quantify this weathering process was impossible. As a result of this study, some specific features should be taken into account in the estimation of mafic rocks weathering rates and calculations of atmospheric CO₂ consumption by weathering in such a particular environment. The relative enrichment in Na with respect to Ca and Mg observed in rivers from both granitic and basaltic watersheds raises the possibility of contribution to the river chemistry of other sources than primary silicate weathering reactions. We suggest that either Mg-vermiculite and CaMg-amphibole formation in soils limits Ca and Mg export in waters, or there are highly weatherable Ca- and Mg-rich minerals present in granitic rocks.

According to the calculations, the weathering rates of ultramafic rocks are higher than those for the granitic till, but dominated moraine depositions in this region hide the evidence of a real weathering process. Therefore, values estimated for the olivinite rock

in this study appear to be lower than the weathering rates estimated on the basis of surface water fluxes for Karelian and Siberian mafic rocks in previous studies. Retention of Mg and Ca in soil due to precipitation of secondary phases such as Mg-vermiculite or process of adsorption on mineral, organic or organo-mineral phases, can serve as an explanation of this discrepancy.

- In the second part of this work, we investigated colloidal speciation of trace elements in boreal waters from Northern and Southern Karelia using two methods – ultrafiltration and dialysis – in order to recognize the factors responsible for the chemical composition of surface water draining different lithology. Several groups of elements can be distinguished according to their behaviour during filtration and association with these two types of colloids: (i) species very weakly affected or unaffected by ultrafiltration, which are present as truly dissolved inorganic species or weak organic complexes (Ca, Mg, Li, Na, K, Cs, Si, B, As, Sr, Ba, W, Sb and Mo); (ii) elements present in the fraction smaller than 1-10 kDa, which are liable to form strong organic complexes (Ni, Zn, Cu, Cd, Ba, W and, in some rivers, Sr and Cr), and (iii) elements strongly associated with colloidal iron in all ultrafiltrates and dialysates, with up to 95% concentrated in large colloidal particles (> 10 kDa) (Mn, Al, Ga, REEs, Pb, V, Cr, Ti, Zr, Th, U, Co, Y and Hf).

For almost 30 elements affected by size separation during filtration, dialysis yields a 2 to 3 times higher proportion of colloidal forms (1 kDa – 0.22 µm) compared to frontal ultrafiltration. Nevertheless, dialysis is able to provide a fast and artefact-free *in-situ* separation of colloidal and dissolved components. Its main advantages over the more widely used ultrafiltration technique are i) the absence of charge separation; ii) no clogging of the filter membrane induced by forced filtration, and iii) a reduction in the various sources of contamination (filter, apparatus, tubing and recipient) provided the constant chemical composition and colloidal stability of the external pool is maintained.

- Assessment of the role of the rock lithology (granitic environment versus basaltic) in TE speciation and organo-mineral colloids formation in boreal waters demonstrates that within ±10% uncertainty, there is no difference in TE distribution between truly dissolved forms (< 1 kDa) and two colloidal pools (1 kDa – 10 kDa and 10 kDa – 0.22 µm) in surface waters draining acidic and basic rocks. We also note the existence of a significant pool of large colloidal particles (10 kDa – 0.22 µm) that

accounts for 10 to 40% of major cations (Ca, Mg and Na) and other divalent alkaline-earth elements (Sr and Ba) that are usually considered as being in truly dissolved forms. The transition metals (Cu, Zn, Ni and Co), which are known to be strongly complexed with organic matter, are present in both colloidal and dissolved form, with similar proportions in each fraction (< 1 kDa, 1 – 10 kDa and 10 kDa – 0.22 µm) pools. Finally, for most elements significantly affected by the presence of colloids (Al, Ti, Y, REEs, Zr, Th and U) more than 70% is contained in the 1 kDa – 0.22 µm fraction, while the small colloidal particles (1 – 10 kDa) account for only a minor proportion (10 to 20%) compared to large colloidal particles (10 kDa – 0.22 µm, from 50 to 90%).

- Geochemical modelling using Visual MINTEQ code with available database of the complexation of several TE with natural organic matter generally agrees with the experimental results although it does not allow us to reproduce quantitatively the distribution of all colloidal versus dissolved forms. This is consistent with a previous hypothesis that some TEs, notably trivalent and tetravalent metals, are associated with the inorganic (Fe-bearing) part of the colloids, and not just complexed with humic or fulvic acids. Though data of this study do not allow straightforward discrimination, our observations are compatible with three possible pathways of colloid formation, i.e., i) in the uppermost surface horizon via the release of dissolved TE, Fe and organic matter from decomposing plant litter, ii) in interstitial soil solutions via production/migration of colloids between soil horizons, and iii) at the redox front between Fe(II)-bearing anoxic groundwaters and surficial OM-rich waters of the riparian or wetland zone.

- In order to get further insights in the stability constants of association reactions between TE and natural organo-mineral colloids, we further treated in the laboratory the filtered samples. Ex-situ dialysis experiments through 1-kDa membrane of natural filtered waters conducted at various pH in the laboratory allowed straightforward evaluation of the degree of trace metal binding to natural colloids. Using available speciation code (Visual MINTEQ with implemented NICA-Donnan model for ion binding humic acid) we found that it allows reasonable description of the proportion of colloidal Ca, Mg, Sr, Ba, Mn, Co, Ni, Cd, Pb forms measured in the experiment at pH from 3 to 8 assuming that all colloidal metal is bound to humic and fulvic acid. The degree of binding of Al, Fe, REEs, Th and U is strongly overestimated by the model and the decrease of humic (HA) and fulvic (FA) binding constant by at least 3-5 orders of

magnitude is necessary to approach the experimental pH-dependence. While for Cu (and probably U) such a modification is consistent with large variation of stability constants reported in literature, unreasonably large modifications for Al, Fe, REEs and Th binding with HA and FA are necessary to approach the experimental data and even then, the fit is extremely poor. Therefore, an alternative explanation for this discrepancy could be the association of trivalent and tetravalent elements with the bulk of Fe-rich (mineral) colloids, as it was already reported in previous works.

- It was also proven that colloidal speciation of most trace elements in water depends on pH. According to our results, the decrease of pH from 6 to 5 will bring about two to three-fold increase in the proportion of non-colloidal (< 1 kDa) forms of most potentially toxic metals (Al, Cu, Cd, Co, Ni, Pb, Th, U). These conventionally dissolved species are potentially bioavailable since the pore sizes of cell wall transport channels (10-30 Å in bacteria, 35-50 Å in plant cells) and that of 1 kDa dialysis membrane (1-3 nm) are comparable. Therefore, significant increase in the bioavailability of trace metals may occur upon acidification of natural waters induced by local anthropogenic pollution or the global warming (atmospheric CO₂ increase). From the other hand, increase of DOC concentration in surface waters due to global warming as it is observed in Nordic Countries, British Isles, and Northern and Eastern United States (by approx. 10% over 10 years) may as well increase the proportion of metals bounded to colloidal organic matter thus compensating for the effect of acidification.

5.2. Perspectives

In the course of this study, a number of new scientific challenges have been identified. Like any multidisciplinary study, while providing the answers to the pre-identified objectives, it opens a number of new frontiers and provides the necessary background to tackle new questions. In the near next future, in order to further advance in our understanding of biogeochemistry of boreal systems, several new issues have to be addressed:

- Further stable-isotope (Ca, Cu, Fe) geochemical studies and experimental modelling of colloid formation are required to ascertain the mechanism of TE

interaction with organo-mineral colloids of the boreal zone. Recently, it was shown that two types of colloids, iron oxyhydroxides and Fe-C colloidal matter, exhibit different Fe-isotope composition (Ingri et al., 2006). Since both types of colloids are important for trace metal transport in the river systems, important isotopic fractionation can be anticipated. Study of stable isotope fractionation will allow i) better constrain the isotopic signature of element fluxes to the ocean; ii) provide new traces for the origin of colloids in surface waters of the boreal zone.

- In order to better distinguish the relative role of mineral and organic parts of colloids in the binding of trace metals, some pretreatment of natural waters via UV irradiation and H₂O₂ treatment can be performed. This treatment will partially decompose the organic matter and, followed by standard dialysis or ultrafiltration procedure it will allow quantifying the binding constants or distribution coefficients for TE with mineral part of colloids.
- To get further insights in the structure of organo-mineral colloids collected in natural waters or formed in the laboratory via lixiviation of plant litter/peat soil, detailed microscopic/spectroscopic study is necessary. The size of colloids subjected to different treatment can be assessed via laser granulometry, while the chemical structure of organo-mineral associates can be characterized using X-ray Synchrotron microscopy (NEXAFS for C and Fe).
- In order to better characterize all three possible families of colloids encountered in the Podzol boreal zone (organic of the plant litter, Fe-Al-organic of the soil solution and Fe-organic of the river water), separation and in-situ characterization of the first two families are necessary. This can be achieved via using temporary or permanently installed soil waters collectors (porous cups or lysimeters) as well as specially designed laboratory experiments.
- Further progress can still be done for the understanding the origin of element in the rivers. In addition to the effect of soil minerals and rocks dissolution and the groundwater input, surface soil water transport of plant litter degradation products can be better assessed. For this, thorough measurements of major group of plants litter chemical composition, its degradation in soil and further transport to the rivers via subsurface and surface flow should be assessed. According to the balance calculation by

Zakharova et al. (2007) for Karelia region, up to 30-40% of major elements and silica in the river water may be originated from the plant litter degradation. At present, we have no evaluation for the role of plant litter in the transport of other major and trace elements, notably those present in the form of colloids and further in-situ and laboratory experiments are necessary.

BIBLIOGRAPHY

- AFNOR (1996) *Qualité des sols. Recueil de normes Françaises*, Association Française de Normalisation, Paris.
- Aggarwal, S. G.; Chandrawanshi, C. K.; Patel, R. M.; Agarwal, S.; Kamavisdar, A. & Mundhara, G. L. (2001), 'Acidification of surface waters in Central India', *Water, Air and Soil Pollution* 130, 855-862.
- Akselsson, C.; Holmqvist, J.; Kurz, D. & Sverdrup, H. (2006), 'Relations between elemental content in till, mineralogy of till and bedrock mineralogy in the province of Småland, southern Sweden', *Geoderma* 136, 643-659.
- Alapieti, T. & Tuomo (1982), 'The Koillismaa layered igneous complex, Finland : its structure, mineralogy and geochemistry, with emphasis on the distribution of chromium', *Bull. Geol. Surv. Finl.* 319, 116.
- Alfaro-De la Torre, M. C.; Beaulieu, P. & Tessier, A. (2000), 'In situ measurement of trace metals in lakewater using the dialysis and DGT techniques', *Anal. Chim. Acta* 418, 53-68.
- Allard, T.; Menguy, N.; Salomon, J.; Calligaro, T.; Weber, T.; Calas, G. & Benedetti, M. F. (2004), 'Revealing forms of iron in river-borne material from major tropical rivers of the Amazon Basin (Brazil)', *Geochim. Cosmochim. Acta* 68(14), 3079-3094.
- Allard, B. (2006), 'A comparative study on the chemical composition of humic acids from forest soil, agricultural soil and lignite deposit Bound lipid, carbohydrate and amino acid distributions', *Geoderma* 130(1-2), 77-96.
- Allard, B. & Derenne, S. (2007), 'Oxidation of humic acids from an agricultural soil and a lignite deposit: Analysis of lipophilic and hydrophilic products', *Org. Geochem.* 38, 2036-2057.
- Allen, C.; Darmody, R.; Thorn, C.; Dixon, J. & Schlyter, P. (2001), 'Clay mineralogy, chemical weathering and landscape evolution in Arctic-Alpine Sweden', *Geoderma* 99, 277-294.
- Allison, J. D.; Brown, D. S. & Novo-Gradac, K. J. (1991), 'MINTEQA2/PRODEFA2, A geochemical assessment model for environmental systems: version 3.0 user's manual', (EPA/600/3-91/021), 115.
- Allison, J. & Perdue, E. (1994), In: *Humic Substances in the Global Environment and Implications on Human Health*, Elsevier Science B.V., Amsterdam, chapter Modeling metal-humic interaction with Minteqa2, pp. 927-942.
- Amelin, Y. & Semenov, V. (1990), 'On the age and sources of magmas for the early Proterozoic layered intrusions of Karelia (abstracts of papers)', *Isotopnoe*

datirovanie endogenykh rudnykh formacii (Isotopic dating of endogenic ore associations), Tbilisi, 40-42.

- Amelin, Y. V.; Heaman, L. & Semenov, V. (1995), 'U-Pb geochronology of layered mafic intrusions in the eastern Baltic Shield: implications for the timing and duration of Paleoproterozoic continental rifting', *Precambrian Res.* 75, 31-46.
- Amelin, Y. V. & Semenov, V. S. (1996), 'Nd and Sr isotopic geochemistry of mafic layered intrusions in the eastern Baltic shield: implications for the evolution of Paleoproterozoic continental mafic magmas', *Contrib. Mineral. Petrol.* 124, 255-272.
- Anderson, H.; Berrow, M.; Farmer, V.; Hepburn, A.; Russell, J. & Walker, A. (1982), 'A reassessment of podzol formation processes', *J. Soil Sci.* 33, 125-136.
- Andersson, K.; Dahlqvist, R.; Turner, D.; Stolpe, B.; Larsson, T.; Ingri, J. & Andersson, P. (2006), 'Colloidal rare earth elements in a boreal river: Changing sources and distributions during the spring flood', *Geochim. Cosmochim. Acta* 70, 3261-3274.
- Andersson, P. S.; Porcelli, D.; Wasserburg, G. J. & Ingri, J. (1998), 'Particle transport of ^{234}U / ^{238}U in the Kalix river and in the Baltic Sea', *Geochim. Cosmochim. Acta* 62(3), 385-392.
- Andersson, P. S.; Porcelli, D.; Gustafsson, O.; Ingri, J. & Wasserburg, G. J. (2001a), 'The importance of colloids for the behavior of uranium isotopes in the low-salinity zone of a stable estuary', *Geochim. Cosmochim. Acta* 65(1), 13-25.
- Andersson, Per S.; Dahlqvist, Ralf; Ingri, Johan & Örjan Gustafsson (2001b), 'The isotopic composition of Nd in a boreal river: A reflection of selective weathering and colloidal transport', *Geochim. Cosmochim. Acta* 65(4), 521-527.
- Apps, M.; Kurz, W.; Luxmoore, R.; Nilsson, L.; Sedjo, R.; Schmidt, R.; Simpson, L. & Vinson, T. (1993), 'Boreal forests and tundra', *Water, Air and Soil Pollution* 70(1-4), 39-53.
- Ariés, S.; Valladon, M.; Polvé, M. & Dupré, B. (2000), 'A routine method for oxide and hydroxide interference corrections in ICP-MS chemical analysis of environmental and geological samples', *Geostandards Newsletter* 24, 19-31.
- Åström, M. & Corin, N. (2000), 'Abundance, sources and speciation of trace elements in humus-rich streams affected by acid sulphate soils', *Aquat. Geochem.* 6(3), 367-383.
- Åström, M. (2001), 'The effect of acid soil leaching on trace element abundance in a medium-sized stream, W. Finland', *Appl. Geochem.* 16, 387-396.
- Balashov, Y. A.; Bayanova, T. B. & Mitrofanov, F. P. (1993), 'Isotope data on the age and genesis of layered basic-ultrabasic intrusions in the Kola Peninsula and northern Karelia, northeastern Baltic Shield', *Precambrian Res.* 64, 197-205.

-
- Barkov, A.; Gannibal, L.; Ryungenen, G. & Balashov, Y. (1991), 'Zircon dating of the Kivakka layeres massif, Northern Karelia. Abstracts of papers', *All-Union seminar on methods of isotopic geology, Zvenigorod, 21-25 October 1991, St. Petersburg*, 21-23.
- Bau, M. (1999), 'Scavenging of dissolved yttrium and rare earths by precipitating iron oxyhydroxide: Experimental evidence for Ce oxidation, Y-Ho fractionation, and lanthanide tetrad effect', *Geochim. Cosmochim. Acta* 63, 67-77.
- Benedetti, M.; Milne, C.; Kinniburgh, D.; van Riemsdijk, W. & Koopal, L. (1995), 'Metal ion binding to humic substances: Application of the non ideal competitive adsorption model', *Environ. Sci. Technol.* 29, 446-457.
- Beneš, P. & Steinnes, E. (1974), 'In situ dialysis for the determination of the state of trace elements in natural waters', *Water Res.* 8(11), 947-953.
- Bennett, P. C. (1991), 'Quartz dissolution in organic-rich aqueous systems', *Geochim. Cosmochim. Acta* 55(7), 1781-1797.
- Berggren D. (1989) Speciation of aluminum, cadmium, copper, and lead in humus soil solutions – a comparison of the ion exchange column procedure and equilibrium dialysis. *Int. Environ. Anal. Chem.* 35, 1–15.
- Berner, R. A.; Lasaga, A. C. & Garrels, R. M. (1983), 'The carbonate-silicate geochemical cycle and its effect on atmospheric carbon dioxide over the past 100 million years', *American Journal of Science* 283, 641-683.
- Berner, R. (1992), 'Weathering, plants, and the long-term carbon cycle', *Geochim. Cosmochim. Acta* 56(8), 3225-3231.
- Berner, R. (1995), 'Chemical weathering and its effect on atmospheric CO₂ and climate', *Reviews in mineralogy and geochemistry* 31(1), 565-583.
- Berner, R. A. & Maasch, K. A. (1996), 'Chemical weathering and controls on atmospheric O₂ and CO₂: Fundamental principles were enunciated by J. J. Ebelmen in 1845', *Geochim. Cosmochim. Acta* 60(9), 1633-1637.
- Berner, R. A. & Kothavala, Z. (2001), 'Geocarb III: a revised model of atmospheric CO₂ over phanerozoic time', *American Journal of Science* 301, 182-204.
- Bibikova, E.; Skiodl, T.; Bogdanova, S.; Gorbatschev, R. & Slabunov, A. (2001), 'Titanite-rutile thermochronometry across the boundary between the Archaean Craton in Karelia and the Belomorian Mobile Belt, eastern Baltic Shield', *Precambrian Res.* 105, 315-330.
- Bibikova, E. V.; Samsonov, A. V.; Petrova, A. Y. & Kirnozova, T. I. (2005), 'The Archean geochronology of Western Karelia', *Stratigraphy and Geological Correlation* 13(5), 459-475.

-
- Björkvald, L.; Buffam, I.; Laudon, H. & Mört, C. (2008), 'Hydrogeochemistry of Fe and Mn in small boreal streams: The role of seasonality, landscape type and scale', *Geochim. Cosmochim. Acta* 72(12), 2789-2804.
- Bluth, G. J. S. & Kump, L. R. (1994), 'Lithologic and climatologic controls of river chemistry', *Geochim. Cosmochim. Acta* 58(10), 2341-2359.
- Boeglin, J. & Probst, J. (1998), 'Physical and chemical weathering rates and CO₂ consumption in a tropical lateritic environment: the upper Niger basin', *Chem. Geol.* 148(3-4), 137-156.
- Borg H. and Andersson P. (1984) Fractionation of trace metals in acidified fresh waters by in situ dialysis. *Verh. Int. Verein Limnol.* 22, 725–729.
- Borg, H.; Andersson, P. & Johansson, K. (1989), 'Influence of acidification on metal fluxes in Swedish forest lakes', *Sci. Total Environ.* 87-88, 241-253.
- Botch, M.; Kobak, K.; Vinson, T. & Kolchugina, T. (1995), 'Carbon pools and accumulation in peatlands of the former Soviet Union', *Glocal Biogeochem. Cycles* 9, 37-46.
- Brady, P. V. (1991), 'The effect of silicate weathering on global temperature and atmospheric CO₂', *Journal of Geophysical Research* 96(B11), 18101-18106.
- Braun, J.; Viers, J.; Dupré, B.; Polve, M.; Ndam, J. & Muller, J. (1998), 'Solid/ liquid REE fractionation in the lateritic systems of the Goyoum, East Cameroon: The implication for the present dynamics of the soil covers of the humid tropical regions', *Geochim. Cosmochim. Acta* 62(2), 273-299.
- van Breemen, N. & Buurman, P. (1998), *Soil Formation*, chapter Podzolization, pp. 245-270.
- Buffle J. (1988), Complexation reactions in aquatic systems: an analytical approach. Ellis Horwood Ltd., Chichester, UK.
- Buffle, J. & van Leeuwen, H. (1992), *Environmental particles*, Lewis Publishers.
- Buurman, P. (1984), *Podzols*. Van-Nostand Reinhold Soil Science Series. ISBN-0-442-21129-5. Campbell, I.B., Claridge, G.G., 1987. *Antartica-Soils, Weathering Process and Climate*. Elsevier, New York.
- Buurman, P. & Jongmans, A. (2005), 'Podzolisation and soil organic matter dynamics', *Geoderma* 125(1-2), 71-83.
- Buschmann, J. & Sigg, L. (2004), 'Antimony(III) binding to humic substances: influence of pH and type of humic acid', *Environ. Sci. Technol.* 38, 4535-4541.
- Bychkova, Y. V. (2003), 'Principles of a contrast rhythmic layering structure of Kivakka intrusion (Zakonomernosti stroeniya kontrastnoi pitmicheskoi rassloennosti v

-
- Kivakkskom intruzive) (in Russian)', PhD thesis, MGU, Kaf. Geokhimii Geologicheskogo f-ta.
- Bychkova, Y. & Koptev-Dvornikov, E. (2004), 'Rithmical layering of Kivakka type: geology, petrology, petrochemistry, hypothesis of formation (in Russian)', *Petrology* 12(3), 281-302.
- Bychkova, Y. V.; Koptev-Dvornikov, E. V.; Kononkova, N. N. & Kameneva, E. E. (2007), 'Composition of rock-forming minerals in the Kivakka layered massif, Northern Karelia, and systematic variations in the chemistries of minerals in the rhythmic layering subzone', *Geochem. Int.* 45(2), 131–151.
- de Caritat, P.; Reimann, C.; Bogatyrev, I.; Chekushin, V.; Finne, T. E.; Halleraker, J. H.; Kashulina, G.; Niskavaara, H.; Pavlov, V. & Ayras, M. (2001), 'Regional distribution of Al, B, Ba, Ca, K, La, Mg, Mn, Na, P, Rb, Si, Sr, Th, U and Y in terrestrial moss within a 188,000 km² area of the central Barents region: influence of geology, seaspray and human activity', *Appl. Geochem.* 16, 137-159.
- Carpita, N.; Sabularse, D.; Montezinos, D. & Delmer, D. (1979), 'Determination of the pore size of cell walls of living plant cells', *Science* 205(4411), 1144-1147.
- Chien, S. C.; Wang, M. & Huang, C. (2006), 'Reactions of compost-derived humic substances with lead, copper, cadmium, and zinc', *Chemosphere* 64, 1353-1361.
- Colombini, M. (1980), 'Pore size and properties of channels from mitochondria isolated from Neurospora crassa', *J. Membrane Biol.* 53, 1432-1424.
- Condie, K. C. (1993), 'Chemical composition and evolution of the upper continental crust: Contrasting results from surface samples and shales', *Chem. Geol.* 104(1-4), 1-37.
- Courchesne, F. & Hendershot, W.H. (1997), Essai. La Genèse des podzols. *Geogr. Phys. Quarter.* 51, 235–250.
- Dahlqvist, R.; Andersson, K.; Ingri, J.; Larsson, T.; Stolpe, B. & Turner, D. (2007), 'Temporal variations of colloidal carrier phases and associated trace elements in a boreal river', *Geochim. Cosmochim. Acta* 71, 5339-5354.
- Dahlqvist, R.; Benedetti, M. F.; Andersson, K.; Turner, D.; Larsson, T.; Stolpe, B. & Ingri, J. (2004), 'Association of calcium with colloidal particles and speciation of calcium in the Kalix and Amazon rivers', *Geochim. Cosmochim. Acta* 68(20), 4059-4075.
- Dahlqvist, R.; Andersson, P. S. & Ingri, J. (2005), 'The concentration and isotopic composition of diffusible Nd in fresh and marine waters', *Earth Planet. Sci. Lett.* 233, 9-16.
- Dahlqvist, R.; Andersson, P.; Ingri, J. & Porcelli, D. (2006), 'Vertical REE profiles in water and DGT in the central Arctic Ocean', *Goldschmidt Conference Abstracts*.

-
- Dahlqvist, R.; Andersson, K.; Ingri, J.; Larsson, T.; Stolpe, B. & Turner, D. (2007), 'Temporal variations of colloidal carrier phases and associated trace elements in a boreal river', *Geochim. Cosmochim. Acta* 71, 5339-5354.
- Dai, M. & Martin, J. (1995), 'First data on trace metal level and behaviour in two major Arctic river-estuarine systems (Ob and Yenisey) and in the adjacent Kara Sea, Russia', *Earth Planet. Sci. Lett.* 131(3-4), 127-141.
- Dai, M.; Martin, J. & Cauwet, G. (1995), 'The significant role of colloids in the transport and transformation of organic carbon and associated trace metals (Cd, Cu and Ni) in the Rhône delta (France)', *Mar. Chem.* 51, 159-175.
- D'Amico, M.; Julitta, F.; Previtali, F. & Cantelli, D. (2008), 'Podzolization over ophiolitic materials in the western Alps (Natural Park of Mont Avic, Aosta Valley, Italy)', *Geoderma* 146, 129-137.
- Darmody, R.; Thorn, C.; Harder, R.; Schlyter, J. & Dixon, J. (2000), 'Weathering implications of water chemistry in an arctic-alpine environment, northern Sweden', *Geomorphology* 34, 89-100.
- Davies, J.; Jenkins, A.; Monteith, D.; Evans, C. & Cooper, D. (2005), 'Trends in surface water chemistry of acidified UK Freshwaters, 1988-2002', *Environmental Pollution* 137, 27-39.
- Debon, F.; Enrique, P. & Autran, A. (1995), 'Magmatisme Hercynien', *Synthèse géologique et géophysique des Pyrénées. Edt BRGM* 1, Cycle Hercynien (eds. A. Barnolas and J. C. Chiron), 361-499.
- Degueldre, C.; Triay, I.; Kim, J.; Vilks, P.; Laaksoharju, M. & Miekeley, N. (2000), 'Groundwater colloid properties: a global approach', *Appl. Geochem.* 15, 1043-1051.
- DePaolo, D. & Wasserburg, G. (1976), 'Inferences about magma sources and mantle structure from variations of $^{143}\text{Nd}/^{144}\text{Nd}$ ', *Geophys. Res. Lett.* 3, 249-252.
- DePaolo, D. J. (1981), 'Neodymium isotopes in the Colorado Front Range and crust-mantle evolution in the Proterozoic', *Nature* 291, 193-196.
- DePaolo, D. (1988), *Neodimium isotope geochemistry*, Springer-Verlag, New York.
- Dessert, C.; Dupré, B.; Francois, L. M.; Schott, J.; Gaillardet, J.; Chakrapani, G. & Bajpai, S. (2001), 'Erosion of Deccan Traps determined by river geochemistry: impact on the global climate and the $^{87}\text{Sr}/^{86}\text{Sr}$ ratio of seawater', *Earth Planet. Sci. Lett.* 188, 459-474.
- Dessert, C.; Dupré, B.; Gaillardet, J.; François, L. M. & Allègre, C. J. (2003), 'Basalt weathering laws and the impact of basalt weathering on the global carbon cycle', *Chem. Geol.* 202, 257– 273.

-
- Dia, A.; Gruau, G.; Olivié-Lauquet, G.; Riou, C.; Molénat, J. & Curmi, P. (2000), 'The distribution of rare earth elements in groundwaters: Assessing the role of source-rock composition, redox changes and colloidal particles', *Geochim. Cosmochim. Acta* 64(24), 4131-4151.
- Dixon, R.; Solomon, A.; Brown, S.; Houghton, R.; Trexier, M. & Wisniewski, J. (1994), 'Carbon pools and flux of global forest ecosystems', *Science* 263(5144), 185-190.
- Dobrovolsky, V. V. Matveeva, G. E., ed. (1983), *Geography of microelements. Global dispersion*, "Mysl" Moskva.
- Dokuchaev, V. (1880), 'O podzole', *Trudy Vol'nogo ekonomicheskogo obschestva* 1(2).
- van Dongen, Bart E.; Zencaka, Zdenek & Örjan Gustafsson (2008), 'Differential transport and degradation of bulk organic carbon and specific terrestrial biomarkers in the surface waters of a sub-arctic brackish bay mixing zone', *Mar. Chem.* 112(3-4), 203-314.
- Drever, J. I. (1982), *The geochemistry of natural waters*, Prentice-Hall, Inc.
- Duchaufour, P. (1951), 'Lessivage et podsolisation', *Revue forestière française* 10, 652-674.
- Duchaufour, P. (1997), *Abrégé de pédologie*. Editions Masson, 5 ed.
- Dupré, B.; Gaillardet, J.; Rousseau, D. & Allègre, C. J. (1996), 'Major and trace elements of river-borne material: The Congo Basin', *Geochim. Cosmochim. Acta* 60(8), 1301-1321.
- Dupré, B.; Viers, J.; Dandurand, J.; Polvé, M.; Bénézeth, P.; Vervier, P. & Braun, J. (1999), 'Major and trace elements associated with colloids in organic-rich river waters: ultrafiltration of natural and spiked solutions', *Chem. Geol.* 160, 63-80.
- Dupré, B.; Dessert, C.; Oliva, P.; Godderis, Y.; Viers, J.; François, L.; Millot, R. & Gaillardet, J. (2003), 'Rivers, chemical weathering and Earth's climate', *C. R. Geoscience* 335, 1141-1160.
- Erlandsson, M. (2008), 'Credible acidification assessments in a changeable environment', PhD thesis, Swedish University of Agricultural Sciences.
- Evans, C.; Cullen, J.; Alewell, C.; Kopácek, J.; Marchetto, A.; Moldan, F.; Prechtel, A.; Rogora, M.; Veselý, J. & Wright, R. (2001), 'Recovery from acidification in European surface waters', *Hydrology and Earth System Sciences* 5(3), 283-297.
- Evans, C.; Monteith, D. & Cooper, D. (2005), 'Long-term increases in surface water dissolved organic carbon: observations, possible causes and environmental impacts', *Environ. Pollut.* 137, 55-71.

-
- Evdokimova, T. (1957), 'Soil formation process on metamorphic rocks of Karelia', *Pochvovedenie (Soviet Soil. Sci.)* 9, 60-69.
- Eyrolle, F. & Benaim, J. (1999), 'Metal available sites on colloidal organic compounds in surface waters (Brazil)', *Water Res.* 33(4), 995-1004.
- Eyrolle, F.; Benedetti, M. F.; Benaim, J. Y. & Février, D. (1996), 'The distributions of colloidal and dissolved organic carbon, major elements, and trace elements in small tropical catchments', *Geochim. Cosmochim. Acta* 60(19), 3643-3656.
- Fedo, C. M.; Nesbitt, H. W. & Young, G. M. (1995), 'Unraveling the effects of potassium metasomatism in sedimentary rocks and paleosols, with implications for paleoweathering conditions and provenance', *Geology* 23(10), 921-924.
- Feoktistov, V. M. (2004), 'Water chemical composition of Karelian rivers and their dissolved chemical discharge into the White Sea', *Water Resour.* 31(6), 631-638.
- Förstner, U. (1987), *Inbook: Metals speciation, separation, and recovery*, Lewis publishers, Inc., Chelsea, Michigan, chapter Changes in metal mobilities in aquatic and terrestrial cycles.
- Frey, K. E. & Smith, L. C. (2005), 'Amplified carbon release from vast West Siberian peatlands by 2100', *Geophysical Research Letters* 32, L09401.
- Fytianos, K. (2001), 'Speciation analysis of heavy metals in natural waters: a review', *Journal of AOAC International* 84(6), 1763.
- Gaillardet, J.; Dupré, B. & Allègre, C. (1995), 'A global geochemical mass budget applied to the Congo Basin rivers: Erosion rates and continental crust composition', *Geochim. Cosmochim. Acta* 59(17), 3469-3485.
- Gaillardet, J.; Dupré, B.; Allègre, C. J. & Négrel, P. (1997), 'Chemical and physical denudation in the Amazon River Basin', *Chem. Geol.* 142, 141-173.
- Gaillardet, J.; Dupré, B.; Louvat, P. & Allègre, C. (1999), 'Global silicate weathering and CO₂ consumption rates deduced from the chemistry of large rivers', *Chem. Geol.* 159, 3-30.
- Gaillardet, J.; Viers, J. & Dupré, B. (2003), *Surface and ground water, weathering, and soils. Treatise on geochemistry*, Elsevier-Pergamon, Oxford, chapter Trace elements in river waters, pp. 225-272.
- Galloway, J. N. (2001), 'Acidification of the world: natural and anthropogenic', *Water, Air and Soil Pollution* 130, 17-24.
- Garrels, R. & Mackenzie, F. (1971), *Evolution of sedimentary rocks*, Norton, New York.
- Georgievsky, A. (1888), 'K voprosu o podzole', *Materialy po izucheniyu russkikh pochv*, 4.

-
- Giesler, R.; Ilvesniemi, H.; Nyberg, L.; van Hees, P.; Starr, M.; Bishop, K.; Kareinen, T. & Lundström, U. (2000), 'Distribution and mobilization of Al, Fe and Si in three podzolic soil profiles in relation to the humus layer', *Geoderma* 94, 249-263.
- Gimpel, J.; Zhang, H.; Davison, W. & Edwards, A. (2003), 'In situ trace metal speciation in lake surface waters using DGT, dialysis, and filtration', *Environ. Sci. Technol.* 37(1), 138-146.
- Gislason, S. R.; Arnorsson, S. & Armannsson, H. (1996), 'Chemical weathering of basalt in Southwest Iceland; effects of runoff, age of rocks and vegetative/glacial cover', *American Journal of Science* 296, 837-907.
- Glinka, K. (1932), *Pochvovedenie*, Moscow-Leningrad: Selkhozgiz.
- Goldstein, S.; O'Nions, R. & Hamilton, P. (1984), 'A Sm-Nd study of atmospheric dusts and particulates from major river system', *Earth Planet. Sci. Lett.* 70, 221-236.
- Grard, A.; François, L.; Dessert, C.; Dupré, B. & Goddérat, Y. (2005), 'Basaltic volcanism and mass extinction at the Permo-Triassic boundary: Environmental impact and modeling of the global carbon cycle', *Earth Planet. Sci. Lett.* 234(1-2), 207-221.
- Guieu, C.; Huang, W.; Martin, J. & Yong, Y. (1996), 'Outflow of trace metals into the Laptev Sea by the Lena River', *Mar. Chem.* 53, 255-267.
- Guo, L.; Hunt, B. J. & Santschi, P. H. (2001), 'Ultrafiltration behavior of major ions (Na, Ca, Mg, F, Cl, and SO₄) in natural waters', *Wat. Res.* 35(6), 1500-1508.
- Guo, L. & Santschi, P. H. (1996), 'A critical evaluation of the cross-flow ultrafiltration technique for sampling colloidal organic carbon in seawater', *Mar. Chem.* 55(1-2), 113-127.
- Guo, L.; Semiletov, I. & Gustafsson, O. et al. (2004), 'Characterization of Siberian Arctic coastal sediments: Implications for terrestrial organic carbon export', *Global Biogeochem. Cycles* 18, 1-11.
- Gustafsson, J., 'A Windows version of MINTEQA2',
<http://www.lwr.kth.se/English/OurSoftware/vminteq/index.htm>.
- Gustafsson, J. (1999), 'WinHumicV for Win95/98/NT
(<http://amov.ce.kth.se/people/gustafjp/winhumicv.htm>)'.
- Gustafsson, O. & Gschwend, P. M. (1997), 'Aquatic colloids: Concepts, definitions, and current challenges', *Limnol. Oceanogr.* 42(3), 519-528.
- Gustafsson, O.; Widerlund, A.; Andersson, P. S.; Ingri, J.; Roos, P. & Ledin, A. (2000), 'Colloid dynamics and transport of major elements through a boreal river – brackish bay mixing zone', *Mar. Chem.* 71, 1-21.

-
- Hättestrand, C. (1997), Ribbed moraines in Sweden-distribution pattern and paleoglaciological implications. *Sediment. Geol.* 111, 41-56.
- Hoffman, M. R.; Yost, E. C.; Eisenreich, S. J. & Maier, W. J. (1981), 'Characterization of soluble and colloidal-phase metal complexes in river water by ultrafiltration. A mass-balance approach', *Environ. Sci. Technol.* 15(6), 655-661.
- Hoffmann, S. R.; Shafer, M. M.; Babiarz, C. L. & Armstrong, D. E. (2000), 'A critical evaluation of tangential-flow ultrafiltration for trace metal studies in freshwater systems. 1. Organic carbon', *Environ. Sci. Technol.* 34, 3420-3427.
- Hölemann, J.; Schirmacher, M. & Prange, A. (2005), 'Seasonal variability of trace metals in the Lena River and the southeastern Laptev Sea: Impact of the spring freshet', *Global and Planetary Change* 48, 112-125.
- Ingri, J. & Widerlund, A. (1994), 'Uptake of alkali and alkaline-earth elements on suspended iron and manganese in the Kalix River, northern Sweden', *Geochim. Cosmochim. Acta* 58(24), 5433-5442.
- Ingri, J.; Torssander, P.; Andersson, P. S.; Morth, C. & Kusakabe, M. (1997), 'Hydrogeochemistry of sulfur isotopes in the Kalix River catchment, northern Sweden', *Appl. Geochem.* 12, 483-496.
- Ingri, J.; Widerlund, A.; Land, M.; Gustafsson, O.; Andersson, P. S. & Öhlander, B. (2000), 'Temporal variations in the fractionation of the rare earth elements in a boreal river; the role of colloidal particles', *Chem. Geol.* 166, 23-45.
- Ingri, J.; Widerlund, A. & Land, M. (2005), 'Geochemistry of major elements in a pristine boreal river system; Hydrological compartments and flow paths', *Aquat. Geochem.* 11, 57-88.
- Ingri, J.; Malinovsky, D.; Rodushkin, I.; Baxter, D. C.; Widerlund, A.; Andersson, P.; Gustafsson, O.; Forsling, W. & Öhlander, B. (2006), 'Iron isotope fractionation in river colloidal matter', *Earth Planet. Sci. Lett.* 245, 792-798.
- Jacobsen, S. B. & Wasserburg, G. (1980), 'Sm-Nd isotopic evolution of chondrites', *Earth Planet. Sci. Lett.* 50(1), 139-155.
- Johannesson, K. H.; Tang, J.; Daniels, J. M.; Bounds, W. J. & Burdige, D. J. (2004), 'Rare earth element concentrations and speciation in organic-rich blackwaters of the Great Dismal Swamp, Virginia, USA', *Chem. Geol.* 209, 271-294.
- Kempton, P. D.; Downes, H.; Neymark, L. A.; Wartho, J. A.; Zartman, R. E. & Sharkov, E. V. (2001), 'Garnet granulite xenoliths from the northern Baltic Shield – the underplated lower crust of a paleoproterozoic large igneous province?', *J. Petrol.* 42(4), 731-763.
- Kharkar, D.; Turekian, K. & Bertine, K. (1968), 'Stream supply of dissolved silver, molybdenum, antimony, selenium, chromium, cobalt, rubidium and cesium to the oceans', *Geochim. Cosmochim. Acta* 32(3), 285-298.

-
- Kinniburgh, D. G.; van Riemsdijk, W. H.; Koopal, L. K.; Borkovec, M.; Benedetti, M. F. & Avena, M. J. (1999), 'Ion binding to natural organic matter: competition, heterogeneity, stoichiometry and thermodynamic consistency', *Colloids and Surfaces. A: Physicochemical and Engineering Aspects* 151, 147-166.
- Klyunin, S.; Grokhovskaya, T.; Zakharov, A. & Solov'eva, T. (1994), 'Geology and platinum-bearing potential of the Olanga group of massifs, Northern Karelia', *Geology and genesis of PGE deposits*, Nauka, Moscow, 111-126.
- Köppen, W.P. (1931), *Grundriss der Klimakunde*, Walter de Gruyter, 2nd ed., Berlin.
- Koptev-Dvornikov, E.; Kireev, B.; Pchelintseva, N. & Khvorov, D. (2001), 'Distribution of cumulative mineral assemblages, major and trace elements over the vertical section of the Kivakka intrusion, Olanga group of intrusions, Northern Karelia', *Petrology* 9(1), 3-27.
- Kulikov, V. & Kulikova, V. (1982), 'On the summary section of the early Precambrian of the Vetreny belt (in Russian)', *Geology and Stratigraphy of the Karelian Precambrian Rocks*. Petrozavodsk, Year Book Information, 21-26.
- Kulikov, V. (1988), 'High-magnesian volcanism in the early Proterozoic', *Komatiites and High-Magnesian Volcanics in the Early Precambrian of the Baltic Shield* (ed. O. A. Bogatikov). Nauka, 20-88.
- Kulikov, V. (1999), 'Komatititic Basalts of the Vetreny Belt (Karel. Nauch. Tsentr, Petrozavodsk) (in Russian)', *Selected Works of the Karelian Scientific Center of Russian Academy of Sciences*, 60-61.
- Kulikov, V.; Kulikova, V.; Bychkova, Y. & Zudin, A. (2003), 'Sumiiskii riftovyi vulkanizm paleoproterozooya yugo-vostochnoi chasti Karel'skogo kratona', *Materialy II Vserossiiskogo simpoziuma po vulkanologii i paleovulkanologii "Vulkanizm i geodinamika"*, Ekaterinburg, 99-104.
- Kulikov, V.; Bychkova, Y.; Kulikova, V.; Koptev-Dvornikov, E. & Zudin, A. (2005), 'Role of deep-seated differentiation in formation of Paleoproterozoic Sinegorie lava plateau of komatiite basalts, southeastern Fennoscandia', *Petrology* 13(5), 469-488.
- Kulikova, V. V. & Kulikov, V. S. (1981), 'New Data on Archean Peridotitic Komatiites in East Karelia', *Dokl. Akad. Nauk SSSR* 259(3), 693-697.
- Kump, L. R.; Brantley, S. L. & Arthur, M. A. (2000), 'Chemical weathering, atmospheric CO₂, and climate', *Annu. Rev. Earth Planet. Sci. Lett.* 28, 611-667.
- Land, M. & Öhlander, B. (1997), 'Seasonal variations in the geochemistry of shallow groundwater hosted in granitic till', *Chem. Geol.* 143, 205-216.
- Land, M.; Ingri, J. & Öhlander, B. (1999a), 'Past and present weathering rates in northern Sweden', *Appl. Geochem.* 14, 761-774.

-
- Land, M.; Öhlander, B.; Ingri, J. & Thunberg, J. (1999b), 'Solid speciation and fractionation of rare earth elements in a spodosol profile from northern Sweden as revealed by sequential extraction', *Chem. Geol.* 160, 121–138.
- Land, M.; Ingri, J.; Andersson, P. S. & Öhlander, B. (2000), 'Ba/Sr, Ca/Sr and $^{87}\text{Sr}/^{86}\text{Sr}$ ratios in soil water and groundwater: implications for relative contributions to stream water discharge', *Appl. Geochem.* 15, 311-325.
- Land, M. & Öhlander, B. (2000), 'Chemical weathering rates, erosion rates and mobility of major and trace elements in a boreal granitic till', *Aquat. Geochem.* 6, 435–460.
- Land, M.; Thunberg, J. & Öhlander, B. (2002), 'Trace metal occurrence in a mineralised and a non-mineralised spodosol in northern Sweden', *J. Geochem. Explor.* 75, 71–91.
- Laudon, H.; Köhler, S. & Buffam, I. (2004), 'Seasonal TOC export from seven boreal catchments in northern Sweden', *Aquat. Sci.* 66, 223-230.
- Lavrov, M. (1979), 'Ultramafics and layered peridotite-gabbro-norite intrusions in the Precambrian of Northern Karelia (in Russian)', Nauka, Leningrad.
- Lesovaya, S.; Goryachkin, S.; Pogozhev, E.; Polekhovsky, Y.; Zavarzin, A. & Zavarzina, A. (2008), 'Soils on hard rocks in the Northwest of Russia: Chemical and mineralogical properties, genesis and classification problems', *Eurasian Soil Science* 41(4), 363-376.
- Lobach-Zhuchenko, S.; Levchenkov, O.; Cherulaev, V. & Krylov, I. (1986), 'Geological evolution of the Karelian granite-greenstone terrain', *Precambrian Res.* 33(1-3), 45-65.
- Lobach-Zhuchenko, S.; Chekulayev, V.; Sergeev, S.; Levchenkov, O. & Krylov, I. (1993), 'Archaeon rocks from southeastern Karelia (Karelian granite greenstone terrain)', *Precambrian Res.* 62(4), 375-397.
- Lobach-Zhuchenko, S.; Arrestova, N.; Chekulaev, V.; Levsky, L.; Bogomolov, E. & Krylov, I. (1998), 'Geochemistry and petrology of 2.40-2.45 Ga magmatic rocks in the north-western Belomorian Belt, Fennoscandian Shield, Russia', *Precambrian Res.* 92, 223-250.
- Louvat, P. & Allègre, C. J. (1997), 'Present denudation rates on the island of Réunion determined by river geochemistry: Basalt weathering and mass budget between chemical and mechanical erosions', *Geochim. Cosmochim. Acta* 61(17), 3645-3669.
- Louvat, P. & Allègre, C. J. (1998), 'Riverine erosion rates on Sao Miguel volcanic island, Azores archipelago', *Chem. Geol.* 148(3-4), 177-200.
- Lozovik, P. & Potapova, I. (2006), 'Input of chemical substances with atmospheric precipitation onto the territory of Karelia', *Water Resour.* 33(1), 104-111.

-
- Ludwig, W.; Amiotte-Suchet, P.; Munhoven, G. & Probst, J. (1998), 'Atmospheric CO₂ consumption by continental erosion: present-day controls and implications for the last glacial maximum', *Global and Planetary Change* 16-17, 107-120.
- Lundström, U. & Öhman, L. (1990), 'Dissolution of feldspars in the presence of natural, organic solutes', *European Journal of Soil Science* 41(3), 359-369.
- Lundström, U.S. (1993), The role of organic acids in soil solution chemistry in a podzolized soil. *J. Soil Sci.* 44, 121-133.
- Lundström, U. S.; van Breemen, N. & Bain, D. (2000a), 'The podzolization process. A review.', *Geoderma* 94, 91-107.
- Lundström, U.; van Breemen, N.; Bain, D.; van Hees, P.; Giesler, R.; Gustafsson, J.; Ilvesniemi, H.; Karlton, E.; Melkerud, P.; Olsson, M.; Riise, G.; Wahlberg, O.; Bergelin, A.; Bishop, K.; Finlay, R.; Jongmans, A.; Magnusson, T.; Mannerkoski, H.; Nordgren, A.; Nyberg, L.; Starr, M. & Strand, L. T. (2000b), 'Advances in understanding the podzolization process resulting from a multidisciplinary study of three coniferous forest soils in the Nordic Countries', *Geoderma* 94, 335-353.
- Maksimova, M. (1967), 'Inorganic and organic composition of major ions in rivers of Karelian coast of the White Sea (in Russian)', *Gidrobiologicheskie issledovaniya na Karelskom poberezhie Belogo morya. Nauka, Leningrad*, 9-20.
- Martin, J. & Whitfield, M. (1983), In: *Trace metals in Sea Water*, Plenum, New-York, chapter The significance of the river input of chemical elements to the oceans, pp. 265-296.
- Martin, J.; Guan, D.; Elbaz-Poulichet, F.; Thomas, A. & Gordeev, V. (1993), 'Preliminary assessment of the distributions of some trace elements (As, Cd, Cu, Fe, Ni, Pb and Zn) in a pristine aquatic environment: the Lena River estuary (Russia)', *Mar. Chem.* 43, 185-199.
- Melkerud, P.; Bain, D.; Jongmans, A. & Tarvainen, T. (2000), 'Chemical, mineralogical and morphological characterization of three podzols developed on glacial deposits in Northern Europe', *Geoderma* 94, 125-148.
- Meybeck, M. (1987), 'Global chemical weathering of surficial rocks estimated from river dissolved loads', *Am. J. Sci.* 287(5), 401-428.
- Millot, R.; Gaillardet, J.; Dupré, B. & Allègre, C. J. (2002), 'The global control of silicate weathering rates and the coupling with physical erosion: new insights from rivers of the Canadian Shield', *Earth Planet. Sci. Lett.* 196, 83-98.
- Millot, R.; Gaillardet, J.; Dupré, B. & Allègre, C. J. (2003), 'Northern latitude chemical weathering rates: Clues from the Mackenzie River Basin, Canada', *Geochim. Cosmochim. Acta* 67(7), 1305-1329.

-
- Milne, C. J.; Kinniburgh, D. G. & Tipping, E. (2001), 'Generic NICA-Donnan model parameters for proton binding by humic substances', *Environ. Sci. Technol.* 35(10), 2049-2059.
- Milne, C. J.; Kinniburgh, D. G.; van Riemsdijk, W. H. & Tipping, E. (2003), 'Generic NICA-Donnan model parameters for metal-ion binding by humic substances', *Environ. Sci. Technol.* 37(5), 958-971.
- Moiseenko, T. (1995), 'Critical loads of SO₄ for surface waters in the Kola region of Russia', *Water, Air and Soil Pollution* 85, 469-473.
- Mokma, D.; Yli-Halla, M. & Lindqvist, K. (2004), 'Podzol formation in sandy soils of Finland', *Geoderma* 120, 259-272.
- Moran, S. & Woods, W. (1997), 'Cd, Cr, Cu, Ni and Pb in the water column and sediments of the Ob-Irtysh Rivers, Russia', *Mar. Poll. Bull.* 35, 270-279.
- Muir, A. (1961), 'The podzol and podzolic soils', *Adv. Agron.* 13, 1-56.
- Murashkina, M.; Southard, R. & Pettygrove, G. (2007), 'Silt and fine sand fractions dominate K fixation in soils derived from granitic alluvium of the San Joaquin Valley, California', *Geoderma* 141, 283-293.
- Mylon, S.; Twining, B.; Fisher, N. & Benoit, G. (2003), 'Relating the speciation of Cd, Cu, and Pb in two Connecticut rivers with their uptake in algae', *Environ. Sci. Technol.* 37, 1261-1267.
- Neaman, A.; Chorover, J. & Brantley, S. L. (2005), 'Implications of the evolution of organic acid moieties for basalt weathering over geological time', *Am. J. Sci.* 305, 147-185.
- Nesbitt, H. & Young, G. (1982), 'Early Proterozoic climates and plate motions inferred from major element chemistry of lutites', *Nature* 299, 715-717.
- Nolan A. L, McLaughlin M. J. and Mason S. D. (2003) Chemical speciation of Zn, Cd, Cu, and Pb in pore waters of agricultural and contaminated soils using Donnan dialysis. *Environ. Sci. Technol.* 37, 90-98.
- Oelkers, E. H. & Schott, J. (1998), 'Does organic acid adsorption affect alkali-feldspar dissolution rates?', *Chem. Geol.* 151, 235-245.
- Öhlander, B.; Ingri, J. & Ponter, C. (1991), 'Geochemistry of till weathering in the Kalix River Watershed, northern Sweden. Reports in Forest Ecology and Forest Soils, Swedish University of Agricultural Sciences', In: *Chemical Weathering Under Field Conditions* (ed. K. Rosén). Report 63, 1-18.
- Öhlander, B.; Land, M.; Ingri, J. & Widerlund, A. (1996), 'Mobility of rare earth elements during weathering of till in northern Sweden', *Appl. Geochem.* 11, 93-99.

-
- Öhlander, B.; Ingri, J.; Land, M. & Schoberg, H. (2000), 'Change of Sm-Nd isotope composition during weathering of till', *Geochim. Cosmochim. Acta* 64(5), 813-820.
- Öhlander, B.; Thunberg, J.; Land, M.; Hoglund, L. O. & Quishang, H. (2003), 'Redistribution of trace metals in a mineralized spodosol due to weathering, Liikavaara, northern Sweden', *Appl. Geochem.* 18, 883-899.
- Oliva, P.; Viers, J.; Dupré, B.; Fortune, J. P.; Martin, F.; Braun, J.; Nahon, D. & Robain, H. (1999), 'The effect of organic matter on chemical weathering: Study of a small tropical watershed: Nsimi-Zoétélé site, Cameroon', *Geochim. Cosmochim. Acta* 63(23/24), 4013-4035.
- Oliva, P.; Dupré, B.; Martin, F. & Viers, J. (2004), 'The role of trace minerals in chemical weathering in a high-elevation granitic watershed (Estibère, France): Chemical and mineralogical evidence', *Geochim. Cosmochim. Acta* 68(10), 2223-2244.
- Oliver, B.; Thurman, E. & Malcolm, R. (1983), 'The contribution of humic substances to the acidity of colored natural waters', *Geochim. Cosmochim. Acta* 47, 2031-2035.
- Olivié-Lauquet, G.; Allard, T.; Benedetti, M. & Muller, J. (1999), 'Chemical distribution of trivalent iron in riverine material from a tropical ecosystem: A quantitative EPR study', *Wat. Res.* 33(11), 2726-2734.
- Olivié-Lauquet, G.; Allard, T.; Bertaux, J. & Muller, J. (2000), 'Crystal chemistry of suspended matter in a tropical hydrosystem, Nyong basin (Cameroon, Africa)', *Chem. Geol.* 170(1-4), 113-131.
- Olsson, M. T. & Melkerud, P. (2000), 'Weathering in three podzolized pedons on glacial deposits in northern Sweden and central Finland', *Geoderma* 94, 149-161.
- Orr, J.; Fabry, V.; Aumont, O.; Bopp, L.; Doney, S. & et al., R. F. (2005), 'Anthropogenic ocean acidification over the twenty-first century and its impact on calcifying organisms', *Nature* 437, 681-686.
- Pédrot, M.; Dia, A.; Davranche, M.; Coz, M. B.; Henin, O. & Gruau, G. (2008), 'Insights into colloid-mediated trace element release at the soil/water interface', *J. Colloid Interface Sci.* 325, 187-197.
- Perelman, A. (1974), 'Pochva kak biokosnaya sistema zemnoi kory', *Trudy X Mezhdunarodnogo kongressa pochvovedov. Moscow: Nauka* 6.
- Peuraniemi, V. (1982), Geochemistry of till and mode of occurrence of metals in some moraine types in Finland. *Geol. Surv. Fin. Bull.* 322, 75.
- Peuraniemi, V.; Aario, R. & Pulkkinen, P. (1997), 'Mineralogy and geochemistry of the clay fraction of till in northern Finland', *Sedimentary Geology* 111, 313-327.

-
- Pham, M. H. & Garnier, J. (1998), 'Distribution of trace elements associated with dissolved compounds (<0.45 µm – 1 nm) in freshwater using coupled (frontal cascade) ultrafiltration and chromatographic separations', *Environ. Sci. Technol.* 32(4), 440-449.
- Pokrovsky, O. & Schott, J. (2002), 'Iron colloids/organic matter associated transport of major and trace elements in small boreal rivers and their estuaries (NW Russia)', *Chem. Geol.* 190, 141-179.
- Pokrovsky, O. S.; Dupré, B. & Schott, J. (2005a), 'Fe-Al-organic colloids control of trace elements in peat soil solutions', *Aquat. Geochem.* 11, 241–278.
- Pokrovsky, O.; Schott, J.; Kudryavtsev, D. I. & Dupré, B. (2005b), 'Basalt weathering in Central Siberia under permafrost conditions', *Geochim. Cosmochim. Acta* 69(24), 5659-5680.
- Pokrovsky, O. S.; Schott, J. & Dupré, B. (2006a), 'Trace element fractionation and transport in boreal rivers and soil porewaters of permafrost-dominated basaltic terrain in Central Siberia', *Geochim. Cosmochim. Acta* 70, 3239–3260.
- Pokrovsky, O.; Schott, J. & Dupré, B. (2006b), 'Basalt weathering and trace elements migration in the boreal Arctic zone', *J. Geochem. Explor.* 88, 304-307.
- Ponomareva, V. (1964), *Teoria podzoloobrazovatel'nogo processa (Theory of the podzol-formation process)*, M.-L.: Nauka.
- Ponter, C.; Ingri, J. & Bostrom, K. (1992), 'Geochemistry of manganese in the Kalix River, northern Sweden', *Geochim. Cosmochim. Acta* 56, 1485-1494.
- Pontér, C.; Ingri, J.; Burmann, J. & Bostrom, K. (1990), 'Temporal variations in dissolved and suspended iron and manganese in the Kalix River, northern Sweden', *Chem. Geol.* 81, 121-131.
- Porcelli, D.; Andersson, P. S.; Wasserburg, G. J.; Ingri, J. & Baskaran, M. (1997), 'The importance of colloids and mires for the transport of uranium isotopes through the Kalix River watershed and Baltic Sea', *Geochim. Cosmochim. Acta* 61(19), 4095-411.
- Pourret, O.; Davranche, M.; Gruau, G. & Dia, A. (2007), 'Organic complexation of rare earth elements in natural waters: Evaluating model calculations from ultrafiltration data', *Geochim. Cosmochim. Acta* 71, 2718-2735.
- Prado, A. G.; Torres, J. D.; Martins, P. C.; Pertusatti, J.; Bolzon, L. B. & Faria, E. A. (2006), 'Studies on copper(II)- and zinc(II)-mixed ligand complexes of humic acid', *Journal of Hazardous Materials* B136, 585-588.
- Puchtel, I.; Hofmann, A.; Mezger, K.; Shchipansky, A.; Kulikov, V. & Kulikova, V. (1996), 'Petrology of a 2.41 Ga remarkably fresh komatiitic basalt lava lake in Lion Hills, central Vetreny Belt, Baltic Shield', *Contrib. Mineral. Petrol.* 124(3-4), 273-290.

-
- Puchtel, I. S.; Haase, K. M.; Hofmann, A. W.; Chauvel, C.; Kulikov, V. S.; Garbe-Schonberg, C. & Nemchin, A. A. (1997), 'Petrology and geochemistry of crustally contaminated komatiitic basalts from the Vetreney Belt, southeastern Baltic Shield: Evidence for an early Proterozoic mantle plume beneath rifted Archean continental lithosphere', *Geochim. Cosmochim. Acta* 61(6), 1205-1222.
- Pullin, M. J. & Cabaniss, S. E. (2003), 'The effects of pH, ionic strength, and iron-fulvic acid interactions on the kinetics of non-photochemical iron transformations. I. Iron(II) oxidation and iron(III) colloid formation', *Geochim. Cosmochim. Acta* 67(21), 4067-4077.
- Rad, S.; Louvat, P.; Gorge, C.; Gaillardet, J. & Allègre, C. J. (2006), 'River dissolved and solid loads in the Lesser Antilles: New insight into basalt weathering processes', *J. Geochem. Explor.* 88, 308-312.
- Reimann, C.; de Caritat, P.; Halleraker, J. H.; Volden, T.; Ayras, M.; Niskavaara, H.; Chekushins, V. A. & Pavlovs, V. A. (1997), 'Rainwater composition in eight arctic catchments in Northern Europe (Finland, Norway and Russia)', *Atmos. Environ.* 31(2), 159-170.
- Reimann, C. & Melezhik, V. (2001), 'Metallogenic provinces, geochemical provinces and regional geology – what causes large-scale patterns in low density geochemical maps of the C-horizon of podzols in Arctic Europe?', *Appl. Geochem.* 16(7-8), 963-983.
- Remaury, M.; Oliva, P.; Guillet, B.; Martin, F.; Toutain, F.; Dagnac, J.; Belet, J.; Dupré, B. & Gauquelin, T. (2002), 'Nature and genesis of spodic horizons characterized by inverted color and organic content in a subalpine podzolic soil (Pyrenees Mountains, France)', *Bulletin de la Société Géologique de France* 172(1), 77-86.
- Reuss, J.; Cosby, B. & Wright, R. (1987), 'Chemical processes governing soil and water acidification', *Nature* 329, 27-32.
- Revyako, N.; Bychkova, Y. & Kostitsyn, Y. (2007), 'Isotope evidence of the interaction of basic melt with crust rocks on the example of Kivakka layered intrusion (Karelia) (in Russian)', *Proceeding of the International conference "Ultrabasic-basic complexes of fold regions"*. Irkutsk, 2007, 487-490.
- Righi, D., Chauvel, A. (1987), *Podzols and Podzolization*. Assoc. Franc. Etude Sol. INRA, Plaisir et Paris, Paris.
- Ryabchikov, I.; Suddaby, P.; Girnis, A.; Kulikov, V.; Kulikova, V. & Bogatikov, O. (1988), 'Trace-element geochemistry of Archaean and Proterozoic rocks from eastern Karelia, USSR', *Lithos* 21, 183-194.
- Salminen, R.; Gregorauskiene, V. & Tarvainen, T. (2008, in press), 'The normative mineralogy of 10 soil profiles in Fennoscandia and north-western Russia', *Appl. Geochem..*

-
- Sarala, P. (2005), 'Till geochemistry in the ribbed moraine area of Peräpohjola, Finland', *Appl. Geochem.* 20, 1714-1736.
- Sawhney, B. L. (1989), *Minerals in soil environments*, Soil Science Society of America, chapter 16: Interstratification in layer silicates, pp. 789-828.
- Sayre, A. (1994), *Taiga*, New York: Twenty-First Century Books.
- Schroeder, P. A.; Melear, N. D.; West, L. T. & Hamilton, D. A. (2000), 'Meta-gabbro weathering in the Georgia Piedmont, USA: implications for global silicate weathering rates', *Chem. Geol.* 163, 235-245.
- Schweda, P.; Araujo, P. D. R. & Sjoeberg, L. (1991), 'Soil chemistry, clay mineralogy and noncrystalline phases in soil profiles from southern Sweden and Gårdsjön.', In: Rosén, K. (Ed.), *Chemical weathering under field conditions*, Reports in Forest Ecology and Forest Soils. Swedish University of Agricultural Sciences Report 63, 49-62.
- Seip, H. M. (1986), 'Surface water acidification', *Nature* 322, 118.
- Semenov, V.; Koptev-Dvornikov, E.; Berkovskii, A.; Kireev, B.; Pchelintseva, N. & Vasil'eva, M. (1995), 'Layered troctolite-gabbro-norite Tsipringa intrusion, Northern Karelia: Geologic structure and petrology', *Petrology* 3(6), 588-610
- Serreze, M.; Bromwich, D.; Clark, M.; Etringer, A.; Zhang, T. & Lammers, R. (2002), 'Large-scale hydro-climatology of the terrestrial Arctic drainage system', *J. Geophys. Res. - Atmospheres* 108(D2), 1-28.
- Shmygalev, V. (1968), 'Mafic and ultramafic intrusions of the Olanga group', *Vulkanicheskie i giperbazitovye kompleksy proterozoika Karelii (Proterozoic volcanic and ultramafic complexes of Karelia)*, Petrozavodsk 1, 209-219.
- Sholkovitz, E. (1976), 'Flocculation of dissolved organic and inorganic matter during the mixing of river water and seawater', *Geochim. Cosmochim. Acta* 40(7), 831-845.
- Sholkovitz, E. R. (1995), 'The aquatic chemistry of rare earth elements in rivers and estuaries', *Aquat. Geochem.* 1, 1-34.
- Sigg, L.; Black, F.; Buffle, J.; Cao, J.; Cleven, R.; Davison, W.; Galceran, J.; Gunkel, P.; Kalis, E.; Kistler, D.; Martin, M.; Noël, S.; Nur, Y.; Odzak, N.; Puy, J.; Riemsdijk, W. V.; Temminghoff, E.; Tercier-Waeber, M.; Toepperwien, S.; Town, R. M.; Unsworth, E.; Warnken, K. W.; Weng, L.; Xue, H. & Zhang, H. (2006), 'Comparison of analytical techniques for dynamic trace metal speciation in natural freshwaters', *Environ. Sci. Technol.* 40(6), 1934-1941.
- Skjelkvale, B. L.; Stoddard, J. L. & Andersen, T. (2001), 'Trends in surface water acidification in Europe and North America (1989-1998)', *Water, Air and Soil Pollution* 130, 787-792.

-
- Skjelkvale, B.; Stoddard, J.; Jeffries, D.; Tørseth, K.; sen, T. H.; Bowman, J.; Mannio, J.; Monteith, D.; Mosello, R.; Rogora, M.; Rzychon, D.; Vesely, J.; Wieting, J.; Wilander, A. & Worsztynowicz, A. (2005), 'Regional scale evidence for improvements in surface water chemistry 1990-2001', *Environmental Pollution* 137, 165-176.
- Slaveykova, V. & Wilkinson, K. (2002), 'Physicochemical aspects of lead bioaccumulation by Chlorella vulgaris', *Environ. Sci. Technol.* 36, 969-975.
- Starr, M.; Lindroos, A.; Ukonmaanaho, L.; Tarvainen, T. & Tanskanen, H. (2003), 'Weathering release of heavy metals from soil in comparison to deposition, litterfall and leaching fluxes in a remote, boreal coniferous forest', *Appl. Geochem.* 18, 607-613.
- Starr, M. & Lindroos, A. (2006), 'Changes in the rate of release of Ca and Mg and normative mineralogy due to weathering along a 5300-year chronosequence of boreal forest soils', *Geoderma* 133, 269-280.
- State Geological Map of Russian Federation, 2001. Sheet Q-(35)-37. In: Bogdanov, Yu.B. (Ed.), Explication Note. Ministry of Natural Resources, St-Petersbourg. VSEGEI.
- Stefansson, A. & Gislason, S. R. (2001), 'Chemical weathering of basalts, Southwest Iceland: effect of rock crystallinity and secondary minerals on chemical fluxes to the ocean', *Am. J. Sci.* 301, 513-556.
- Stevenson, F. & Chen, Y. (1991), 'Stability constants of copper(II)-humate complexes determined by modified potentiometric titration', *Soil Science Society of America Journal* 55, 1586-1591.
- Stumm, W. & Morgan, J. (1996), *Aquatic Chemistry*, Wiley Intersciences.
- Taylor, S. & McLennan, S. (1985), *The continental crust: its composition and evolution*, Blackwell Scientific Publications, Oxford.
- Thiede, J.; Bauch, H. A.; Hjort, C. & Mangerud, J. (2001), 'The late Quaternary stratigraphy and environments of northern Eurasia and the adjacent Arctic seas - new contributions from QUEEN', *Global and Planetary Change* 31(1-4), vii-x.
- Thorn, C. E.; Dixon, J. C.; Darmody, R. G. & Allen, C. E. (2006), 'A 10-year record of the weathering rates of surficial pebbles in Kärkevagge, Swedish Lapland', *Catena* 65, 272-278.
- Thurman, E. M. (1985), *Organic geochemistry of natural waters*, Martinus Nijhoff/Dr W. Junk Publishers: Boston.
- Tipping, E. & Hurley, M. (1992), 'A unifying model of cation binding by humic substances', *Geochim. Cosmochim. Acta* 56(10), 3627-3641.

-
- Tipping, E. (1994), 'WHAM - A chemical equilibrium model and computer code for waters, sediments, and soils incorporating a discrete site/electrostatic model of ion-binding by humic substances', *Computers & Geosciences* 20(6), 973-1023.
- Tipping, E. (1996), 'CHUM: a hydrochemical model for upland catchments', *Journal of Hydrology* 174, 305-330.
- Tipping, E. (1998), 'Humic ion-binding model VI: an improved description of the interactions of protons and metal ions with humic substances', *Aquatic Geochemistry* 4, 3-48.
- Tipping, E. (2002), *Cation Binding by Humic Substances*, Vol. 12, Cambridge University Press.
- Trias, J.; Jarlier, V. & Benz, R. (1992), 'Porins in the cell wall of mycobacteria', *Science* 258(5087), 1479-1481.
- Tyler, G. (2004), 'Vertical distribution of major, minor, and rare elements in a Haplic Podzol', *Geoderma* 119, 277-290.
- Unsworth, E. R.; Warnken, K. W.; Zhang, H.; Davison, W.; Black, F.; Buffle, J.; Cao, J.; Cleven, R.; Galceran, J.; Gunkel, P.; Kalis, E.; Kistler, D.; Leeuwen, H. P. V.; Martin, M.; Noël, S.; Nur, Y.; Odzak, N.; Puy, J.; Riemsdijk, W. V.; Sigg, L.; Temminghoff, E.; Tercier-Waeber, M.; Toepperwien, S.; Town, R. M.; Weng, L. & Xue, H. (2006), 'Model predictions of metal speciation in freshwaters compared to measurements by in situ techniques', *Environ. Sci. Technol.* 40(6), 1942-1949.
- Ure, A. & Davidson, C. (1995), *Chemical speciation in the environment*, Blackie Academic Professional, London, UK.
- Vasiliev, M. V. (2006), 'Osobennosti intruzivnyh sistem Vetrenogo poyasa (in Russian)', Master's thesis, Geologicheskii f-t MGU.
- Vasyukova, E.; Pokrovsky, O.; Viers, J.; Oliva, P.; Dupré, B.; Martin, F. & Candaudap, F., 'Trace elements in organic- and iron-rich surficial fluids of boreal zone: Assessing colloidal forms via dialysis and ultrafiltration', *Geochim. Cosmochim. Acta* (submitted).
- Viers, J.; Dupré, B.; Polve, M.; Dandurand, J. & Braun, J. (1997), 'Chemical weathering in the drainage basin of a tropical watershed (Nsimi-Zoetele site, Cameroon): comparison between organic-poor and organic-rich waters', *Chem. Geol.* 140, 181-206.
- Viers, J.; Dupré, B.; Braun, J.; Deberdt, S.; Angeletti, B.; Ngoupayou, J. N. & Michard, A. (2000), 'Major and trace element abundances, and strontium isotopes in the Nyong basin rivers (Cameroon): constraints on chemical weathering processes and elements transport mechanisms in humid tropical environments', *Chemical Geology* 169, 211-241.

Viers, J.; Barroux, G.; Pinelli, M.; Seyler, P.; Oliva, P.; Dupré, B. & Boaventura, G. R. (2005), 'The influence of the Amazonian floodplain ecosystems on the trace element dynamics of the Amazon River mainstem (Brazil)', *Sci. Total Environ.* 339, 219-232.

Viers, J.; Oliva, P.; Dandurand, J.; Dupré, B. & Gaillardet, J. (2007), *In Surface and Ground Water, Weathering, and Soils (ed. J.I. Drever)*. Vol.5, *Treatise on Geochemistry*, Elsevier-Pergamon, Oxford, chapter Chemical weathering rates, CO₂ consumption, and control parameters deduced from the chemical composition of rivers, pp. 1-25.

Viers, J.; Dupré, B. & Gaillardet, J. (2008), 'Chemical composition of world rivers suspended sediments: new insights from a new database', *submitted to Sci. Total Environ.*

Wikipedia web-site: <http://fr.wikipedia.org/wiki/Image:Taiga.png>

World Reference Base for soil Resources (2006), IUSS Working Group WRB, FAO.

Yeghicheyan, D.; J., Carignan; M., Valladon; M., Bouhnik Le Coz; F., Le Cornec; M., Castrec-Rouelle; M., Robert; L., Aquilina; E., Aubry; C., Churlaud; A., Dia; S., Deberdt; B., Dupré; R., Freydier; G., Gruau; O., Hénin; de Kersabiec A. M.; J., Macé; L., Marin; N., Morin; P., Petitjean & E., Serrat (2001), 'A compilation of silicon and thirty one trace elements measured in the natural river water reference material SLRS-4 (NRC-CNRC)', *Geostandards Newsletter* 25(2-3), 465-474.

Zakharova, E.; Pokrovsky, O. S.; Dupré, B. & Zaslavskaya, M. B. (2005), 'Chemical weathering of silicate rocks in Aldan Shield and Baikal Uplift: insights from long-term seasonal measurements of solute fluxes in rivers', *Chem. Geol.* 214, 223–248.

Zakharova, E.; Pokrovsky, O. S.; Dupré, B.; Gaillardet, J. & Efimova, L. (2007), 'Chemical weathering of silicate rocks in Karelia region and Kola peninsula, NW Russia: Assessing the effect of rock composition, wetlands and vegetation', *Chem. Geol.* 242, 255-277.

Zilliacus, H. (1989), 'Genesis of De Geer moraines in Finland', *Sedimentary geology* 62(2-4), 309-317.

Zhulidov, A.; Headley, J.; Robarts, R.; Nikanorov, A.; Ishenko, A. & Champ, M. (1997), 'Concentrations of Cd, Pb, Zn and Cu in pristine wetlands of the Russian Arctic', *Mar. Poll. Bull.* 35, 242-251.

LIST OF FIGURES

Fig. 1.1. Scheme describing the main matter exchange between different reservoirs (soil-rock system, vegetation, and atmosphere) of a watershed.....	19
Fig. 1.2. Distribution of mineral and organic colloids as a function of size in aquatic systems.....	23
Fig. 1.3. Schematic representation of a typical podzol soil of the boreal forest.....	29
Fig. 1.4. Geographical distribution of the taiga zone (after the Köppen-Geiger climate classification world map) corresponding to “Dfc” and “Dfd” zones	33
Fig. 1.5. Map of the White Sea with the studied Vetryny Belt paleorift zone and Kivakka intrusion zone.....	34
Fig. 2.1. Map of the studied areas Vetryny Belt and Kivakka intrusion showing soil and water sample points, and geological situation.....	48
Fig. 2.2. Representative X-ray diffractograms of soil profiles K-14 and No.15.....	65
Fig. 2.3. SEM images of minerals found in soils illustrating neo-formed material and erosion on the surface of minerals.....	66
Fig. 2.4. Photos of podzols V-4, K-14, K-37 and regosol K-29.....	67
Fig. 2.5. Ration of Chemical Index of Alteration (CIA) of soils to that of rocks for soils developed on basic rocks and on acidic rocks from Vetryny Belt and Kivakka intrusion.....	71
Fig. 2.6. Photo of a podzol (K-7) developed on granito-gneiss from the Kivakka intrusion zone.....	72
Fig. 2.7. Upper crust normalized REE patterns for soils from Kivakka intrusion, Vetryny Belt, and a mixed diagram on which E and B horizons of different soils are plotted.....	73
Fig. 2.8. Upper crust normalized extended elements patterns for soils developed on both granitic and basic rocks from the Kivakka intrusion zone and Vetryny Belt zone.....	76
Fig. 2.9. Ternary molar diagram with rock and soil composition for the studied sites...	78
Fig. 2.10. Ca/Na molar ratios vs. Mg/Na molar ratios showing different materials (soils, rocks and waters) from Kivakka intrusion and Vetryny Belt zones.....	79
Fig. 2.11. Scatter diagram of $^{87}\text{Sr}/^{86}\text{Sr}$ vs. $^{87}\text{Rb}/^{86}\text{Sr}$ for the whole set of rocks, rock minerals, soils and waters for Kivakka intrusion and Vetryny belt.....	81
Fig. 3.1. Map of the studied area showing main geomorphological regions and sampling locations in the Vetryny Belt zone, the White Sea coast and the Kivakka intrusion zone.....	105

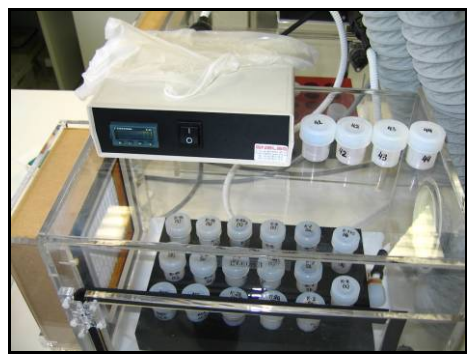
Fig. 3.2. Proportion of colloidal matter in dialysates versus filtrates.....	112
Fig. 3.3. Correlation between charge balance and OC in successive filtrates and dialysates from 2.5 μm to 1 kDa.	113
Fig. 3.4. Distribution of OC and Fe among filtrates in various pore size classes.....	114
Fig. 3.5. Correlation between Fe and OC concentrations in various filtrates.....	115
Fig. 3.6. [Fe] to [Organic Carbon] ratio in filtrates and ultrafiltrates for different samples.....	116
Fig. 3.7. Correlation between Mn and Fe concentration in various filtrates.....	117
Fig. 3.8. Cobalt and nickel correlations with organic matter and iron in 0.22 (0.45) μm filtrates for rivers draining different rocks.....	118
Fig. 3.9. Pb concentration as a function of Fe and OC concentrations in successive filtrates from 5 μm to 1 kDa.....	118
Fig. 3.10. Aluminium correlations with organic matter and iron in 0.22 (0.45) μm filtrates for rivers draining different rocks.....	119
Fig. 3.11. Al and Ga concentration as a function of Fe concentration in successive filtrates from 5 μm to 1 kDa.....	120
Fig. 3.12. Ytterbium and La correlations with organic matter and iron in 0.22 (0.45) μm filtrates for rivers draining different rocks.....	121
Fig. 3.13. Upper-crust normalized REE pattern of 0.22 (0.45) μm and 1 (10) kDa (ultra)filtrates for Ruiga river (No.9), creek over ultramafites (No.15) and swamp water (K-23).	122
Fig. 3.14. Ce and Yb concentrations as a function of Fe and OC in successive filtrates from 5 μm to 1 kDa.....	123
Fig. 3.15. Titanium-Fe correlation in 0.22 (0.45) μm filtrates for rivers draining different rocks.....	124
Fig. 3.16. Ti, Zr, Hf, and Th concentrations as a function of Fe concentration in successive filtrates from 5 μm to 1 kDa.....	124
Fig. 3.17. V and As concentration as a function of Fe concentration in successive filtrates from 5 μm to 1-10 kDa.....	125
Fig. 3.18. TE distribution between dissolved matter (< 1 kDa) and two colloidal pools (1 kDa – 10 kDa and 10 kDa – 0.22 μm) both for acidic- and basic rock-dominated catchments for Fe, Al, Ca, V, Co, La, Th and U.....	127
Fig. 3.19. Calculated proportions of organic complexes for Na, Ca, Mg, Mn, Co, Al, Ni, Zn, Cd, Fe, Pb, Cu, REEs, Th and U in four samples in 0.22 μm fraction.....	129

Fig. 4.1. Map of the studied region showing sampling points location.....	145
Fig. 4.2. Schematic representation of dialysis experiment procedure.....	147
Fig. 4.3. DOC and Fe concentrations in 0.22 µm fraction as a function of pH for seven natural waters.....	149
Fig. 4.4. Dependence of colloidal organic carbon and Fe on pH in all studied samples.....	150
Fig. 4.5. Molar [Fe] to [Organic Carbon] ratio in 0.22 µm filtrates and 1 kDa dialysates for studied samples.....	151
Fig. 4.6. Percentage of colloidal forms (1 kDa – 0.22 µm) in all samples (average)....	153
Fig. 4.7. Dependence of Fe, Mn, Ni, Cd, Cr, Cu, Y, La, Ce and U in colloidal (< 1 kDa) form on pH in seven studied samples.....	154
Fig. 4.8. Dependence of Li, Si, Ti, V, As, Rb, Sb and Cs in dissolved (< 1 kDa) form on pH in seven studied samples.....	156
Fig. 4.9. Dependence of Al and Ga in dissolved (< 1 kDa) form on pH in seven studied samples.	157
Fig. 4.10. Results of vMINTEQ speciation calculation for Ca, Mg, Sr, Ba, Mn, Co, Ni, Cd, Pb.	158
Fig. 4.11. Results of vMINTEQ speciation calculation for Al, Fe, Cu, Y, V, La, Th and U.....	160
Fig. 4.12. Results of vMINTEQ speciation calculation for Cu with adjusted stability constants of Cu-humate and Cu-fulvate complexes.....	162
Fig. 4.13. Results of vMINTEQ speciation calculation for Eu and Dy with adjusted stability constants of metal-humate and metal-fulvate complexes.....	162
Fig. 4.14. Results of vMINTEQ speciation calculation for Fe, Al, U and Th with adjusted stability constants of metal-humate and metal-fulvate complexes.....	163
Fig. 4.15. Correlation between the concentration of Fe and trace elements in colloidal fraction of studied natural waters for Al, Ti, Y, La, Ce, Hf, Th, U.....	167
Fig. 4.16. Iron-normalized TE partition coefficient K_d vs. pH for Ti, La, Th and U.....	168

LIST OF TABLES

Table 2.1. Soils and surface waters studied and their bedrock composition.....	52
Table 2.2. Chemical analysis of the bulk fraction and Rb-Sr and Sm-Nd isotope data for soils from Vetreny Belt and Kivakka layered intrusion.....	53
Table 2.3. Major, trace elements and dissolved organic carbon (DOC) concentrations, and strontium isotopic ratios ($^{87}\text{Sr}/^{86}\text{Sr}$) measured in the dissolved phase (<0.22 (0.45) μm) in river and swamp waters from Vetreny Belt and Kivakka intrusion zone.....	57
Table 2.4. Mineralogical composition of studied soils.....	64
Table 3.1. Studied samples from rivers, lakes and swamps, with their bedrock composition.....	107
Table 4.1. Surface waters studied, their bedrock and chemical composition.....	146

Annexes



ANNEXES – CONTENTS

Annex A	215
Table A-1. The chemical composition of studied altered minerals and rocks assessed from electron microprobe analysis of thin sections of basic rocks and one granite sampled in the zone of Kivakka and Vetreney Belt mafic intrusions.....	216
Table A-2. Trace elements composition for unweathered basalts from Ruiga and Goletz hills of the Vetreney Belt paleorift.....	231
Fig. A-1. Graphical representation of distribution of elements concentrations on depth along the soil profiles.....	232
 Annex B	241
Table B-1. Measured major and trace element concentrations in all filtrates and ultrafiltrates.....	242
Table B-2. Percentage of trace element distribution between dissolved and two colloidal pools for acidic- and basic rock-dominated catchments.....	249
Table B-3. Iron-normalized K_d values for trace element distribution between dissolved phase (< 1 kDa) and colloidal matter (1 kDa – 0.22 μm).....	252
 Annex C	253
Table C-1. Measured major and trace elements concentrations in filtrates (0.22 μm) and dialysates (1 kDa).....	254
Table C-2. The TE distribution between dissolved (< 1 kDa) and colloidal (1 kDa – 0.22 μm) pools for the studied waters at different pH.....	258
Table C-3. Iron-normalized K_d values for TE distribution between dissolved phase (< 1 kDa) and colloidal matter (1 kDa – 0.22 μm) in all samples at different pH.....	261

Annex A

Table A-1. The chemical composition of studied altered minerals and rocks assessed from electron microprobe analysis of thin sections of several basic rocks and one granite collected in the zone of Kivakka and Veturøy Belt mafic intrusions.

ULTRAMAFIC ROCK

Ampibole

sample	15-2-C1-19	15-2-C2-27	15-2-C3-16	15-2-C3-18	15-2-C3-19	15-2-C8-13	15-2-C9-6	average(7)	53.37
SiO ₂	57.77	43.97	57.24	55.77	55.85	47.26	55.72	0.06	33.97
TiO ₂	0	0	0.03	0.23	0	0.13	0	0.04	0.01
Al ₂ O ₃	0.1	4.85	0.62	0.79	2.4	8.78	2.48	2.86	16.08
Cr ₂ O ₃	0.03	0.24	0.03	0.03	0.03	0.06	0	0.06	0.02
Fe ₂ O ₃ (c)	3.23	18.19	5.21	5.69	4.37	8.43	4.45	7.08	6.48
FeO(c)	0.21	0	0	0	0	0	0	0.03	0.04
MnO	0.05	0.14	0.09	0.01	0.11	0.11	0.18	0.10	0.05
MgO	23.27	30.27	23.07	22.96	22.51	21.29	22.52	23.70	29.31
CaO	13.3	0.69	12.04	11.38	12.3	5.91	11.82	9.63	0.08
Na ₂ O	0.06	0.03	0	0.07	0.6	0.92	0.55	0.32	0.25
K ₂ O	0.03	0.04	0.01	0.02	0.06	2.91	0.05	0.45	0.37
NiO	0.18	0.11	0.1	0.07	0	0.1	0	0.08	0.07
H ₂ O(c)	2.2	2.13	2.2	2.17	2.19	2.1	2.19	2.17	12.52
Sum Ox%	100.43	100.66	100.64	99.19	100.42	98	99.97	99.90	99.23

Feldspar

Haematite

sample	15-2-C9-9	sample	15-2-C3-13	sample	15-2-C8-1	average(2)
SiO ₂	40.88	SiO ₂	0.02	SiO ₂	0.05	0.04
TiO ₂	0.04	TiO ₂	51.32	TiO ₂	51.99	51.66
Al ₂ O ₃	0	Al ₂ O ₃	0.44	Al ₂ O ₃	0	0.22
Cr ₂ O ₃	0.02	Cr ₂ O ₃	2.09	Cr ₂ O ₃	0.05	1.07
Fe ₂ O ₃	5.74	Fe ₂ O ₃ (c)	1.9	Fe ₂ O ₃ (c)	0.44	1.17
MgO	40.08	FeO(c)	42.84	FeO(c)	44.67	43.76
CaO	0.03	MnO	0.9	MnO	0.94	0.92
NiO	0.17	MgO	1.33	MgO	0.59	0.96
Na ₂ O	0	CaO	0	CaO	0.07	0.04
K ₂ O	12.3	ZnO	0	ZnO	0	0.00
H ₂ O(c)	12.66	NiO	0.04	NiO	0.03	0.04
Sum Ox%	99.34	12.7	99.84	Sum Ox%	100.89	99.87
An	63	61	60	61	60	60

Ilmenite

Serpentine

sample	15-2-C9-9	sample	15-2-C3-13	sample	15-2-C8-1	average(2)
SiO ₂	40.88	SiO ₂	0.02	SiO ₂	0.05	0.04
TiO ₂	0.04	TiO ₂	51.32	TiO ₂	51.99	51.66
Al ₂ O ₃	0	Al ₂ O ₃	0.44	Al ₂ O ₃	0	0.22
Cr ₂ O ₃	0.02	Cr ₂ O ₃	2.09	Cr ₂ O ₃	0.05	1.07
Fe ₂ O ₃	5.74	Fe ₂ O ₃ (c)	1.9	Fe ₂ O ₃ (c)	0.44	1.17
MgO	40.08	FeO(c)	42.84	FeO(c)	44.67	43.76
CaO	0.03	MnO	0.9	MnO	0.94	0.92
NiO	0.17	MgO	1.33	MgO	0.59	0.96
Na ₂ O	0	CaO	0	CaO	0.07	0.04
K ₂ O	12.3	ZnO	0	ZnO	0	0.00
H ₂ O(c)	12.66	NiO	0.04	NiO	0.03	0.04
Sum Ox%	99.34	12.7	99.84	Sum Ox%	100.89	99.87
An	63	61	60	61	60	60

Pyroxene

sample	15-2-C1-2	15-2-C1-3	15-2-C1-4	15-2-C1-5	15-2-C1-6	15-2-C1-7	15-2-C1-9	15-2-C1-12	15-2-C1-14	15-2-C1-15	15-2-C1-16	15-2-C1-17	15-2-C1-18	15-2-C1-20
SiO ₂	52.49	52.93	52.08	53.14	53.26	52.54	52.62	55.33	54.74	55.38	55.14	55.32	52.83	52.14
TiO ₂	0.2	0.3	0.65	0.15	0.17	0.42	0.18	0.45	0.54	0.52	0.45	0.51	0.32	0.85
Al ₂ O ₃	2.04	1.93	2.15	2.12	1.63	2.1	2.11	0.77	1.13	0.77	0.7	0.78	2.19	2.08
Cr ₂ O ₃	0.93	0.8	0.84	0.85	0.88	0.84	0.84	0.25	0.28	0.18	0.23	0.2	0.92	0.7
Fe ₂ O _{3(c)}	0.01	0	1.45	0.02	0.03	1.55	1.1	0.54	0.35	0	0	0.68	0	0.52
FeO(c)	5.83	6.38	5.35	6.78	6.59	5.13	5.13	11.47	11.58	11.72	11.78	11.77	5.7	5.65
MnO	0.23	0.2	0.21	0.16	0.22	0.22	0.17	0.33	0.25	0.25	0.36	0.25	0.28	0.2
MgO	17.83	18.44	17.45	18.85	18.01	17.51	18.36	29.52	29.16	29.22	29.46	17.6	16.64	
CaO	18.74	18.25	19.61	17.82	18.77	19.99	19	1.68	1.67	1.66	1.59	1.6	19.66	20.57
Na ₂ O	0.23	0.13	0.23	0.06	0.17	0.22	0.15	0	0	0	0	0	0.09	0.26
K ₂ O	0	0	0.01	0	0.04	0	0	0	0	0	0	0.01	0	0.02
Sum Ox%	98.55	99.37	100.03	99.97	99.77	100.53	99.67	100.34	99.7	99.56	99.47	100.58	99.6	99.62
sample	15-2-C2-1	15-2-C2-2	15-2-C2-3	15-2-C2-4	15-2-C2-5	15-2-C2-6	15-2-C2-7	15-2-C2-10	15-2-C2-11	15-2-C2-12	15-2-C2-15	15-2-C2-23	15-2-C2-24	15-2-C2-25
SiO ₂	55.04	54.84	55.04	55.65	55.37	55	54.32	54.82	55.18	55.76	52.41	55.37	53.01	54.5
TiO ₂	0.15	0.13	0.2	0.12	0.13	0.18	0.18	0.2	0.12	0.12	0.25	0.13	0.16	
Al ₂ O ₃	1.32	1.27	1.38	1.12	1.09	1.37	1.38	1.36	1.08	1.14	2.02	1.43	1.32	
Cr ₂ O ₃	0.52	0.49	0.47	0.42	0.4	0.5	0.52	0.47	0.42	0.47	0.86	0.53	0.46	0.55
Fe ₂ O _{3(c)}	0.9	0.15	0.93	0	0.63	0.65	1.6	0.58	0.28	0.37	1.13	0	3.1	1.06
FeO(c)	10.64	11.25	10.3	10.85	10.4	10.47	10.72	11.06	10.51	10.53	5.73	11.55	10.62	10
MnO	0.22	0.23	0.28	0.19	0.16	0.27	0.31	0.33	0.18	0.21	0.09	0.2	0.31	0.29
MgO	29.3	28.78	29.5	29.46	29.64	29.37	28.77	28.83	29.45	29.74	29.06	27.8	29.18	
CaO	2.24	2.27	2.21	2.23	2.29	2.21	2.16	2.24	2.27	2.35	18.98	2.18	2.19	2.35
Na ₂ O	0	0	0	0	0	0	0	0	0	0	0.28	0	0	0
K ₂ O	0	0	0	0	0	0	0.01	0.02	0	0	0	0	0.07	0
Sum Ox%	100.32	99.42	100.31	100.04	100.1	100.01	99.97	99.92	99.5	100.7	99.39	100.57	100.48	99.41
sample	15-2-C2-26	15-2-C2-28	15-2-C2-30	15-2-C2-31	15-2-C3-1	15-2-C3-3	15-2-C3-4	15-2-C3-5	15-2-C3-7	15-2-C3-8	15-2-C3-9	15-2-C3-10	15-2-C3-11	
SiO ₂	55.05	54.94	54.91	54.77	54.7	53.32	52.37	55.3	53.22	54.4	54.73	55.17	55.09	55.34
TiO ₂	0.16	0.19	0.08	0.16	0.14	0.07	0.43	0.45	0.15	0.51	0.4	0.49	0.46	0.46
Al ₂ O ₃	1.34	1.29	1.01	1.45	1.48	1.69	2.15	0.73	1.8	1.22	1.23	1.18	1.01	0.75
Cr ₂ O ₃	0.46	0.54	0.44	0.51	0.54	1.02	0.83	0.31	1.06	0.4	0.37	0.37	0.33	0.16
Fe ₂ O _{3(c)}	0.25	0.71	0.56	0.97	1.66	0.38	0.87	0.16	0.09	0.5	0.4	0.22	0.18	0.5
FeO(c)	10.62	10.49	9.97	9.94	9.53	5.47	5.68	12.34	5.72	11.35	11.64	11.84	12.24	11.86
MnO	0.19	0.2	0.15	0.3	0.3	0.28	0.18	0.31	0.15	0.33	0.26	0.32	0.25	0.26
MgO	29.16	29.38	29.58	29.21	29.65	18.64	17.16	29.37	18.55	28.8	28.91	29.07	28.85	29.62
CaO	2.19	2.23	2.54	2.24	18.95	20.16	1.17	18.94	1.9	1.86	1.9	1.83	1.83	1.29
Na ₂ O	0	0	0	0	0	0.12	0.16	0	0.12	0	0	0	0	0
K ₂ O	0.02	0	0.01	0.02	0	0	0.01	0.01	0	0.02	0	0	0.01	0.01
Sum Ox%	99.68	99.92	98.95	99.89	100.24	99.93	100.16	99.81	99.44	99.79	100.57	100.25		

Pyroxene (continued)

sample	15-2-C3-14	15-2-C3-15	15-2-C5-3	15-2-C5-4	15-2-C5-12	15-2-C5-14	15-2-C5-15	15-2-C5-16	15-2-C6-1	15-2-C6-4	15-2-C6-7	15-2-C6-10	15-2-C6-11
SiO ₂	55.38	52.34	53.28	51.52	54.82	52.87	54.72	54.51	52.66	51.91	52.02	53.54	55.32
TiO ₂	0.4	0.3	0.07	0.21	0.22	0.16	0.16	0.22	0.74	0.8	0.18	0.39	0.54
Al ₂ O ₃	0.52	2.08	1.35	2.51	1.29	2.55	1.53	1.46	1.81	2.22	2.19	0.44	0.64
Cr ₂ O ₃	0.11	0.88	0.84	0.74	0.54	0.54	0.54	0.54	0.73	0.69	0.81	0.29	0.13
Fe ₂ O ₃ (c)	1.14	0.49	0.31	1.69	0.55	1.59	1.17	0	0.42	1.35	0.03	1.11	0
FeO(c)	11.5	6.19	5.95	3.91	10.96	9.74	9.54	10.31	5.36	5.43	6.19	4.32	12.27
MnO	0.29	0.19	0.12	0.27	0.17	0.15	0.28	0.34	0.25	0.22	0.17	0.23	0.24
MgO	29.83	18.01	19.66	18.1	29.09	28.29	29.7	28.94	18.34	17.06	16.94	16.49	29.23
CaO	1.25	18.46	17.5	19.04	2.16	2.05	2.19	2.24	19.31	19.85	19.9	22.41	1.47
Na ₂ O	0	0.16	0.05	0.2	0	0	0	0	0	0.02	0.02	0.31	0
K ₂ O	0.01	0	0	0	0	0	0.13	0	0	0.01	0.02	0.04	0
Sum Ox%	100.44	99.08	99.13	98.18	99.79	98.09	99.82	98.49	99.13	99.75	99.25	99.36	98.95

sample	15-2-C7-2	15-2-C8-3	15-2-C8-5	15-2-C8-8	15-2-C8-9	15-2-C8-11	15-2-C8-12	15-2-C8-14	15-2-C10-1	15-2-C10-4	average (66)
SiO ₂	51.97	52.43	52.95	55.25	52.66	51.97	55.25	53.38	53.12	52.49	53.57
TiO ₂	0.36	0.16	0.25	0.08	0.14	0.24	0.39	0.14	0.17	0.42	0.41
Al ₂ O ₃	2.14	1.71	1.59	0.11	1.68	1.85	0.24	1.45	1.73	2.15	1.61
Cr ₂ O ₃	0.78	0.98	1.04	0.05	0.9	0.97	0.04	0.81	0.93	0.95	0.62
Fe ₂ O ₃ (c)	1.54	1.42	0.37	1.09	0.2	1.81	0.06	0.71	0.99	0.45	0.45
FeO(c)	5.13	4.69	5.41	13.29	6.09	4.6	13.36	4.98	5	5.72	7.92
MnO	0.13	0.19	0.24	0.25	0.22	0.21	0.29	0.24	0.23	0.11	0.23
MgO	17.13	18.13	18.37	28.78	18.9	17.52	28.8	18.29	18.93	17.39	21.95
CaO	19.98	19.67	19	1.02	17.89	19.76	1.11	19.76	18.86	20.09	12.90
Na ₂ O	0.23	0.09	0.18	0	0.04	0.21	0	0.18	0.12	0.13	0.11
K ₂ O	0	0.01	0	0	0.01	0	0	0	0	0	0.01
Sum Ox%	99.4	99.48	99.38	99.91	98.7	99.15	99.54	99.93	100.06	99.9	99.77

Spinel

sample	15-2-C1-8	15-2-C1-13	15-2-C2-19	average(3)
SiO ₂	0.06	0	0.13	0.06
TiO ₂	3.47	2.79	3.08	3.11
Al ₂ O ₃	6.1	5.46	16.77	9.44
Cr ₂ O ₃	26.57	23.15	28.53	26.08
Fe ₂ O ₃ (c)	26.81	31.43	13.78	24.01
FeO	32.62	31.54	32.96	32.37
MnO	0.59	0.54	0.62	0.58
MgO	0.89	0.83	1.43	1.05
ZnO	0.56	0.25	1.35	0.72
NiO	0	0.17	0.02	0.06
Sum Ox%	97.67	96.16	98.66	97.50

Olivine	sample	15-2-C1-10	15-2-C1-11	15-2-C1-23	15-2-C1-24	15-2-C1-25	15-2-C1-26	15-2-C1-27	15-2-C1-28	15-2-C2-14	15-2-C2-18	15-2-C2-21	15-2-C3-21
	SiO ₂	38.36	37.96	39.13	38.07	37.94	37.98	38.1	38.9	37.65	38.41	38.36	
	TiO ₂	0	0.02	0.05	0	0	0	0	0.04	0	0.03	0	
	Al ₂ O ₃	0	0	0	0	0	0	0	0	0	0	0	
	Cr ₂ O ₃	0.07	0.03	0.04	0	0.05	0.05	0	0.04	0.02	0.02	0	
	FeO	23.99	24.12	19.44	25.11	24.02	24.27	23.75	22.44	26.15	22.93	21.61	
	MnO	0.37	0.36	0.32	0.29	0.3	0.27	0.33	0.22	0.5	0.38	0.35	
	MgO	37.63	37.74	40.33	36.42	36.7	37.15	37.36	39.17	35.53	38.74	39.71	
	CaO	0.09	0.02	0.14	0.07	0.11	0.1	0.08	0.23	0.08	0.12	0.12	
	NiO	0.14	0.15	0.2	0.24	0.16	0.17	0.29	0.25	0.16	0.14	0.2	
	Sum Ox%	100.65	100.4	99.63	100.2	99.26	99.98	99.91	101.29	100.99	100.77	100.34	
	sample	15-2-C7-8	15-2-C7-14	15-2-C7-16	15-2-C7-17	15-2-C8-4	15-2-C9-1	15-2-C9-2	15-2-C9-10	15-2-C9-12	15-2-C10-7	average(21)	
	SiO ₂	35.72	38.85	38.8	37.37	41.21	38.71	38.7	39.02	37.37	38.83	38.26	
	TiO ₂	0.02	0	0	0.01	0.01	0	0	0	0	0	0.01	
	Al ₂ O ₃	0	0	0	0	0.79	0	0	0	0	0	0.00	
	Cr ₂ O ₃	0.04	0.04	0.04	0	0.03	0.01	0.04	0.02	0.01	0.05	0.03	
	FeO	34.86	20.45	20.32	27.7	25.75	20.11	20.46	19.53	27.75	20.07	23.44	
	MnO	0.54	0.25	0.35	0.52	0.39	0.3	0.28	0.27	0.45	0.34	0.34	
	MgO	28.22	40.56	40.15	34.24	31.73	40.91	40.81	40.74	34.59	40.86	37.86	
	CaO	0.1	0.17	0.04	0.14	1.35	0.23	0.12	0.15	0	0.1	0.11	
	NiO	0.24	0.16	0.22	0.13	0.21	0.14	0.22	0.21	0.1	0.19	0.19	
	Sum Ox%	99.74	100.48	99.93	100.12	101.48	100.41	100.64	99.93	100.27	100.43	100.34	

BASALT

Amphibole		sample	1/1-10-3	1/1-10-4	1/1-10-5	1/1-10-6	1/1-10-7	1/1-10-8	1/1-10-9	1/1-10-11	1/1-10-12	1/1-10-13	1/1-10-15	1/1-9-17	1/1-9-18	1/1-9-19	1/1-9-21
SiO ₂	55.47	53.67	53.21	54.48	55.75	53.62	55.91	54.54	54.12	54.48	54.96	59.31	53.64	56.29			
TiO ₂	0.14	0	0.05	0.81	0.05	0	0	0.01	0.19	0.01	0	0	0.08	0			
Al ₂ O ₃	0.45	3.34	4.17	1.14	1.17	3.88	0.7	2.46	2.14	0.9	0.18	3.13	0.77				
Cr ₂ O ₃	0.65	0.11	0.24	0.21	0.12	0.02	0.29	0.19	0.61	0.05	0.2	0.02	0.26	0.05			
Fe ₂ O _{3(c)}	18.15	5.91	7.6	15.64	16.2	5.61	18.22	10.57	7.38	2.14	15.95	9.39	12.12	8.26			
FeO(c)	0	3.02	2.22	0	0	3.9	0	0	2.48	6.11	0	0	0	0.22			
MnO	0.74	0.22	0.17	0.56	0.5	0.24	0.63	0.38	0.19	0.19	0.72	0.33	0.26	0.29			
MgO	21.49	18.76	18.26	19.32	20.03	17.87	20.8	18.76	18.53	18.63	20.06	26.26	18.76	20.48			
CaO	0.99	12.29	11.73	5.1	5.32	11.78	2.12	10.08	11.84	12.9	5.21	0.58	10.03	11.83			
Na ₂ O	0	0.42	0.61	0.08	0.08	0.63	0.08	0.48	0.3	0.15	0.11	0	0.42	0.07			
K ₂ O	0.02	0.03	0.05	0	0	0.01	0.01	0.02	0.01	0.05	0.01	0.06	0.06	0			
NiO	0.06	0.16	0.16	0.04	0.03	0.15	0.06	0.08	0.03	0.06	0.09	0	0.07	0			
H ₂ O(c)	2.18	2.14	2.15	2.19	2.14	2.19	2.15	2.16	2.16	2.12	2.16	2.21	2.17	2.18			
Sum Ox%	100.33	100.1	100.64	99.74	101.44	99.84	101.02	99.72	100.69	99.01	100.36	98.34	100.98	100.43			
sample		1/1-9-22	1/1-9-23	1/1-9-24	1/1-9-26	1/1-9-29	1/1-9-30	1/1-9-32	1/1-6-32	1/1-6-33	1/1-6-35	1/1-6-39	1/1-6-41	1/1-6-44	1/1-6-45	1/1-5-50	
SiO ₂	56.34	56.99	54.12	51.6	53.97	54.14	53.76	54.27	56.31	52.89	51.87	50.72	52.62	54.97			
TiO ₂	0	0.07	0.14	2.97	0.02	0.98	0.15	0.06	0.03	0.15	0.26	0.08	0.09	0.02			
Al ₂ O ₃	1.15	0.8	2.58	1.34	2.55	2.02	3.63	2.81	0.41	3.23	4.44	6.54	4.65	1.07			
Cr ₂ O ₃	0.05	0.13	0.24	0.05	0	0.03	0.39	0.4	0.26	0.54	0.73	0.03	0.05	0.11			
Fe ₂ O _{3(c)}	3.64	15.32	13.26	1.06	2.88	6.6	10.87	16.16	1.03	7.31	5.2	7.01	9.96	16.38			
FeO(c)	3.74	0	0	7.88	5.51	2.82	0	0	5.13	1.8	3.99	3.49	0	0			
MnO	0.11	0.45	0.41	0.24	0.21	0.25	0.26	0.64	0.1	0.22	0.2	0.24	0.28	0.54			
MgO	19.89	22.8	19.38	18.01	18.5	18.89	19.31	18.88	20.24	18.57	17.57	16.77	18.3	20.38			
CaO	12.43	2.63	7.72	13.19	12.74	11.91	10.01	5.88	13.04	11.79	11.84	11.68	10.91	4.26			
Na ₂ O	0.12	0.06	0.4	0.03	0.27	0.23	0.49	0.47	0.04	0.45	0.79	1.01	0.75	0.12			
K ₂ O	0.01	0.04	0.08	0.04	0.01	0.01	0.08	0.01	0.01	0	0.05	0.05	0.18	0			
NiO	0.1	0.19	0.01	0.14	0.16	0.04	0.11	0.01	0.08	0.14	0.06	0.2	0.1	0.19			
H ₂ O(c)	2.15	2.22	2.17	2.08	2.11	2.15	2.18	2.19	2.13	2.13	2.11	2.12	2.15	2.17			
Sum Ox%	99.74	101.68	100.52	98.64	98.95	100.07	101.23	101.87	98.81	99.22	99.09	99.93	100.03	100.21			
sample		1/1-5-54	1/1-5-57	1/1-5-63	1/1-4-64	1/1-4-65	1/1-4-66	1/1-4-67	1/1-4-68	1/1-4-70	1/1-4-71	1/1-4-72	1/1-4-74	1/1-4-75	1/1-3-77		
SiO ₂	55.52	54.86	53	56.08	54.98	56.24	56.05	55.56	53.14	53.24	53.69	54.49	53.72	56.01			
TiO ₂	0.05	0.23	0.16	0	0.53	0	0	0.02	0.5	0.06	0.12	0.02	0	0.02			
Al ₂ O ₃	1.18	2.75	3.84	1.21	0.99	1.08	0.16	0.71	2.72	3.68	3.35	1.34	2.76	1.19			
Cr ₂ O ₃	0.1	0.27	0.86	0.16	0.04	0.11	0	0.2	0.31	0.04	0.33	0.37	0.26	0.03			
Fe ₂ O _{3(c)}	17.69	5.46	6.46	17.66	2.61	19.25	18.55	12.49	9.58	14.87	15.86	5.68	7.71				
FeO(c)	0	3.5	2.31	4.83	0	5.83	0	0	0	0.28	0	0	2.9	0.53			
MnO	0.72	0.19	0.11	0.76	0.18	0.7	0.73	0.34	0.22	0.47	0.48	0.48	0.19	0.24			
MgO	20.49	18.87	18.22	19.34	20.25	19.25	21.19	21.33	18.99	18.74	18.81	20.09	18.68	20.33			
CaO	2.87	12.1	11.48	12.64	3.07	12.97	0.65	1.16	8.86	11.33	7.71	5.25	11.86				
Na ₂ O	0.18	0.4	0.65	0.1	0.02	0.01	0.03	0.01	0	0.07	0.54	0.56	0.42	0.08			
K ₂ O	0.02	0	0.01	0.02	0.01	0.03	0.01	0	0	0.07	0	0.01	0.01	0			
NiO	0.03	0	0	0.07	0.09	0.11	0.15	0.12	0.14	0.12	0.06	0.07	0.05	0.11			
H ₂ O(c)	2.19	2.16	2.13	2.16	2.17	2.15	2.18	2.15	2.18	2.15	2.15	2.16	2.16	2.17			
Sum Ox%	101.03	100.81	99.31	100.54	100.58	100.56	100.32	100.65	100.1	100.05	102.17	100.36	98.66	100.4			

Amphibole (continued)

sample	1/1-3-81	1/1-3-82	1/1-3-87	1/1-3-88	1/1-3-90	1/1-2-93	1/1-2-96	1/1-2-100	1/1-2-101	1/1-2-103	1/1-1-107	1/1-1-108	1/1-1-110	1/1-1-111
SiO ₂	52.46	53.88	56.97	54.7	52.69	55.98	54	56.63	54.14	55.84	51.63	55.38	54.88	53.37
TiO ₂	0.15	0.16	0	0.01	0.02	0	0.2	0.03	0.2	0	0.26	0.02	0.06	1.14
Al ₂ O ₃	3.65	1.75	0.8	1.3	4.29	0.59	3.01	1.41	2.9	1.41	5.31	0.85	2.29	0.72
Cr ₂ O ₃	0.18	0.4	0.02	0.22	0.03	0.05	0.26	0.1	0.72	0	0.56	0.12	0.35	0.12
Fe ₂ O _{3(c)}	10.34	15.08	2.75	18.03	5.78	4.57	8.35	2.9	4.19	5.2	9.83	18.85	12	17.11
FeO(c)	0	4.45	0	3.47	2.99	0.83	3.9	2.92	2.75	1	0	0	0	0
MnO	0.34	0.59	0.17	0.68	0.22	0.05	0.12	0.07	0.13	0.16	0.27	0.64	0.44	0.63
MgO	18.43	19.22	19.92	19.96	18.12	20.39	19.18	20.33	19.43	19.9	17.46	20.37	19.19	19.74
CaO	11.12	6.54	12.56	4.42	12.07	11.5	12.91	12.26	12.25	10.97	2.3	9.34	5.74	5.74
Na ₂ O	0.53	0.22	0.04	0.11	0.64	0	0.54	0.06	0.51	0.16	0.98	0	0.35	0.04
K ₂ O	0.03	0.02	0.03	0.01	0.06	0.02	0.01	0.01	0.02	0.04	0.01	0	0.02	0.02
NiO	0.05	0.01	0.06	0.03	0.1	0.08	0.07	0.09	0	0	0.06	0.12	0.07	0.07
H ₂ O(c)	2.13	2.15	2.16	2.13	2.15	2.16	2.14	2.17	2.16	2.15	2.18	2.18	2.16	2.16
Sum Ox%	99.41	100.01	99.93	101.64	99.61	99.54	100.23	100.61	99.57	99.87	100.49	100.84	101.21	100.87
sample	1/1-1-112	1/1-1-113	1/1-1-114	1/1-1-115	1/1-1-117	1/1-1-118	1/1-1-119	1/1-1-120	1/1-1-122	1/1-1-123	1/1-1-124	1/1-1-125	1/1-1-126	1/1-1-127
SiO ₂	56	51.95	53.6	54.88	55.9	55.15	52.8	56.35	53.03	54.48	49.06	55	53.46	54.97
TiO ₂	0	0.07	0.05	0.08	0.09	0.02	0.04	0	0.07	0.16	7.77	0	0.04	0.12
Al ₂ O ₃	1.07	4.7	3.27	2.05	1.78	0.63	3.34	0.59	1.71	1.83	2.19	1.47	1.62	2.15
Cr ₂ O ₃	0.06	0.49	0.14	0.23	0.33	0.13	0.22	0.11	0.5	0.07	0.25	0.07	0.26	0.41
Fe ₂ O _{3(c)}	7	6.11	7.49	11.49	12.42	17.34	12.03	18.9	15.67	8.82	13.67	6.4	17.8	16.44
FeO(c)	1.01	3.48	1.52	0.21	0.42	0.64	0.43	0.68	0.6	0.17	0.39	0.25	0.65	0.41
MnO	0.14	0.2	0.21	0.43	0.42	0.26	0.66	0.52	21.57	21.67	20.69	17.95	19.9	19.44
MgO	20.14	17.39	18.8	19.54	21.26	20.66	18.52	20.66	19.67	20.69	17.95	19.9	19.48	19.44
CaO	11.74	11.65	11.47	9.03	4.85	3.15	9.4	1.22	5.24	10.39	6.36	12.23	4.11	9.73
Na ₂ O	0.14	0.63	0.59	0.27	0.23	0	0.56	0.02	0.25	0.02	0.37	0.21	0.22	0.27
K ₂ O	0.01	0.06	0.03	0	0.03	0.02	0.01	0	0.02	0.09	0.04	0.01	0.04	0.03
NiO	0.08	0	0.02	0.02	0.11	0.1	0.08	0.07	0.03	0.12	0.15	0.08	0.04	0.11
H ₂ O(c)	2.16	2.11	2.14	2.17	2.18	2.16	2.14	2.18	2.13	2.15	2.14	2.14	2.17	2.17
Sum Ox%	99.53	98.83	99.34	100.2	99.6	100	99.57	100.69	98.91	99	100.33	99.63	99.87	100.34
sample	1/1-7-129	1/1-7-132	1/1-7-133	1/1-8-137	1/1-8-138	1/1-8-139	1/1-8-140	1/1-8-141	1/1-8-142	1/1-8-143	1/1-8-144	1/1-8-145	1/1-8-146	1/1-8-147
SiO ₂	52.53	53.86	55.15	54.21	56.26	54.6	54.89	56.16	57.16	53.07	54.65	53.84	54.86	54.96
TiO ₂	0.28	0	0.02	0.12	0.01	0.1	0.02	0.03	0	0.03	0.09	0.06	0	0.10
Al ₂ O ₃	3.78	2.87	0.76	3.23	1.35	2.34	1.87	1.11	1.19	3.84	2.36	2.73	2.38	2.42
Cr ₂ O ₃	0.88	0.03	0.14	0.32	0	0.21	0.02	0.07	0.07	0	0.03	0.17	0.09	0.22
Fe ₂ O _{3(c)}	6.89	4.52	18.13	11.73	6.3	11.88	6.42	8.11	6.33	7.81	9.25	9.66	11.21	7.94
FeO(c)	2.52	4.38	0	1.5	0	0	2.43	0	1.2	0	0.14	0.25	0.13	1.28
MnO	0.27	0.21	0.82	0.4	0.13	0.27	0.07	0.18	0.04	0.19	0.25	0.23	0.31	0.39
MgO	18.13	18.57	20.86	19.1	20.16	19.21	19.48	20.76	21.74	18.83	20.24	19	18.88	22.57
CaO	11.78	12.41	1.63	9.57	11.94	9.44	12.01	10.69	12.19	11.75	9.87	11.18	9.86	7.99
Na ₂ O	0.61	0.37	0	0.49	0.14	0.35	0.12	0.07	0	0.48	0.13	0.49	0.4	0.11
K ₂ O	0.04	0	0.02	0.05	0	0.31	0	0.01	0.11	0.32	0.06	0	0.11	0.25
NiO	0.07	0.13	0.07	0.11	0.12	0.02	0.24	0.07	0.16	0.17	0.07	0.14	0.14	0.07
H ₂ O(c)	2.13	2.11	2.16	2.18	2.17	2.15	2.18	2.15	2.18	2.14	2.16	2.15	2.17	2.16
Sum Ox%	99.44	99.81	101.45	100.11	100.69	99.8	99.58	99.99	99.61	99.51	99.78	100.3	99.41	100.19

Pyroxene

sample	1/1-6-34	1/1-6-37	1/1-6-38	1/1-6-42	1/1-6-43	1/1-5-47	1/1-5-48	1/1-5-49	1/1-5-51	1/1-5-52	1/1-5-55	1/1-5-56	1/1-5-58	1/1-3-80	
SiO ₂	52.08	51.42	51.93	51.69	51.8	53.52	53.83	52.06	51.56	52.04	51.97	52.56	51.52		
TiO ₂	0.24	0.3	0.29	0.29	0.26	0.17	0.2	0.3	0.2	0.27	0.28	0.24	0.27	0.35	
Al ₂ O ₃	2.86	3.16	2.79	2.98	3.36	1.69	1.38	2.9	2.7	2.69	2.96	2.71	2.82	3.39	
Cr ₂ O ₃	0.76	0.81	0.76	0.8	0.82	0.44	0.49	0.75	0.61	0.67	0.82	0.8	0.72	0.95	
Fe ₂ O _{3(c)}	1.06	0.91	0.9	1.27	1.18	0.23	0	1.48	1.88	1.25	0.95	0.96	0.64	0.53	
FeO(c)	4.85	4.7	5.09	4.26	4.93	5.81	5.97	4.31	4.78	5.4	4.79	4.51	5.11	5.53	
MnO	0.2	0.16	0.17	0.2	0.27	0.25	0.1	0.22	0.23	0.26	0.26	0.17	0.19	0.07	
MgO	17.91	17.48	18.42	17.79	17.64	18.56	19.18	17.93	17.64	18.82	17.47	17.77	18.4	17.2	
CaO	19.69	19.93	18.89	19.82	19.74	19.2	18.41	19.87	19.29	17.87	20.07	19.98	19.41	19.96	
Na ₂ O	0.06	0.04	0.02	0.11	0.05	0.09	0.07	0.12	0.14	0.08	0.16	0.09	0.03	0.01	
K ₂ O	0	0	0	0	0.01	0	0	0	0	0	0	0	0	0	
Sum Ox%	99.71	98.92	99.25	99.22	100.05	99.96	99.62	99.93	99.03	99.56	99.2	100.14	99.53		
sample	1/1-3-85	1/1-2-97	1/1-2-98	1/1-2-102	1/1-2-102	1/1-8-150	average(19)								
SiO ₂	52.56	51.71	52.14	52.65	51.26	52.14	52.14								
TiO ₂	0.28	0.22	0.3	0.36	0.06	0.26	0.26								
Al ₂ O ₃	2.88	2.8	2.79	2.76	2.4	3.018	2.74								
Cr ₂ O ₃	0.76	0.77	0.76	0.53	0.53	0.02	0.73								
Fe ₂ O _{3(c)}	0.14	1.27	1.27	0.35	0.07	0	0.95								
FeO(c)	5.94	4.87	5.3	6.97	1.03	5.00	5.00								
MnO	0.18	0.15	0.17	0.13	0	0.18	0.18								
MgO	17.85	18.51	17.46	17.02	0.04	18.02	18.02								
CaO	19.23	18.42	20.24	19.35	12.82	19.44	19.44								
Na ₂ O	0.11	0.09	0.02	0.17	4.38	0.08	0.08								
K ₂ O	0	0	0	0.09	0.21	0.00	0.00								
Sum Ox%	99.93	98.81	99.53	99.74	100	99.53	99.53								

Feldspar

sample	1/1-2-105	sample	1/1-9-25
SiO ₂	52.58	SiO ₂	61.61
TiO ₂	0.07	TiO ₂	0
Al ₂ O ₃	29.06	Al ₂ O ₃	0.03
Fe ₂ O ₃	1.21	FeO	1.19
MgO	0.38	MnO	0
CaO	11.63	MgO	29.91
Na ₂ O	4.79	H ₂ O(c)	4.6
K ₂ O	0.26	Sum Ox%	97.35
Sum Ox%	99.98	An	56

Talc

sample	1/1-9-25
SiO ₂	61.61
TiO ₂	0
Al ₂ O ₃	0.03
FeO	1.19
MnO	0
MgO	29.91
H ₂ O(c)	4.6
Sum Ox%	97.35

Spinel	sample	1/1-3-79											
		1/1-10-1	1/1-10-2	1/1-9-16	1/1-9-20	1/1-5-46	1/1-5-53	1/1-5-60	1/1-5-61	1/1-4-62	1/1-4-66	1/1-4-69	1/1-4-73
SiO ₂	0.05	0.13	0.1	0.09	0.15	0.05	0.13	0.09	0.05	0.05	0.07	0.07	0.12
TiO ₂	0.67	5.67	0.83	0.94	0.51	0.75	0.69	0.62	0.68	0.68	0.28	0.41	0.4
Al ₂ O ₃	8.09	10.08	7.83	7.56	11.91	9.43	7.87	7.56	7.87	8.06	0.03	9.12	10.47
Cr ₂ O ₃	46.61	36.97	44.87	44.51	45.04	38.29	42.89	44.57	43.35	44.99	0.08	46.15	47.01
Fe ₂ O _{3(c)}	11.09	7.3	11.76	12.03	7.97	16.18	13.89	12.82	13.48	12.09	0	9.89	7.41
FeO	31.7	36.26	31.84	31.73	32.03	31.62	31.84	31.67	31.46	31.43	44.66	30.98	31.51
MnO	0.87	0.81	0.76	0.77	0.72	0.76	0.71	0.74	0.78	0.72	1.31	0.85	0.73
MgO	0.32	0.27	0.33	0.37	0.49	0.22	0.22	0.22	0.2	0.27	0.37	0.22	0.31
ZnO	0.93	0.79	0.61	0.57	0.97	0.77	0.68	0.75	0.77	0.95	0.06	1.02	1.07
NiO	0.09	0.1	0	0.02	0.06	0.03	0.03	0.07	0.06	0.03	0	0.06	0
Sum Ox%	100.42	98.38	98.94	98.58	99.84	98.1	98.99	99.06	98.74	99.4	98.73	99.24	99.68
Spinels	sample	average(22)											
		1/1-2-94	1/1-2-95	1/1-2-99	1/1-1-106	1/1-7-121	1/1-7-130	1/1-8-135	1/1-8-136	0.1	0.07	0.1	0.09
SiO ₂	0.08	0.1	0.02	0.05	0.12	0.07	0.07	0.07	0.07	0.1	0.62	0.62	4.69
TiO ₂	0.75	0.61	0.59	0.67	1.99	0.81	0.75	0.75	0.75	0.79	4.39	4.29	8.29
Al ₂ O ₃	8.14	8.71	8.68	8.22	9.65	8.8	8.8	8.8	8.8	9.99	45.25	45.25	40.83
Cr ₂ O ₃	45.87	45.82	44.61	45.7	38.16	44.64	43.98	43.98	43.98	43.98	13.31	13.31	10.36
Fe ₂ O _{3(c)}	10.36	10.75	11.78	10.7	12.85	10.61	12.73	12.73	12.73	12.73	31.61	31.61	32.89
FeO	31.39	31.74	31.54	31.7	32.63	31.4	31.77	31.77	31.77	31.77	0.82	0.82	0.82
MnO	0.85	0.67	0.82	0.68	0.81	0.77	0.77	0.77	0.77	0.77	0.82	0.82	0.82
MgO	0.37	0.35	0.39	0.33	0.22	0.37	0.37	0.37	0.37	0.37	0.26	0.26	0.31
ZnO	0.77	0.91	0.64	0.63	0.67	0.9	0.66	0.66	0.66	0.66	0.68	0.68	0.77
NiO	0.03	0.12	0	0.01	0.05	0.05	0.05	0.05	0.05	0.05	0.06	0.06	0.04
Sum Ox%	98.61	99.77	99.06	98.7	97.15	98.44	99	99	99	99	99.46	99.46	99.46

ARCHEAN GRANITE

<u>Fedspars</u>	sample	AR1-C5-1	AR1-C5-2	AR1-C5-3	AR1-C5-4	AR1-C5-5	AR1-C1-7	AR1-C2-3	AR1-C3-1	AR1-C3-2	AR1-C3-3	AR1-C3-4	AR1-C3-5	AR1-C4-5	AR1-C6-1
SiO ₂	64.47	64.46	62.63	62.41	64.67	63.14	64.73	63.28	63.05	63.34	62.29	63.03	62.97	62.5	
TiO ₂	0	0	0.09	0.01	0.05	0.09	0	0	0	0	0.02	0.07	0	0.04	0
Al ₂ O ₃	18.28	18.16	23.61	23.37	18.01	23.14	18.64	23.4	23.32	23.6	23.03	22.99	23.28	23.11	
Fe ₂ O ₃	0	0	0.03	0.19	0.07	0.2	0.07	0.01	0	0.04	0.03	0	0.15	0.05	
CaO	0	0.04	5.32	5.5	0.04	4.99	0.01	4.99	5.03	5.15	4.91	4.77	4.82	5.31	
BaO	0.54	0.49	0	0	0.51	0	0.48	0	0	0.01	0	0	0.06	0	
Na ₂ O	0.71	0.95	8.86	8.74	0.63	9.4	0.88	9.13	9.05	8.61	8.85	8.87	9.2	8.69	
K ₂ O	15.43	14.91	0.1	0.1	15.8	0.16	15.07	0.27	0.26	0.27	0.27	0.27	0.3	0.29	
Sum Ox%	99.43	99	100.63	100.32	99.78	101.14	99.87	101.07	100.71	101.03	99.44	99.93	100.82	99.95	
An	0	0	25	26	0	22	0	23	23	24	23	23	22	25	

Fedspar (continued)

sample	AR1-C6-2	AR1-C6-3	AR1-C6-4	average(17)
SiO ₂	62.55	62.61	62.48	63.36
TiO ₂	0.12	0.03	0	0.03
Al ₂ O ₃	23.28	23.35	23.26	21.85
Fe ₂ O ₃	0.12	0.11	0.07	0.06
CaO	5.25	5.2	5.08	3.63
BaO	0	0.08	0.1	0.15
Na ₂ O	8.63	8.72	8.95	6.61
K ₂ O	0.31	0.29	0.28	4.54
Sum Ox%	100.26	100.39	100.22	100.22
<i>An</i>	25	24	23	17

Mica

sample	AR1-C1-1	AR1-C1-2	AR1-C1-3	AR1-C1-5	AR1-C2-1	AR1-C2-2	AR1-C2-4	AR1-C4-1	AR1-C4-2	AR1-C4-3	AR1-C4-4	AR1-C4-9	average(12)
SiO ₂	36.61	36.95	36.67	37.02	36.4	36.97	36.54	36.38	36.87	36.23	36.81	36.04	36.62
TiO ₂	3.19	2.89	2.65	3.21	3.89	3.05	3.25	3.14	3.46	2.98	2.96	3.33	3.16
Al ₂ O ₃	15.51	14.87	15.18	15.52	15	15.5	15.28	15.03	15.13	15.48	14.97	15.09	15.21
Cr ₂ O ₃	0	0.05	0	0.06	0.06	0	0.02	0	0.05	0.05	0.08	0.04	0.03
FeO	20.19	20.06	20.18	20.64	20	19.48	19.85	20.01	19.89	20.19	19.73	20.08	20.03
ZnO	0.09	0.22	0	0	0	0.05	0.03	0.17	0.25	0	0.24	0	0.09
MnO	0.25	0.16	0.21	0.18	0.15	0.22	0.23	0.25	0.17	0.3	0.22	0.12	0.21
MgO	9.89	10.06	9.95	10.01	10.25	9.98	10	10.3	10.02	10.12	10.06	9.95	10.01
CaO	0.03	0.01	0	0.05	0	0.01	0.01	0	0.03	0	0.03	0.1	0.02
Na ₂ O	0	0	0	0	0	0	0.06	0	0	0	0	0	0.01
K ₂ O	9.61	9.72	9.32	9.62	9.54	9.27	9.23	9.39	9.51	9.52	9.25	9.41	9.45
BaO	0.17	0.19	0.2	0.25	0.34	0.1	0.11	0.23	0.18	0.1	0.17	0.3	0.20
NiO	0.01	0.07	0	0	0.05	0	0	0	0	0	0	0	0.01
F	0.79	0.59	0.5	0.31	0.18	0.55	0.7	0.72	0.79	0.68	0.51	0.79	0.59
Cl	0.08	0.11	0.1	0.05	0.08	0.12	0.08	0.08	0.05	0.1	0.08	0.05	0.08
H ₂ O(c)	3.52	3.59	3.61	3.79	3.81	3.61	3.53	3.52	3.53	3.54	3.62	3.46	3.59
O=F	0.33	0.25	0.21	0.13	0.07	0.23	0.3	0.33	0.29	0.21	0.33	0.25	0.33
O=Cl	0.02	0.03	0.02	0.01	0.02	0.03	0.02	0.02	0.01	0.02	0.02	0.01	0.02
Sum Ox%	99.6	99.26	98.34	100.56	99.65	98.65	98.96	99.59	98.93	98.5	97.97	99.05	99.05

OLIVINITE

Amphibole

sample	K14-C1-8	K14-C1-10	K14-C1-16	K14-C7-2	K14-C7-15	K14-C7-17	K14-C5-35	K14-C4-8	K14-C4-5a	K14-C4-5b	K14-C4-5c	K14-C4-5d	average(12)
SiO ₂	57.01	56.21	58.2	56.59	56.34	53.06	46.75	44.98	56.81	57.55	58.36	56.85	54.90
TiO ₂	0	0.01	0	0.03	0.02	0	0.08	0	0.07	0	0	0	0.02
Al ₂ O ₃	0.39	2.99	0.39	1.07	0.84	2.86	11.6	14.65	1.71	0.9	0.68	1.42	3.29
Cr ₂ O ₃	0.05	0.01	0.04	0.08	0	0	0.03	0	0.01	0	0.08	0	0.03
Fe ₂ O _{3(c)}	1.36	3.4	0.51	3.4	3.21	4.12	6.33	7.33	2.76	3.35	2.75	1.32	3.32
FeO(c)	0.97	0	2.07	0	0	0	0.55	0	0.81	0	0	1.59	0.50
MnO	0.02	0.12	0.1	0.13	0.02	0.1	0.17	0	0.15	0.23	0.09	0.07	0.10
MgO	23.54	22.27	22.84	23.64	24.5	24.25	17.93	17.05	22.2	23.37	23.82	22.64	22.34
CaO	13.97	12.7	13.4	12.74	11.74	10.9	12.21	11.53	13.03	12.61	12.53	13.58	12.58
Na ₂ O	0	0.37	0.05	0.09	0.02	0.28	2.14	2.88	0.16	0.04	0.06	0.09	0.52
K ₂ O	0	0.03	0	0.01	0.02	0.02	0.13	0.15	0	0.02	0.04	0.04	0.04
NiO	0.14	0.05	0.01	0.05	0	0.05	0.08	0.16	0.07	0.02	0	0.05	0.06
F									0.02	0	0.2	0.05	0.05
Cl									0.53	0.02	0.05	0.01	0.13
H ₂ O(c)	2.18	2.2	2.19	2.18	2.14	2.14	2	2.18	2.2	2.11	2.16	2.16	2.16
O=F									0.01	0	0.09	0.02	0.02
O=Cl									0.12	0	0.01	0	0.03
Sum Ox%	99.63	100.35	99.82	100.02	98.89	97.78	100.12	100.16	99.91	100.68	99.85	99.85	99.89

Olivine

sample	K14-C1-1	K14-C1-2	K14-C1-3	K14-C1-4	K14-C1-6	K14-C1-13	K14-C1-14	K14-C2-21	K14-C4-9	K14-C4-10	K14-C4-11	K14-C7-1	K14-C7-4
SiO ₂	40.7	40.47	40.42	40.66	40.31	40.06	40.05	40.45	40.26	40.2	40.47	40.18	40.62
TiO ₂	0	0	0.01	0.03	0	0	0	0	0	0	0	0	0
Cr ₂ O ₃	0.04	0.02	0.03	0.06	0.05	0.04	0.05	0.01	0.03	0	0.03	0	0
FeO	15.1	15.73	15.08	15.01	15.45	15.18	14.92	15.3	15.79	15.32	15.07	14.81	15.61
MnO	0.27	0.27	0.26	0.31	0.23	0.29	0.19	0.2	0.24	0.21	0.26	0.29	0.2
MgO	44.26	44.61	44.72	44.6	44.76	44.92	44.5	44.48	44.22	44.93	44.7	45.08	44.9
CaO	0.04	0.05	0.01	0.02	0.06	0.04	0.09	0.08	0.04	0.01	0.03	0.05	0.04
NiO	0.3	0.23	0.33	0.37	0.35	0.34	0.35	0.3	0.29	0.32	0.31	0.32	0.31
Total Ox%	100.71	101.36	100.87	101.05	101.22	100.89	100.14	100.83	100.88	100.99	100.87	100.71	101.69
sample	K14-C7-5	K14-C7-6	K14-C7-7	K14-C7-9	K14-C7-10	K14-C7-11	K14-C7-12	K14-C7-13	K14-C7-14	K14-C7-31	K14-C7-33	K14-C5-1	K14-C5-2
SiO ₂	40.37	39.97	40.41	40.15	40.34	40.15	40.28	40.23	40.17	40.52	40.15	39.75	40.05
TiO ₂	0	0	0	0	0	0	0	0	0	0	0	0	0
Cr ₂ O ₃	0.07	0.02	0	0.02	0.02	0	0	0.04	0.03	0.07	0	0.01	0
FeO	15.33	16.73	14.95	15.44	15.66	15.5	15.08	15.45	15.31	15.04	17.56	15.04	15.02
MnO	0.17	0.31	0.2	0.15	0.21	0.2	0.14	0.18	0.31	0.25	0.35	0.25	0.33
MgO	44.74	42.98	44.7	44.82	44.47	44.46	44.59	44.96	44.77	45.28	42.93	44.88	45.05
CaO	0.04	0.03	0.04	0.03	0.08	0.03	0.04	0.07	0.03	0	0.02	0.06	0.02
NiO	0.37	0.31	0.27	0.34	0.31	0.32	0.4	0.41	0.22	0.36	0.37	0.47	0.3
Total Ox%	101.09	100.35	100.57	100.96	101.07	100.66	100.57	101.33	100.88	101.44	101.39	100.46	100.78

Olivine (continued)

sample	K14-C5-3	K14-C5-4	K14-C5-7	K14-C5-8	K14-C5-9	K14-C5-10	K14-C5-11	K14-C5-12	K14-C5-13	K14-C5-14	K14-C5-18	K14-C5-21	K14-C5-22
SiO ₂	40.42	39.97	39.71	40.28	40.11	40.51	40.39	40.43	40.31	40.44	40.18	40.51	40.27
TiO ₂	0	0	0	0	0	0	0	0	0	0	0	0	0
Cr ₂ O ₃	0.03	0	0	0.01	0.01	0	0	0.03	0.03	0	0.02	0	0.02
FeO	15.05	15.37	15.55	15.18	14.85	15.3	14.8	14.9	14.85	14.8	14.47	14.82	14.58
MnO	0.18	0.25	0.19	0.24	0.21	0.26	0.35	0.21	0.22	0.27	0.29	0.22	0.23
MgO	44.72	45.23	44.51	45.02	44.88	45.03	44.91	44.93	44.97	44.49	44.78	44.78	44.86
CaO	0.07	0.04	0.04	0.07	0.11	0.04	0.06	0.07	0.06	0.06	0.06	0.04	0.04
NiO	0.38	0.37	0.33	0.39	0.27	0.38	0.33	0.39	0.28	0.32	0.28	0.32	0.36
Total Ox%	100.84	101.23	100.34	100.89	100.59	101.38	100.96	100.98	100.86	100.86	99.78	100.71	100.36
sample	K14-C5-23	K14-C5-24	K14-C5-25	K14-C5-26	K14-C5-27	K14-C5-28	K14-C5-33	K14-C5-34	K14-C5-36	K14-C5-37	K14-C5-38	K14-C5-39	K14-C5-40
SiO ₂	40.47	40.27	39.97	40.33	40.12	40.45	39.65	39.76	40.25	40.1	40.17	40.17	40.17
TiO ₂	0	0	0	0.02	0	0	0	0	0.05	0	0	0	0
Cr ₂ O ₃	0.04	0.01	0.03	0	0.07	0.01	0.03	0	0.05	0.01	0	0.04	0
FeO	15.08	15.19	14.96	15.11	15.27	15.17	16.95	17.11	16.07	14.94	14.82	15.26	14.88
MnO	0.28	0.23	0.23	0.19	0.3	0.15	0.22	0.24	0.2	0.19	0.26	0.19	0.31
MgO	44.99	45.43	44.88	44.69	44.09	45.31	43.29	42.77	43.63	44.91	44.76	44.85	45.01
CaO	0.04	0	0.03	0.07	0.04	0.02	0	0.02	0	0.04	0.03	0.09	0.07
NiO	0.34	0.31	0.3	0.37	0.32	0.31	0.37	0.42	0.32	0.27	0.35	0.4	0.41
Total Ox%	101.23	101.44	100.4	100.76	100.22	101.42	100.5	100.32	100.57	100.45	100.39	101	100.85
sample	K14-C5-41	K14-C6-1	K14-C6-4	K14-C6-5	K14-C6-6	K14-C6-7	K14-C6-8	K14-C6-11	K14-C6-12	K14-C6-13	K14-C6-14	K14-C6-15	K14-C6-16
SiO ₂	40.23	40.25	40.63	40.55	40.19	40.14	40.85	40.8	40.23	40.97	40.53	40.43	40.17
TiO ₂	0	0	0	0.05	0.02	0.01	0	0	0	0	0.02	0	0
Cr ₂ O ₃	0.04	0.04	0	0.03	0	0.02	0	0	0	0.05	0	0.04	0
FeO	15.1	14.94	15.06	14.96	15.07	15.63	15.36	14.76	15.05	16.18	15.38	14.98	14.99
MnO	0.21	0.24	0.32	0.29	0.29	0.21	0.24	0.21	0.2	0.25	0.21	0.25	0.23
MgO	44.73	44.46	45.26	45.17	44.65	44.47	44.86	45.62	45.02	44.45	45.37	44.56	44.67
CaO	0.02	0.05	0.05	0.04	0.07	0.03	0.03	0.01	0.02	0.02	0.02	0.02	0.04
NiO	0.26	0.3	0.22	0.39	0.34	0.34	0.26	0.31	0.34	0.34	0.33	0.37	0.4
Total Ox%	100.59	100.28	101.54	101.44	100.67	100.9	100.89	101.76	101.43	101.5	102.27	100.78	100.76
sample	K14-C6-17	K14-C6-18	K14-C6-19	K14-C6-23	K14-C6-24	K14-C6-25	K14-C6-26	K14-C6-27	K14-C6-28	K14-C6-29	K14-C6-30	K14-C6-31	average(77)
SiO ₂	40.43	40.29	40.02	40.21	40.22	40.18	40.09	40.46	40.37	40.18	39.94	40.7	40.28
TiO ₂	0	0	0	0	0	0	0.06	0	0	0	0	0.01	0.00
Cr ₂ O ₃	0	0	0.01	0.02	0.01	0.04	0.02	0.04	0	0	0	0.02	0.02
FeO	15.34	15.37	15.26	14.72	15.58	15.28	15.43	15.26	14.83	15.28	14.91	15.55	15.27
MnO	0.19	0.26	0.26	0.25	0.27	0.27	0.22	0.25	0.24	0.22	0.21	0.26	0.24
MgO	44.54	44.8	44.57	44.41	44.46	44.99	44.7	44.77	44.55	44.35	44.7	44.87	44.67
CaO	0.05	0.01	0.05	0.06	0.04	0.04	0.05	0.09	0.03	0.05	0.06	0.01	0.04
NiO	0.34	0.28	0.3	0.28	0.47	0.39	0.2	0.41	0.1	0.31	0.28	0.42	0.33
Total Ox%	100.88	101	100.47	99.94	101.05	101.21	100.77	101.29	100.33	100.36	100.78	100.17	100.87

Serpentine														
sample	K14-C1-5	K14-C1-15	K14-C5-5	K14-C5-6	K14-C5-15	K14-C5-16	K14-C5-29	K14-C5-30	K14-C5-31	K14-C5-32	K14-C6-20	K14-C6-21	K14-C6-22	average(13)
SiO ₂	39.81	41.38	40.77	40.24	40.6	40.45	39.9	41.31	40.37	40.14	37.22	37.49	35.06	39.59
TiO ₂	0.03	0	0	0.06	0.02	0	0.02	0	0	0.04	0	0.01	0	0.01
Al ₂ O ₃	0.01	0.14	0	0	0	0	0	0.03	0	0	0.15	0.09	0.07	0.04
Cr ₂ O ₃	0.03	0	0.02	0	0.01	0.02	0.02	0.02	0.05	0.04	0	0	0.01	0.02
Fe ₂ O ₃	8.13	6.26	8.17	8.86	9.18	9.1	8.97	8.81	7.07	7.07	14.79	14.59	14.47	9.65
MnO	0.01	0.15	0.08	0.08	0.14	0.07	0.1	0.12	0.14	0.06	0.23	0.23	0.23	0.13
MgO	38.75	37.76	38.95	38.27	37.84	36.88	38.03	38.03	38.27	40.02	37.38	35.32	34.09	37.26
CaO	0.03	0.13	0.06	0.08	0.06	0.06	0.05	0.05	0.05	0	0.08	0.13	0.09	0.07
K ₂ O	0.01	0	0	0.01	0	0.02	0	0	0	0	0	0	0.01	0.00
NiO	0.33	0.1	0.18	0.08	0.11	0.05	0.12	0.14	0.33	0.24	0.37	0.1	2.98	0.39
H ₂ O(c)	12.59	12.57	12.76	12.66	12.7	12.54	12.84	12.75	12.37	12.39	12.24	11.84	12.53	12.53
Total Ox%	99.73	98.49	100.94	100.34	100.65	99.19	99.79	101.58	100.73	100.61	99.06	97.55	99.70	99.70

Pyroxene													
sample	K14-C4-12	K14-C4-15	K14-C7-3	K14-C7-8	K14-C7-19	K14-C7-20	K14-C7-21	K14-C7-25	K14-C7-26	K14-C7-27	K14-C7-32	K14-C7-35	K14-C5-19
SiO ₂	55.52	55.55	51.6	52.85	55.85	54.97	55.85	55.44	55.7	55.98	54.94	56.01	55.82
TiO ₂	0.09	0.3	1.23	0.31	0.36	0.09	0.15	0.15	0.2	0.25	0.45	0.32	0.13
Al ₂ O ₃	2.14	1.75	3.02	2.89	1.57	2.17	1.85	1.85	1.71	1.8	1.42	1.35	1.71
Cr ₂ O ₃	0.71	0.35	0.79	0.68	0.36	0.72	0.42	0.51	0.57	0.45	0.32	0.26	0.49
Fe ₂ O ₃ (c)	0	0	1.28	1.39	0	1.29	0	0	0	0	0.9	0	0
FeO(c)	9.26	9.27	3.86	3.05	9.26	7.04	9.59	9.4	9.99	9.8	9.39	10.02	9.97
MnO	0.22	0.35	0.08	0.2	0.23	0.22	0.22	0.19	0.19	0.18	0.17	0.2	0.29
MgO	29.21	29.62	15.75	17.63	30.33	26.93	29.8	30.3	29.96	30.12	30.91	31.26	30.59
CaO	3.54	3.05	22.28	20.82	1.78	8.08	1.92	2.18	1.45	2.08	1.13	0.84	1.57
Na ₂ O	0	0	0.48	0.46	0	0.04	0	0	0	0	0	0	0
K ₂ O	0	0	0	0.01	0	0.01	0	0.02	0	0	0	0	0
Total Ox%	100.68	100.24	100.39	100.28	99.75	101.56	99.82	100.02	99.78	100.65	99.65	100.26	100.57

Pyroxene													
sample	K14-C5-20	K14-C6-2	K14-C6-3	K14-C6-9	K14-C6-32	K14-C6-33	K14-C6-34	K14-C6-35	K14-C6-36	K14-C6-37	K14-C6-38	K14-C6-39	average(22)
SiO ₂	56.14	52.98	52.34	52.78	53.69	53	52.51	52.44	53.65	54.35	53.2	52.9	54.35
TiO ₂	0.24	0.34	0.19	0.79	0.26	0.28	0.26	0.26	0.31	0.26	0.26	0.26	0.32
Al ₂ O ₃	1.72	2.66	3.08	3.07	2.65	3	3.1	3.24	2.72	2.72	2.72	2.72	2.29
Cr ₂ O ₃	0.5	0.82	0.94	0.6	0.78	0.86	0.89	0.89	0.89	0.72	0.72	0.72	0.62
Fe ₂ O ₃ (c)	0	0.24	0.21	0.34	0	0	1.59	0.2	0	0	0	0	0.34
FeO(c)	9.89	5.74	5.31	5.2	6.58	5.71	4.03	4.68	7.01	7.46	7.01	7.46	7.46
MnO	0.17	0.25	0.17	0.23	0.23	0.23	0.17	0.18	0.06	0.13	0.20	0.20	0.20
MgO	30.51	18.55	17.42	17.44	20.91	18.64	17.77	15.72	21.53	24.59	24.59	24.59	24.59
CaO	1.25	17.76	19.27	19.21	14.14	18.06	19.61	21.88	13.4	9.79	9.79	9.79	9.79
Na ₂ O	0	0.4	0.34	0.58	0.26	0.26	0.43	0.46	0.2	0.18	0.18	0.18	0.18
K ₂ O	0	0	0	0	0	0	0	0	0.01	0.01	0.01	0.01	0.00
Total Ox%	100.42	99.75	99.26	100.26	99.51	99.98	100.36	99.91	99.63	100.12	100.12	100.12	100.12

Feldspar												
sample	K14-C4-13	K14-C4-14	K14-C7-16	K14-C7-18	K14-C7-22	K14-C7-23	K14-C7-24	K14-C7-28	K14-C7-29	K14-C7-30	K14-C7-36	average(11)
SiO ₂	53.85	53.44	53.26	53.98	52.79	52.73	53.44	52.64	52.14	49.86	50.71	52.62
TiO ₂	0.06	0.04	0	0.05	0	0	0.07	0.04	0	0.02	0.1	0.03
Al ₂ O ₃	28.44	28.99	29.69	29.02	28.76	29.5	28.89	29.04	29.61	29.94	29.33	29.20
Fe ₂ O ₃	0.33	0.3	0.39	0.34	0.32	0.38	0.37	0.3	0.26	0.24	0.4	0.33
CaO	11.94	12.5	12.98	12.2	12.45	12.82	12.16	12.92	13.71	9.77	10.27	12.16
Na ₂ O	4.89	4.79	4.21	4.74	4.46	4.47	4.88	4.25	3.9	7.57	6.67	4.98
K ₂ O	0.04	0.05	0.09	0.04	0.15	0.04	0.24	0.2	0.25	0.27	0.13	
Total Ox%	99.55	100.11	100.63	100.36	98.92	99.94	99.84	99.43	99.82	97.64	97.76	99.45
<i>An</i>	57	59	63	59	60	61	58	62	65	41	45	57

Spinel	
sample	K14-C7-34
SiO ₂	0.03
TiO ₂	1.49
Al ₂ O ₃	12.03
Cr ₂ O ₃	24.05
Fe ₂ O ₃ (c)	27.69
FeO	31.17
MnO	0.35
MgO	1.76
ZnO	0.27
NiO	0.15
Total Ox%	98.97

NORITE

Amphibole

sample	N-C2-5	N-C2-6	average(2)
SiO ₂	55.23	54.52	54.88
TiO ₂	0.63	0.26	0.45
Al ₂ O ₃	2.07	2.66	2.37
Cr ₂ O ₃	0.22	0.39	0.31
Fe ₂ O ₃ (c)	4.82	2	3.41
FeO(c)	1.58	5.61	3.60
MnO	0.13	0.14	0.14
MgO	20.33	18.65	19.49
CaO	12.32	12.76	12.54
Na ₂ O	0	0.02	0.01
K ₂ O	0.11	0.18	0.15
NiO	0.05	0.03	0.04
H ₂ O(c)	2.16	2.13	2.15
Sum Ox%	99.66	99.34	99.50

Talc

sample	N-C2-4	N-C2-4	average(2)
SiO ₂	60.89	60.89	
TiO ₂	0.09	0.09	
Al ₂ O ₃	1.41	1.41	
FeO	4.13	4.13	
MnO	0.08	0.08	
MgO	28.07	28.07	
H ₂ O(c)	4.63	4.63	
Sum Ox%	99.31	99.31	

Pyroxene

sample	N-C2-2	N-C2-3	N-C4-4	N-C1-7	N-C1-11	N-C2-1	N-C2-3	N-C2-4	N-C2-5	average(9)
SiO ₂	52.46	51.89	52.13	55.04	52.83	51.97	55.14	55.52	55.09	53.56
TiO ₂	0.92	0.94	0.62	0.34	0.48	0.98	0.14	0.05	0.19	0.52
Al ₂ O ₃	1.94	2.17	2.14	1.14	1.83	2.11	1.22	1.43	1.35	1.70
Cr ₂ O ₃	0.43	0.45	0.67	0.36	0.5	0.45	0.45	0.37	0.31	0.42
Fe ₂ O ₃ (c)	0	0.73	0	1.13	0	0	0	0	0	0.27
FeO(c)	6.9	5.05	6.05	12.65	5.22	5.55	13.75	13.62	13.07	9.10
MnO	0.23	0.14	0.18	0.37	0.11	0.11	0.39	0.36	0.29	0.24
MgO	15.9	15.37	15.66	28.19	15.95	15.37	27.67	28.01	28.02	21.13
CaO	21.04	22.83	21.65	22.23	22.41	22.31	1.62	1.43	2.13	13.07
Na ₂ O	0.13	0.23	0.19	0	0.09	0.19	0	0	0	0.09
K ₂ O	0	0	0.02	0	0	0	0	0	0.01	0.00
Sum Ox%	99.94	99.81	99.29	101.45	99.43	99.06	100.31	100.73	100.9	100.10

<u>Epidote</u>	sample	N-C5-3	N-C5-4	N-C5-6	N-C5-7	N-C5-10	N-C5-13	N-C5-14	N-C1-1	N-C1-2	average(9)
SiO ₂	38.38	40.59	41.08	38.36	38.23	38.94	39.87	43.33	38.4	39.69	39.69
TiO ₂	0	0.01	0.02	0	0	0.06	0.06	0.03	0.03	0.02	0.02
Al ₂ O ₃	24.45	26.99	29.88	25.78	25.53	27.31	29.19	23.8	23.49	26.27	26.27
Cr ₂ O ₃	0.03	0.01	0	0	0	0	0.04	0	0.05	0.01	0.01
Fe ₂ O ₃	11.23	7.17	3.52	9.86	10.38	7.39	5.58	8.8	12.3	8.47	8.47
Mn ₂ O ₃	0.15	0.22	0.02	0.29	0.16	0.15	0.64	0.22	0.13	0.22	0.22
MgO	0.08	0	0	0	0	0	0	0.23	0	0.26	0.26
CaO	22.88	22.89	23.55	23.75	23.55	24.06	23.61	20.63	23.5	23.16	23.16
H ₂ O(c)	1.89	1.94	1.97	1.91	1.9	1.93	1.96	1.97	1.89	1.93	1.93
Sum Ox%	99.09	99.82	100.05	99.95	99.75	99.83	100.97	101.01	99.78	100.03	100.03

<u>Feldspar</u>	sample	N-C5-2	N-C5-5	N-C5-9	N-C2-7	N-C1-4	N-C5-1	N-C3-3	N-C3-4	N-C3-5	N-C3-6	N-C3-7	N-C3-8	N-C3-9	N-C4-5
SiO ₂	51.11	50.55	50.22	49.75	50.03	49.64	50.3	50.59	50.57	48.83	49.7	49.87	49.48	50.44	50.44
TiO ₂	0	0	0.04	0.06	0	0.03	0	0	0.06	0.04	0.05	0	0	0	0
Al ₂ O ₃	30.19	30.35	30.96	30.91	31.13	30.89	31.4	31.11	30.96	32.04	31.8	31.38	31.96	30.99	30.99
Fe ₂ O ₃	0.37	0.63	0.48	0.54	0.38	0.47	0.27	0.38	0.39	0.41	0.43	0.51	0.45	0.58	0.58
CaO	14.21	14.71	15.03	15.11	15.21	15.48	14.95	14.45	14.44	16.03	15.41	15.45	15.3	15.31	15.31
BaO	0	0	0	0	0	0	0	0.08	0.08	0.06	0	0	0	0	0
Na ₂ O	3.29	3.29	3.12	3.17	3.1	2.7	3.21	3.41	3.4	2.5	2.71	2.84	2.83	3.12	3.12
K ₂ O	0.24	0.02	0.06	0.03	0.06	0.14	0.11	0.17	0.17	0.19	0.14	0.12	0.07	0.18	0.18
Sum Ox%	99.42	99.55	99.91	99.6	99.88	99.34	100.32	100.19	100.05	100.04	100.24	100.18	100.1	100.62	100.62
An	69	71	72	73	75	71	69	69	77	75	74	75	75	72	72

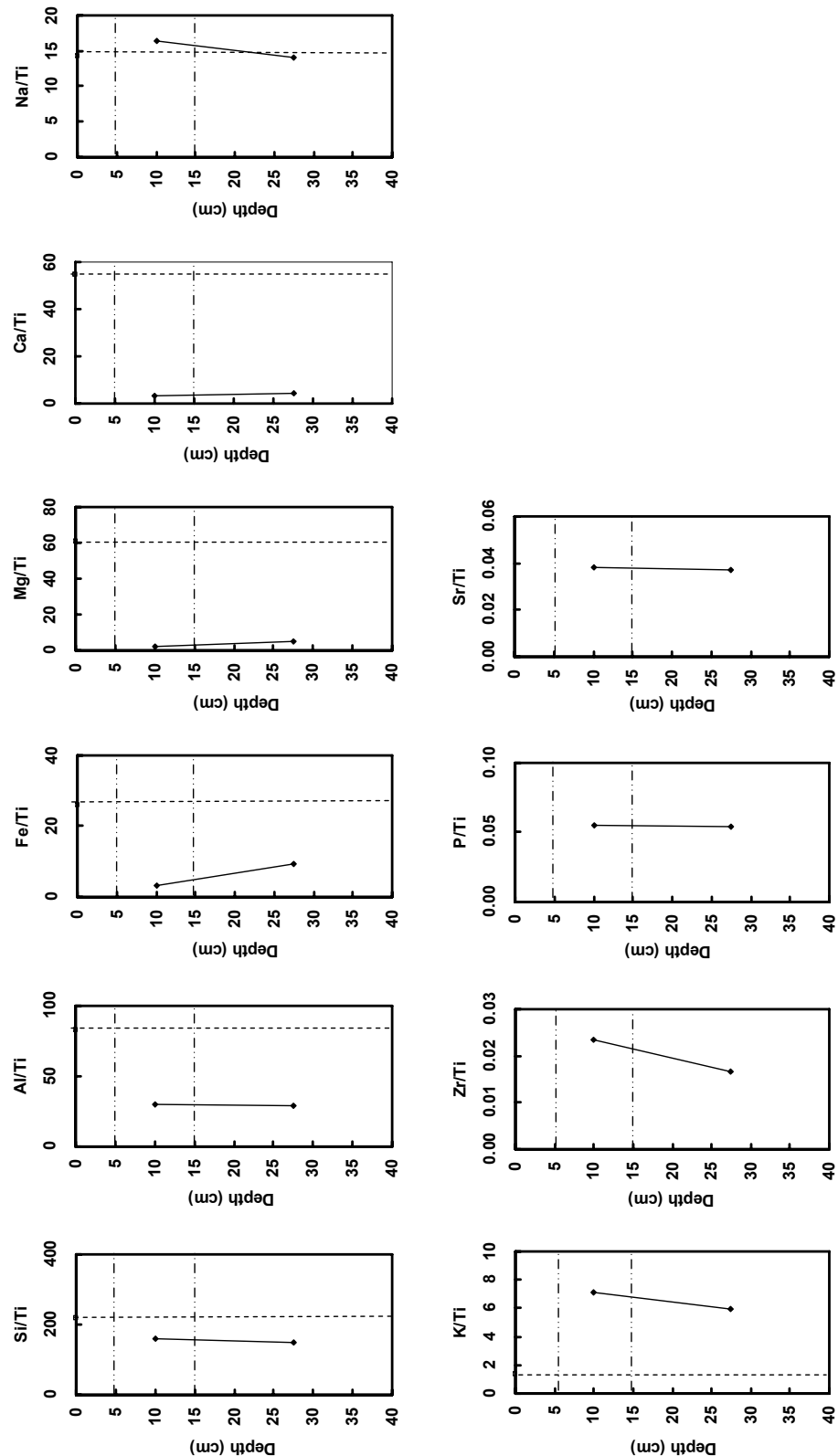
sample	N-C4-8	N-C1-2	N-C1-8	N-C1-9	N-C1-10	N-C2-2	average(20)
SiO ₂	50.53	49.29	49.93	49.36	50.05	49.94	50.05
TiO ₂	0.02	0	0.05	0	0.15	0.04	0.02
Al ₂ O ₃	31.22	31.25	31.86	31.6	31.81	31.68	31.16
Fe ₂ O ₃	0.49	0.33	0.31	0.44	0.33	0.68	0.44
CaO	15.55	16.25	15.59	15.49	15.6	15.66	15.06
BaO	0.05	0	0.03	0	0	0	0.02
Na ₂ O	2.95	2.44	3.06	2.88	2.79	3	3.04
K ₂ O	0.21	0.12	0.02	0.07	0.13	0.12	0.12
Sum Ox%	101.02	99.69	100.84	99.84	100.86	101.13	99.91
An	74	78	74	75	75	74	73

Table A-2. Trace elements composition for unweathered basalts from Ruiga and Goletz hills of the Vetryny Belt paleorift.

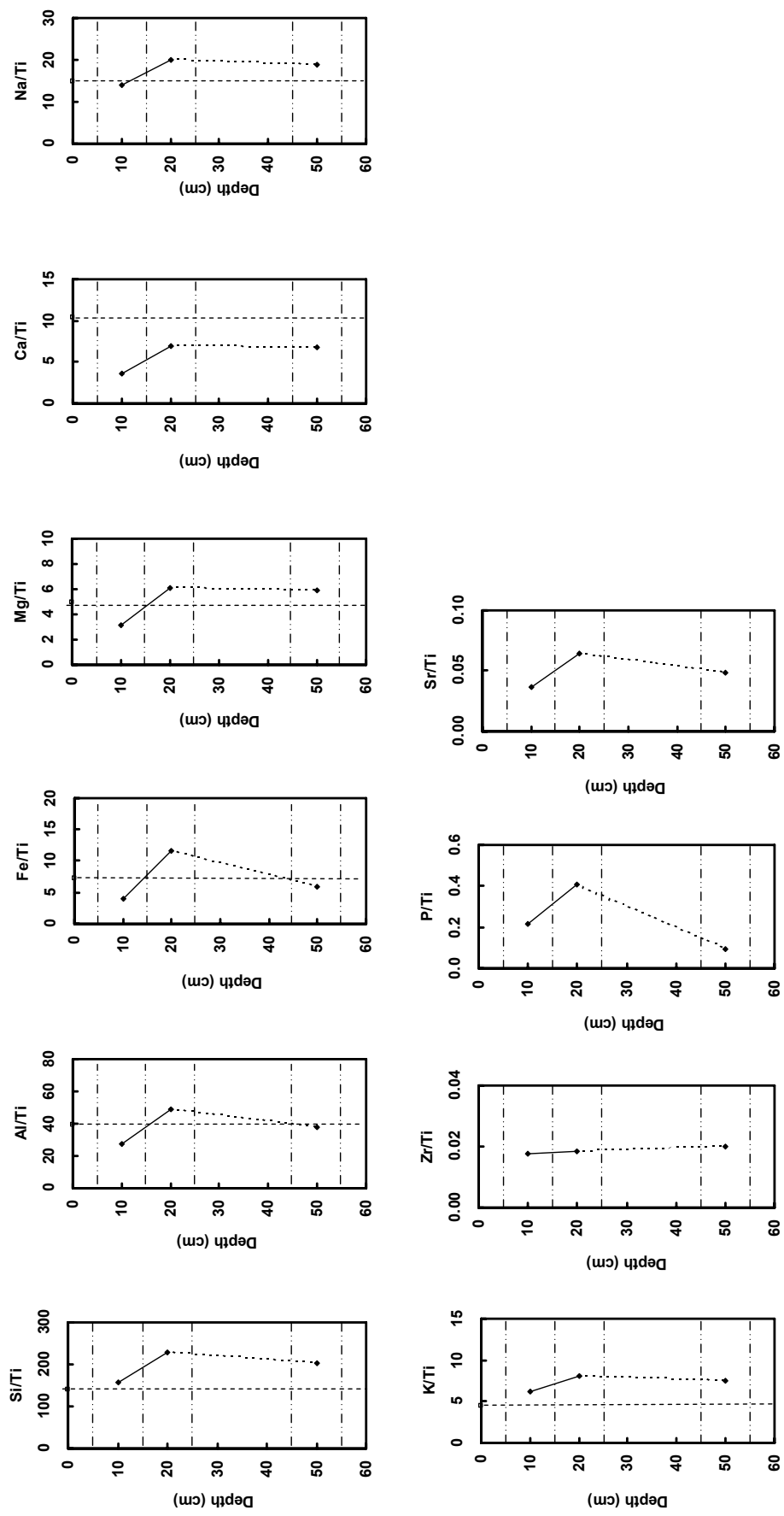
Sample	Basalt from Ruiga hill					Basalt from Goletz hill					
	Element	4108/10	4108/9	4108/7	4108/5	average	4102	4101	4106	4104/1	4105/1
Ti	2 609.5	73.9	879.6	2 254.1	1 454.3	nd	nd	nd	nd	nd	nd
V	167.80	nd	46.80	nd	107.30	nd	nd	nd	nd	nd	nd
Cr	154.2	nd	1 699.0	1 475.9	1 109.7	nd	nd	660.5	1 261.5	nd	961.0
Co	35.60	1.186	81.58	75.36	48.43	37.04	38.17	50.05	59.35	66.66	50.25
Ni	nd	nd	nd	nd	nd	nd	109.10	nd	nd	nd	109.10
Cu	33.62	1.11	12.67	43.61	22.75	105.46	0.00	91.86	58.10	74.06	65.90
Zn	57.30	1.67	20.59	56.95	34.13	0.00	0.00	nd	62.70	nd	20.90
Rb	10.60	0.28	2.07	12.81	6.44	10.93	6.57	3.24	5.02	7.98	6.75
Sr	105.05	3.17	19.91	52.60	45.18	84.66	nd	nd	75.31	nd	79.99
Zr	27.96	0.90	19.26	43.90	23.00	22.39	23.68	45.74	40.99	39.09	34.38
Ba	232.18	5.69	43.63	163.58	111.27	297.09	194.69	91.05	71.30	97.55	150.34
La	7.93	0.21	2.58	7.54	4.57	10.70	10.92	7.22	7.67	5.14	8.33
Ce	16.28	0.44	5.42	15.54	9.42	22.03	22.59	15.40	15.67	10.97	17.33
Pr	2.12	0.06	0.70	1.99	1.21	2.87	2.92	2.07	2.08	1.47	2.28
Nd	8.83	0.24	2.92	8.28	5.07	11.98	12.11	9.06	9.00	6.43	9.71
Sm	2.02	0.057	0.65	1.82	1.14	2.71	2.75	2.21	2.08	1.58	2.27
Eu	0.68	0.018	0.19	0.50	0.35	0.86	0.85	0.67	0.69	0.50	0.71
Gd	1.94	0.056	0.62	1.69	1.08	2.92	2.76	2.28	2.11	1.63	2.34
Tb	0.32	0.009	0.10	0.27	0.18	0.46	0.45	0.38	0.35	0.27	0.38
Dy	2.04	0.059	0.65	1.73	1.12	2.85	2.90	2.41	2.22	1.72	2.42
Ho	0.43	0.012	0.14	0.36	0.24	0.60	0.61	0.50	0.46	0.36	0.51
Er	1.26	0.036	0.41	1.06	0.69	1.77	1.79	1.46	1.34	1.05	1.48
Tm	0.17	0.005	0.06	0.14	0.09	0.24	0.24	0.20	0.19	0.14	0.20
Yb	1.14	0.032	0.39	0.96	0.63	1.51	1.54	1.29	1.19	0.93	1.29
Lu	0.16	0.005	0.06	0.14	0.09	0.20	0.20	0.18	0.17	0.13	0.17
Pb	3.05	0.079	1.15	3.47	1.94	3.14	2.90	2.52	0.92	1.40	2.18
Th	1.00	0.028	0.32	1.13	0.62	1.27	1.28	0.76	0.61	0.55	0.90
U	0.19	0.005	0.06	0.22	0.12	0.30	0.30	0.16	0.12	0.11	0.20

Fig. A-1. Graphical representation of distribution of elements concentrations on depth along the soil profiles. Vertical dotted line corresponds to the element/Ti ratio in parent rock.

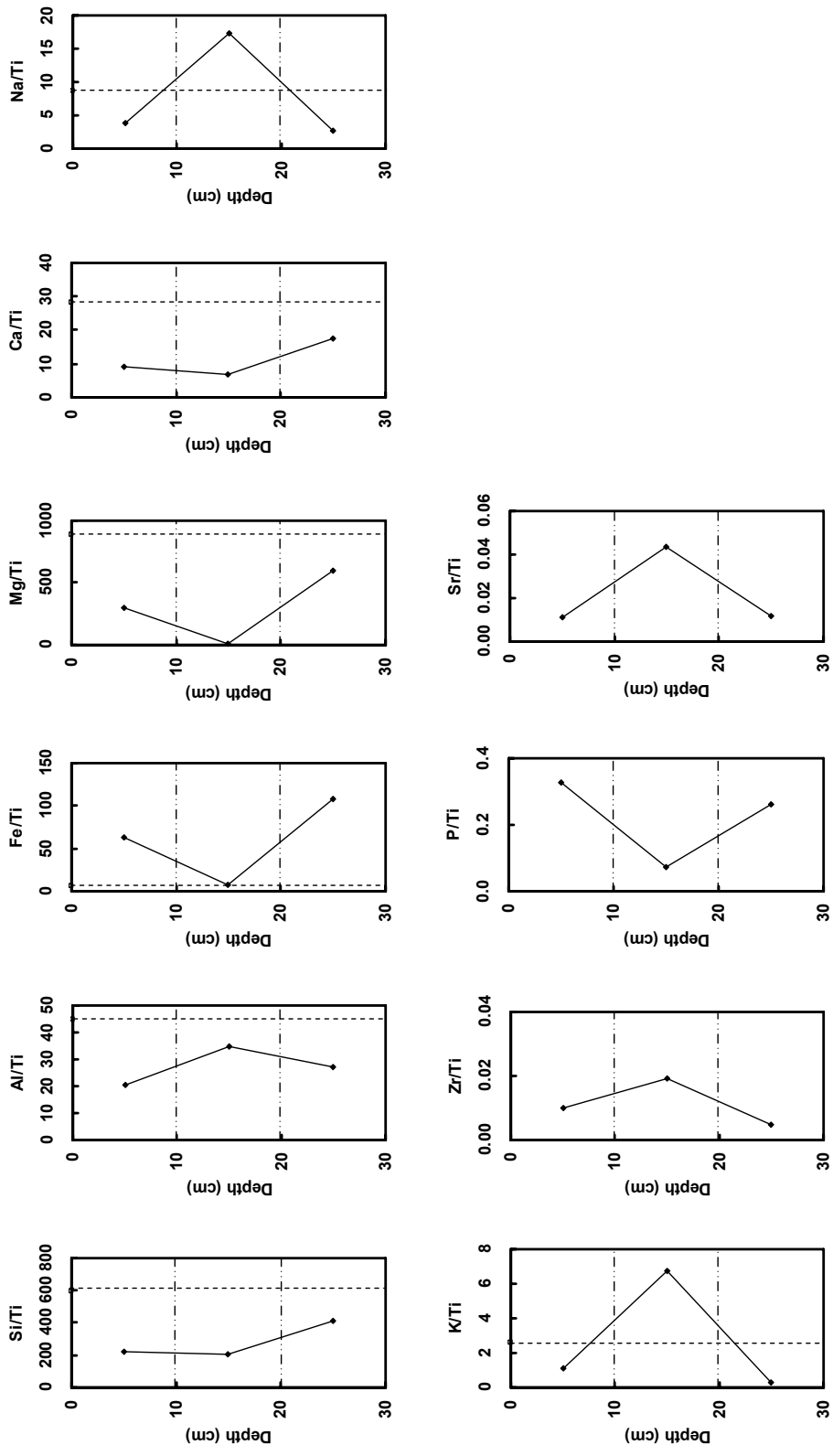
K-7: soil over TTG



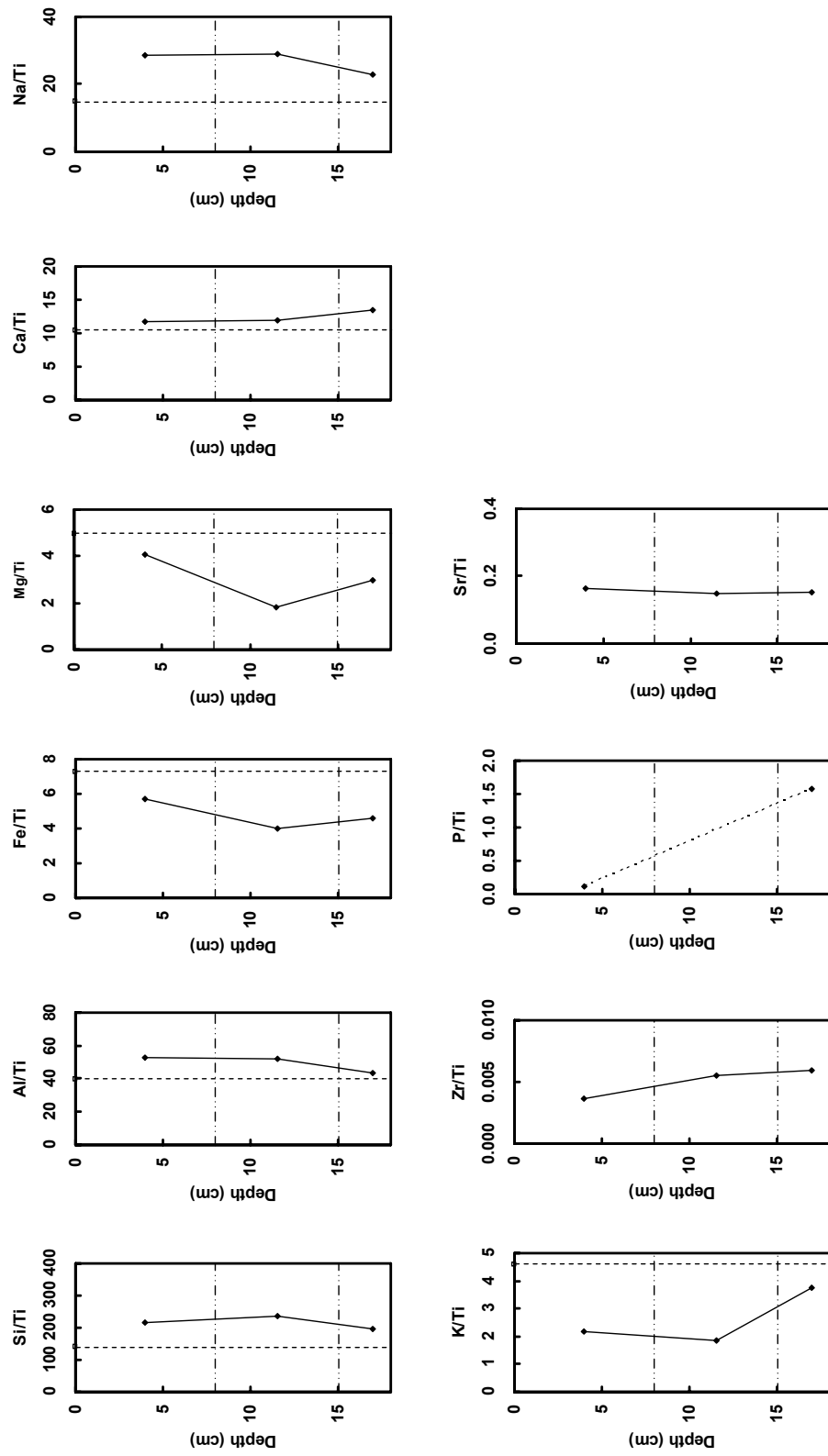
K-8: soil over TTG



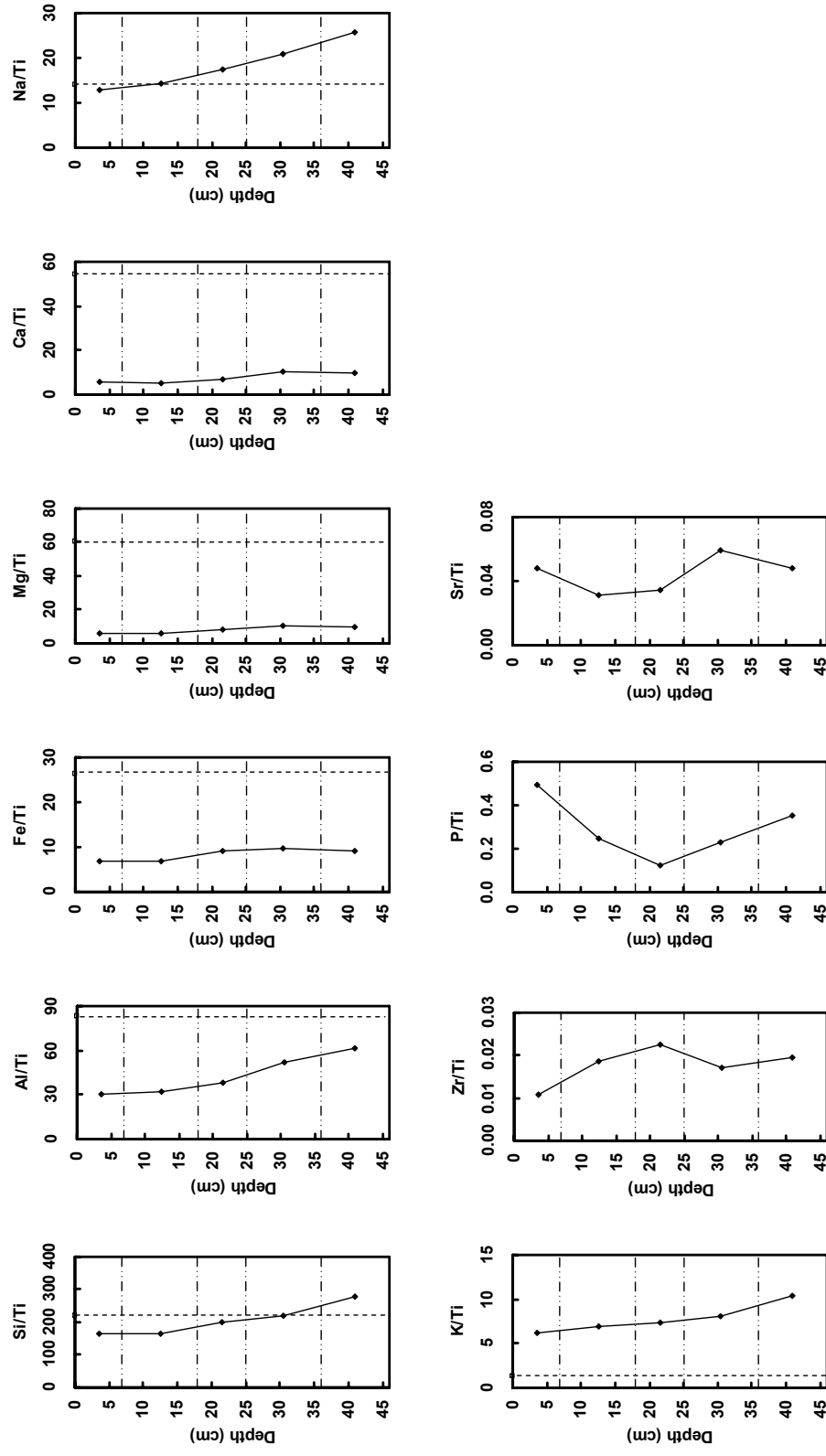
K-14: soil over olivinite



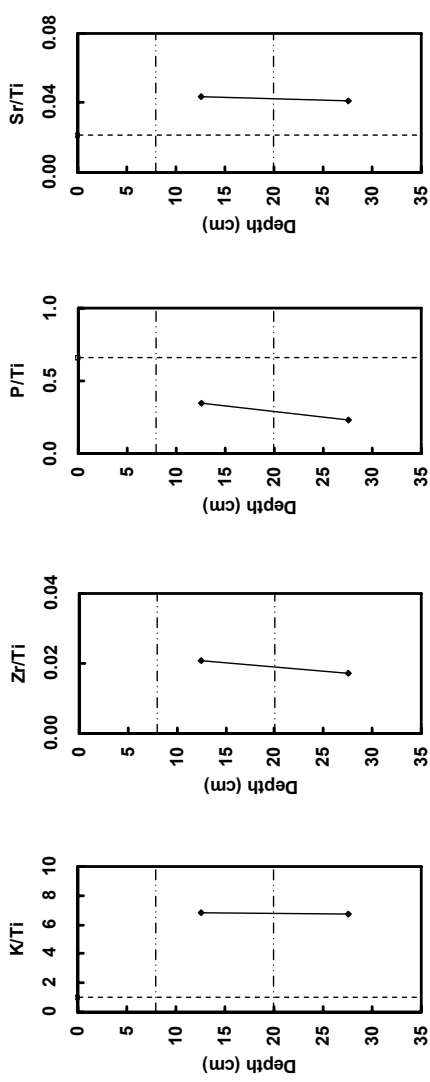
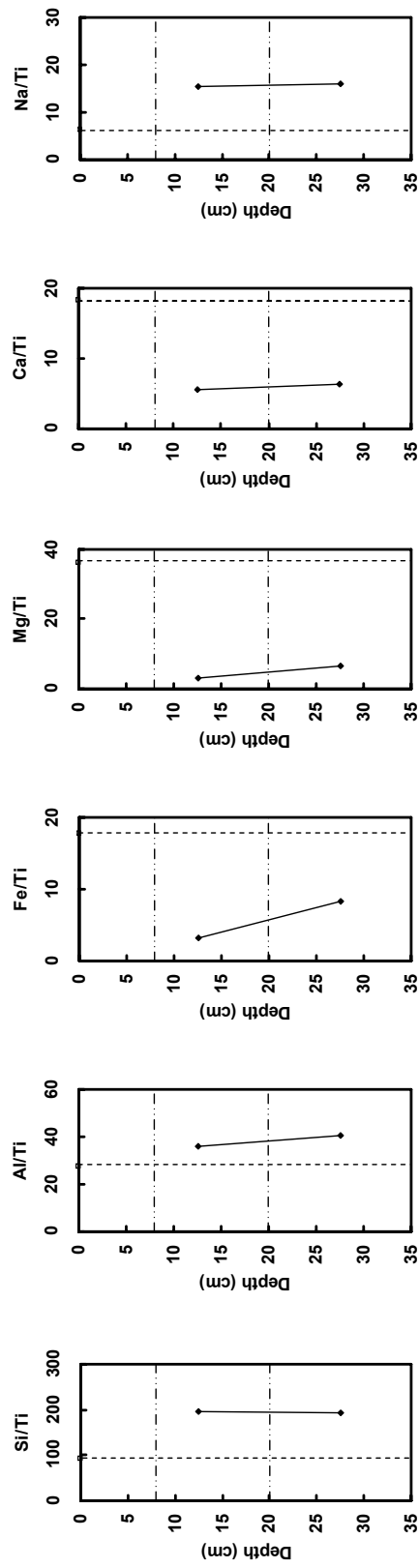
K-29: soil over TTG



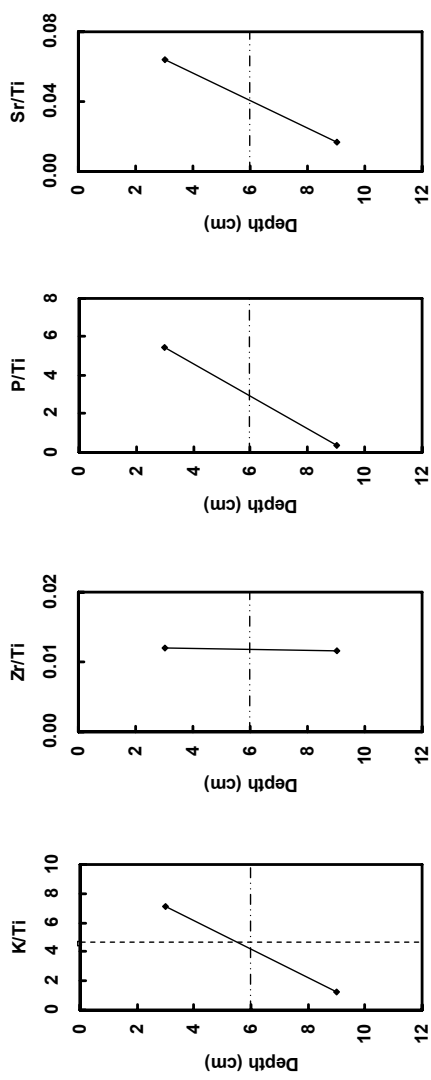
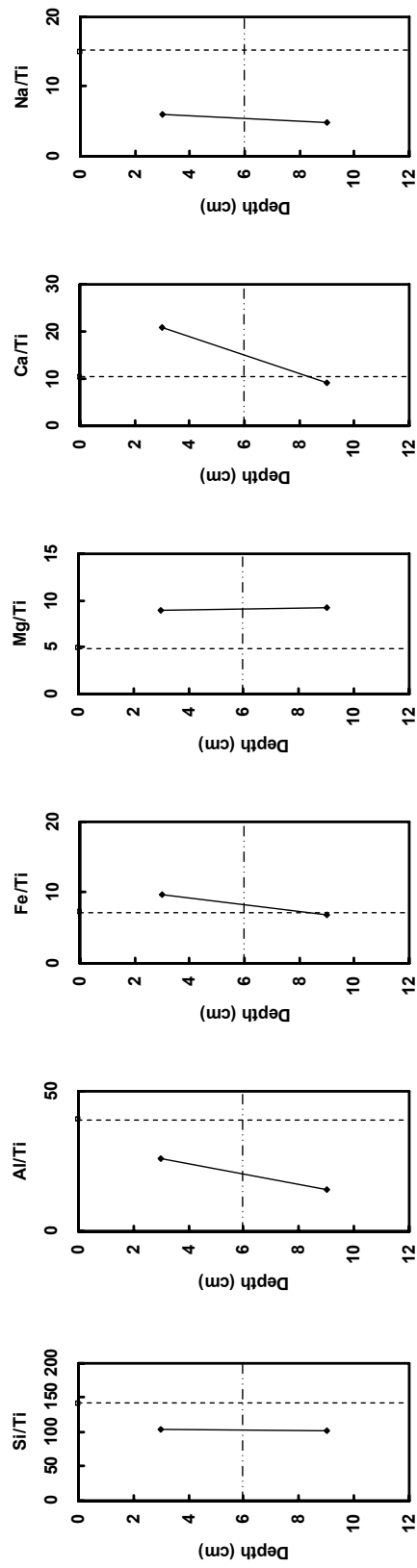
K-37: soil over gabbro-norite



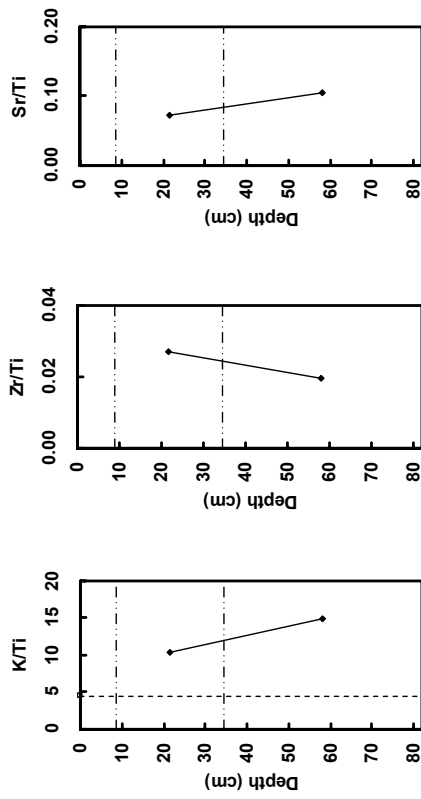
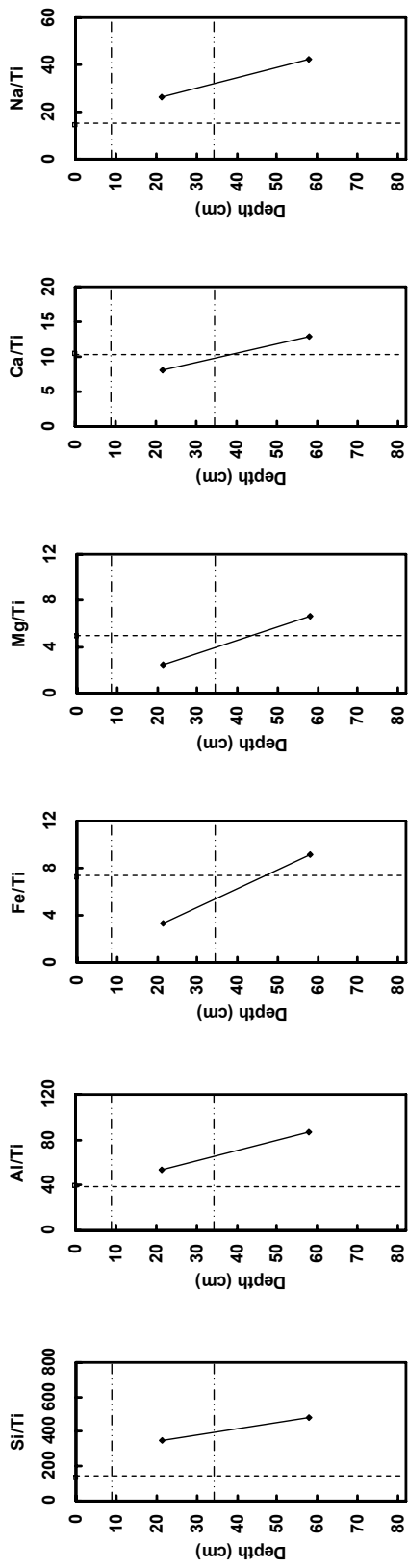
V-7: soil over basalt



V-9: soil over granite



V-16: soil over granite



Annex B

Table B-1. Measured major and trace element concentrations in all filtrates and ultrafiltrates. All concentrations are in $\mu\text{g/l}$ except DOC and alkalinity (mg/l). No. - ultrafiltration.

Sample	No.6 0.22 μm	No.6 10 kD dialysis	No.6 3 μm	No.8 0.22 μm	No.8 100 kD UF	No.8 10 kD UF	No.8 1 kD UF	No.8 0.22 μm	No.9 100 kD UF	No.9 10 kD UF	No.9 1 kD UF	No.9 0.22 μm	No.10 100 kD dialysis	No.9 100 kD UF	No.9 10 kD UF	No.9 1 kD UF	No.11 0.22 μm	
PH	6.81	nd	nd	nd	nd	nd	nd	nd	nd	nd	nd	nd	nd	nd	nd	nd	nd	
Na	3.968	3.794	nd	2.679	2.749	2.636	2.636	cnd	2.574	2.337	2.299	2.293	2.482	nd	nd	nd	nd	
K	9.49	nd	751	666	732	610	3.043	838	655	502	411	293	514	304	1800	517	304	
Mg	6.357	4.525	5.103	3.119	3.130	3.043	2.526	2.233	2.286	2.867	2.910	2.875	2.365	425	328	922	328	
Ca	12.783	11.285	9.379	5.479	5.443	4.761	4.797	3.625	3.638	3.659	1.841	1.835	1.823	1.265	421	1296	4.84 ± 0.12	
[Alk]	81.48 ± 0.24	nd	nd	23.9 ± 0.36	22.65 ± 0.54	22.88 ± 0.15	20.89 ± 0.34	nd	4.6 ± 0.32	4.85 ± 0.21	6.14 ± 0.42	6.67 ± 0.34	4.57 ± 0.76	3.95 ± 0.33	4.23 ± 0.13	4.21 ± 0.17	4.26	
Cl	1.264	1.556	1.596	nd	2.690	2.368	2.040	cnd	2.195	1.400	1.270	1.342	cnd	1.382	900	809	809	
SO ₄	201	271	189	nd	521	443	432	400	421	cnd	671	750	556	429	360	420	310	
NO ₃	110	187	101	nd	250	210	182	80	125	nd	<dl	120	<dl	<dl	100	100	100	
F	124	<dl	129	nd	64	52	57	53	nd	49	40	40	<dl	58	42	<dl	<dl	
Si	5.415	5.580	5.360	5.460	5.040	4.950	4.930	4.900	5.070	5.040	4.820	4.900	4.820	4.930	4.820	3.970	4.540	
DOC	10.70	3.64	2.55	29.10	27.70	25.00	nd	19.60	4.97	25	34.40	32.80	32.00	13.00	3.87	2.03	98.50	
Al	18	2	256	243	89	82	27	24	27	750	nd	717	696	241	46	42	264	310
Mn	4.301	2.841	3.143	1.544	1.398	1.235	1.356	894	1.028	760	132	145	106	32	21	59	57	
Fe	nd	13	nd	2.536	2.464	104	9	61	62	2.660	1.805	1.888	1.290	219	168	135	135	
Li	5.416	6.001	4.778	1.929	1.988	2.100	2.240	1.999	1.698	1.655	1.005	0.979	1.278	1.246	nd	0.600	0.233	
B	4.504	nd	4.222	3.022	3.289	3.935	1.301	nd	3.255	3.211	3.095	3.095	3.862	4.847	2.806	3.674	1.637	
Ti	0.182	0.192	cnd	3.738	3.595	0.988	0.819	0.189	0.160	0.173	10.173	7.886	7.275	6.948	0.496	0.124	1.415	
V	0.124	0.069	0.019	1.433	1.411	0.402	0.220	0.320	0.351	0.279	1.782	1.123	1.028	0.812	0.734	0.519	0.539	
Cr	0.154	0.151	nd	1.854	1.854	1.209	0.785	2.045	2.045	cnd	2.141	2.087	2.087	1.025	1.025	1.169	1.169	
Co	6.544	6.611	6.665	6.051	4.986	5.176	2.989	2.825	2.100	1.095	1.053	1.029	0.688	0.166	0.094	0.668	1.226	
Ni	0.736	cnd	cnd	3.288	3.479	1.404	2.058	2.058	2.199	1.970	3.854	3.620	3.659	2.776	1.557	cnd	1.236	
Cu	0.092	cnd	cnd	4.386	cnd	5.927	5.859	3.250	0.837	6.169	0.698	0.830	0.689	0.700	0.718	0.335	0.137	
Zn	3.423	cnd	cnd	12.968	10.328	6.863	7.556	6.059	6.951	5.934	4.919	6.886	6.585	6.374	cnd	3.501	3.102	
Ga	0.077	0.102	0.063	0.113	0.122	0.054	0.054	0.084	0.082	0.074	0.068	0.047	0.043	0.040	0.014	0.008	0.020	
As	1.497	0.934	0.844	2.445	2.247	1.401	1.412	1.273	1.982	1.284	0.715	0.664	0.643	0.639	0.583	0.326	0.235	
Rb	1.000	1.016	0.955	1.689	1.689	1.618	1.521	1.653	1.653	0.491	0.521	0.488	0.499	0.541	0.370	0.847	0.411	
Sr	43.94	33.91	35.54	25.70	25.72	23.59	18.12	18.25	18.39	13.31	12.84	12.53	8.31	3.55	2.97	11.99	9.24	
Y	0.051	0.008	0.004	0.341	0.323	0.154	0.137	0.038	0.030	0.041	0.469	0.444	0.432	0.416	0.180	0.021	0.030	
Zr	0.055	nd	nd	0.798	0.767	0.688	0.488	0.439	0.078	0.078	0.078	0.065	0.621	0.580	0.559	0.179	nd	
Nb	0.001	0.001	0.020	0.019	0.008	0.008	0.008	0.002	0.002	nd	0.040	0.038	0.037	0.033	0.005	0.001	0.007	
Mo	0.065	0.059	0.048	0.056	0.053	0.053	0.050	0.048	0.048	cnd	0.010	0.016	0.016	0.006	0.014	0.006	0.020	
Cd	0.011	0.064	0.014	0.020	0.020	0.019	0.019	0.019	0.019	cnd	0.110	0.023	0.023	0.029	0.081	0.011	nd	
Sn	nd	0.036	0.020	0.019	0.019	0.019	0.019	0.028	0.026	0.026	0.022	0.022	0.022	0.029	0.011	0.016	0.051	
Sb	0.015	0.021	0.0143	0.0143	0.0143	0.0143	0.0143	0.0179	0.070	0.070	0.070	0.041	0.040	0.038	0.041	0.020	0.014	
Cs	0.015	0.016	0.016	0.024	0.024	0.024	0.024	0.024	0.023	0.023	0.023	0.023	0.023	0.023	0.006	0.008	0.002	
Ba	37.57	33.77	30.01	16.82	15.40	11.68	10.76	7.74	10.13	9.31	8.65	7.89	7.67	3.64	1.66	3.35	7.75	
La	0.064	0.026	0.009	0.646	0.703	0.256	0.203	0.201	0.058	0.051	0.929	0.928	1.022	0.900	0.509	0.047	0.015	
Ce	0.128	0.015	0.006	1.575	1.469	0.346	0.339	0.083	0.110	0.120	1.906	1.722	1.665	1.611	0.060	0.022	0.553	
Pr	0.015	0.002	0.001	0.160	0.153	0.048	0.039	0.010	0.011	0.014	0.240	0.218	0.199	0.198	0.068	0.003	0.005	
Nd	0.061	0.009	0.003	0.636	0.599	0.156	0.040	0.046	0.056	0.056	0.899	0.823	0.808	0.775	0.075	0.031	0.249	
Sm	0.016	0.003	nd	0.113	0.110	0.043	0.034	0.008	0.008	0.011	0.159	0.145	0.142	0.049	0.005	0.002	0.358	
Eu	0.002	0.001	nd	0.026	0.026	0.006	0.006	0.002	0.002	0.003	0.023	0.023	0.023	0.023	0.004	0.001	0.013	
Gd	0.007	0.002	0.001	nd	0.012	0.004	0.004	0.001	0.001	0.001	0.113	0.108	0.105	0.045	0.005	0.003	0.034	
Lu	0.001	nd	nd	0.019	0.019	0.013	nd	0.005	0.002	0.002	0.021	0.021	0.021	0.016	0.005	nd	0.003	
Hf	0.001	nd	nd	0.006	0.006	0.005	0.005	0.005	0.005	0.005	0.008	0.008	0.008	0.003	0.006	nd	0.007	
Dy	0.007	0.001	nd	0.070	0.067	0.030	0.026	0.006	0.005	0.009	0.084	0.087	0.085	0.030	0.003	0.001	0.044	
Ho	0.002	nd	nd	0.015	0.015	0.007	0.006	0.001	0.001	0.003	0.019	0.017	0.016	0.007	0.001	nd	0.009	
Er	0.004	0.001	nd	0.042	0.039	0.006	0.006	0.005	0.005	0.005	0.048	0.048	0.048	0.044	0.004	0.002	0.026	
Tm	0.001	nd	nd	0.006	0.006	0.003	0.003	0.003	0.003	0.003	0.007	0.007	0.007	0.006	0.004	0.003	0.004	
Yb	nd	0.001	nd	0.039	0.036	0.020	0.017	0.005	0.005	0.005	0.042	0.042	0.042	0.039	0.020	0.003	nd	
Gd	0.001	nd	nd	0.006	0.006	0.003	0.003	0.003	0.003	0.003	0.006	0.006	0.006	0.006	0.003	0.001	0.003	
Lu	0.001	nd	nd	0.019	0.019	0.013	nd	0.005	0.005	0.005	0.021	0.021	0.021	0.016	0.006	nd	0.006	
Hf	0.001	nd	nd	0.006	0.006	0.005	0.005	0.005	0.005	0.005	0.008	0.008	0.008	0.008	0.003	nd	0.007	
W	nd	0.006	0.003	0.005	0.005	0.005	0.005	0.005	0.005	0.005	0.012	0.012	0.012	0.012	0.006	nd	nd	
Pb	0.015	0.043	0.006	0.991	0.326	0.060	0.060	0.022	0.022	0.022	0.280	0.227	0.214	0.026	0.002	0.001	0.104	
Th	0.006	0.001	nd	0.127	0.121	0.058	0.058	0.058	0.058	0.058	0.137	0.137	0.137	0.022	0.001	0.002	0.023	
Lu	0.025	0.011	0.006	0.084	0.084	0.085	0.085	0.104	0.120	0.002	0.024	0.024	0.024	0.024	0.001	0.001	0.023	

Table B-1, continued.

Table B-1, continued.

Sample	Filter	No.24	No.24	No.25	No.24	No.25	K ₁	K ₁	K ₁	K ₃	K ₄	K ₅	K ₇	K ₇	K ₇	
		5 µm	0.22 µm	10 kD dialysis	1 kD dialysis	0.22 µm	5 µm	0.45 µm	10 kD UF	1 kD UF	0.45 µm	0.45 µm	5 µm	0.45 µm	10 kD UF	1 kD UF
PH	6.84	nd	nd	nd	nd	4.94	nd	nd								
Na	2.755	3.097	2.255	2.186	3.169	4.71	5.07	493	nd	nd						
K	7.31	3.82	4.73	nd	3.15	75	75	104	167	nd	396	1.796	1.781	1.806	1.843	1.667
Mg	847	864	442	406	576	198	183	125	nd	nd	560	502	573	533	729	546
Ca	2.743	2.493	1.390	1.874	1.160	587	561	336	nd	nd	138	2086	2106	1.977	1.860	1.789
[Al] _{Cl}	7.35 ± 0.01	8.03 ± 1.06	nd	6.35 ± 0.09	2.54 ± 0.66	nd	1.62 ± 0.13	nd	nd	nd	405	368	9745	8394	8226	7922
SO ₄	3.970	1.970	nd	cnd	nd	nd	nd	nd	nd	nd	nd	nd	nd	nd	nd	nd
NO ₃	<dl	nd	nd	nd	nd	nd	<dl	nd	nd							
F	64	60	nd	nd	73	<dl	nd	nd								
Si	2.480	2.450	2.183	2.400	2.90	2.970	79	40	57	72	nd	40	283	3210	3432	3385
DOC	17.30	18.10	3.50	2.99	23.60	nd	5.71	7.63	2.93	2.68	nd	nd	nd	nd	nd	nd
Al	1.26	57	5	4	205	128	109	100	44	25	58	121	40	10.42	4.46	3.61
Mn	38	8	16	5	17	3	3	2	2	2	2	2	13	1.498	nd	nd
Fe	2.237	272	18	4	1.088	53	49	13	15	7	3	18	21	4.195	2.590	1.2
Li	0.840	0.791	0.470	0.581	0.633	0.132	0.170	0.192	0.129	0.108	0.100	0.321	0.423	0.599	0.401	0.277
B	4.796	nd	2.928	nd	2.764	1.310	1.283	nd	nd							
Ti	2.421	0.495	0.066	0.121	1.275	0.561	0.391	0.084	0.144	0.100	0.043	0.174	0.321	0.555	0.272	0.259
V	0.863	0.161	0.081	0.099	0.283	0.334	0.314	0.295	0.395	0.357	0.216	0.230	0.356	0.169	0.022	0.022
Cr	0.689	0.681	0.099	0.169	0.785	0.210	0.186	0.142	0.219	0.133	0.113	0.125	0.145	0.217	0.316	0.064
Co	0.154	0.042	0.088	0.014	0.143	0.199	0.193	0.181	0.143	0.143	0.108	0.084	0.182	0.085	0.093	0.014
Ni	0.360	0.307	cnd	cnd	0.469	2.193	0.546	0.492	0.492	0.233	0.216	0.233	0.398	0.293	0.372	0.200
Cu	0.482	cnd	0.261	cnd	0.948	0.458	0.888	0.769	0.769	cnd	0.326	0.161	0.464	0.598	0.402	0.190
Zn	2.372	cnd	cnd	0.014	4.004	4.754	4.000	4.257	cnd	cnd	0.341	4.257	2.866	2.759	2.963	1.223
Ga	0.035	0.007	0.003	0.002	0.015	0.008	0.005	0.003	0.003	0.002	0.001	0.001	0.002	0.005	0.001	0.001
As	0.316	0.340	0.158	0.169	0.283	0.200	0.201	0.182	0.215	0.178	0.156	0.131	0.125	0.134	0.090	0.086
Rb	0.915	0.881	0.752	0.634	0.629	0.405	0.39	0.051	0.553	0.056	0.034	0.178	0.033	1.102	1.472	1.055
Sr	16.98	13.97	6.43	5.98	14.33	2.48	2.36	1.47	nd	nd	1.31	1.55	52.91	50.89	52.30	41.80
Y	0.174	0.110	0.003	0.002	0.149	0.023	0.013	0.005	0.008	0.002	0.003	0.015	0.017	0.065	0.004	0.003
Zr	0.155	0.157	0.002	0.001	0.289	0.015	0.015	0.015	0.006	0.004	0.004	0.002	0.010	0.040	0.041	0.020
Nb	0.010	0.003	nd	nd	0.007	0.005	nd	0.003	0.003	0.001	0.002	0.001	0.024	0.008	0.002	nd
Mo	0.174	0.024	0.111	0.029	0.075	0.034	0.034	0.023	0.027	0.016	0.014	0.009	0.022	0.024	0.017	0.016
Cd	0.013	0.014	cnd	cnd	0.014	0.014	0.013	0.012	cnd	cnd	0.011	0.019	0.016	0.008	0.007	0.014
Sn	0.023	nd	0.020	0.043	nd	nd	nd	nd	nd	nd	0.030	0.030	0.013	0.039	0.013	nd
Sb	0.044	cnd	0.028	0.024	0.045	0.036	0.036	0.035	0.035	nd	0.039	0.023	0.014	0.017	0.010	0.012
Cs	0.015	0.014	0.012	0.009	0.010	0.001	0.001	0.001	0.002	0.001	0.004	0.004	0.005	0.007	0.007	0.006
Eu	0.010	0.006	nd	nd	0.010	0.010	0.010	0.010	0.002	nd	nd	nd	nd	nd	nd	nd
Gd	0.037	0.024	0.001	0.002	0.060	0.006	0.006	0.006	0.002	0.018	0.006	0.038	0.022	0.239	0.162	0.081
Tb	0.005	0.003	nd	nd	0.006	0.001	nd	nd								
Dy	0.028	0.018	nd	nd	0.032	0.004	0.002	0.005	0.007	0.001	nd	nd	nd	nd	nd	nd
Ho	0.006	0.003	nd	nd	0.007	0.001	nd	nd								
Er	0.016	0.011	nd	nd	0.019	0.003	0.002	nd	nd							
Tm	0.003	nd	nd	nd	0.003	nd	nd	nd	nd	nd	nd	nd	nd	nd	nd	nd
Yb	0.017	0.010	nd	nd	0.020	0.001	nd	nd								
Lu	0.003	nd	nd	nd	0.003	nd	nd	nd	nd	nd	nd	nd	nd	nd	nd	nd
Hf	0.006	0.002	0.020	0.020	0.133	0.005	nd	nd								
W	0.013	0.005	0.053	0.053	nd	nd	nd	nd	nd	nd	nd	nd	nd	nd	nd	nd
Pb	0.316	0.033	cnd	cnd	0.047	0.047	0.001	0.001	0.001	nd	nd	nd	nd	nd	nd	nd
Th	0.034	0.049	0.047	0.047	0.001	0.001	0.001	0.001	0.001	nd	nd	nd	nd	nd	nd	nd

Table B-1, continued.

Table B-1, continued.

Sample	K _{23-B}	K _{23-B}	K ₂₅	K ₂₅	K ₂₆	K ₂₆	K ₂₇	K ₂₇	K ₃₀	K ₃₀	K ₃₃	K ₃₃	K ₃₈	K ₃₈	K ₃₉	K ₃₉	K ₄₀	K ₄₀	K ₄₁	K ₄₁	K ₄₃	K ₄₃	K ₄₃	K ₄₃	
Filter	10 kDa dialysis	1 kDa dialysis	0.45 µm	<0.2 µm in situ																					
pH	nd	nd	4.82	6.49	6.37	5.434	10.300	2.233	2.732	7.45	4.56	6.13	1.164	845	743	5.00	5.00	5.00	5.00	5.00	5.00	5.00	nd	nd	
Na	1.243	1.182	8.18	627	5.291	2.302	3.562	2.880	3.86	9.07	1.399	1.194	1.164	249	133	21	1.197	1.180	1.094	1.094	1.094	1.094	1.094	nd	nd
K	851	717	63	1.182	397	8.439	12.905	8.254	8.898	8.743	1.395	1.194	1.164	217	165	165	1.451	1.451	1.327	1.327	1.327	1.327	1.327	nd	nd
Mg	4.304	4.053	888	1.182	497	20.574	35.137	23.323	10.596	17.435	9.09	2.328	644	3.246	3.246	3.246	3.246	3.246	3.246	3.246	3.246	3.246	3.246	3.246	3.052
Ca	12.564	11.201	1.404	2.96 ± 0.07	401	587	1.746	684	2.864	495	1.252	0.18	1.180	220	736	2.72 ± 0.02	nd	1.511	1.511	1.511	1.511	1.511	1.511	nd	nd
[Al] _i	nd	nd	1.70	1.182	985	1.182	1.182	1.182	1.182	1.182	1.182	1.182	1.182	nd	nd										
Cl	nd	nd	1.39	1.182	nd	nd																			
SO ₄	nd	nd	<dl	nd	nd																				
NO ₃	nd	nd	nd	nd	nd	nd	nd	nd	nd	nd	nd	nd	nd	nd	nd	nd	nd	nd	nd	nd	nd	nd	nd	nd	nd
F	nd	nd	3.728	7.040	26.50	nd	5.78	50.06	nd	6.32	5.08	16.65	6.41	11.60	5.28	124.42	nd	4.96	34.07	34.07	34.07	34.07	34.07	28.62	14.62
Si	4.186	nd	nd	nd	nd	nd	nd	nd	nd	nd	nd	nd	nd	nd	nd	nd	nd	nd	nd	nd	nd	nd	nd	nd	nd
DOC	nd	nd	2.96 ± 0.19	2.64 ± 0.19	1.182	1.182	1.182	1.182	1.182	1.182	1.182	1.182	1.182	nd	nd										
Al	54	23	415	21	22	1.182	1.182	1.182	1.182	1.182	1.182	1.182	1.182	1.182	1.182	1.182	1.182	1.182	1.182	1.182	1.182	1.182	1.182	1.182	1.182
Mn	1.081	982	26	9	433	61	1.182	1.182	1.182	1.182	1.182	1.182	1.182	1.182	1.182	1.182	1.182	1.182	1.182	1.182	1.182	1.182	1.182	1.182	1.182
Fe	7.438	5.311	1.505	22	318	118	5	1.182	1.182	1.182	1.182	1.182	1.182	1.182	1.182	1.182	1.182	1.182	1.182	1.182	1.182	1.182	1.182	1.182	1.182
Li	0.469	0.391	0.960	0.158	0.889	0.925	0.513	0.247	0.272	0.272	0.272	0.272	0.272	0.272	0.272	0.272	0.272	0.272	0.272	0.272	0.272	0.272	0.272	0.272	
B	1.762	1.227	1.799	1.302	4.874	5.025	1.587	2.105	0.896	1.707	0.874	1.217	0.874	1.325	1.325	1.325	1.325	1.325	1.325	1.325	1.325	1.325	1.325	1.325	1.325
Tl	0.369	0.155	3.513	0.196	0.392	0.368	0.192	0.141	0.122	0.538	0.476	0.893	0.923	0.923	0.923	0.923	0.923	0.923	0.923	0.923	0.923	0.923	0.923	0.923	
V	nd	nd	0.935	0.559	0.598	0.251	0.030	0.786	0.056	0.115	0.166	0.344	0.385	0.440	0.465	0.485	0.485	0.485	0.485	0.485	0.485	0.485	0.485	0.485	
Cr	0.680	0.362	2.750	0.139	0.261	0.137	0.059	0.018	0.062	0.083	0.030	0.200	0.256	0.240	0.240	0.240	0.240	0.240	0.240	0.240	0.240	0.240	0.240	0.240	
Co	9.495	8.047	0.989	0.058	0.137	0.136	0.047	0.027	0.029	0.124	0.035	0.331	0.384	0.384	0.384	0.384	0.384	0.384	0.384	0.384	0.384	0.384	0.384	0.384	
Ni	1.596	3.152	2.028	0.136	0.136	0.136	0.047	0.027	0.029	0.031	0.031	0.031	0.031	0.031	0.031	0.031	0.031	0.031	0.031	0.031	0.031	0.031	0.031		
Cu	0.370	0.181	1.262	0.348	0.406	0.094	0.073	0.073	0.035	0.035	0.035	0.035	0.035	0.035	0.035	0.035	0.035	0.035	0.035	0.035	0.035	0.035	0.035		
Zn	6.783	4.010	9.799	4.294	0.677	0.005	0.002	0.007	0.001	0.003	0.010	0.003	0.003	0.003	0.003	0.003	0.003	0.003	0.003	0.003	0.003	0.003	0.003	0.003	
Ga	0.047	0.030	0.012	0.002	0.002	0.002	0.002	0.002	0.002	0.002	0.002	0.002	0.002	0.002	0.002	0.002	0.002	0.002	0.002	0.002	0.002	0.002	0.002	0.002	
As	0.534	0.423	0.284	0.124	0.076	0.124	0.165	0.165	0.102	0.078	0.127	0.127	0.127	0.127	0.127	0.127	0.127	0.127	0.127	0.127	0.127	0.127	0.127	0.127	
Rb	2.504	2.363	0.316	0.730	1.641	1.641	0.380	0.380	0.777	0.777	1.791	0.514	0.455	0.455	0.455	0.455	0.455	0.455	0.455	0.455	0.455	0.455	0.455	0.455	0.455
Sr	30.14	26.35	7.39	1.78	38.57	51.86	14.05	17.20	15.91	15.91	15.91	15.91	15.91	15.91	15.91	15.91	15.91	15.91	15.91	15.91	15.91	15.91	15.91	15.91	
Y	0.314	0.159	0.517	0.016	0.075	0.075	0.002	0.002	0.002	0.002	0.002	0.002	0.002	0.002	0.002	0.002	0.002	0.002	0.002	0.002	0.002	0.002	0.002	0.002	
Zr	0.140	0.049	0.735	0.031	0.031	0.003	0.002	0.002	0.002	0.002	0.002	0.002	0.002	0.002	0.002	0.002	0.002	0.002	0.002	0.002	0.002	0.002	0.002	0.002	
Nb	0.024	0.005	0.024	0.024	0.005	0.005	0.005	0.005	0.005	0.005	0.005	0.005	0.005	0.005	0.005	0.005	0.005	0.005	0.005	0.005	0.005	0.005	0.005	0.005	
Mo	0.455	0.220	0.066	0.028	0.028	0.003	0.002	0.002	0.002	0.002	0.002	0.002	0.002	0.002	0.002	0.002	0.002	0.002	0.002	0.002	0.002	0.002	0.002	0.002	
Cd	0.015	0.024	nd	nd																					
Sn	0.043	0.030	0.042	0.022	0.022	0.002	0.002	0.002	0.002	0.002	0.002	0.002	0.002	0.002	0.002	0.002	0.002	0.002	0.002	0.002	0.002	0.002	0.002	0.002	0.002
Sb	0.005	0.003	0.004	0.003	0.003	0.002	0.002	0.002	0.002	0.002	0.002	0.002	0.002	0.002	0.002	0.002	0.002	0.002	0.002	0.002	0.002	0.002	0.002	0.002	
Cs	0.018	0.006	0.023	0.013	0.013	0.009	0.009	0.009	0.009	0.009	0.009	0.009	0.009	0.009	0.009	0.009	0.009	0.009	0.009	0.009	0.009	0.009	0.009	0.009	
Eu	0.018	0.006	0.023	0.013	0.013	0.009	0.009	0.009	0.009	0.009	0.009	0.009	0.009	0.009	0.009	0.009	0.009	0.009	0.009	0.009	0.009	0.009	0.009	0.009	
Gd	0.041	0.017	0.017	0.017	0.017	0.002	0.002	0.002	0.002	0.002	0.002	0.002	0.002	0.002	0.002	0.002	0.002	0.002	0.002	0.002	0.002	0.002	0.002	0.002	
Tb	0.006	0.002	0.002	0.002	0.002	0.002	0.002	0.002	0.002	0.002	0.002	0.002	0.002	0.002	0.002	0.002	0.002	0.002	0.002	0.002	0.002	0.002	0.002	0.002	
Dy	0.039	0.015	0.015	0.019	0.019	0.003	0.003	0.003	0.003	0.003	0.003	0.003	0.003	0.003	0.003	0.003	0.003	0.003	0.003	0.003	0.003	0.003	0.003	0.003	
Pr	0.071	0.031	0.029	0.013	0.013	0.004	0.004	0.004	0.004	0.004	0.004	0.004	0.004	0.004	0.004	0.004	0.004	0.004	0.004	0.004	0.004	0.004	0.004	0.004	
Nd	0.293	0.127	0.588	0.023	0.0																				

Table B-1, continued.

Table B-1, continued.

Sample	Y-1	Y-2	Y-3	Y-4	Y-5	Y-6	Y-7
Filter	10kD dialysis	1kD dialysis	5 μm	0.22 μm	10kD dialysis	1kD dialysis	0.22 μm
PH	nd	nd	6.04	nd	nd	3.92	nd
Na	39.022	37.389	11.891	nd	nd	6.683	nd
K	4.725	4.458	1.426	nd	1.506	9.00	5.237
Mg	3.668	3.219	3.118	nd	2.850	9.67	nd
Ca	1.348	1.167	3.699	4.527	2.830	3.734	1.299
[Al] ^N	33.64 ± 1.5	nd	23.22 ± 0.15	27.05 ± 0.38	nd	32.03 ± 1.24	1.93 ± 0.12
Cl	48.034	nd	16.389	13.948	10.340	nd	2.02 ± 0.1
SO ₄	6.448	nd	4.376	3.554	4.230	nd	10.596
NO ₃	<dl	nd	<dl	<dl	<dl	nd	4.882
F	nd	nd	nd	nd	nd	nd	<dl
Si	10.821	10.612	9.789	nd	9.587	9.676	294
DOC	15.44	nd	31.28	19.67	8.24	5.11	47.16
Al	370	192	480	357	107	68	890
Mn	10	8	129	125	96	93	45
Fe	63	25	1.337	1.117	93	46	1.072
Li	10.778	9.504	5.584	1.665	6.798	5.799	2.441
B	66.497	63.161	22.566	33.976	25.227	29.045	nd
T	5.889	2.356	6.909	5.817	3.688	2.201	32.819
V	29.533	26.593	1.315	1.195	0.931	0.888	1.488
Cr	2.180	1.294	2.565	2.528	0.892	0.627	1.229
Co	0.680	0.485	0.610	0.586	0.310	0.275	0.313
Ni	3.867	2.132	1.170	1.254	0.508	0.430	1.278
Cu	1.123	0.941	0.475	0.351	0.341	0.414	0.728
Zn	3.485	3.324	4.310	3.054	cmtd	4.375	43
Ga	0.026	0.012	0.045	0.043	0.026	0.019	3.360
Rb	21.568	19.493	0.512	0.539	0.338	0.639	0.389
Sr	4.260	3.988	1.386	1.363	1.337	1.324	4.043
Y	26.43	21.62	34.91	34.15	28.35	28.18	12.53
Zr	0.554	0.229	0.331	0.304	0.066	0.037	8.95
Nb	0.053	0.030	0.032	0.033	0.024	0.024	0.026
Mo	nd	nd	0.082	0.081	0.084	0.080	0.069
Cd	0.039	0.041	0.007	0.008	0.013	0.014	0.144
Sn	0.024	0.018	0.012	nd	0.014	0.011	0.027
Sb	0.323	0.275	0.026	0.026	0.029	0.022	0.173
Cs	0.010	0.010	0.013	0.012	0.012	0.013	0.054
Ba	2.37	1.75	1.291	12.38	11.11	10.47	13.21
La	0.851	0.418	1.029	0.937	0.142	0.080	3.636
Ce	2.263	0.996	2.316	2.126	0.333	0.183	7.689
Pr	0.244	0.110	0.254	0.236	0.039	0.020	0.895
Nd	0.944	0.427	0.954	0.865	0.148	0.075	3.180
Sm	0.143	0.064	0.140	0.133	0.023	0.002	0.033
Eu	0.018	0.018	0.012	0.021	0.004	0.001	0.050
Gd	0.101	0.046	0.090	0.077	0.015	0.006	0.272
Tb	0.013	0.006	0.011	0.010	0.002	0.001	0.034
Dy	0.077	0.031	0.061	0.055	0.010	0.006	0.053
Ho	0.017	0.007	0.013	0.011	0.002	0.001	0.014
Er	0.050	0.023	0.038	0.031	0.008	0.004	0.090
Tm	0.008	0.004	0.005	0.005	0.001	0.001	0.012
Yb	0.053	0.024	0.032	0.030	0.007	0.004	0.017
Lu	0.009	0.004	0.005	0.004	0.001	0.001	0.026
Hf	0.022	0.011	0.015	0.014	0.003	0.003	0.004
W	0.043	0.036	0.014	0.008	0.012	0.014	0.006
Pb	0.273	0.187	0.421	0.442	0.197	0.136	0.870
Th	0.073	0.027	0.101	0.133	0.012	0.006	0.876
U	0.195	0.085	0.077	0.075	0.002	0.001	0.051

Table B-2. Percentage of TE distribution between dissolved phase (< 1 kDa) and two colloidal pools (1 kDa – 10 kDa and 10 kDa – 0.22 µm) for both acidic- and basic rock-dominated catchments. V - Vetrynen Belt, K - Kivakkka intrusion, and Y - White Sea coast series, respectively. "nd" stands for not determined.

Table B-2, continued.

Sample	No.24	No.24	No.24	No.24	No.24	K-1	K-1	K-1	K-1	K-7	K-7	K-7	K-7	K-23	K-23	K-23	K-23	K-43
	<1 kDa	1 kDa-10 kDa	10 kDa-0.22 μm	<1 kDa	1 kDa-10 kDa	10 kDa-0.45 μm	<1 kDa	1 kDa-10 kDa	10 kDa-0.45 μm	<1 kDa	1 kDa-10 kDa	10 kDa-0.45 μm	<1 kDa	1 kDa-10 kDa	10 kDa-0.45 μm	<1 kDa	1 kDa-10 kDa	10 kDa-0.45 μm
Na	70.6	2.2	27.2	78.0	nd	nd	nd	nd	nd	86.3	7.3	6.4	nd	nd	nd	nd	nd	nd
K	nd	nd	nd															
Mg	45.9	4.1	50.0	47.5	25.4	27.1	85.0	3.4	11.7	54.4	8.9	36.7	nd	nd	nd	nd	nd	nd
Ca	46.5	9.2	44.2	57.9	37.0	5.1	74.9	6.4	18.7	41.4	5.9	52.6	63.2	12.1	24.7	61.1	5.1	
Si	98.0	nd	nd	nd	nd	nd	83.1	nd	nd	78.5	5.9	nd	nd	nd	nd	98.5	nd	nd
DOC	16.5	2.8	80.7	32.9	14.0	53.1	20.0	14.6	65.4	28.2	14.8	57.0	86.4	10.6	2.9	15.2	8.0	76.9
Al	7.0	1.4	91.6	22.7	17.8	59.5	11.5	4.2	84.3	7.4	67.9	24.7	9.4	12.5	78.2	6.1	4.5	89.4
Mn	60.5	nd	nd	61.7	14.8	5.3	0.2	94.5	nd	nd	nd	nd	63.4	6.4	30.1	68.2	3.7	28.1
Fe	1.6	5.0	93.4	6.0	7.9	86.2	0.3	nd	nd	0.6	52.6	46.8	64.6	25.9	9.5	9.3	2.4	88.2
Li	73.5	nd	nd	63.2	12.8	24.0	65.4	2.9	31.7	77.3	12.0	10.7	80.9	16.1	3.0	97.7	nd	nd
B	nd	nd	nd	nd	nd	nd	nd	nd	nd	77.3	7.0	15.7	94.6	nd	nd	93.1	nd	nd
Ti	24.5	nd	nd	11.1	14.4	74.5	71.2	3.6	25.2	6.6	89.1	4.3	2.9	5.1	91.9	1.9	0.6	97.5
V	61.3	nd	nd	nd	nd	nd	12.9	0.2	86.9	16.3	nd	nd	38.4	25.8	35.8	2.4	0.7	96.9
Cr	24.8	nd	nd	61.0	10.5	28.5	30.2	nd	nd	nd	51.0	nd	14.4	12.6	73.0	6.5	15.8	77.6
Co	32.6	nd	nd	55.7	18.2	26.1	15.3	4.9	79.8	27.8	68.4	3.8	51.9	9.3	38.8	53.5	7.3	39.3
Ni	nd	nd	nd	43.8	24.8	31.3	28.6	8.0	63.5	17.5	42.3	40.2	36.5	16.6	47.0	36.0	9.9	54.1
Cu	17.1	nd	nd	21.0	14.4	57.6	49.9	5.2	45.0	36.2	nd	nd	30.1	31.5	38.4	38.8	30.0	30.0
Zn	38.7	nd	nd	35.5	54.1	10.5	26.6	25.0	48.4	nd	nd	nd	52.3	36.2	11.6	41.0	4.0	55.0
Ga	36.5	1.9	61.6	49.0	19.5	31.5	79.4	nd	nd	10.3	58.4	31.3	45.0	26.2	28.8	20.9	12.2	66.9
As	49.7	nd	nd	77.8	10.7	11.5	60.7	2.8	36.5	45.8	12.7	41.5	60.4	15.8	23.8	32.8	3.6	63.7
Rb	72.0	13.4	14.6	86.2	nd	nd	82.2	3.5	14.2	86.8	nd	nd	90.5	5.4	4.1	96.2	nd	nd
Sr	42.8	3.2	54.0	55.5	26.5	18.0	82.1	5.2	12.6	40.4	16.3	43.2	67.1	9.7	23.2	66.2	6.4	27.3
Y	2.0	0.8	97.3	13.5	7.2	79.3	2.0	1.3	96.6	5.5	90.7	3.8	10.9	13.7	75.4	5.3	6.5	88.2
Zr	0.4	0.9	98.7	14.5	10.4	75.1	nd	nd	nd	0.0	89.3	10.7	3.9	7.3	88.8	1.4	2.6	96.1
Nb	5.0	nd	nd	nd	nd	nd	nd	nd	nd	1.2	70.8	28.0	12.9	44.2	42.9	0.0	6.3	93.7
Mo	nd	nd	nd	39.5	4.1	46.5												
Cd	nd	nd	nd	nd	25.9	3.3												
Sn	1.4	nd	nd	58.3	37.0	4.7	30.9	nd	nd	11.7	31.9	56.4	nd	nd	nd	58.9	5.9	35.2
Sb	5.0	0.9	94.2	nd	nd	nd	nd	nd	nd	48.5	28.7	22.8	66.5	30.5	3.0	52.9	7.2	39.9
Cs	67.7	22.0	10.3	97.2	nd	nd	81.8	nd	nd	73.9	nd	nd	nd	nd	nd	81.8	nd	nd
Ba	41.2	8.1	50.7	51.5	25.8	22.7	68.8	6.1	25.1	43.0	15.1	42.0	64.1	14.1	21.8	50.8	4.4	44.8
La	18.7	15.4	65.8	5.2	6.7	88.2	6.4	nd	nd	4.5	69.9	25.6	11.1	23.9	65.0	4.1	2.9	93.0
Ce	1.6	1.2	97.3	8.3	3.8	87.9	1.3	0.8	98.0	4.1	71.0	24.9	10.0	13.9	76.2	3.3	4.3	92.4
Pr	1.2	0.9	97.9	6.9	8.2	84.9	1.3	1.1	97.6	4.1	69.3	26.6	10.6	13.7	75.7	0.0	8.2	91.8
Nd	1.6	0.3	98.1	9.2	9.4	81.4	1.7	0.4	97.9	4.2	70.1	25.7	11.2	14.6	74.2	3.8	5.0	91.8
Sm	2.2	1.0	96.8	2.0	32.6	65.4	3.2	0.2	96.5	4.6	67.6	27.8	11.0	14.2	74.8	4.3	6.0	89.7
Eu	nd	nd	nd	66.2	nd	nd	nd	nd	nd	4.3	63.0	32.7	12.8	28.1	59.1	6.9	4.1	93.0
Gd	1.3	3.2	95.5	24.6	21.8	53.6	1.6	nd	nd	3.6	61.7	34.7	9.0	12.4	78.6	5.1	3.3	91.6
Tb	0.8	nd	nd	nd	19.8	25.4	54.7	0.9	nd	nd	4.5	63.8	31.7	8.8	14.4	76.8	5.0	5.2
Dy	1.6	nd	nd	nd	12.1	1.1	86.8	2.0	nd	nd	4.5	66.6	28.9	8.9	13.4	77.6	4.2	4.5
Ho	3.3	nd	nd	13.0	24.7	62.3	1.2	0.0	98.8	4.9	71.2	23.9	10.2	14.2	75.6	5.5	4.1	90.4
Er	2.9	1.6	95.5	16.2	2.9	80.9	0.8	0.6	98.6	4.0	67.3	28.7	11.2	14.8	73.9	6.2	5.4	88.4
Tm	nd	nd	nd	nd	23.6	26.8	49.6	0.6	nd	nd	6.8	71.4	21.8	12.0	17.4	70.5	9.2	2.1
Yb	nd	nd	nd	nd	10.7	9.7	79.6	1.5	nd	nd	5.5	64.6	30.0	12.4	14.6	73.0	6.9	5.9
Lu	nd	nd	nd	nd	nd	nd	nd	0.9	nd	nd	5.3	63.5	31.2	13.4	15.0	71.7	7.3	5.1
Hf	nd	nd	nd															
W	nd	nd	nd	nd	nd	nd	nd	nd	nd	33.6	nd	nd	nd	nd	nd	nd	nd	nd
Pb	0.5	nd	nd	47.8	1.1	51.0	26.7	nd	nd	4.1	81.1	14.9	nd	nd	nd	29.9	nd	nd
Th	1.1	nd	nd	10.0	1.6	88.4	nd	nd	nd	nd	nd	nd	3.5	6.8	88.7	1.7	2.1	96.2
U	1.7	nd	nd	nd	23.4	16.8	59.8	nd	nd	3.4	67.6	29.1	8.9	6.9	84.2	3.8	2.8	93.4

Table B-2, continued.

Sample	K-44	K-44	K-44	Y-1	Y-1	Y-1	Y-1	Y-3	Y-3	Y-5	Y-5
	<1 kDa	1 kDa-10 kDa	10 kDa-0.45 µm	<1 kDa	1 kDa-10 kDa	10 kDa-0.22 µm	<1 kDa	1 kDa-10 kDa	10 kDa-0.22 µm	<1 kDa	10 kDa-0.22 µm
Na	69.1	18.8	12.1	93.1	5.6	0.5	nd	nd	nd	nd	nd
K	nd	nd	nd	93.8	5.6	0.5	nd	nd	nd	nd	nd
Mg	43.9	7.0	49.0	72.4	10.1	17.5	nd	nd	nd	nd	nd
Ca	39.4	17.6	43.0	51.4	8.0	40.6	82.5	3.9	13.7	56.2	13.0
Si	93.6	1.1	5.3	nd	nd	nd	nd	nd	nd	58.0	5.7
DOC	nd	nd	nd	0.0	19.6	80.4	26.0	15.9	58.1	35.2	9.6
Al	15.7	7.6	76.7	18.8	17.5	63.7	19.1	11.0	70.0	33.9	13.0
Mn	43.1	10.2	46.7	47.9	13.7	38.5	24.8	2.4	22.9	62.2	10.0
Fe	1.7	2.2	96.1	6.1	9.5	84.4	4.1	4.2	91.6	36.6	8.1
Li	nd	nd	nd	nd	nd	nd	nd	nd	nd	nd	nd
B	nd	nd	nd	89.0	4.7	6.3	85.5	nd	nd	nd	nd
Ti	1.8	1.8	96.5	4.2	6.4	89.4	3.5	2.9	93.7	5.3	4.5
V	9.4	3.4	87.2	nd	nd	nd	74.3	3.6	22.1	37.0	11.0
Cr	6.1	18.1	75.8	23.9	16.4	59.8	16.0	46.9	6.0	64.7	8.4
Co	26.8	8.4	64.9	59.0	25.0	34.6	28.1	37.3	34.3	47.1	29.9
Ni	18.6	16.2	65.2	nd	nd	nd	nd	nd	nd	56.7	14.4
Cu	28.1	40.2	31.7	65.9	12.8	21.3	nd	nd	nd	48.2	7.3
Zn	54.7	nd	42.4	2.1	55.5	nd	nd	nd	nd	33.6	11.1
Ga	23.3	1.3	75.4	19.3	23.1	57.6	42.9	16.5	nd	59.9	8.9
As	43.0	8.7	48.3	nd	nd	nd	62.1	nd	nd	15.1	8.4
Rb	nd	nd	nd	92.0	6.3	1.7	97.2	0.9	nd	53.6	7.3
Sr	41.1	15.3	43.7	56.2	12.5	31.3	82.5	3.4	14.1	82.6	4.9
Y	5.5	7.2	87.3	10.6	13.0	76.3	12.3	9.4	78.3	18.9	10.7
Zr	1.2	3.3	95.5	6.0	10.8	83.1	4.8	4.3	90.9	10.1	6.6
Nb	30.6	nd	nd	15.2	11.6	73.2	24.0	0.6	75.5	8.3	7.6
Mo	68.9	nd	nd	nd	nd	nd	98.9	nd	nd	22.4	6.6
Cd	nd	nd	nd	nd	nd	nd	nd	nd	nd	64.3	0.8
Sn	35.4	nd	nd	36.9	12.0	51.2	nd	nd	nd	31.8	nd
Sb	59.0	21.8	19.1	164.1	nd	87.4	nd	nd	nd	53.0	16.4
Cs	82.2	17.2	0.6	102.1	nd	nd	nd	nd	nd	84.5	5.5
Ba	37.6	8.1	54.3	36.0	12.6	51.3	84.5	5.1	10.3	56.4	10.1
La	3.8	4.5	91.6	8.0	10.1	81.9	8.5	6.6	84.9	12.8	8.6
Ce	4.0	5.1	90.8	8.2	10.4	81.3	8.6	7.1	84.3	14.9	9.2
Pr	4.4	5.7	89.9	8.8	10.7	80.5	8.6	8.1	83.3	16.2	9.7
Nd	4.7	6.2	89.1	9.1	11.0	79.9	8.7	8.4	82.9	17.5	10.0
Sm	5.9	5.2	88.8	8.5	10.6	80.9	7.6	9.7	82.7	17.5	10.5
Eu	8.9	2.9	88.2	10.2	4.7	85.3	2.6	16.0	81.4	35.3	nd
Gd	5.3	5.7	89.0	9.8	11.7	78.5	8.0	11.1	80.9	19.3	12.5
Yb	8.9	4.5	86.6	11.8	13.9	74.2	14.0	8.8	77.2	24.4	12.6
Lu	13.3	nd	nd	13.5	17.1	69.4	13.8	10.5	76.1	19.1	9.7
Dy	6.2	4.1	89.6	8.6	12.5	78.9	10.4	7.5	82.1	18.8	10.6
Ho	9.1	1.9	88.9	9.6	12.8	77.6	11.7	9.2	79.2	20.7	10.3
Er	6.7	3.7	89.6	10.8	12.5	76.7	11.7	13.6	74.7	20.1	12.1
Tm	11.1	0.7	88.2	11.8	13.7	74.4	12.4	13.3	74.3	19.8	12.7
Hf	10.3	nd	nd	64.3	13.7	22.0	nd	nd	nd	16.4	77.6
W	nd	nd	nd	nd	nd	nd	nd	nd	nd	48.5	7.3
Pb	7.0	4.8	88.2	12.8	5.9	81.2	30.8	13.8	56.4	20.2	7.9
Th	1.8	2.4	95.8	3.3	5.5	91.2	4.2	5.1	90.7	4.9	4.6
U	10.1	0.6	89.3	8.0	10.4	81.6	7.5	7.5	85.5	20.6	6.5

Table B-3. Iron-normalized K_d values for TE distribution between dissolved phase ($< 1 \text{ kDa}$) and colloidal matter ($1 \text{ kDa} - 0.22 \mu\text{m}$). "nd" stands for not determined; B

Sample	No. & Bedrock	No. 9	No. 15	No. 18	K-1	K-23	K-43	K-44	No. 22	No. 24	K-7	Y-1	Y-3	Y-5	average	average	
		B	B	B	B	B	B	B	G (summer)	G (summer)	G (winter)	G (winter)	G (winter)	G (winter)	G (summer)	G (winter)	
Al	0.223	nd	0.275	0.054	0.217	0.073	1.581	0.092	0.037	0.211	0.021	0.284	0.182	1.129	0.359	0.532	
Mn	0.022	0.055	0.055	0.040	0.040	0.002	0.048	0.023	nd	0.010	0.049	0.072	0.015	0.353	0.036	0.146	
Li	0.005	0.007	0.021	nd	0.037	0.002	0.002	nd	0.138	0.006	0.001	nd	nd	0.012	0.048	nd	
Ti	5.403	2.125	0.083	0.510	0.083	2.295	0.948	0.584	0.049	0.001	1.484	1.198	nd	1.870	0.211	1.341	
V	0.105	0.013	0.017	0.020	nd	0.030	4.243	0.166	0.284	0.010	0.018	nd	0.015	0.985	0.656	0.104	0.500
Cr	0.069	0.155	0.184	0.003	0.041	0.055	1.477	0.264	0.006	0.048	0.006	0.210	0.130	1.361	0.281	0.020	0.567
Co	0.049	0.114	0.084	0.013	0.051	0.015	0.090	0.047	nd	0.033	0.015	0.046	0.049	0.443	0.058	0.024	0.179
Ni	0.058	0.000	0.135	0.001	0.082	0.028	0.183	0.075	nd	0.007	0.125	0.082	0.623	0.070	0.007	0.277	
Cu	0.249	0.057	0.001	nd	0.240	0.010	0.162	0.044	nd	0.078	0.003	0.034	nd	1.147	0.109	0.040	0.591
Zn	0.019	0.013	0.075	nd	0.116	nd	0.148	0.014	nd	0.025	0.008	0.089	nd	0.388	0.064	0.016	0.238
Ga	0.013	0.068	0.088	0.010	0.066	0.051	0.389	0.057	nd	0.028	0.001	0.275	0.057	3.259	0.093	0.014	1.197
As	0.019	0.021	0.028	0.010	0.018	0.007	0.211	0.023	0.257	0.016	0.002	nd	0.026	0.503	0.042	0.092	0.264
Rb	0.001	0.036	0.071	0.000	0.051	0.009	0.053	0.025	nd	0.006	0.006	0.001	nd	0.008	0.007	0.003	
Sr	0.010	0.038	0.297	0.081	0.409	0.100	1.854	0.294	nd	0.021	0.001	0.051	0.009	0.366	0.032	0.939	0.142
Y	0.177	0.535	nd	nd	0.377	nd	7.385	1.453	0.120	4.093	nd	0.134	0.552	0.307	2.484	0.468	0.462
Zr	0.524	15.321	nd	nd	nd	0.463	nd	0.039	0.166	0.301	nd	0.022	0.853	5.157	5.012	2.107	2.344
Nb	0.034	1.614	nd	nd	nd	nd	nd	0.158	0.549	nd	nd	0.136	0.368	6.407	0.537	0.233	2.304
Mo	0.004	nd	nd	nd	nd	0.009	0.008	0.008	nd	0.006	nd	0.006	nd	0.000	0.000	0.003	
Cd	0.040	0.116	0.007	0.000	0.008	0.013	0.043	nd	nd	0.003	0.935	nd	0.001	0.012	0.032	0.003	0.629
Sn	0.025	0.340	0.096	0.001	0.046	0.044	0.072	0.031	0.136	1.123	0.006	0.113	nd	1.241	0.082	0.422	0.677
Sb	0.041	0.021	nd	nd	nd	0.006	0.092	0.012	nd	0.306	nd	0.006	nd	0.514	0.034	0.306	0.260
Cs	0.002	0.009	0.076	nd	0.002	0.002	0.023	0.004	nd	0.008	0.001	nd	nd	0.017	0.004	nd	
Ba	0.017	0.054	0.084	0.001	0.060	0.008	0.100	0.028	nd	0.023	0.001	0.117	0.008	0.448	0.044	0.012	0.191
La	0.332	0.601	0.188	0.032	1.170	0.123	2.382	0.429	0.026	0.069	0.040	0.759	0.460	3.949	0.655	0.045	1.723
Ce	0.290	0.856	0.400	0.091	0.704	0.138	3.035	0.408	0.011	1.000	0.212	0.735	0.456	3.321	0.740	0.408	1.504
Pr	0.251	0.889	0.360	0.086	0.854	0.136	nd	0.369	nd	1.298	0.206	0.686	0.459	3.001	0.421	0.752	1.382
Nd	0.248	0.727	0.315	0.105	0.629	0.135	2.590	0.348	nd	0.975	0.163	0.658	0.450	2.730	0.637	0.569	1.279
Sm	0.222	0.670	0.238	0.049	3.165	0.122	2.304	0.272	nd	0.712	0.082	0.707	0.520	2.739	0.880	0.397	1.322
Eu	0.096	0.587	0.193	0.042	0.033	0.128	1.392	0.176	nd	0.081	0.579	1.625	1.061	3.045	0.655	0.045	1.723
Gd	0.143	0.949	0.230	0.166	0.195	0.156	1.925	0.306	nd	1.192	0.172	0.606	0.491	2.417	0.509	0.682	1.171
Tb	0.101	0.557	0.274	nd	0.258	0.124	1.961	0.216	nd	1.910	0.298	0.580	0.522	2.449	0.499	1.044	1.184
Dy	0.167	0.694	0.269	0.095	0.463	0.124	2.331	0.258	nd	0.978	0.133	0.699	0.369	2.501	0.554	0.555	1.190
Ho	0.103	0.595	0.369	nd	0.427	0.114	1.766	0.171	nd	0.471	0.235	0.618	0.326	2.222	0.506	0.353	1.055
Er	0.101	0.439	0.204	0.050	0.329	0.140	1.549	0.241	nd	0.534	0.338	0.544	0.324	2.298	0.381	0.436	1.056
Tm	0.028	0.341	0.161	nd	0.206	0.080	1.017	0.138	nd	0.462	0.491	0.304	0.462	2.342	0.281	0.462	1.045
Yb	0.075	0.362	0.197	0.039	0.531	0.101	1.401	0.176	nd	0.182	0.490	0.263	1.799	0.360	0.182	0.851	
Lu	0.018	0.285	0.146	nd	0.024	0.104	1.308	0.112	nd	0.314	0.422	0.269	1.663	0.285	0.314	0.785	
Hf	0.009	0.468	nd	nd	nd	nd	1.199	0.150	nd	nd	0.456	0.152	2.962	0.457	nd		
Pb	0.212	0.626	0.299	0.010	0.069	0.138	0.242	0.230	nd	0.350	0.008	0.447	0.096	2.296	0.228	0.228	1.529
Th	0.452	2.837	0.279	nd	0.574	nd	5.903	0.936	nd	1.442	nd	1.915	0.975	nd	2.130	0.790	1.445
	0.541	0.583	0.176	nd	0.208	0.167	2.621	0.153	nd	0.076	0.897	0.756	0.570	nd	0.756	0.486	1.187

Annex C

Table C-1. Measured major and trace elements concentrations in filtrates (0.22 µm) and dialysates (1 kDa) at different pH. All concentrations are given in µg/l except for DOC (mg/l). "nd" stands for not determined; "cntd" - contaminated; "nat" - natural pH value.

Table C-1, continued.

Table C-1, continued.

pH	M-1			2.61			4.08			6.32			7.22			3.16			5.81			7.08			
	[< 0.22 µm]	[< 1 kDa]																							
Na	776	646	3.213	2.842	846	655	cnd	cnd	4.044	4.522	cnd	cnd													
K	120	90	94	90	100	87	128	122	83	cnd	cnd	86	433	892	242	952	51	51	63	cnd	cnd	63	118	cnd	
Mg	563	503	540	473	659	371	708	552	908	1.008	952	1.136	1.219	1.093	453	994	178	1.073	1.073	1.073	1.073	1.073	1.073	1.073	
Ca	2.400	2.268	2.185	1.914	2.566	1.363	2.603	1.833	2.04	4.85	533	508	519	499	504	503	499	504	503	503	503	503	503	503	
Si	1.778	1.584	1.814	1.635	2.160	1.834	2.104	1.435	41.37	27.75	44.21	11.15	45.22	7.84	44.44	44.44	6.41	6.41	6.41	6.41	6.41	6.41	6.41	6.41	
DOC	14.72	cnd	16.70	17.24	18.16	cnd	14.35	nd	41.37	27.75	44.21	11.15	45.22	7.84	44.44	44.44	6.41	6.41	6.41	6.41	6.41	6.41	6.41	6.41	
Al	105	100	108	51	126	15	128	33	186	136	209	15	204	4	190	4	192	4	192	4	192	4	192	4	192
Mn	10.4	10.5	13.5	11.5	10.0	4.2	10.3	3.4	41.8	41.4	41.1	12.4	43.4	4.4	45.0	4.4	45.0	4.4	45.0	4.4	45.0	4.4	45.0	4.4	45.0
Fe	567	616	621	251	689	16	674	11	849	612	919	46	932	8	950	8	950	8	950	8	950	8	950	8	950
Li	0.304	0.190	0.248	0.336	0.260	0.147	0.406	0.306	0.731	nd	0.627	0.621	0.548	0.670	0.656	nd									
B	1.066	1.020	0.894	nd	1.217	1.222	1.410	nd	3.282	4.049	3.290	4.018	3.231	4.311	3.231	4.311	3.231	4.311	3.231	4.311	3.231	4.311	3.231	4.311	
Ti	0.517	cnd	0.760	0.094	0.947	nd	0.893	nd	1.679	1.663	1.843	1.819	1.809	2.239	1.874	1.874	1.874	1.874	1.874	1.874	1.874	1.874	1.874	1.874	
V	0.179	0.224	0.179	0.094	0.193	0.084	0.207	0.101	0.186	0.152	0.171	0.129	0.112	0.183	0.177	0.177	0.177	0.177	0.177	0.177	0.177	0.177	0.177	0.177	
Cr	0.280	0.296	0.298	0.161	0.330	0.105	0.386	0.151	0.516	0.425	0.542	0.212	0.568	0.155	0.775	0.155	0.775	0.155	0.775	0.155	0.775	0.155	0.775	0.155	
Co	0.082	0.091	0.114	0.107	0.072	0.018	0.079	0.004	0.318	0.327	0.320	0.073	0.340	0.025	0.340	0.025	0.340	0.025	0.340	0.025	0.340	0.025	0.340	0.025	
Ni	0.519	0.571	0.625	0.519	0.628	0.097	0.297	0.423	0.680	0.625	0.625	0.128	0.602	0.046	0.625	0.046	0.625	0.046	0.625	0.046	0.625	0.046	0.625	0.046	
Cu	0.801	0.833	1.382	0.858	0.403	0.184	0.704	0.352	1.336	1.040	1.229	0.249	1.201	0.135	1.477	0.135	1.477	0.135	1.477	0.135	1.477	0.135	1.477	0.135	
Zn	33.82	27.24	19.78	19.67	6.33	5.33	24.51	9.18	15.24	cnd	11.53	3.91	9.38	1.24	10.12	1.25	10.12	1.25	10.12	1.25	10.12	1.25	10.12	1.25	
Ga	0.009	0.010	0.011	0.005	0.003	0.003	0.002	0.011	0.005	0.031	0.017	0.029	0.008	0.022	0.028	0.022	0.028	0.022	0.028	0.022	0.028	0.022	0.028	0.022	
Ge	0.005	0.003	0.005	0.005	0.005	0.005	nd	0.006	0.004	0.049	0.033	0.048	nd	0.049	nd										
As	0.133	0.135	0.135	0.096	0.141	0.085	0.168	0.099	0.365	0.265	0.386	0.168	0.394	0.158	0.394	0.158	0.394	0.158	0.394	0.158	0.394	0.158	0.394	0.158	
Rb	0.246	0.226	0.221	0.211	0.232	0.233	0.227	0.089	0.097	0.086	0.080	0.086	0.064	0.052	0.076	0.076	0.076	0.076	0.076	0.076	0.076	0.076	0.076	0.076	
Sr	14.63	13.41	12.04	14.49	8.74	14.75	11.12	6.78	6.61	6.47	6.22	6.07	6.47	1.02	6.92	4.8	6.92	4.8	6.92	4.8	6.92	4.8	6.92	4.8	
Y	0.081	0.095	0.095	0.044	0.111	0.010	0.108	0.008	0.089	0.058	0.058	0.124	0.008	0.084	0.001	0.081	0.001	0.081	0.001	0.081	0.001	0.081	0.001		
Zr	0.060	0.063	0.081	0.017	0.088	0.005	0.098	nd	0.211	0.136	0.136	0.128	0.141	0.102	0.006	0.134	0.006	0.134	0.006	0.134	0.006	0.134	0.006		
Mo	0.019	0.041	0.036	0.014	0.046	0.048	0.101	0.078	0.012	0.014	0.018	0.018	0.018	0.018	0.018	0.018	0.018	0.018	0.018	0.018	0.018	0.018	0.018		
Cd	3.221	3.700	3.191	0.117	0.090	0.024	0.004	0.004	3.148	2.953	1.254	0.203	1.238	0.051	0.051	0.051	0.051	0.051	0.051	0.051	0.051	0.051	0.051		
Sn	nd	nd	nd	nd	nd	nd	nd	nd	0.035	0.138	0.036	0.013	0.032	0.025	0.025	0.025	0.025	0.025	0.025	0.025	0.025	0.025	0.025		
Sb	0.022	0.025	0.027	0.026	0.020	0.016	0.030	0.022	0.035	0.032	0.030	0.030	0.032	0.030	0.030	0.030	0.030	0.030	0.030	0.030	0.030	0.030	0.030		
Cs	0.007	0.008	0.005	0.002	0.002	0.004	0.004	0.004	0.003	0.003	0.002	0.002	0.001	0.002	0.001	0.002	0.001	0.002	0.001	0.002	0.001	0.002	0.001		
Ba	7.63	7.69	7.45	6.61	8.59	4.26	7.56	4.44	8.09	7.50	7.50	7.50	7.50	7.50	7.50	7.50	7.50	7.50	7.50	7.50	7.50	7.50	7.50		
La	0.183	0.229	0.225	0.077	0.251	0.015	0.245	0.011	0.128	0.072	0.090	0.072	0.072	0.072	0.072	0.072	0.072	0.072	0.072	0.072	0.072	0.072	0.072		
Ce	0.327	nd	0.421	0.154	0.465	0.026	0.441	0.015	0.156	0.081	0.081	0.166	0.003	0.169	0.003	0.169	0.003	0.169	0.003	0.169	0.003	0.169	0.003		
Pr	0.046	0.056	0.056	0.022	0.022	0.022	0.022	0.015	0.233	0.012	0.075	0.042	0.094	0.004	0.094	0.004	0.094	0.004	0.094	0.004	0.094	0.004	0.094		
Nd	0.164	0.219	0.217	0.082	0.254	0.015	0.254	0.015	0.038	0.002	0.022	0.013	0.019	0.002	0.019	0.002	0.019	0.002	0.019	0.002	0.019	0.002	0.019		
Sm	0.028	0.034	0.036	0.013	0.037	nd	0.005	0.002	0.002	0.011	0.012	0.006	0.004	0.005	0.004	0.005	0.004	0.005	0.004	0.005	0.004	0.005	0.004		
Eu	0.009	0.011	0.009	0.005	0.002	0.011	0.001	0.001	0.001	0.001	0.001	0.001	0.001	0.001	0.001	0.001	0.001	0.001	0.001	0.001	0.001	0.001	0.001		
Tm	0.001	0.001	0.001	nd	0.001	0.001	0.001	0.001	0.001	0.001	0.001	0.001	0.001	0.001	0.001	0.001	0.001	0.001	0.001	0.001	0.001	0.001	0.001		
Tb	0.002	0.004	0.003	0.001	0.001	0.004	0.004	0.004	0.004	0.004	0.004	0.004	0.004	0.004	0.004	0.004	0.004	0.004	0.004	0.004	0.004	0.004	0.004		
Dy	0.014	0.019	0.017	0.007	0.020	0.001	0.017	0.001	0.017	nd	0.001	0.013	0.006	0.013	0.006	0.013	0.006	0.013	0.006	0.013	0.006	0.013	0.006		
Ho	0.003	0.003	0.002	0.003	0.002	nd	0.003	0.006	0.004	nd	0.004	0.004	0.004	0.004	0.004	0.004	0.004	0.004	0.004	0.004	0.004	0.004	0.004		
Er	0.007	0.011	0.009	0.005	0.010	0.001	0.008	0.001	0.008	nd	0.006	0.006	0.006	0.006	0.006	0.006	0.006	0.006	0.006	0.006	0.006	0.006	0.006		
Tm	0.001	0.001	0.001	nd	0.001	0.001	0.001	0.001	0.001	nd															

Table C-1, continued.

pH	S-40			5.27			7.06			7.44		
	[< 0.22 µm]	[< 1 kDa]										
Na	7.830	5.710	cnd	cnd								
K	1.190	cnd	125	cnd	133	cnd	117	cnd	131	cnd	141	cnd
Mg	1.533	1.099	993	546	939	272	1.029	237	1.156	173	1.156	173
Ca	1.672	1.288	1.101	517	1.045	1.82	1.021	1.021	1.021	1.021	1.016	1.016
Si	1.247	884	863	869	866	845	860	866	860	860	856	856
DOC	39.29	22.85	42.06	10.30	43.15	7.24	42.69	7.57	42.69	7.57	42.69	7.57
Al	1.43	50	105	6	97	1	107	56	107	56	107	56
Mn	7.4	4.8	4.8	1.8	4.7	0.5	5.1	0.5	5.1	0.5	5.1	0.5
Fe	564	199	396	7	375	3	403	14	403	14	403	14
Li	0.650	0.726	0.417	0.477	0.593	0.538	0.443	0.443	0.443	0.443	0.443	0.443
B	8.576	7.599	6.003	7.011	5.883	6.335	5.973	6.335	5.973	6.335	5.973	6.335
Ti	3.083	0.530	2.875	0.087	2.244	0.101	2.270	0.165	2.270	0.165	2.270	0.165
V	0.464	0.227	0.281	0.187	0.274	0.221	0.310	0.316	0.310	0.316	0.310	0.316
Cr	0.671	0.290	0.438	0.138	0.477	0.115	0.595	0.292	0.595	0.292	0.595	0.292
Co	0.204	0.124	0.147	0.036	0.141	0.011	0.155	0.014	0.155	0.014	0.155	0.014
Ni	0.459	0.263	0.321	0.048	0.293	0.021	0.334	0.030	0.334	0.030	0.334	0.030
Cu	1.857	0.792	1.416	0.263	1.458	0.135	1.705	0.505	1.705	0.505	1.705	0.505
Zn	37.10	26.31	23.57	6.67	22.41	1.98	26.71	2.56	26.71	2.56	26.71	2.56
Ga	0.044	0.013	0.023	0.002	0.011	0.006	0.031	nd	0.031	nd	0.031	nd
Ge	0.037	0.009	0.026	0.007	0.026	0.004	0.021	nd	0.021	nd	0.021	nd
As	0.478	0.220	0.365	0.145	0.359	0.133	0.347	0.177	0.347	0.177	0.347	0.177
Rb	0.224	0.159	0.149	0.122	0.138	0.106	0.147	0.131	0.147	0.131	0.147	0.131
Sr	12.41	8.07	8.12	3.21	8.04	1.39	8.56	1.21	8.56	1.21	8.56	1.21
Y	0.094	0.025	0.062	0.003	0.102	0.004	0.077	0.043	0.077	0.043	0.077	0.043
Zr	0.272	0.068	0.123	0.032	0.138	0.033	0.152	0.048	0.152	0.048	0.152	0.048
Mo	0.006	0.004	0.011	0.018	0.023	nd	0.024	nd	0.024	nd	0.024	nd
Cd	4.477	2.783	2.396	2.434	2.199	0.077	0.059	0.033	0.059	0.033	0.059	0.033
Sn	0.050	0.006	0.034	0.004	0.036	0.016	0.078	0.045	0.078	0.045	0.078	0.045
Sb	0.049	0.027	0.038	0.020	0.038	0.016	0.039	0.024	0.039	0.024	0.039	0.024
Cs	0.008	0.005	0.003	0.003	0.002	0.001	0.006	0.005	0.006	0.005	0.006	0.005
Ba	11.12	6.79	7.08	2.03	6.82	0.65	7.88	0.65	7.88	0.65	7.88	0.65
La	0.074	nd	0.049	nd	0.038	nd	0.054	0.008	0.054	0.008	0.054	0.008
Ce	0.129	0.024	0.091	nd	0.092	nd	0.095	0.001	0.095	0.001	0.095	0.001
Pr	0.017	0.004	0.012	nd	0.012	nd	0.013	nd	0.013	nd	0.013	nd
Nd	0.069	0.016	0.047	0.002	0.050	nd	0.055	0.001	0.055	0.001	0.055	0.001
Sm	0.019	0.008	0.013	0.001	0.013	0.013	0.014	0.001	0.014	0.001	0.014	0.001
Eu	0.006	0.002	0.004	nd	0.004	nd	0.005	nd	0.005	nd	0.005	nd
Gd	0.013	0.003	0.013	nd	0.012	nd	0.011	nd	0.011	nd	0.011	nd
Tb	0.002	nd	0.001	nd	0.002	nd	0.002	nd	0.002	nd	0.002	nd
Dy	0.010	0.002	0.007	nd	0.009	nd	0.008	nd	0.008	nd	0.008	nd
Ho	0.002	0.001	0.001	nd	0.002	nd	0.002	nd	0.002	nd	0.002	nd
Er	0.004	0.001	0.004	nd	0.003	nd	0.004	nd	0.004	nd	0.004	nd
Tm	0.001	nd	nd	nd	0.001	nd	nd	nd	nd	nd	nd	nd
Yb	0.005	0.001	0.003	nd	0.003	nd	0.004	nd	0.004	nd	0.004	nd
Lu	0.001	nd	nd	nd								
Hf	0.010	0.002	0.004	0.001	0.005	0.001	0.004	0.003	0.004	0.003	0.004	0.003
W	0.008	0.004	0.004	0.004	0.006	0.007	0.006	nd	0.006	nd	0.006	nd
Pb	0.044	0.030	0.017	0.019	0.016	0.017	0.017	0.017	0.017	0.017	0.017	0.017
Tl	1.006	0.322	0.693	0.018	0.453	nd	0.785	0.012	0.785	0.012	0.785	0.012
Th	0.014	0.002	0.011	nd	0.011	nd	0.010	0.001	0.010	0.001	0.010	0.001
U	0.002	0.001	0.002	nd								

Table C-2. The trace elements distribution (in %) between dissolved (< 1 kDa) and colloidal (1 kDa - 0.22 μm) pools for the studied waters at different pH. "nd" stands for not determined.

No.12		No.15									
pH	4.20	5.12	6.18 _{nat}	6.84	7.50	7.50	3.75	4.78	5.15 _{nat}	5.89	6.87
%	< 1 kDa	0.22 μm	< 1 kDa	0.22 μm	< 1 kDa	0.22 μm	< 1 kDa	0.22 μm	< 1 kDa	0.22 μm	< 1 kDa
DOC	63.5	36.5	53.6	46.4	53.7	35.6	64.4	30.2	69.8	60.5	39.5
Li	84.9	15.1	74.4	25.6	94.5	5.5	89.2	10.8	87.0	nd	nd
B	69.6	30.4	94.8	5.2	nd	88.1	11.9	89.7	10.3	54.7	45.3
Na	nd	nd	92.1	7.9	99.7	0.3	nd	nd	nd	nd	nd
Mg	nd	nd	nd	nd	nd	nd	nd	nd	nd	nd	nd
Al	56.9	43.1	46.3	53.7	40.6	59.4	21.1	78.9	29.5	64.3	35.7
Si	nd	nd	nd	nd	nd	nd	nd	nd	nd	nd	nd
K	nd	nd	nd	nd	nd	nd	nd	nd	nd	nd	nd
Ca	nd	nd	93.2	6.8	85.7	14.3	68.9	31.1	92.2	7.8	nd
Tl	16.7	83.3	12.4	87.6	11.4	88.6	8.3	91.7	13.2	86.8	24.8
V	40.6	59.4	51.4	48.6	67.3	32.7	59.3	40.7	85.0	15.0	23.6
Cr	45.7	54.3	42.1	57.9	45.2	54.8	30.1	69.9	24.0	76.0	55.4
Mn	72.3	27.7	66.8	33.2	34.1	65.9	nd	nd	nd	94.7	5.3
Fe	27.1	72.9	15.5	84.5	12.6	87.4	4.1	95.9	2.2	97.8	38.7
Co	67.0	33.0	56.5	43.5	42.8	57.2	17.1	82.9	15.4	84.6	15.8
Ni	63.2	36.8	56.6	43.4	55.3	44.7	38.5	61.5	26.9	81.9	53.4
Cu	60.2	39.8	52.2	47.8	61.7	38.3	36.9	63.1	26.5	73.1	88.4
Zn	36.2	63.8	21.5	78.5	31.1	68.9	8.9	91.1	6.3	93.7	70.6
Ga	41.8	58.2	42.0	58.0	38.0	62.0	40.1	59.9	67.8	32.2	60.7
Ge	62.4	37.6	nd	nd	nd	nd	nd	nd	nd	nd	nd
As	66.1	33.9	72.0	28.0	81.3	18.7	63.9	36.1	67.2	32.8	64.8
Rb	79.3	20.7	93.5	6.5	85.9	14.1	81.8	18.2	85.3	14.7	nd
Sr	72.7	27.3	72.0	28.0	57.9	47.1	52.3	37.9	62.1	95.5	4.5
Y	55.0	45.0	43.4	56.6	33.0	67.0	15.6	84.4	4.9	95.1	68.4
Zr	35.1	64.9	23.4	76.6	19.8	80.2	10.7	89.3	6.0	94.0	34.4
Nb	11.0	89.0	5.7	94.3	25.6	74.4	nd	nd	nd	nd	nd
Mo	25.1	74.9	53.7	46.3	nd	37.3	62.7	97.2	2.8	nd	35.2
Cd	66.0	34.0	56.7	43.3	62.9	37.1	29.4	70.6	16.3	83.7	87.9
Sn	43.6	56.4	82.6	17.4	nd	54.8	45.2	57.0	43.0	48.1	51.9
Sb	71.3	28.7	86.8	13.2	95.3	4.7	90.9	9.1	88.8	nd	nd
Cs	68.6	31.4	83.5	16.5	81.6	18.4	74.8	25.2	74.2	25.8	99.9
Eu	52.2	33.7	60.1	39.9	40.5	59.5	35.3	64.7	27.1	89.7	13.3
La	46.5	53.5	33.3	66.7	25.0	75.0	12.1	87.9	3.7	96.3	54.7
Ce	47.6	52.4	34.8	65.2	25.5	74.5	12.4	87.6	3.2	96.8	56.3
Pr	49.1	50.9	36.5	63.5	27.6	72.4	12.6	88.0	3.3	96.7	58.5
Nd	50.2	49.8	37.2	62.8	27.7	72.3	12.4	87.6	3.0	97.0	40.1
Sm	50.5	49.5	42.1	57.9	27.4	72.6	13.2	86.8	2.7	97.3	58.0
Tm	51.4	47.8	27.3	72.7	25.8	74.2	10.3	89.7	0.8	93.0	7.1
Gd	54.0	46.0	40.7	59.3	24.6	75.4	17.8	82.2	1.8	98.2	71.8
Tb	53.3	46.7	40.1	59.9	28.2	71.8	13.3	86.7	1.4	98.6	43.8
Lu	65.7	34.3	47.2	52.8	32.8	67.2	20.6	79.4	nd	nd	nd
Dy	51.0	49.0	39.3	60.7	26.3	73.7	12.6	87.4	3.3	96.7	41.5
Ho	55.7	44.3	44.0	56.0	30.8	69.2	14.0	86.0	2.3	97.8	42.2
Er	55.5	44.5	44.8	55.2	28.3	71.7	15.3	84.7	2.9	98.2	68.2
Tm	51.4	48.6	48.1	51.9	27.2	72.8	13.0	87.0	nd	nd	nd
Yb	52.1	47.9	45.3	54.7	37.3	62.7	18.3	81.7	4.7	95.3	59.4
Hf	32.7	67.3	31.6	68.4	33.9	66.1	nd	nd	nd	nd	nd
W	nd	nd	58.9	41.1	nd	nd	4.0	96.0	9.4	nd	nd
Pb	35.0	65.0	59.5	40.5	64.9	35.1	56.7	43.3	70.6	44.2	55.8
Tl	74.4	25.6	nd	nd	nd	94.5	5.5	nd	nd	nd	nd
Th	26.8	73.2	12.4	87.6	8.6	91.4	4.1	95.9	1.9	98.1	39.3
U	45.3	54.7	29.1	70.9	17.8	82.2	7.9	92.1	4.3	95.7	60.7

Table C-2, continued.

Table C-2, continued.

pH	K ₂₃			K ₄₃			M-1			
	3.48	4.41	5.00	3.35	4.21	5.05	2.61	4.08	6.32	7.22
%	<1 kDa - 0.22 μm	<1 kDa - 0.22 μm	1 kDa - 0.22 μm	<1 kDa - 0.22 μm	1 kDa - 0.22 μm	<1 kDa - 0.22 μm	<1 kDa - 0.22 μm	1 kDa - 0.22 μm	1 kDa - 0.22 μm	1 kDa - 0.22 μm
DOC	82.3	17.7	74.0	26.0	59.5	40.5	81.0	19.0	69.3	30.7
Li	nd	nd	nd	nd	nd	nd	nd	nd	nd	nd
B	nd	nd	nd	nd	nd	nd	nd	nd	nd	nd
Mg	nd	nd	nd	nd	nd	nd	nd	nd	nd	nd
A	85.5	14.5	59.0	41.0	64.4	nd	96.5	3.5	72.5	27.5
Si	88.9	11.1	85.0	15.0	90.5	nd	83.1	16.9	71.7	28.3
K	nd	nd	nd	nd	nd	nd	nd	nd	nd	nd
Ca	nd	nd	nd	nd	nd	nd	nd	nd	nd	nd
Co	97.7	2.3	84.9	15.1	39.7	60.3	45.3	27.8	nd	nd
Ni	93.9	6.1	81.4	18.6	54.4	45.6	47.5	52.5	nd	nd
Cu	89.0	11.0	75.1	24.9	51.5	48.5	47.4	98.4	1.6	nd
Zn	nd	80.2	10.8	70.1	20.9	36.5	63.5	nd	nd	nd
Ga	68.6	31.4	33.1	66.9	nd	nd	nd	nd	nd	nd
Ge	nd	nd	nd	nd	nd	nd	nd	nd	nd	nd
As	86.6	13.4	83.0	17.0	66.2	33.8	78.4	21.6	nd	nd
Rb	nd	nd	nd	90.1	9.9	90.7	9.3	nd	nd	nd
Sr	nd	99.4	0.6	75.4	24.6	74.2	25.8	nd	nd	nd
Y	89.0	11.0	61.8	38.2	17.9	82.1	8.7	98.3	3.2	nd
Zr	74.2	25.8	44.4	55.6	15.5	84.5	12.0	88.0	86.6	nd
Nb	52.5	47.5	21.1	78.9	9.3	90.7	10.4	89.6	59.2	nd
Mo	53.8	46.2	55.5	44.5	nd	nd	nd	nd	nd	nd
Cd	nd	86.9	13.1	41.1	58.9	17.5	82.5	nd	nd	nd
Sn	41.3	58.7	22.2	34.2	65.8	50.4	49.6	nd	nd	nd
Sb	nd	nd	96.2	38.8	14.2	80.1	19.9	nd	nd	nd
Cs	97.9	2.1	nd	93.2	6.8	98.2	1.8	84.1	15.9	nd
Ba	nd	nd	95.6	4.4	60.1	39.9	47.5	52.5	nd	nd
La	80.1	19.9	46.5	53.5	10.4	89.6	4.0	96.0	93.5	nd
Ce	80.6	19.4	48.6	54.4	5.5	91.0	3.3	88.7	7.0	nd
Pr	81.0	19.0	45.5	54.5	9.5	90.5	3.6	96.4	7.5	nd
Nd	84.3	15.7	48.4	51.6	10.0	90.0	3.8	96.2	88.0	nd
Sr	84.6	15.4	51.8	48.2	11.0	89.0	4.3	95.7	87.7	nd
Sm	95.9	2.0	92.0	9.8	52.5	47.5	13.7	86.3	84.6	nd
Tm	70.4	29.6	38.5	61.5	17.9	82.1	9.9	90.1	83.4	nd
Yb	89.6	10.4	63.4	46.8	11.7	88.3	3.7	96.3	81.0	nd
Lu	89.1	10.9	66.7	33.3	21.2	87.4	12.6	87.4	79.4	nd
Hf	88.9	10.1	47.9	52.1	nd	nd	nd	nd	nd	nd
Dy	84.0	16.0	54.3	45.7	13.3	86.7	7.1	92.9	90.7	nd
Pb	53.3	16.6	53.8	46.2	15.7	84.3	7.7	92.3	12.1	nd
Er	87.8	12.2	62.3	37.7	18.0	82.0	7.8	92.2	89.4	nd
Tl	nd	nd	nd	nd	nd	nd	nd	nd	nd	nd
Th	96.0	4.0	66.5	33.5	15.2	84.8	19.2	80.8	91.3	nd

Table C-2, continued.

pH	S-32			S-40			S-44		
	3.16	5.81	7.08	3.22	5.27	7.06	3.22	5.27	7.06
< 1 kDa	1 kDa - 0.22 μm	1 kDa - < 1 kDa	1 kDa - 0.22 μm	< 1 kDa	1 kDa - 0.22 μm	1 kDa - 0.22 μm	< 1 kDa	1 kDa - 0.22 μm	1 kDa - 0.22 μm
DOC	67.1	32.9	25.2	74.8	17.3	82.7	14.4	85.6	75.5
Li	nd	nd	99.0	1.0	nd	nd	nd	nd	17.7
B	nd	nd	nd	nd	nd	nd	nd	nd	82.3
Na	nd	nd	nd	nd	nd	nd	nd	nd	nd
Mg	nd	nd	47.7	52.3	27.2	72.8	12.4	87.6	77.0
Al	73.2	26.8	7.4	92.6	2.2	97.8	nd	nd	nd
Si	nd	nd	nd	nd	nd	nd	0.8	70.9	nd
K	nd	nd	nd	nd	nd	nd	nd	nd	nd
Ca	nd	nd	41.4	58.6	17.9	82.1	13.9	86.1	nd
Ti	39.5	60.5	10.3	89.7	13.2	6.6	93.4	77.0	nd
V	81.8	18.2	75.3	24.7	57.1	42.9	98.7	3.3	nd
Cr	82.4	17.6	39.2	60.8	27.4	72.6	41.9	58.1	nd
Mn	99.0	1.0	30.3	69.7	10.1	89.9	1.6	98.4	nd
Fe	72.1	27.9	5.0	95.0	0.8	99.2	0.1	99.9	nd
Co	nd	nd	22.7	77.3	7.2	92.8	4.1	95.9	nd
Ni	97.7	2.3	20.4	79.6	7.7	92.3	4.4	95.6	nd
Cu	77.9	22.1	20.3	79.7	11.2	88.8	37.5	62.5	nd
Zn	nd	nd	33.9	66.1	13.2	86.8	12.4	87.6	nd
Ga	55.8	44.2	28.2	71.8	88.4	11.6	nd	nd	nd
Ge	66.8	33.2	nd	nd	nd	nd	nd	nd	nd
As	72.5	27.5	43.5	56.5	40.1	59.9	46.9	53.1	nd
Rb	nd	nd	92.1	7.9	81.5	18.5	84.3	15.7	nd
Sr	97.5	2.5	34.4	65.6	15.8	84.2	7.0	93.0	nd
Y	65.1	34.9	6.1	93.9	1.3	98.7	0.9	99.1	nd
Zr	64.4	35.6	nd	nd	5.5	94.5	8.1	91.9	nd
Nb	nd	nd	41.5	58.5	35.6	64.4	57.2	42.8	nd
Mo	nd	nd	nd	nd	nd	nd	nd	nd	nd
Cd	93.8	6.2	16.2	83.8	4.1	95.9	3.5	96.5	nd
Sn	nd	nd	35.6	64.4	72.0	28.0	55.5	44.5	nd
Sb	91.3	8.7	83.4	16.6	68.0	32.0	64.3	35.7	nd
Cs	nd	nd	67.1	32.9	64.8	35.2	66.9	33.1	nd
Ba	92.7	7.3	23.8	76.2	8.7	91.3	2.5	97.5	nd
La	56.1	43.9	nd	nd	nd	nd	nd	nd	nd
Ce	51.8	48.2	2.1	97.9	nd	nd	nd	nd	nd
Pr	54.8	45.2	3.6	96.4	nd	nd	nd	nd	nd
Nd	56.3	43.7	3.8	96.2	nd	nd	nd	nd	nd
Sm	58.3	41.7	8.8	91.2	nd	nd	nd	nd	nd
Eu	67.3	32.7	12.4	87.6	6.9	93.1	nd	nd	nd
Tm	67.2	32.8	5.1	94.9	nd	nd	nd	nd	nd
Gd	55.0	45.0	nd	nd	nd	nd	nd	nd	nd
Tb	56.5	43.5	5.0	95.0	nd	nd	nd	nd	nd
Dy	43.6	56.4	3.3	96.7	nd	nd	nd	nd	nd
Ho	63.1	36.9	9.5	90.5	nd	nd	nd	nd	nd
Er	62.4	37.6	nd	1.7	98.3	nd	nd	nd	nd
Tm	nd	nd	nd	nd	nd	nd	nd	nd	nd
Yb	67.7	32.3	13.8	86.2	nd	nd	nd	nd	nd
Lu	60.2	39.8	nd	nd	nd	nd	nd	nd	nd
Hf	71.2	28.8	nd	49.7	50.3	29.8	70.2	20.5	nd
W	nd	nd	nd	nd	nd	nd	nd	nd	nd
Pb	65.8	34.2	2.5	97.5	nd	nd	nd	nd	nd
Tl	nd	nd	nd	nd	nd	nd	nd	nd	nd
Th	46.6	53.4	9.2	90.8	10.3	89.7	3.4	96.6	nd
U	50.0	50.0	nd	nd	nd	nd	nd	nd	nd

Table C-3. Iron-normalized K_d values for TE distribution between dissolved phase ($< 1 \text{ kDa}$) and colloidal matter ($1 \text{ kDa} - 0.22 \mu\text{m}$) in all samples at different pH.

“nd” stands for not determined.

AUTEUR : Ekaterina VASYUKOVA

TITRE : Altération chimique des roches et migration des éléments dans la zone boréale (Nord-Ouest de la Russie)

DIRECTEURS DE THESE : Bernard DUPRE, Oleg POKROVSKY, Alexander SHISHKIN

LIEU ET DATE DE SOUTENANCE : 27 janvier 2009, Université Paul Sabatier, Laboratoire des Mécanismes et Transferts en Géologie (LMTG), OMP, 14 av. Edouard Belin, 31400 Toulouse

RESUME :

Cette thèse a pour but d'améliorer notre compréhension des processus d'altération des roches mafiques silicatées, de la spéciation des éléments et de leur migration dans le milieu boréal (bassin versant de la mer Blanche, Nord-Ouest de la Russie). Les objectifs principales du travail sont *i*) de caractériser et décrire les mécanismes responsables de l'altération chimique et de la formation des minéraux dans la zone subarctique, *ii*) évaluer le rôle de la lithologie (environnement granitique versus basaltique) dans la spéciation des éléments traces (ET) et la formation des colloïdes organo-minéraux dans les eaux de surface des bassins versants boréaux des hautes latitudes, et *iii*) révéler la dépendance de la spéciation des ET en fonction du pH de la solution pour prédire des changements éventuels dans la bioaccumulation des éléments dans les eaux naturelles à cause de leur acidification. L'originalité de cette thèse est de combiner, pour la première fois sur les mêmes objets naturels, les techniques physico-chimique, minéralogique et isotopique afin de mieux comprendre les facteurs qui contrôlent les cycles biogéochimiques des éléments dans les régions subarctiques.

MOTS-CLES : géochimie, zone boréale, subarctic, élément trace, colloïde, spéciation, eaux naturelles, ultrafiltration, dialyse, podzol, roche mafic, altération chimique

DISCIPLINE ADMINISTRATIVE : Géochimie de Surface

INTITULE ET ADRESSE DU LABORATOIRE :

Laboratoire des Mécanismes et Transferts en Géologie (LMTG), Université de Toulouse, CNRS, OMP, 14 av. Edouard Belin, 31400 Toulouse

The chemical weathering of rocks and migration of elements in the boreal zone (North-West Russia)

The objective of this thesis is to improve our understanding of the weathering processes of mafic silicate rocks and element speciation and migration in the boreal environments (White Sea basin, North-Western Russia). Specific goals are to i) characterize and describe the mechanisms governing the chemical weathering and mineral formation in subarctic zone, ii) assess the role of the rock lithology (granitic environment vs. basaltic) in trace elements (TE) speciation and organo-mineral colloids formation in surface waters of boreal high latitude river basins, and iii) reveal the pH-dependence of TE speciation in order to predict possible changes in elements bioavailability in natural water due to their acidification caused by environmental changes. The main originality of the work is to combine, for the first time on the same natural objects, the geochemical, isotope, physico-chemical and mineralogical techniques to better understand the factors that control biogeochemical cycling of elements in the subarctic region.